Final Report

Contract BED26-977-16

Prediction of Safety Opportunities Using Automated Traffic Signal Performance Measures

Mohamed Abdel-Aty, Ph.D., P.E.
Zubayer Islam, Ph.D.
Yang-Jun Joo, Ph.D.
BM Tazbiul Hassan Anik, Ph.D.

University of Central Florida

Department of Civil, Environmental & Construction Engineering

Orlando, FL 32816-2450

UNIVERSITY OF
CENTRAL FLORIDA

June 2025

DISCLAIMER

The opinions, findings, and conclusions expressed in this publication are those of the authors and not necessarily those of the State of Florida Department of Transportation.

TECHNICAL REPORT DOCUMENTATION PAGE

1. Report No. 5	2. Government Accession No.	3. Recipient's Catalog No.	
4. Title and Subtitle Prediction of Safety Opportunities Using Automated Traffic Signal Performance Measures		5. Report Date June 2025	
		6. Performing Organization Code	
7. Author(s) Mohamed A. Abdel-Aty, Ph.D., P.E.; Zubayer Islam, Ph.D.; Yang-Jun Joo, Ph.D.; BM Tazbiul Hassan Anik		8. Performing Organization Report No.	
9. Performing Organization Name and Address Department of Civil, Environmental & Construction Engineering, University of Central Florida 12800 Pegasus Drive, Suite 211 Orlando, FL 32816-2450		10. Work Unit No. (TRAIS)	
		11. Contract or Grant No. BED26-977-16	
12. Sponsoring Agency Name and Address Florida Department of Transportation, District 5		13. Type of Report and Period Covered Draft Final Deliverable	
		14. Sponsoring Agency Code	
15. Supplementary Note			

16. Abstract

This report presents the Smart Signal Performance Monitor (SSPM) system, developed to enhance intersection safety in Florida. The SSPM utilizes Automated Traffic Signal Performance Measures (ATSPM) to provide data-driven signalization recommendations. Raw ATSPM data is transformed into performance measures like Signal Phasing and Timing (SPaT) metrics, vehicle volume, conflicts, red-light running (RLR), and pedestrian activity. Algorithms were developed to recommend six key strategies: Yellow/Red Clearance Time Adjustment using a causal forest model; Protected vs. Permitted Left-Turn Phasing via gap analysis and volume estimation; Pedestrian Recall using a Beta-Binomial model and k-means clustering; and Leading Pedestrian Interval (LPI) with No Right Turn on Red (NRTOR) based on pedestrian-vehicle conflict propensity. The SSPM architecture features a Transform-Recommend-Rank (TRR) Server (for processing, recommendations, and ranking intersections by a composite safety score), a Database Server, and a Frontend Server with interactive dashboards. Tested with June 2024 data from 19 Seminole County intersections, the SSPM demonstrates an end-to-end pipeline for monitoring intersection safety and recommendations for signal strategies. Future work includes integrating live ATSPM feeds and expanding system coverage, which will provide FDOT with a network-wide proactive management tool for intersection safety.

17. Key Words Automated Traffic Signal Performance Measures, Traffic signal, Safety evaluation		18. Distribution Statement	
19. Security Classif. (of this report)	20. Security Classif. (of this page) Unclassified	21. No. of Pages 247	22. Price

TABLE OF CONTENTS

LIST OF FIGURES

LIST OF TABLES

EXECUTIVE SUMMARY

This report details the development and implementation of the Smart Signal Performance Monitor (SSPM) system, a comprehensive platform designed to enhance intersection safety and operational efficiency in Florida's District 5, with an initial focus on Seminole County. Leveraging Automated Traffic Signal Performance Measures (ATSPM) data, the SSPM system provides data-driven recommendations for traffic signalization strategies.

The project began with the collection of two primary data types: detector configuration data from the Normalized Operational Equipment Management Initiative (NOEMI) and controller event log data from SunStore. Recognizing the variability and potential inaccuracies in this data, a critical step involved a thorough data quality assessment. The Event Sequence Quality Checker (ESQC) was developed and employed to verify detector functionality and the integrity of event sequences, ensuring that subsequent analyses were based on reliable data. Detector configurations, which vary significantly across intersections, were systematically categorized by phase and movement type (left-turn, through, right-turn, and shared) to manage this complexity and facilitate consistent data transformation.

The core of the system involves transforming raw controller event log data into a rich set of performance measures. These include Signal Phasing and Timing (SPaT) metrics, vehicle volume, occupancy time, gap, headway, split failures, vehicle-vehicle conflicts, red-light running (RLR) incidents, pedestrian activity indicators, pedestrian delay, and pedestrian-vehicle conflict propensity. These measures are calculated at a granular cycle level and can be aggregated to various time intervals (e.g., 15 minutes, hourly) for trend analysis and recommendation generation.

Building on these performance measures, the project developed algorithms to recommend key traffic signalization strategies:

- **Yellow and Red Clearance Time Adjustment**: A causal forest model estimates the impact of signal timing adjustments on conflict rates per vehicle, providing data-driven recommendations for optimizing these critical intervals.
- **Protected vs. Permitted Left-Turn Phasing**: Recommendations are based on a gap analysis of opposing through movements and an estimation of left-turn volumes derived from turning movement count survey and stop-bar detector occupancy data.
- **Pedestrian Recall**: A Beta-Binomial model estimates the probability of pedestrian presence, and k-means clustering identifies critical hours when pedestrian recall should be active.
- **Leading Pedestrian Interval (LPI) and No Right Turn on Red (NRTOR)**: These interconnected strategies are recommended based on an analysis of pedestrian-vehicle (right-turn) conflict propensity, calculated using pedestrian and vehicle exposure during concurrent phases.

The SSPM system architecture integrates three main components:

- **Transform–Recommend–Rank (TRR) Server**: This backend engine processes raw ATSPM data, applies the aforementioned algorithms to generate safety recommendations, and ranks intersections based on a composite safety score derived from normalized performance measures (vehicle-vehicle conflicts, RLR, pedestrian delay).
- **Database Server**: Stores all transformed performance measures, safety recommendations, and intersection rankings, making them accessible via a set of RESTful APIs for dynamic querying.

- **Frontend Server**: A React-based user interface provides operators with interactive dashboards. The "Recommendation View" enables the exploration of performance measure trends (Measure Dashboard) and the visualization of specific strategy recommendations (Recommendation Dashboard). The "Rank View" enables users to identify high-risk intersections based on customizable safety score weightings and selected time intervals.

The SSPM system, tested with data from June 2024 for 19 intersections in Seminole County, demonstrates a viable end-to-end pipeline from raw data ingestion to actionable safety insights. While currently reliant on historical batch data, future work includes migration to live ATSPM feeds and a cloud-based (AWS) environment for enhanced scalability and real-time operational support. The prototype provides FDOT with a powerful tool to proactively manage traffic signal operations, prioritize interventions, and ultimately improve road safety across the district.

CHAPTER 1: INTRODUCTION

Signalized intersections are crucial nodes within the urban transportation network where the risk of conflicts and crashes can be substantial. Traditional approaches to traffic signal management have often been reactive, relying on historical crash data or periodic manual reviews to identify safety deficiencies. However, the advent of Automated Traffic Signal Performance Measures (ATSPM) presents a significant opportunity to shift towards a more proactive and data-driven paradigm for improving safety at these locations. ATSPM systems offer high-resolution data from traffic signal controllers, capturing detailed information about signal timing, vehicle actuation, and pedestrian activity.

By analyzing ATSPM data, traffic engineers can identify emerging safety issues and implement changes before crashes occur. While ATSPMs have been widely recognized for their utility in optimizing traffic flow and operational efficiency, their application for direct safety enhancements through targeted countermeasures is an area of evolving research and practice. There is a clear need to develop systematic methodologies and practical tools that can translate raw ATSPM data into actionable safety insights and recommendations for specific signalization strategies.

This report details the research undertaken to address this need. It presents the development of algorithms and a comprehensive system designed to utilize ATSPM data for identifying and predicting safety improvement opportunities at signalized intersections within Florida's District 5. The primary objective is to equip traffic operators with data-driven tools to enhance safety through informed adjustments to traffic signal operations, focusing on countermeasures such as yellow and red clearance timing, left-turn phasing, and pedestrian treatments. This work aims to transform

raw data into meaningful performance measures and, ultimately, into recommendations that can lead to safer intersection environments.

This report proceeds as follows. **Chapter 2** provides a foundational overview of ATPSM and details the two essential data sources: detector configuration files and controller event logs. **Chapter 3** presents an extensive review of related works, encompassing project reports from US and state Departments of Transportation (DOT), existing GitHub repositories related to ATSPM systems, and a systematic review of academic literature on the mobility and safety applications of ATSPMs. This chapter also summarizes best practices for various operational countermeasures at intersections as recommended in technical manuals. **Chapter 4** describes the data collection methodologies implemented for this project, focusing on acquiring detector configuration data from the Normalized Operational Equipment Management Initiative (NOEMI) and controller event log data from SunStore for ATSPM-equipped intersections, primarily in Seminole county. It also details the process of grouping detector configurations and the development of the Event Sequence Quality Checker (ESQC) to assess data quality. **Chapter 5** elaborates on the algorithm development process. This includes the transformation of controller event log data into meaningful cycle-level performance measures such as Signal Phasing and Timing (SPaT), volume, occupancy, headway, and conflicts. It further details the methodologies for exploratory data analysis and the algorithms developed to provide recommendations for six key safety strategies: yellow and red clearance time adjustment, choice of protected versus permitted left-turns, pedestrian recall, Leading Pedestrian Interval (LPI), and No Right Turn on Red (NRTOR). **Chapter 6** introduces the system architecture of the Smart Signal Performance Monitor (SSPM), a system developed to implement the derived algorithms and deliver actionable safety recommendations. This chapter outlines the core components of the SSPM, including the Transform-Recommend-Rank (TRR)

server, the database server, and the frontend server, which features interactive dashboard views for performance measure analysis, safety recommendations, and intersection safety ranking. Subsequent chapters are intended to cover the evaluation of the SSPM system, the functionalities of its report generation module, and a final summary of the research and implementation. Through the integration of real-time data processing, advanced analytics, and user-friendly interfaces, this work endeavors to make a significant contribution to advancing transportation safety technologies.

CHAPTER 2: OVERVIEW OF ATSPM

ATSPM relies on two primary types of data: the detector configuration and the controller event log data. While the detector configuration data is crucial for interpreting detector actuation events associating vehicle detections with specific traffic movements, the controller event data is essential for analyzing signal timing performance and identifying vehicle movement events. This chapter investigates the detailed data structure and parameters to provide intersection performance analysis provided by ATSPM Documentation from Purdue University[1].

2.1. Detector Configuration

Detector Configuration Data encompasses the structural and operational details of traffic detectors installed at intersections. It has the following key components:

a) Approach: descriptions of where each detector is positioned within the approach.

b) Detector width and lengths: Effective detecting width and length of detector

c) Lane Type: Identification of which traffic movements (e.g., through, left turn, right turn, and the specific phases) each detector is designed to monitor.

d) Detector Types: Specifications of the detection technology employed (e.g., inductive loops, video detection, radar).

e) Channel Number: A unique identifier assigned to each detector input

f) Phase Number: Specific traffic phases assigned to each detector

g) Stopbar Distance: Detecting location from the stopbar detector

---

[1] Purdue University ATSPM document

ATSPM detector configuration information varies in format across different administrative entities. FDOT utilizes Normalized Operational Equipment Management Initiative (NOEMI) reports to manage traffic operations throughout Florida's roadway network. These reports include details on specific intersections, covering operation and maintenance activities. **Figure 2-1** shows a section of the NOEMI report that addresses the configuration of the detectorFigure 2-1. The NOEMI report provides key information necessary for interpreting ATSPM controller event log data, which is discussed in detail in the next chapter. However, it is updated infrequently, often with several years between revisions, and relies primarily on manual processes.

ID	Approach	Lane Type	Width	Length	Lane No. from Left	Type	Channel	Phase	Stopbar Distance	Slot Number	Length
1	1 N CHARLES RICHARD BEALL BLVD NB	Left	12	190	1	Inductive Loop	1	1	0	null	40
2	1 N CHARLES RICHARD BEALL BLVD NB	Through	12	null	2	Inductive Loop	9	6	150	null	6
2	1 N CHARLES RICHARD BEALL BLVD NB	Through	12	null	2	Inductive Loop	11	6	330	null	6
3	1 N CHARLES RICHARD BEALL BLVD NB	Through	14	null	3	Inductive Loop	10	6	150	null	6
3	1 N CHARLES RICHARD BEALL BLVD NB	Through	14	null	3	Inductive Loop	12	6	330	null	6
4	1 N CHARLES RICHARD BEALL BLVD NB	Right	12	175	4						
5	2 N PINE MEADOW DR WB	Left	10	135	1	Inductive Loop	6	4	0	null	40
6	2 N PINE MEADOW DR WB	Through Right	12	null	2	Inductive Loop	7	4	0	null	40
7	3 N CHARLES RICHARD BEALL BLVD SB	Left	12	205	1	Inductive Loop	8	5	0	null	40
8	3 N CHARLES RICHARD BEALL BLVD SB	Through	12	null	2	Inductive Loop	2	2	150	null	6
8	3 N CHARLES RICHARD BEALL BLVD SB	Through	12	null	2	Inductive Loop	4	2	330	null	6
9	3 N CHARLES RICHARD BEALL BLVD SB	Through	14	null	3	Inductive Loop	3	2	150	null	6
9	3 N CHARLES RICHARD BEALL BLVD SB	Through	14	null	3	Inductive Loop	5	2	330	null	6
10	3 N CHARLES RICHARD BEALL BLVD SB	Right	12	170	4						
11	4 DOGWOOD TRL EB	Left	12	85	1	Inductive Loop	13	8	0	null	40
12	4 DOGWOOD TRL EB	Through Right	12	null	2	Inductive Loop	14	8	0	null	40

Figure 2-1. An Example of Detector Configuration Data in the FDOT NOEMI Report

The accuracy of detector configuration is crucial, as it specifies the precise location of events recorded in log data. Inaccurate or outdated information leads to false or misleading intersection performance measurements. Although NOEMI reports provide configuration information for over 1800 intersections in Florida, this study focuses on a select number of intersections with verified data accuracy for further analysis.

2.2. ATSPM Controller Event Log data

ATSPM Controller Event Log data encompasses information gathered and stored by traffic signal controllers and detectors. This data is typically collected in real-time or near-real-time, offering continuous insights into intersection operations. The ATSPM database primarily archives data on events such as vehicle detections and changes in traffic signals up to 0.1 seconds.

Each event generated by the signal controller consists of four bytes: two for the event timestamp, one for the event code type, and one for the event parameter. The event code identifies the specific activity reported by the controller, such as phase initiation or termination, detection activation or deactivation, or errors. Consequently, the event code byte can report up to 256 distinct activities. **Table 2-1** provides detailed descriptions of each event parameter.

Table 2-1. Parameters of ATSPM Controller Event Log Data

Parameter	Description	Field Type
SignalID	This column identifies the specific traffic signal or intersection. It's typically a unique numerical or alphanumeric code assigned to each intersection in the network.	integer
TimeStamp	This column records the exact date and time when an event occurred. It usually includes both the date and time, often down to 0.1 seconds for precise temporal analysis.	DateTime
EventCode	This column contains a numerical code representing a specific type of event or action at the traffic signal. Different numbers correspond to different events, such as signal phase changes, vehicle detections, pedestrian button presses, and preemption events.	integer
EventParam	This column provides additional information, or parameters related to the event specified by detector channel numbers and phases.	integer

Table 2-2 provides a brief description of each event code. It is composed of traffic signal events, vehicle detection events, preemption, coordination, and maintenance events.

Table 2-2. Parameters of ATSPM Controller Event Log data

Event Type	**Event Code**	**Event Code Types**	**Descriptions**
Traffic signal	0–20	Active Phase Events	Any phase-related status changes, such as activation or termination.
	21–30	Active Pedestrian Phase Events	Pedestrian-related phase status changes.
	31–40	Barrier/Ring Events	Barrier and yellow permissive events.
	41–60	Phase Control Events	Phase hold, call, and omit status changes.
	61–80	Phase Overlap Events	Overlap status changes
Vehicle detection	81–100	Detector Events	Detector activity and error status changes.
Preemption	101–130	Preemption Events	Preemption status changes
Coordination	131-170	Coordination Events	Coordinated timing status changes, such as cycle length and split times.
Maintenance	171–199	Cabinet/System Events	Controller property-related status changes, including alarms, clock updates, and power failures.
User-defined functions	200-255	User-defined event	Future user-defined functions

The type of event happening at intersections typically includes the beginning or end of a signal phase and the activation or deactivation of a detector. An illustrated overview of the high-resolution event data is presented in Table 2-3.

Table 2-3 Example of High-Resolution Event Data from ATSPM

Signal ID	Time Stamp	Event Code	Event Parameter	Remarks
1067	2019-10-01 04:33.5	1	7	Phase 7 Green Begin
1067	2019-10-01 04:35.3	82	4	Detector 4 On
1067	2019-10-01 04:38.8	81	4	Detector 4 Off
1067	2019-10-01 04:39.6	8	7	Phase 7 Yellow Begin
1067	2019-10-01 04:43.1	82	8	Detector 8 On
1067	2019-10-01 04:43.2	81	8	Detector 8 Off
1067	2019-10-01 04:43.3	10	7	Phase 7 Red Clearance Begin
1067	2019-10-01 04:46.3	11	7	Phase 7 Red Clearance End
1067	2019-10-01 04:47.5	82	5	Detector 5 On
1067	2019-10-01 04:48.1	81	5	Detector 5 Off

In the United States, the ATSPM controllers typically adhere to the 'dual-ring, eight-phase' scheme for controlling traffic at intersections. This scheme ensures the non-overlapping, sequential progression of traffic phases over time, where the phases typically represent the left-turn and through movements of every roadway approach at an intersection. The diagram in **Figure 2-2(b)** (analogous to the intersection in **Figure 2-2(a)**) demonstrates a typical 'dual-ring, eight-phase' scheme, which includes rings and phase groups. The rings in the diagram denote the pathways for sequencing traffic phases, whereas phase groups separated by barriers represent a roadway approaching an intersection.

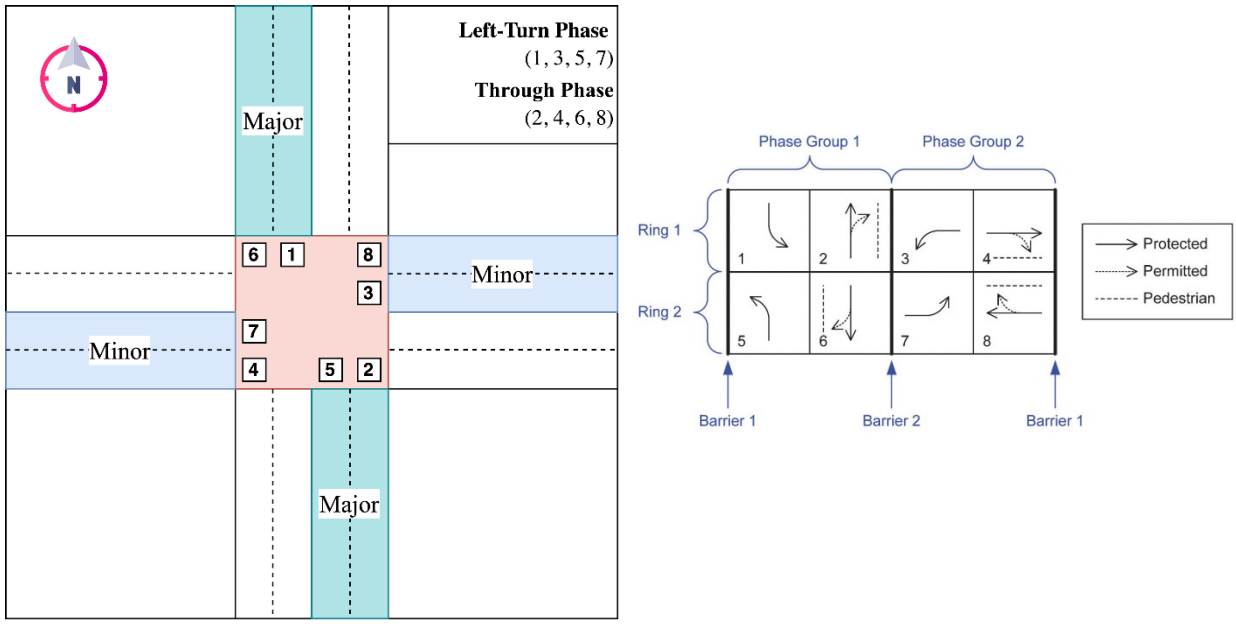

(a) Typical Intersection Depicting Traffic Phases

(b) Configuration of 'Dual-Ring, Eight-Phase' Operation

Figure 2-2 Typical 'Dual-Ring, Eight-Phase' Scheme (Major Roadway Along North-South)

Phase group 1 generally corresponds to the 'major' roadway, and phase group 2 to the 'minor' roadway. The 'dual-ring, eight-phase' scheme functions on a set of rules as follows:

h) At any given time, one phase from each of the two rings can operate.

i) All operational phases must be within the same phase group.

j) Each phase within a particular ring can operate concurrently with any phase from the alternate ring, provided they belong to the same phase group.

k) The operation of phases in phase group 1 (i.e., 'major' roadway) is completely incompatible with those in phase group 2 (i.e., 'minor' roadway).

l) The rings are permitted to cross the barrier when all the rings have arrived at this point.

The cycle length is the duration between successive crossings of barrier 2.

CHAPTER 3: RELATED WORK

This section reviews research reports from various projects from the Department of Transportation (DOT) and GitHub repositories related to existing ATSPM systems to minimize redundant efforts in this project. According to the Federal Highway Administration's (FHWA) ATSPM site[2], six relevant reports are available, sponsored by agencies such as the United States DOT, Indiana DOT, Utah DOT, and the American Association of State Highway and Transportation Officials (AASHTO). Utah and Oregon DOTs have also published GitHub repositories for processing ATSPM data. We examined the features of these repositories, including data characteristics, collection frequency, and their potential applicability to this project. We also identify any attributes that may require further development to achieve the project's objectives. Given the diverse objectives of each agency's analyses, this review is organized by an agency and mainly addresses the report's unique efforts for conciseness.

The review specifically focuses on the features of ATSPM data and use cases relevant to this study, which aims to evaluate the safety of intersections using ATSPM data and apply this information to recommend signalization strategies. Therefore, a discussion of how to install and maintain the ATSPM system is excluded from this review. We mainly analyze the types of data provided by ATSPM, whether this data has been used to recommend signalization strategies at intersections, and their deployment strategy.

---

[2] USDOT ATSPM summary

3.1. Atspm Project Reports and GitHub Repositories Published By DOT

3.1.1. ATSPM Reports By DOT

3.1.1.1. United States Department of Transportation (USDOT)

The United States Department of Transportation (USDOT) published two detailed reports on the ATSPM system in 2020 with Atkins and Leidos, respectively. These reports comprehensively analyze traffic signal performance measures using ATSPM, highlighting the use cases in early adopter agencies and quantitive cost and benefit analysis. A summary of the two published USDOT reports is discussed in the following subsections.

USDOT'2020 by Atkins

This report reported eight detailed use cases of ATSPM, addressing those cases' deployment strategies and the benefits they obtained. Those early adopters adopted various deployment strategies. Most agencies use the open-source ATSPM software developed by the Utah DOT. This approach involves maintaining high-resolution controller data storage and hosting a local installation of the software. The other approach is cooperating with traffic controller vendors. Some traffic controller vendors offer integrated ATSPM capabilities within their central traffic signal management software. In this model, a third-party provider hosts the ATSPM data, often in the cloud. This method typically involves installing supplemental data collection equipment and paying subscription fees. The USDOT reports provide several technical applications:

a) ATSPM systems collect high-resolution data from traffic signal controllers, including events like phase changes and detector actuation.
b) The data collected is processed using specialized software to generate performance measures such as approach delay, speeds, volumes, and arrivals on red.

c) The systems provide real-time monitoring capabilities, alerting engineers to issues such as detector malfunctions or signal failures.

d) Various data visualization tools are developed to help engineers and stakeholders understand traffic performance metrics easily.

The agencies reported in USDOT's 2020 report tried to provide real-time performance data and alerts, improving traffic flow, safety, and operational efficiency. The collaborative efforts across various state and local agencies demonstrate the system's scalability and effectiveness in different urban settings. USDOT's 2020 report states that the project has been successfully implemented in various regions across the United States, demonstrating its versatility and effectiveness. Notable case studies include:

a) Utah Department of Transportation (UDOT):

- UDOT's ATSPM system, developed in collaboration with Purdue University and FHWA, includes a suite of data visualization reports to evaluate traffic progression and identify unused green time.
- UDOT has significantly reduced public complaints and improved operational efficiency using ATSPM at 99 percent of its 1,271 traffic signals.

b) Georgia Department of Transportation (GDOT):

- GDOT's deployment uses the open-source ATSPM software from UDOT. The system aids in managing signal operations, particularly during events like the I-85 bridge collapse, by developing alternate routing plans and adjusting signal timing.
- GDOT has connected 6,775 signals to the ATSPM system, improving overall traffic signal management.

c) Pennsylvania Department of Transportation (PennDOT):

- PennDOT's ATSPM goals focus on reducing delays, emissions, and crashes while promoting economic benefits. They have implemented a unified command and control platform integrating various ATSPM inputs to manage 2,184 signals statewide.

d) Seminole County, Florida:

- Seminole County's ATSPM program, developed with FDOT and UDOT, supports a wide range of performance metrics. The county has upgraded 387 signals to record high-resolution data.

The key benefit of ATSPM, as demonstrated in the report, is that the system offers several benefits over traditional signal retiming methods. Traditionally, signal retiming is done every 3-5 years at a cost of roughly $4,500 per intersection, often relying on public complaints and periodic data collection. ATSPM, however, allows for continuous performance monitoring, leading to proactive identification and correction of deficiencies. This shift to proactive management improves safety, enables targeted maintenance, and enhances overall traffic operations. The FHWA's Every Day Counts (EDC-4) initiative promoted ATSPM, resulting in a significant increase in its adoption. By the end of EDC-4, 57% of states were demonstrating, evaluating, or institutionalizing ATSPM, a substantial increase from the initial 11 states.

USDOT'2020 by Leidos

This report mainly tried to evaluate the economic costs and benefits of early adopter agencies. They report a flexible cost-benefit estimation methodology that covers both short-term and long-term benefits over the lifecycle of ATSPM implementations. **Figure 3-1** shows that the methodology includes 16 cost items and 12 benefit items, each with specific formulas that agencies can adapt to their context.

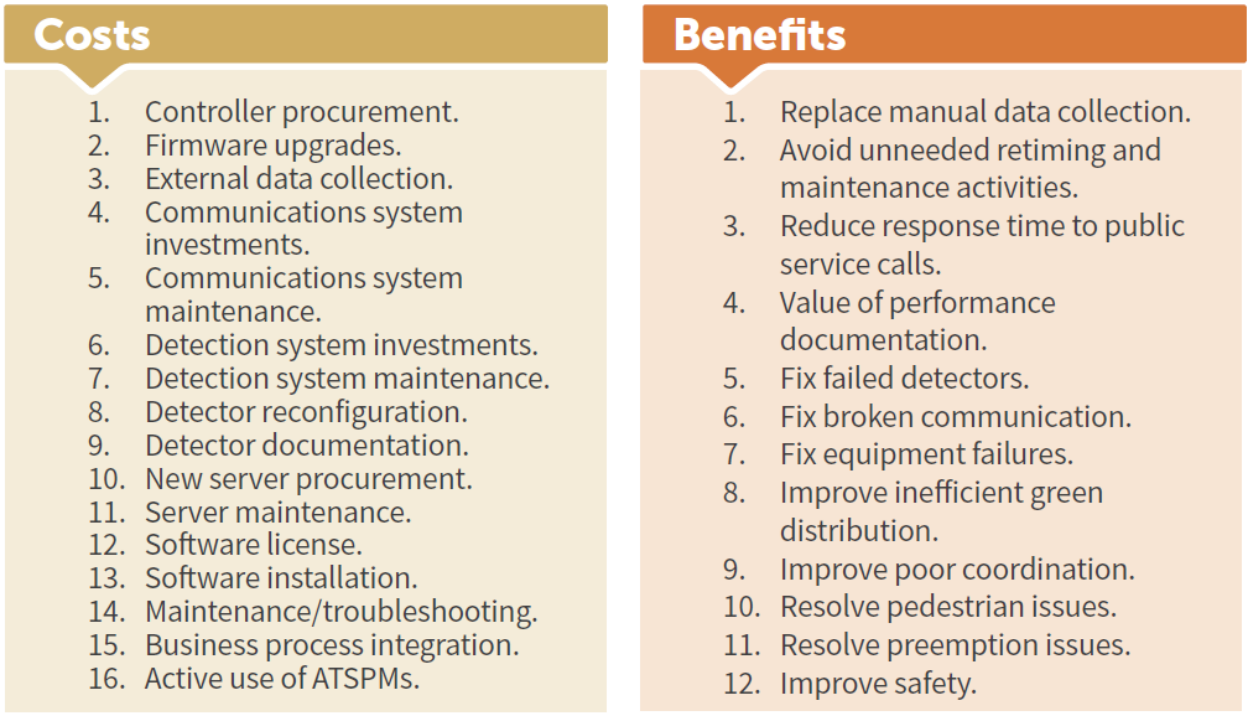

Figure 3-1. Primary Items in the Benefit-Cost Methodology (Leidos, 2020)

This approach allows for a customized analysis based on the available data and specific conditions of different agencies. **Table 3-1** shows the reported cost and benefit analysis, including detailed case studies from six early adopter agencies.

Table 3-1. Cost and Benefit Analysis from Case Studies

Agency	Main implementation	Benefit	No. of intersections	Costs (E.)	Benefit (E.)
Utah DOT	Developed an open-source software package for ATSPMs.	Improved traffic signal monitoring and maintenance, substantial cost savings.	2,111	$11.5M	$108.0M
Georgia DOT	Collaborated with UDOT to enhance the software.	Streamlined signal performance monitoring and reduced response times.	6,804	$0.9M	$9.5M
Pennsylvania DOT	Focused on integrating ATSPMs into local agency operations.	Enhanced detection and response to signal failures.	100 (hypothetical case)	$0.4M	$1.7M
Lake County DOT	Emphasized improving signal timing and reducing maintenance costs.	Significant reduction in vehicle delays	180	$0.3M	$4.1M
Maricopa County DOT	Focused on data-driven improvements to traffic management.	Reduction in travel time and operational costs.	170	$0.5M	$1.5M
Clark County, WA	Faced initial challenges but gained substantial insights into system improvements.		125	This has yet to be fully quantified due to ongoing implementation.	

The USDOT's 2021 report also highlights key lessons from interviews with six early adopter agencies. One of the main findings is that robust executive support is essential for the

effective implementation of ATSPM. Investments in signal maintenance prior to implementing ATSPM can significantly facilitate its integration. Additionally, it is crucial for agencies to adapt the methodology to their unique requirements and contexts. A common issue is that most agencies lack the capacity to analyze data sets to pinpoint problems thoroughly. Innovations like the Measurement, Accuracy, and Reliability Kit (MARK 1), developed by the Georgia Department of Transportation (GDOT), are making strides in this area by summarizing data from various locations.

The development and implementation of ATSPM technology is a collaborative effort involving multiple stakeholders, such as FHW, state DOTs, and academic institutions. This collaboration has fostered the development of innovative data analysis techniques and performance metrics. Furthermore, agencies like the UDOT and the GDOT enhance public transparency by providing access to ATSPM data and analyses through public-facing websites, promoting community engagement and transparency. In essence, ATSPM systems represent a significant leap forward in managing traffic signals, aligning with the dynamic demands of modern transportation networks and yielding safer, more efficient, and cost-effective traffic operations. In summary, ATSPMs have proven to be valuable tools for improving traffic signal management. Their deployment strategies, diverse use cases, and significant benefits highlight their potential to transform how agencies manage and operate traffic signals, ultimately leading to more efficient and safer roadways.

3.1.1.2. Indiana Department of Transportation (INDOT)

The Indiana Department of Transportation (INDOT) has published detailed reports on ATSPM data in 2014 and 2015. These reports provide a comprehensive analysis of traffic signal performance measures based on high-resolution controller event data, highlighting the significance and implementation of these measures for improving traffic signal systems. A brief summary of the published INDOT reports is discussed in the following subsections.

INDOT'2014

In 2014, INDOT published a report emphasizing the critical need for effective traffic signal operations within traffic management, often underestimated in budget and staffing allocations. It highlighted the lack of adequate performance reporting, obscuring the quality of the actual operation. The report aimed to provide a comprehensive suite of control-agnostic, discrete event-based performance measures, including Automated Traffic Signal Performance Measures (ATSPM), applicable universally for analyzing traffic signal systems.

This report discusses various aspects of signal timing that are critical for effective traffic management. It outlines different types of signal operations, such as fixed-time, semi-actuated, fully actuated, and adaptive control, each requiring specific detector data and operational strategies. The report details control elements like interval and phase timing, the role of vehicle detection in linking to signal output and the importance of signal cycles. Actuation methods are highlighted, emphasizing dynamic adjustments based on real-time traffic conditions. Signal coordination strategies aim to synchronize green times across intersections, while preemption and priority functions ensure timely responses for emergency vehicles and transit.

The report presents a comprehensive analysis of various performance measures to assess and optimize traffic signal systems. The capacity performance measures evaluate intersection

utilization through metrics such as traffic volumes, cycle lengths, green time allocation, flow rate, headway, saturation flow rate, vehicle measures of effectiveness, green and red occupancy ratios, and the degree of intersection saturation.

The progression performance measures focus on the efficiency of coordinated signal systems by examining vehicle delays, arrival patterns, percent on green, platoon ratio, arrival type, delay estimates, and the Purdue Coordination Diagram (PCD). The multimodal performance measures assess the accommodation of pedestrians, transit vehicles, and emergency vehicles using metrics like pedestrian delay, level of service (LOS), preemption response time and duration, and transit priority adjustments in green and red phases. Maintenance performance measures ensure system reliability by evaluating communication quality through ping success rates and data transmission failures, data completeness via automated audits and redundancy checks, and detector status by logging error frequency and duration. Every performance measure utilizes specific parameters to provide actionable insights for traffic management improvements. The parameters for every measure are illustrated in **Table 3-2**.

These performance measures, detailed in the report, offer a structured approach to evaluating and enhancing traffic signal systems, ultimately leading to improved traffic flow and management efficiency.

Table 3-2. Summary of Performance Measures and Parameters

Performance Measures	Parameters
Capacity Performance	Traffic Volumes, Cycle Lengths, Green Time Allocation, Flow Rate, Headway, Saturation Flow Rate, Vehicle Measures of Effectiveness, Green and Red Occupancy Ratios, Degree of Intersection Saturation
Progression Performance	Vehicle Delays, Arrival Patterns, Percent on Green, Platoon Ratio, Arrival Type, Delay Estimates, Purdue Coordination Diagram (PCD), Flow Profiles, Shockwave Analysis, Maximum Queue Lengths
Multimodal Performance	Pedestrian Delay, Level of Service (LOS), Preemption Response Time, Preemption Duration, Transit Priority Adjustments in Green and Red Phases, Signal Changes, Vehicle Arrivals, Detection Technologies (GPS, Infrared, Radio-Based Systems)
Maintenance Performance	Communication Quality (Ping Success Rates, Data Transmission Failures), Data Completeness (Automated Audits, Redundancy Checks), Detector Status (Error Frequency, Error Duration)

This INDOT report provides a comprehensive suite of performance measures for current traffic signal systems and paves the way for future advancements in traffic management. With the integration of more sophisticated data collection techniques, such as real-time crowdsourced data and advanced sensor technologies, future traffic signal systems can achieve even greater precision and efficiency. The continuous improvement of data processing algorithms and adopting machine learning models could further enhance the predictive capabilities of traffic management systems. Additionally, expanding the scope of multimodal performance measures to include emerging transportation modes, such as autonomous vehicles and micro-mobility solutions, will be crucial. Future efforts should also focus on the integration of these advanced systems—such as connected vehicle technology, adaptive signal control, and Internet of Things (IoT) devices—into existing infrastructure, ensuring scalability and adaptability.

INDOT'2015

The INDOT report published in 2015 also emphasizes the need to integrate ATSPM into agency operations to enhance efficiency and effectiveness. Traditional traffic signal systems rely on fixed schedules and limited data inputs, leading to suboptimal performance. High-resolution data logging enables detailed analyses of traffic signal performance, identifying inefficiencies and allowing for targeted improvements. This data-driven approach optimizes signal timing plans, improving traffic flow and reducing congestion. The key findings in the report are:

a) Technical Requirements for Implementation:

- High-resolution controller data logging requires understanding the necessary infrastructure, software, and processes to handle increased data volume.
- Identifying suitable detection configurations (e.g., loop detectors, video detectors) and ensuring adequate data storage capacities are crucial.
- Managing latency to ensure seamless data collection, transmission, storage, and visualization is essential for real-time performance analysis.

b) Detection of Vehicles:

- Accurate vehicle detection at intersections is critical for optimizing traffic signal performance.
- Various types of detectors, such as loop detectors and video detectors, provide essential data to signal controllers.
- Detector failures can disrupt traffic flow, but high-resolution event data can identify such failures for timely maintenance and repairs.

c) Evaluation of Local Signal Control:

- High-resolution data and visualizations assess the quality of traffic signal operations at individual intersections, examining metrics such as vehicle delay, queue length, and number of stops.
- The evaluation process examines green time distribution and trends in initiation and termination.
- Performance measures, such as phase failures and split failures, are aggregated to identify spatial and temporal “hot spots” of poor performance.
- Detector failures can also be identified by monitoring inconsistencies in expected traffic patterns, anomalies in signal phase activation, continuous monitoring and alert systems, comparison with adjacent detectors, and correlation with external data sources.

d) System Control Evaluation:

- High-resolution and travel time data manage traffic signal progression along arterial corridors, ensuring coordinated scheduling of green times at neighboring intersections.
- Evaluation involves assessing progression quality and optimizing signal offsets using data-driven techniques like time-space diagrams and vehicle trajectory data.

This INDOT report concludes that integrating high-resolution traffic signal performance measures through ATSPM into agency operations significantly enhances efficiency and effectiveness. Traditional systems relying on fixed schedules and limited data inputs result in suboptimal performance, whereas high-resolution data logging allows for detailed analysis and targeted improvements, leading to optimized signal timing plans, improved traffic flow, and reduced congestion. By addressing technical requirements such as detection, communication, and data processing, and by using data-driven approaches for system control evaluation, agencies can achieve significant improvements in traffic signal management and overall traffic operations.

3.1.1.3. Utah Department of Transportation (UDOT)

The Utah Department of Transportation (UDOT) performed a comprehensive study to explore the potential of Automated Traffic Signal Performance Measures (ATSPM) data in estimating Annual Average Daily Traffic (AADT). Traditionally, UDOT has relied on short-duration traffic counts to fulfill Federal Highway Administration (FHWA) requirements. These counts, conducted at approximately 6000 locations over three years, are labor-intensive, costly, and pose safety risks. The study aimed to determine whether ATSPM data from radar detectors at signalized intersections could be used to estimate AADT, thereby reducing the need for some short duration counts and balancing Continuous Counter Station (CCS) data in estimating seasonal adjustment factors.

Two types of ATSPM detectors were analyzed in this study: Wavetronix SmartSensor Advance detectors and Wavetronix SmartSensor Matrix detectors. Advance detectors are installed 300-400 feet upstream of signalized intersections and provide total through traffic counts. In contrast, Matrix detectors are installed at stop-bar locations and offer lane-by-lane turning movement counts. The study's initial phase involved selecting test locations by mapping CCS and ATSPM detector sites. The selected sites had to be on the same road segment without intermediate access points, providing count data for the same route, direction, and period.

The CCS dataset comprised hourly directional counts from 113 sites for the entire year 2017, totaling 1,846,104 counts. The ATSPM dataset consisted of 15-minute interval counts from 47 signals over the same period, amounting to 15,999,450 counts. The data from CCS and ATSPM pairs were mapped and unified in terms of direction labeling and time intervals for accurate analysis. This mapping process ensured that the datasets could be directly compared and analyzed effectively.

One of the crucial steps in the study was identifying and removing anomalous data, which could be caused by device malfunctions or other issues. Three anomaly detection methods were tested: the Inter Quantile Range (IQR) method, K-Means Clustering, and the Time of Day (TOD) and IQR-based method. The IQR method assumed that any hourly count beyond 1.5 times the IQR from the 75th percentile was an anomaly. The K-Means Clustering method partitioned data into clusters, identifying anomalies based on their distance from cluster averages. The TOD & IQR-based method used historical data to set thresholds for anomalies, particularly for early morning hours. The analysis revealed the following:

- UDOT's use of ATSPM data can reduce the need for labor-intensive, costly short-duration traffic counts. By leveraging ATSPM data, UDOT can minimize the frequency of traditional traffic counts, thereby reducing costs and labor.
- Matrix detectors provide reliable hourly traffic counts and accurate AADT estimates, complementing CCS data. Even without adjustment factors, Matrix detectors provided reliable estimates with average R-squared values of 0.93.
- Anomaly detection, particularly the TOD & IQR method, is crucial for data accuracy. The TOD & IQR method demonstrated superior performance in identifying and removing anomalous data, ensuring the reliability of traffic count data from ATSPM detectors.
- The number of lanes and detector configurations impact the accuracy of traffic counts from ATSPM data. Advance detectors were most accurate on two-lane roadways, while Matrix detectors improved as the number of detector channels increased. Single Matrix detectors were generally more accurate compared to multiple Matrix detectors at intersections.
- This research supports the broader application of ATSPM data for efficient traffic management and planning. Matrix detectors estimated AADT with 88% accuracy compared to CCS sites and accurately estimated monthly seasonal factors with 97.5%

accuracy and day-of-week in month factors with 96.8% accuracy. These capabilities are valuable for making precise adjustments based on seasonal traffic patterns.

3.1.1.4. American Association of State Highway and Transportation Officials (AASHTO)

The main objective of AASHTO's 2020 report is to provide guidance for agencies in implementing a performance measurement approach for traffic signal management. The report aims to help agencies evaluate whether this performance-based approach would be cost-effective for their system and to develop a plan for its implementation. While it also includes a data dictionary and communication materials, these were summarized in the above reports and thus excluded from this review. The report suggests detailed steps to integrate signal performance measures into the management of a traffic signal system, as follows:

- **Select Performance Measures:** Determine which signal performance measures align best with the agency's goals and methods. Identifying key measures is essential to avoid data overload and ensure effective decision-making.
- **Determine Implementation Scale:** Decide whether to implement performance measures across the entire system at once or incrementally. Most agencies opt for an incremental approach, using pilot projects or integrating upgrades with existing maintenance programs.
- **Conduct System Needs Gap Assessment:** Assess gaps in equipment, business processes, organizational structure, or resources required for implementation after selecting performance measures and intersections.
- **Procure Resources:** Identify and acquire the additional resources needed for deployment and long-term maintenance based on the gap assessment results.
- **Configure System:** Set up the equipment and software necessary for data collection, storage, and processing at both the intersection and system levels. Program each intersection with the relevant information.

- **Verify System:** Ensure data consistency and accuracy through a verification process post-installation. Utilize external data from sensor networks or field studies to confirm the precision and correct calculation of performance measures.
- **Apply Performance Measures:** Use performance measures to adjust signal timings, correct mis-programmed parameters, and identify malfunctioning equipment.
- **Integrate into Agency Practice:** Incorporate performance measures into daily operations for continuous monitoring. This practice helps in evaluating the effectiveness of maintenance and operations, guiding resource allocation and funding decisions.

This study provides the various steps involved in both traditional and ATSPM signal retiming. **Figure 3-2** shows that, unlike traditional retiming, performance-based management with ATSPMs allows staff to continuously and proactively monitor the traffic signal system rather than making occasional, reactive changes.

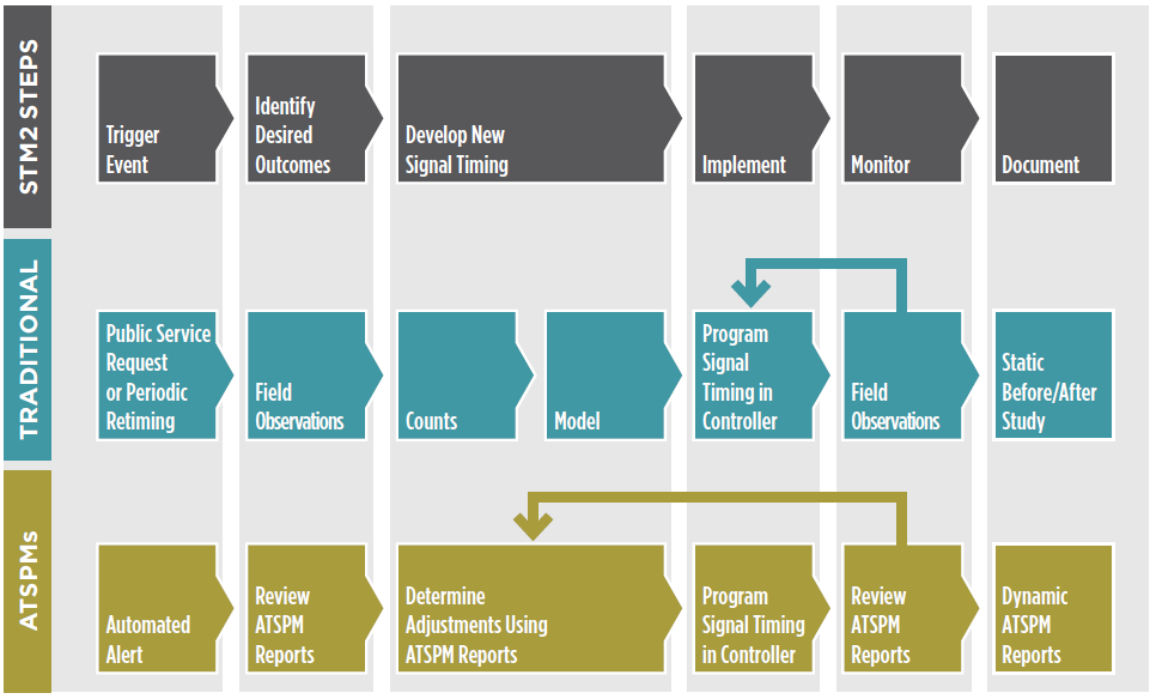

Figure 3-2. Traditional versus Performance-Based Signal Timing Process (AASHTO, 2020)

3.1.2. ATSPM GitHub By DOT

The Utah Department of Transportation (UDOT) developed the ATSPM GitHub repository in 2017 to offer a suite of visual aids that utilize high-resolution data from signal controllers[3]. This open-source software enables real-time analysis and visualization of traffic signal performance, optimizing signal timing and coordination. In addition, the Oregon Department of Transportation (ODOT) published the "ATSPM_Aggregation" GitHub repository In 2023. The repository is a potential Python package designed to aggregate traffic signal performance measures (ATSPMs) in 30-minute and 1-hour intervals from high-resolution controller data[4]. This repository assists traffic engineers and researchers in evaluating traffic signal performance through various metrics. The primary goal is to convert raw data from Automated Traffic Signal Controllers (ATCs) into meaningful performance metrics that can optimize traffic signal timing, improve traffic flow, and enhance overall intersection safety. The repository provides essential tools for processing high-resolution traffic signal data and extracting valuable insights.

---

[3] UDOT ATSPM GitHub repository

[4] Oregon DOT ATSPM GitHub repository

3.1.2.1. Data Characteristics, Aggregation Interval, and Their Applicability

The traits of ATSPM systems include high-resolution data logging, automated data analysis, real-time monitoring, and advanced data visualization tools. These systems capture parameters such as vehicle volumes, delays, green time allocation, arrival on red, split failures, signal coordination metrics, and so on. **Table 3-3** describes the definition of performance measures that can be derived from the ATSPM system. As per the reviewed reports and repositories, these parameters are aggregated at 30-minute and 1-hour intervals. However, aggregating data at more granular, cycle-level intervals could be more critical for detailed traffic signal performance evaluation. Aggregation at the cycle level provides precise insights into each signal cycle's efficiency, allowing for real-time adjustments and optimization of signal timings at intersections. This level of detail is crucial for making real-time adjustments and optimizing signal timings at intersections, addressing specific issues affecting traffic flow and safety, and enhancing overall traffic efficiency and safety.

Table 3-3. Definition of Performance Measures

Measure	**Description**
Green/Yellow/ Red Duration	Measure the amount of green, yellow, and red time served for a particular phase or overlap without requiring detection setup or mapping information.
Phase Termination Type	Indicates how a phase or overlap ends (gapped out, maxed out, or forced off), driven by arrivals in an actuated control system. Acts as a surrogate for capacity utilization without needing detector mapping.
Volume per Time Period	The count of vehicles is interpreted from the number of activations from a setback short-length detector or a dedicated count channel.
Vehicles-per-Hour (vph)	The rate of vehicle arrivals for a one-hour period is typically converted from volume per time period.

Volume/Capacity Ratio (v/c)	The number of vehicle arrivals during a period is divided by the theoretical capacity approximated from the green time served (less any startup loss).
Maximum Vehicle Delay	The greatest number of seconds between a detector activation at the stop bar during red to either the beginning of green or detector deactivation time for RTOR vehicles.
Green/Red Occupancy Ratio	Measure capacity utilization using amounts of detector occupancy during green and red portions of a phase, respectively.
Split Failure	Indication of overcapacity for a lane, phase, or movement triggered by exceeding certain occupancy ratios during green and red phases.
Queue Estimation	Measure the queue length using vehicle arrivals and estimated discharge rates (input-output method) or detector gap durations and counts (shockwave estimation method).
Oversaturation Severity Index	The ratio of unusable green time to total available green time in a cycle.
Time to Service	Measure of the time from the first detection to the beginning of green.
Percent on Green	The percentage of total vehicles arriving during a given cycle is in green.
Purdue Coordination Diagram	Visualization of the quality of a movement's progression over time.
Platoon Ratio	The percentage of vehicles arriving on green is adjusted by the green time proportion per cycle (g/C).
Cyclic Flow Profile	Combines the distribution of vehicle arrivals and the probability of green, aggregated over a set of fixed-length cycles.
Time–Space Diagram	Visualization of estimated vehicle trajectories traversing a distance over time, including locations and phase status of signalized intersections.
Red Light Running	Measures vehicles entering and exiting a stop bar detection zone after the beginning of red.

3.1.2.2. Data Quality Check

Ensuring data quality is fundamental in ATSPM systems. However, previous package does not provide this functionality. Data quality check process involves thorough checks on the data collected for the project, specifically focusing on detector on-off sequences, signal sequences, and anomaly detection. Monitoring the on-off sequences of detectors ensures that data collection is consistent and accurate, highlighting any potential malfunctions or inconsistencies in data recording. Analyzing signal sequences helps identify discrepancies between expected and actual signal performance, ensuring that the traffic signals operate as intended. Additionally, techniques like the Inter Quantile Range (IQR) method and the Time of Day (TOD) and IQR-based method are effective for identifying and removing anomalous data, such as outliers or unexpected variations. These data quality checks are essential for maintaining the reliability of collected data, supporting accurate traffic signal performance analysis, and ultimately aiding the optimization of signalization strategies to enhance intersection safety.

3.1.2.3. Scope to Integrate Emerging Technologies

Emerging technologies like digital twins, sensor fusion, and trajectory data offer significant opportunities to enhance ATSPM systems. Digital twins provide virtual representations of traffic systems, enabling real-time monitoring, simulation, and optimization of traffic signals. This technology can predict traffic patterns and assess the impact of different signalization strategies before implementation. Sensor fusion combines data from sources such as LiDAR, radar, and traditional traffic detectors to create a comprehensive and accurate picture of traffic conditions. Trajectory data offers detailed insights into traffic flow and behavior, which is crucial for precise

traffic signal optimization and identifying safety issues. Using these technologies can provide advanced performance measures and improve overall traffic management.

The findings from the review can significantly benefit the project by offering an effective framework for evaluating intersection safety and recommending effective signalization strategies. The detailed performance measures and high-resolution data logging provide the necessary granularity for analyzing traffic signal performance at a cycle level, enabling precise adjustments to improve traffic flow and safety. Implementing regular data quality checks ensures the reliability and accuracy of the collected data, which is essential for informed decision-making.

Though not within the current scope of the project, integrating emerging technologies like digital twins, sensor fusion, and trajectory data can further enhance ATSPM's analytics capability. Digital twins can simulate various traffic scenarios, helping to predict and mitigate potential issues before they occur. Sensor fusion offers a more comprehensive view of traffic conditions, combining data from multiple sources for better accuracy. Trajectory data provides detailed insights into traffic patterns and behaviors, enabling more targeted interventions.

Overall, the insights gained from the review can lead to a more effective and efficient approach to managing traffic signals, ultimately reducing fatalities and improving overall traffic flow and safety.

3.1.3. Summary

The DOT project report and GitHub repositories offer numerous benefits for traffic signal management and operation. ATSPMs facilitate a proactive approach to traffic signal maintenance by continuously monitoring trends over time. This allows staff to identify issues before the public reports them. Automated alerts can highlight intersections with malfunctioning equipment or high-traffic congestions, enabling technicians to pinpoint failures, understand when issues began, and determine when they were resolved.

ATSPMs continuously collect and analyze real-time data, reducing the need for extensive field observations. This also supports strategies like transit signal priority and further optimizing traffic flow by signal retiming. Shareable reports that summarize the impacts of maintenance and operational activities facilitate transparent communication with stakeholders and policymakers. The data collected through ATSPMs can prioritize short-term maintenance needs and inform long-term infrastructure improvements. These systems also allow agencies to implement adaptive signal control and other advanced systems under various conditions. This is essential for managing traffic during special events, emergencies, or unexpected incidents.

While studies have demonstrated the cost-effective benefits of ATSPMs, most research has focused on intersection efficiency. Consequently, there are few safety features, and the existing GitHub repositories lack the cycle-level aggregation and safety features needed for comprehensive safety evaluations. Further research is required to address these gaps.

3.2. Literature Review on Mobility and Safety Applications of ATSPM

This section provides a systematic review of recent academic literature concerning ATSPM. A comprehensive search through Elsevier's Scopus database yielded 64 relevant journal articles and conference papers from 2018. The majority of these, 27 in total, were published in the Transportation Research Record. As illustrated in **Figure 3-3**, these papers were categorized based on their application areas, with each category's paper count noted in parentheses. Papers were assigned to the most applicable category in cases where multiple applications were covered.

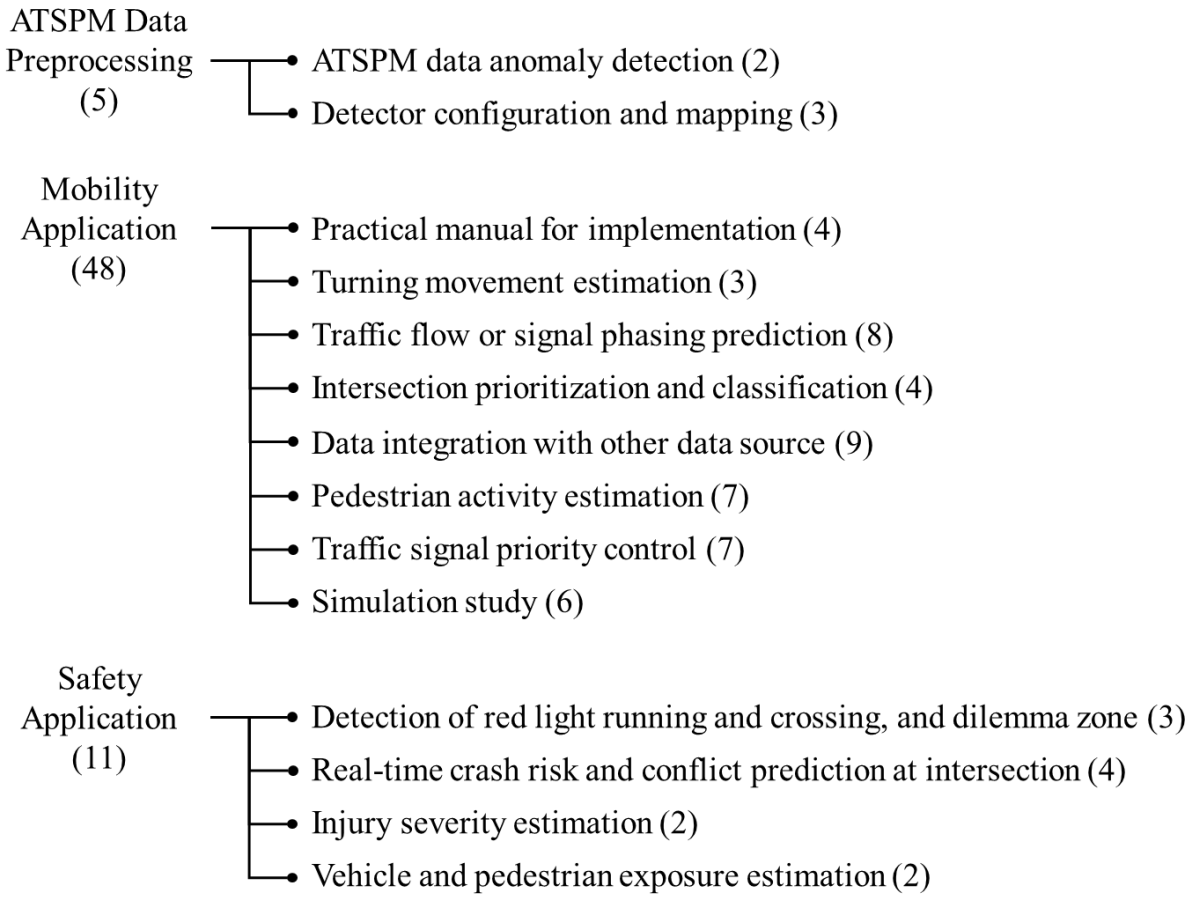

Figure 3-3. Distribution of Research Papers by Application within ATSPM Studies

Our review criteria included only studies that utilized ATSPM data for analytical purposes; those that merely referenced the data were omitted. Notably, these studies employed ATSPM data sourced from within the United States, underscoring their direct relevance to this research. **Figure 3-4** displays a trend analysis of these studies, highlighting a significant surge in publications in 2020, followed by a consistent upward trend.

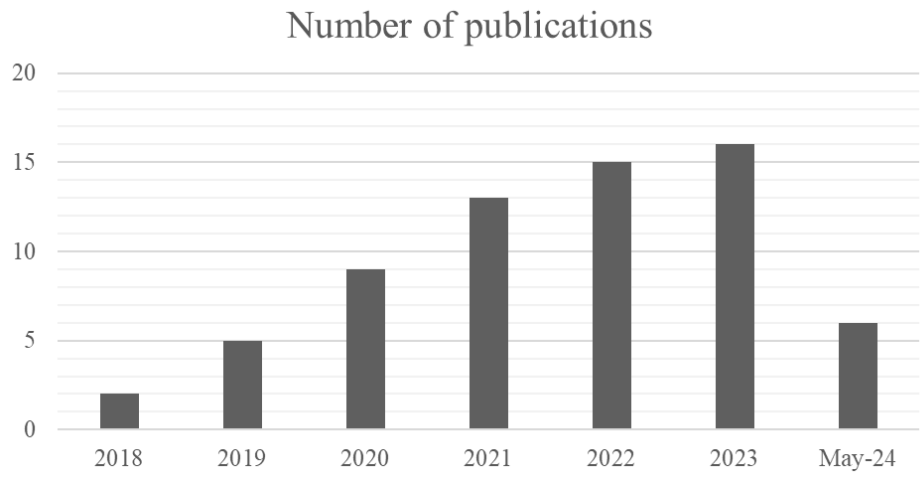

Figure 3-4. Annual Trends in the Utilization of ATSPM Data in Academic Studies.

This review assesses how ATSPM has been employed across the studies, examining the objectives and methodologies. We tried to keep the review concise by only revealing their results if they were clearly noteworthy or worth mentioning. Where applicable, results are quantified to evaluate the potential impacts of ATSPM usage. The review also identifies gaps in the current research area, discussing areas that have not yet been thoroughly explored but are required.

3.2.1. ATSPM Data Preprocessing

Preprocessing of ATSPM data is essential for managing ATSPM data from different agencies into one unified system. In previous studies, identifying and handling unrealistic data in ATSPM data and mapping detectors where event data is recorded are the most important issues for preprocessing ATSPM data. The problem of mapping detectors means identifying the detector configuration, i.e., where and what kind of detectors are installed, due to the heterogeneity of the recording system of ATSPM data managed by different agencies (Zarindast et al., 2024).

3.2.1.1. ATSPM Data Anomaly Detection

In this section, we review papers that focus on improving the quality and usability of ATSPM data by detecting anomalies and implementing quality control measures. These papers took a stepwise approach, observing the anomalies in ATSPM data, predefining their type, and filtering them out (Huang et al., 2018; Wang et al., 2023). For example, Wang et al. (2023) identified various types of anomalies: data switching, data shifting, data missing, and irregular curves. The authors employed a moving average and standard deviation approach to detect these anomalies, calculating z-scores for traffic volume data points. In their study, anomalies were flagged when z-scores exceeded a threshold of 2.0 (Wang et al., 2023).

Huang et al. (2018) addressed the data anomaly issue by combining machine learning with visualization. They used cumulative demand plots to analyze traffic patterns over time, enabling the identification of days with missing or anomalous data. For example, periods where cumulative volume remained unchanged indicated potential data logging issues. Mean-shift clustering was employed to distinguish typical traffic days from atypical ones by comparing daily demand curves. This algorithm clustered days with similar demand patterns and identified outliers, facilitating the detection of anomalous days. The study found other specific detector sensor errors, such as stuck

and false call errors. Stuck call errors occurred when a detector showed occupancy for an excessively long period. False call errors were detected when a sensor recorded unusually high vehicle counts. Also, logging gap distributions were used to examine time intervals between logged events, flagging potential logging failures when there were long gaps. Lastly, phase status logging checked for missing pairs of phase status events.

Those studies emphasized the critical role of high-quality data in traffic signal performance measures and proposed methods to ensure the integrity and usability of this data. However, these studies are based on predefined types of anomalies, so those algorithms cannot detect undefined anomalies. To overcome this limitation, it is necessary to consider a methodology to find anomalies based on data without a predefined definition of normal data in future studies.

3.2.1.2. Detector Configuration Mapping

The accuracy of ATSPM, particularly on detector event data, relies heavily on the accurate detector configuration information. However, unreliable detector configuration information and the inaccuracy of detector-to-phase mappings at ATSPM data are a significant challenge. This issue often arises due to inconsistent management systems, including outdated infrastructure, unrecorded changes, or the addition of new lanes (Mahajan et al., 2020; Zarindast et al., 2024). Zarindast et al. (2024) identify significant variations in how different agencies maintain records of detector configurations. Some agencies may have centralized databases, while others might rely on handwritten documentation or lack electronic records altogether. This inconsistency complicates the process of obtaining accurate and current detector configuration. Therefore, the primary objective of the studies in this section is to accurately map traffic detectors to their respective signal phases in ATSPM data. These studies collectively underscore the importance of precise detector configuration and data quality for the effective use of ATSPM.

Zarindast et al. (2024) address the challenge by developing a data-driven approach that utilizes machine learning algorithms. The study aims to automate the detection and correcting of anomalies in detector configurations. The core of the methodology in this paper is the Occupancy Pattern Association (OPA) algorithm, identifying detector types by examining occupancy patterns and calculating skewness, with presence detectors showing negative skewness and count detectors exhibiting positive skewness. Phase assignment is determined by analyzing the relationship between detector occupancy and the beginning of green. A drop point marks the transition from high to low occupancy after the green phase starts. The phase most frequently associated with these drop points is then identified as the corresponding phase for each detector.

Mahajan et al. (2020) aim to develop a method for mapping detectors to their respective phases and distinguishing between stop bar and advance detectors. The methodology begins with the decomposition of high-resolution data streams into individual signal cycles by identifying repeated signal timing patterns. Once these cycles are identified, they are clustered based on similar phase timing patterns, which discriminate between green and red phases. Initial detector assignments are made by counting vehicle departures during green and red phases under moderate traffic conditions, mapping detectors to phases based on the phase that results in more vehicle departures during green. The distinction between stop bar and advance detectors is distinguished by analyzing low traffic volume cycles, such as those occurring at nighttime. By examining the order of detector activations as a single vehicle progresses through the intersection, the study determines the relative positions of the detectors. Frequent sets of detector activations during low-volume periods further aid in distinguishing detectors close to the stop bar from those located further away.

The current ATSPM systems have detectors of varying lengths at stop bars or as advanced detectors. Emtenan and Day (2020) investigated the impact of various detector configurations and lengths on the accuracy of performance measurements and signal operations. After the simulation-based analysis, the authors noted that longer detection zones tend to overestimate split failures, while shorter zones may underestimate them. They also recommended that detection zones be configured to lengths of approximately 30 to 50 feet, with calibrated GOR thresholds to match the detection zone length for accurate split failure estimation. In general, setback detectors should ideally be placed about 5 seconds of travel time from the stop bar to balance accuracy and practicality in signal operations. Lastly, lane-by-lane detection provides more accurate split failure estimates compared to approach-based detection (Emtenan and Day, 2020). These findings highlight the importance of proper detector configuration in traffic signal systems to ensure accurate performance measurement and effective signal operations.

Those data-driven methods and conclusions offer a practical and scalable solution for diagnosing and correcting detector configuration errors. These papers have in common that they use an empirical approach to determine the configuration of the detector based on physically natural phenomena rather than a random fluctuation of event data. In conclusion, those papers highlight the importance of an organized and standardized way of managing ATSPM data for operations.

3.2.2. Mobility Applications

Mobility application refers to the application of ATSPM in mobility-related fields such as vehicle volume and delay. It is usually used to evaluate various strategies for intersections using the metrics provided by ATSPM or to create new metrics using raw data from ATSPM and validate the metrics.

3.2.2.1. Practical Manual for Implementation

The primary objective of ATSPM is to evaluate the performance of intersections to enhance traffic signal operations and management. Reviewed studies in this section provide detailed manuals on installation (Zhang et al., 2019), traffic signal control strategies (Dobrota et al., 2024; Mitrovic et al., 2023), and new metrics (Dobrota et al., 2023), aiding in the installation and utilization of ATSPM data. These decision-making tools and metrics enable engineers to follow the best practices and reduce unnecessary trial and error and redundant efforts.

Zhang et al. (2019) introduce available performance measures and the system architecture of ATSPM, emphasizing the differences between traditional signal systems and the capabilities of ATSPM. Their study covers technical considerations for installing ATSPM, such as data review and decoding, firmware testing, detector channel mapping, and cybersecurity protocols.

Dobrota et al. (2024) developed a decision-making tool to recommend appropriate traffic signal control strategies by incorporating factors such as corridor characteristics, operational objectives, agency capabilities, and constraints. Their toolbox is designed to offer comprehensive solutions using data that is easily accessible to most agencies, such as annual average daily traffic and vehicle probe data. Similarly, Mitrovic et al. (2023) developed a data-driven decision support tool to identify optimal intersections for deploying adaptive traffic signal control systems, using

ATSPM data to quantify operational attributes. The tool identifies suitable intersections for adaptive traffic signal control deployment, reducing the time and resources required for decision-making. The authors claim its robustness and flexibility apply to various networks.

Dobrota et al. (2023) introduced three new metrics to overcome the shortcomings of traditional performance measures. First, the queued volume in the volume-to-capacity ratio addresses the issue of the volume-to-capacity ratio not distinguishing between queued and free-flowing traffic. Second, cycle utilization measures the extent of time utilization within a cycle, improving the green occupancy ratio by indicating how effectively the green time is utilized throughout the cycle. Lastly, the volume-occupancy capacity utilization, overcoming the limitations of the green occupancy ratio, which does not account for the actual volume of traffic passing through the intersection, potentially leading to misleading interpretations in scenarios where occupancy is high but volume is low.

3.2.2.2. Turning Movement Estimation

An essential aspect of managing traffic congestion in intersections involves accurately estimating travel demand, including turning movements. While these turning movements are crucial for developing effective traffic management strategies, manually collecting turning movement data is labor-intensive and impractical for large-scale, long-term applications. As such, Karapetrovic and Martin (2021) focus on improving the real-time estimation of intersection turning movements, incorporating network geometric data and sparse link flow detections where traffic flow data is collected from a limited number of monitoring points or sensors. ATSPM data aided in calibrating their model and achieved an r-square of 0.70 for the left turn and 0.76 for the right turn on average for 5-min aggregation (Karapetrovic and Martin, 2021). Xu et al. (2023) developed a method for estimating network-level turning movement counts using ATSPM data.

ATSPM data provide detector occupancy time, detector-triggered counts, and green time duration to estimate the turning movement. The proposed model achieves reasonable accuracy, with a median root mean square error of 11 vehicles per 15 minutes for left and 12 vehicles per 15 minutes for right-turn movements (Xu et al., 2023). These approaches enable cost-effective, region-wide turning movement count estimation without additional infrastructure.

Turning movement data is also used to evaluate and optimize various traffic management strategies. For example, Abdelrahman et al. (2020) evaluate the safety and operational performance of displaced left-turn intersections. Using ATSPM data, the authors analyze operational characteristics such as delay and turning volumes to determine the efficiency of displaced left-turn intersections compared to conventional ones. Their study shows that displaced left-turn intersections intersections can reduce intersection delay by 3.567 seconds per vehicle for the same left-turn volume, albeit with some safety trade-offs (Abdelrahman et al., 2020).

3.2.2.3. Traffic Flow or Signal Phasing Prediction

Traffic flow prediction is a traditional task that can be used in various ways. Especially, accurate predictions allow for dynamic adjustment and coordination of traffic signal timings, reducing wait times and improving the flow of vehicles through intersections (Day and Bullock, 2020). In addition, predictive models help route vehicles through less congested paths, thus reducing commuter travel time. Researchers try to predict the traffic flow at the urban network using ATSPM. Previous studies primarily employed machine learning and deep learning models to predict intersection traffic flow (Karnati et al., 2022, 2021; Kazenmayer et al., 2022; Rahman et al., 2022). Using ATSPM data, they estimated traffic volume from vehicle arrivals and departures to develop models for predicting traffic dynamics and optimizing signal timing. Although the performance was critically dependent on the traffic flow and study site, these models

effectively captured non-linear traffic patterns, highlighting the potential for improving traffic management and operational efficiency.

Since cycle-level data can help identify specific times within the signal cycle when traffic problems occur, such as queues building up or vehicles arriving during red lights, some researchers advanced fixed time interval aggregation to cycle length (Day and Bullock, 2020; Mahmoud et al., 2021). For example, Day and Bullock (2020) focused on optimizing traffic signal offsets with predicted cycle-level characteristics. They generated detailed cyclic flow profiles with ATSPM to predict changes in traffic flows resulting from trial offset adjustments. Their method proved successful in approximately 95% of cases, demonstrating that high traffic volumes and precise green time distribution derived from ATSPM data significantly improve traffic signal coordination.

Signal phasing and timing prediction are other prediction targets in the ATSPM data, as they enable dilemma zone warnings to be provided and optimize route planning. To this end, previous studies merged GPS information from multiple vehicles with signal timing data (Islam et al., 2024, 2022). Key features, such as waiting time, approach speed, and acceleration, were extracted based on geolocation data. These features were then used to train a long short-term memory (LSTM) model capable of predicting cycle lengths and phase durations up to six cycles in advance. The authors indicated that the LSTM model could predict cycle lengths with a mean absolute error of approximately 7 seconds and phase durations with an MAE of about 9 seconds.

3.2.2.4. Intersection Prioritization and Classification

ATSPM data has also been instrumental in ranking intersections for improvement or intervention. Studies have developed scoring methods and performance metrics to evaluate various aspects, including safety, capacity, progression, communication, and detection aspects (Day et al., 2018; B. Wang et al., 2022). Day et al. (2018) focus on evaluating corridor performance at the system level by using ATSPM data to develop subscores for communication, detection, safety, capacity allocation, and progression across eight signalized corridors in Indiana. Their findings indicate that maintenance issues significantly impact the overall performance of traffic signal systems, and the developed methodology provides a simplified metric for evaluating corridor performance, highlighting severe deficiencies in any operational aspect.

Mahajan et al. (2019) and Wang et al. (2022) aim to develop a workflow for automatically scoring and ranking intersections based on performance, using ATSPM data to compute measures of effectiveness such as split failures, arrivals on red, arrivals on green, and traffic volume. Clustering and classification techniques identify patterns and bottlenecks in the traffic network, enabling proactive traffic signal management by categorizing intersections into clusters needing timing adjustments or detector error fixes (Mahajan et al., 2019; B. Wang et al., 2022).

Bassett et al. (2023) aim to develop an automated method for flagging intersection approaches needing left-turn phasing changes based on gaps in opposing through traffic, using ATSPM data to validate the gap analysis tool. The method identifies left-turn approaches that require phasing changes, utilizing validated ATSPM data to provide reliable insights and improve efficiency in responding to left-turn complaints (Bassett et al., 2023).

3.2.2.5. Data Integration with Other Data Sources

Several studies have explored and validated vehicle trajectory from alternative data sources to enhance and replicate ATSPMs. Crowdsourced probe vehicle data have demonstrated the potential to offer cost-effective and scalable solutions for traffic signal performance measurement (Emtenan and Day, 2022; Gayen et al., 2023; Saldivar-Carranza et al., 2021, 2024, 2023; Waddell et al., 2020a). Through comparative analysis, vehicle trajectory data were aggregated to evaluate metrics such as delay, percent arrivals on green, number of stops, and volume-to-capacity ratio. **Table 3-4** compares metrics from ATSPM and probe vehicle data with their market penetration rates and aggregation intervals, as presented in the literature.

Probe vehicle data has determined split failure by assessing whether a vehicle stops at least twice before crossing an intersection (Gayen et al., 2023; Saldivar-Carranza et al., 2021, 2023). Another metric probe vehicle data supplement the ATSPM is the downstream blockage, defined as when a queue at the downstream intersection obstructs the progression of vehicles. The results indicate that probe vehicle data can effectively replicate ATSPMs and provide scalable, cost-effective solutions for nationwide implementation.

Furthermore, probe data has been utilized to estimate various metrics, such as travel times (Sengupta et al., 2023), arrival time (Waddell et al., 2020b), and shockwave speeds (Zhang et al., 2023), which cannot be obtained from ATSPM. Sengupta et al. (2023) focus on estimating arterial travel time distributions from ATSPM data. They developed a model that learns simulated probe trajectories from ATSPM data to estimate travel time distributions. The authors claim that their simulation study gave them a reasonable estimate of the travel time distribution using only ATSPM data (Sengupta et al., 2023). Similarly, Waddell et al., 2020b studied obtaining arrival times of vehicles at intersections from probe vehicle data. The study found that using low ping frequency

data can achieve 77% of the benefits of high-resolution data in optimizing signal offsets (Waddell et al., 2020b).

Table 3-4. Compared performance metrics from ATSPM and probe vehicle data

Metric	Source	Waddell et al., 2020a	Saldivar-Carranza et al., 2021	Tahsin Emtenan and Day, 2022	Gayen et al., 2023	Saldivar-Carranza et al., 2023	Saldivar-Carranza et al., 2024
Average delay	**ATSPM and Probe vehicle**	O	O	O			
Percent of arrival on green		O	O	O		O	
Volume-to-capacity ratio				O			
Percent of green duration				O			
Split failure			O		O	O	O
Downstream blockage	**Probe vehicle**		O			O	
Number of stops		O	O		O	O	O
Market penetration rate		0.02-0.04%	2%	-	5%.	2.7%	4.5%
Aggregation interval		1-5min	15 min	5-20min	4 cycles	15min	15min

Vehicle trajectory data from CCTV data differs from probe vehicle data in that it can capture the trajectory of all vehicles, although its range is limited to specific intersections. CCTV can complement and validate the data provided by ATSPMs, yet surprisingly, little research has been conducted on this topic. One study attempted to augment ATSPM data by converting stop

bar sensors into advanced detection events using trajectories from CCTV data (Zhang et al., 2023). The motivation behind this was the absence of advanced detectors in most ATSPM systems. The study reconstructed vehicle trajectories from stop bar detectors using a traffic flow model, enabling the derivation of speed, occupancy, and shockwave speeds.

The review of those papers reveals that probe vehicle data were limited in their ability to utilize real-time information and the types of metrics that could be employed. In addition, probe vehicle-driven metrics should be carefully addressed since they are unreliable for generalizable use when the transmission frequency and market penetration rate are low. Therefore, unique metrics provided by ATSPMs, such as exact vehicle volume, signal phase and timing, shockwave speed, and queue length, could be unique metrics obtained from ATSPMs. This review highlights that the reliability of metrics provided by ATSPM data is largely unexplored. Validating them with high-precision sources such as CCTV or LiDAR and analyzing the situations in which they are prone to significant errors will help ensure the proper utilization of the information provided by ATSPM.

3.2.2.6. Pedestrian Activity Estimation

ATSPM records the activation times and locations of pedestrian push buttons, allowing researchers to infer pedestrian or bicycle volumes. Typically, pedestrians press push buttons only once, even when multiple individuals are waiting, necessitating additional data for accurate pedestrian counts. Previous study estimated crossing volumes by comparing ATSPM data with observed counts from video recordings (Singleton and Runa, 2021). The study found a strong correlation (0.84) between model-predicted and observed volumes, with a notably low mean absolute error of 3 persons per hour, demonstrating the efficacy of using traffic signal data for

pedestrian monitoring. The accuracy remained consistent even during the COVID-19 pandemic, confirming the robustness of the framework (Runa and Singleton, 2023).

Estimated pedestrian volumes have been used to track pedestrian activity. One study assessed the impact of weather on pedestrian signal activity (Runa and Singleton, 2021), while another tracked pedestrian activity during the COVID-19 pandemic (Park et al., 2023; Singleton et al., 2023). Additionally, a study explored the relationship between the pedestrian crossing volumes and the built environment (Singleton et al., 2021) or split failure (Runa et al., 2024).

ATSPM also records the time when the push button and pedestrian signal are actuated, enabling the estimation of pedestrian delay (Karimpour et al., 2022). Karimpour et al., 2022 estimate pedestrian delay at signalized intersections using video-based sensors at four major signalized intersections to obtain actual delay. By combining traffic flow and pedestrian activity, they accurately captured fluctuations in average pedestrian delay, with mean absolute errors of 10 to 13 seconds, outperforming conventional methods.

3.2.2.7. Traffic Signal Priority Control

Signal priority systems can dynamically adjust signal timing to prioritize specific vehicle types, a notable advantage offered by ATSPM systems. This system involves extending the green phase or shortening the red phase to reduce delays for the prioritized vehicle. Although some research has focused on prioritizing freight or snowplows (Lau et al., 2024; Talukder et al., 2022), most studies using ATSPM data have investigated transit signal priority systems. For example, field studies have assessed the performance of transit signal priority systems at signalized intersections without modifying the intersection (Jackson et al., 2023; Leonard et al., 2019). In these studies, V2I communication connected transit buses to traffic signals to request priority, evaluating the system's performance. Similarly, Cvijovic et al. (2022) evaluated algorithms for

connected vehicle-based transit signal priority for regular buses and bus rapid transit (BRT) systems. Using ATSPM data to calibrate traffic conditions and simulate a real-world network, the study found that TSP resulted in significant delay reductions for both regular buses and BRT, with delays decreasing by 33% and 12%, respectively (Cvijovic et al., 2022).

Since the rate of TSP requests being served was initially lower without any modification, several studies have developed different strategies to increase the effectiveness of the transit signal priority system by adjusting the intersection (Sheffield et al., 2021; Wang et al., 2020). Wang et al., 2020 investigated the performance of the transit signal priority system before and after signal retiming data, demonstrating an increase in the transit signal priority served rate from 33.12% to 35.29% after retiming. Sheffield et al. (2021) approached the issue of low-served TSP requests by examining the sensitivity of different transit signal priority request thresholds on bus performance and traffic flow. Utilizing ATSPM data to measure split failures and green time changes when transit signal priority was granted, the study concluded that lower request thresholds significantly improved bus performance with a minor impact on general traffic.

While transit signal priority has been proven effective in various studies, several issues remain. Although transit signal priority implementation improved travel time reliability and reduced delays at intersections, buses often traveled too fast for the system to register their requests ((Jackson et al., 2023). Those observations indicate a need for increased ping frequency or extended detection zones, which increase operational costs. In addition, Jackson et al., 2023 found that buses equipped with signal priority improved their schedule adherence by 2% to 6%, which may be considered minor in less transit-oriented cities. Therefore, the cost-effectiveness of the transit signal priority system needs further evaluation, given the infrastructure and communication system costs it requires. Additionally, a balanced assessment should consider the overall traffic

impact of prioritizing transit buses. Evaluating appropriate preemption strategies for emergency vehicles, such as police cars and ambulances, is also necessary.

3.2.2.8. Simulation Studies

Combined with simulation, ATSPM provided the data needed to conduct various studies, including signal time and trajectory optimization. Those studies used ATSPM to calibrate the simulator to replicate real-world intersections, enabling experiments that would otherwise be impossible or expensive to conduct in a field study.

Signal time optimization aims to reduce the delay, crash, and fuel consumption of the intersection. Most studies have tried to optimize their timing, maintaining the order of phase unchanged (Alshayeb et al., 2023; Parks-Young and Sharon, 2022; Wang et al., 2021). Wang et al. (2021) proposed an adaptive traffic signal control system using connected vehicle data, where ATSPM data were employed to assign optimal green times and design dynamic progression plans for critical paths. Their system reduced average delay by 15.67% and 13.81% compared to fixed coordination and adaptive signal control systems, respectively. Similarly, Parks-Young and Sharon (2022) use actuated and adaptive signal controllers to manage mixed traffic of autonomous and human-operated vehicles. ATSPM data facilitated the development and testing of algorithms for computing safe signal timing bounds. Alshayeb et al. (2023) sought to optimize signal timing to reduce fuel consumption at signalized intersections. The study employed ATSPM data alongside traffic microsimulation and a stochastic genetic algorithm. The optimized signal timing resulted in an 8-12% reduction in fuel consumption under moderate conditions and up to 14% with a higher presence of heavy vehicles without significantly impacting traffic mobility.

In another study, Wang et al. (2022) focused on optimizing the trajectories of connected automated vehicles (CAVs) along signalized arterials to minimize delays and lane-changing related costs under mixed traffic conditions. The researchers utilized ATSPM data to develop a two-stage optimization model for real-time trajectory planning. The model significantly reduced

stop delays for both CAVs and human-driven vehicles, especially under a high market penetration rate scenario (Wang et al., 2022).

Urban networks with many signalized intersections have complex traffic patterns, including varying vehicle flows and signal timings. Without calibration, the model may not reflect these intricacies accurately, leading to unreliable results (Ahmad et al., 2023; Tariq et al., 2021). ATSPM data provided detailed information for calibrating simulation tools. Tariq et al. (2021) aimed to improve the calibration of signalized arterial simulation models using high-resolution signal controller data in conjunction with a multi-objective optimization technique. ATSPM data calibrated parameters such as split utilization ratio, green utilization ratio, arrival on green, and travel time. Ahmad et al. (2023) evaluated traffic operation conditions during wildfire evacuations using connected vehicle data. The study utilized ATSPM data to replicate signal phasing and overall traffic conditions during evacuation.

3.2.3. Safety Applications

The application of ATSPM is a transformative approach in improving traffic safety, particularly by addressing issues such as red-light running (RLR), red-light crossing (RLC), dilemma zones, crash risk and conflict prediction, injury severity prediction, and vehicle and pedestrian exposure estimation. ATSPM enables real-time monitoring and adjustment of traffic signals, reducing RLR and RLC incidents and mitigating dilemma zones where drivers are uncertain whether to stop or proceed during a yellow light. By analyzing detailed traffic data, ATSPM enables accurate predictions of crash risk, conflict, and injury severity, facilitating proactive measures to prevent crashes and mitigate their impact. Additionally, ATSPM assesses vehicle and pedestrian exposure at intersections, providing insights to optimize signal timing and enhance safety measures for all road users. This section will delve into the specific applications of ATSPM in each of these areas, illustrating the significant improvements in traffic safety through this technology.

3.2.3.1. Detection of Red Light Running and Crossing and Dilemma Zone

Red light running (RLR) poses significant safety risks at intersections due to the severe nature of RLR-related crashes. According to a report by the Indiana DOT, RLR can be detected if the red phase and stop bar detector on-off events overlap. This overlap indicates that a vehicle entered and exited the stop bar during the red light. **Figure 3-5** illustrates this detection logic, showing two detector on-off traces alongside the concurrent phase state. The upper graph depicts a detector presence trace with an off-on transition after the start of red and an on-off transition shortly after, suggesting a likely RLR incident. In contrast, the lower graph shows an off-on transition before the start of red, likely representing a vehicle entering during the yellow phase, which is excluded from RLR detection.

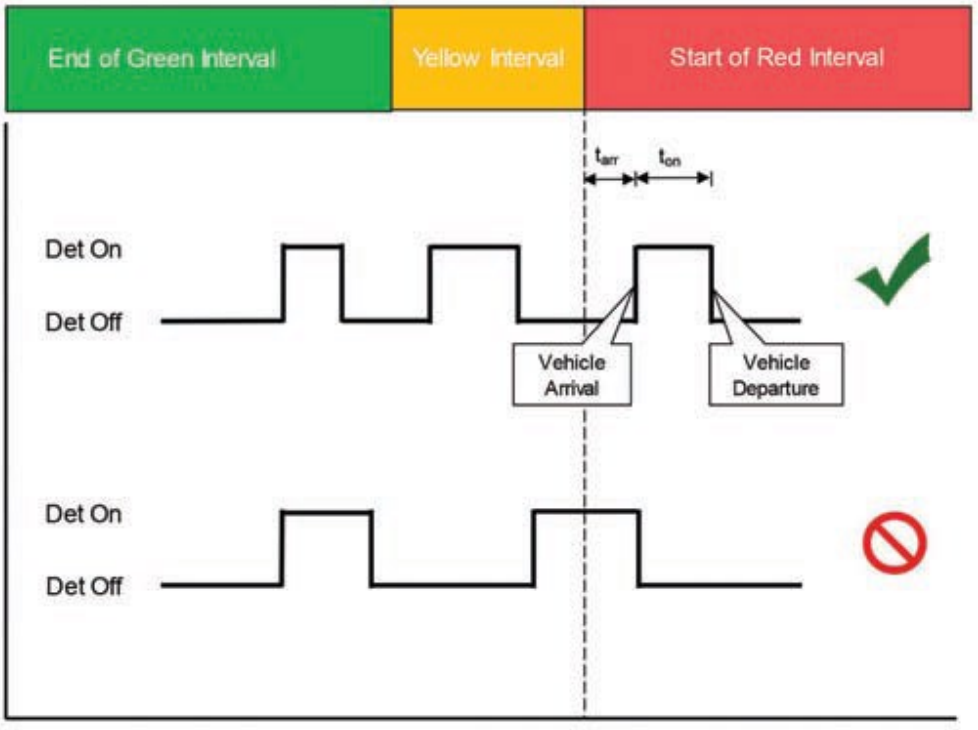

Figure 3-5. Conceptual overview of RLR detection using loop detector and phase event data (Indiana DOT, 2015)

The application of ATSPM is essential in addressing RLR behavior at signalized intersections, a significant cause of intersection-related crashes. Utilizing high-resolution event-based data, ATSPM systems provide detailed performance metrics, signal phasing and timing (SPaT), and traffic data, enabling precise analysis and intervention. The study conducted by Karimpour et al. (2023) used ATSPM data to develop finite mixture models to estimate RLR behavior across multiple intersections in Arizona. Key factors influencing RLR were identified, including traffic flow, intersection delay, number of approach lanes, and cycle length. It was found that increased traffic flow, intersection delay, and number of lanes elevated the likelihood of RLR, while longer cycle lengths reduced it. The study's proposed method outperformed conventional models like the Poisson Generalized Linear Model (PGLM) and the Zero-Inflation Poisson

Regression Model (ZIPM) in accuracy and model fit. This method allows for proactive identification and mitigation of high-risk intersections, significantly contributing to traffic safety by reducing the frequency and severity of RLR incidents.

Zhang et al. (2021) demonstrated the effectiveness of using pose estimation and machine learning models in predicting pedestrian red-light crossing (RLC) intentions at signalized intersections, a crucial aspect of traffic safety. By leveraging CCTV video data and Automated Traffic Signal Performance Measures (ATSPM), the researchers extracted key pedestrian variables such as joint angles, walking speed, waiting time, and green time of vehicle signals. The Random Forest (RF) model achieved the best performance, with a recall value of 0.757 and an AUC value of 0.849 for predicting RLCs, highlighting the significance of factors like walking speed and joint angles. This approach can be integrated into Infrastructure-to-Vehicle (I2V) applications to proactively warn drivers of potential pedestrian RLCs, thereby enhancing intersection safety. The study underscores the potential of combining ATSPM data with advanced computer vision and machine learning techniques to improve traffic safety outcomes and reduce pedestrian-related incidents at signalized intersections.

The dilemma zone is a critical area at signalized intersections where drivers face uncertainty about whether to stop or proceed when the light turns yellow, often resulting in abrupt stops or speeding through the intersection, leading to potential crashes. The study by (Li et al., 2020) highlights the critical role of ATSPM and connected vehicle (CV) technology in mitigating dilemma zone issues at signalized intersections, particularly for heavy vehicles, which have a higher risk due to longer stopping distances and braking performance differences. By leveraging position data from CVs and map-matching them to virtual waypoints, the researchers proposed triggering force gap out (FGO) before a vehicle enters the dilemma zone. ATSPM data recorded

the onset of yellow times and phase terminations, assessing vehicle positions relative to the dilemma zone. Combining CV technology with ATSPM data to trigger FGO reduced dilemma zone incursions by 34% in field tests, demonstrating the effectiveness of this integrated approach in enhancing the detection and mitigation of dilemma zones, thereby promoting safer intersection management.

3.2.3.2. Real-Time Crash Risk and Conflict Prediction at Intersection

Real-time crash risk prediction at intersections is a critical application of ATSPM, aiming to predict the likelihood of crashes (i.e., occurrence and non-occurrence of crashes) in real-time and take proactive measures to prevent them. (Yuan et al., 2019) employed a Long Short-Term Memory Recurrent Neural Network (LSTM-RNN) algorithm to address this challenge, leveraging real-time traffic data collected from traffic detectors through ATSPM. The study utilized the Synthetic Minority Over-sampling Technique (SMOTE) to balance the dataset, which is crucial given the rarity of crash events compared to non-crash events. By analyzing detailed traffic patterns, signal timing, and vehicle movements at 44 intersections in Oviedo, Florida, the LSTM-RNN algorithm demonstrated superior performance in predicting crash risks compared to traditional conditional logistic models. The model achieved a higher sensitivity and a lower false alarm rate, highlighting its potential for practical deployment in traffic management systems to enhance intersection safety.

Further enhancing the capabilities of ATSPM, (Yuan et al., 2021) developed a model for real-time cycle-level crash risk at signalized intersections based on high-resolution event-based data. Unlike previous studies that used fixed time intervals, this research focused on signal cycles, aligning with the cyclical nature of intersection traffic flow. Key factors identified included traffic volume, signal timing, headway and occupancy, traffic variation, shockwave characteristics, and

weather. Using undersampling strategies and developing conditional logistic and binary logistic models, the study focused on predicting crash risk based on these factors. The results indicated that higher cycle volume, arrivals on yellow, and traffic volatility significantly increased the odds of crash occurrence. This study demonstrated that leveraging high-resolution ATSPM data for cycle-level crash risk prediction offers a more accurate and responsive approach to real-time traffic safety management, providing critical insights for mitigating crash risks at signalized intersections.

In addition, (Gong et al., 2020) applied ATSPM data in a multi-objective reinforcement learning framework to enhance adaptive traffic signal control (ATSC) systems for improving intersection safety. This approach utilized high-resolution ATSPM data to dynamically adjust signal timings based on real-time traffic conditions and crash risk predictions. The reinforcement learning model, trained on simulated traffic data, optimized both traffic efficiency and safety metrics. The results showed significant improvements over traditional ATSC methods, demonstrating the potential of integrating ATSPM with advanced machine learning techniques to proactively manage traffic and reduce crash risks at intersections. This innovative application underlines the versatility and effectiveness of ATSPM in addressing various aspects of traffic safety through real-time data analysis and adaptive signal control strategies.

Conflict prediction, distinct from crash risk prediction, focuses on identifying potential conflicts between road users before they escalate into crashes. Zhang and Abdel-Aty (2022) developed a real-time pedestrian conflict prediction model using high-resolution ATSPM data and CCTV footage to derive conflict indicators like Post Encroachment Time (PET) and Time to Collision (TTC). The study utilized multiple machine learning models, with eXtreme Gradient Boosting (XGBoost) demonstrating the best performance, achieving an AUC value of 0.841 and a recall value of 0.739. The model predicted pedestrian conflicts at the signal cycle level, using

variables such as vehicle counts, green time, and pedestrian phase counts as surrogate measures for pedestrian exposure. The ability to predict conflicts one cycle ahead allows for timely adjustments to signal timing and proactive warnings to drivers, significantly enhancing intersection safety. This approach underscores the potential of integrating high-resolution ATSPM data with advanced machine learning techniques to improve real-time traffic safety management.

3.2.3.3. Injury Severity Estimation

Leveraging ATSPM significantly enhances the prediction of injury severity at intersections by utilizing real-time, high-resolution event-based detection records and crash data. (Kidando et al., 2021) applied ATSPM to analyze three years of data (2017-2019) from arterial highways in Tallahassee, Florida. By integrating ATSPM, the study collected detailed traffic flow and signal timing data, providing an accurate representation of traffic conditions leading up to crashes. The research employed Random Forest (RF) and eXtreme Gradient Boosting (XGBoost) classifiers to identify critical factors influencing injury severity, such as the manner of collision, traffic volumes, signal timing, and arrival on red volumes. The XGBoost model outperformed the RF model, highlighting the effectiveness of ATSPM in improving prediction accuracy.

Further analysis by (Kidando et al., 2022) explored the influence of real-time traffic events and signal-based variables on injury severity, incorporating Bayesian inference methods to estimate model parameters. The study identified that approach delay and platoon ratio, derived from ATSPM data, significantly influenced injury severity. The logistic model with a heavy-tailed distribution random effect was found to be the best fit, highlighting the necessity of accounting for site-specific variations. Key factors such as the manner of collision, occupant seat position, number of vehicles involved, gender, age, lighting condition, and day of the week were also significant predictors. The study's findings provide valuable insights for transportation agencies to develop

countermeasures proactively, demonstrating the critical role of ATSPM in enhancing the precision and effectiveness of injury severity prediction at signalized intersections.

3.2.3.4. Vehicle and Pedestrian Exposure Estimation

The estimation of vehicle and pedestrian exposure at intersections is crucial for understanding and improving traffic safety. ATSPM play a pivotal role in this context by providing high-resolution data on traffic flow and signal operations. (Lee et al., 2019) utilized ATSPM data to analyze pedestrian crashes in suburban areas with low pedestrian activities. The study collected data from 219 intersections in Seminole County, Central Florida, including pedestrian calls and pedestrian logs from ATSPM systems. By calculating average daily pedestrian phases requested (ADPR) and average pedestrian phases provided (ADPP), the researchers were able to estimate pedestrian exposure more accurately. The study employed a Bayesian random-parameter Poisson-lognormal model to evaluate the safety-in-numbers (SIN) effect, which suggests that as pedestrian numbers increase, their crash rates decrease. The findings indicated that intersections with higher pedestrian activity exhibited the SIN effect, highlighting the importance of accurate exposure estimation in enhancing pedestrian safety.

(Mahmoud et al., 2021) further demonstrated the utility of ATSPM in estimating pedestrian and bicycle exposure by integrating it with crowdsourced data (Strava), CCTV footage, crash data, and various contextual factors such as land use and socio-demographic characteristics. The study employed multiple statistical and machine learning models, determining that the eXtreme Gradient Boosting (XGBoost) model offered the best performance. This model was then applied to estimate exposure at intersections and along roadway segments, which was crucial for developing Safety Performance Functions (SPFs). The integration of these diverse data sources with ATSPM enabled a comprehensive assessment of exposure, identifying significant hotspots for pedestrian and

bicycle crashes, particularly in urban areas with high activity levels. This research highlights the effectiveness of combining ATSPM with advanced analytical techniques and diverse data sources, providing transportation agencies with robust tools to enhance the safety of vulnerable road users.

3.2.4. Summary of Literature Review

Recent research on ATSPM highlights their significant impact on mobility and safety applications. ATSPM data is utilized to optimize traffic signal timing, reduce congestion, and enhance traffic flow through advanced machine learning models to predict traffic volumes and turning movements. Specific use cases include assessing pedestrian delays, transit signal priority, and evaluating detector configurations. Intersection prioritization leverages ATSPM data for scoring and ranking, employing data-driven techniques and expert input. Validation efforts explore alternative data sources, such as probe vehicle data, to enhance ATSPM's scalability and effectiveness. Addressing data anomalies is critical, with research focusing on improving data quality through machine learning. Safety applications include detecting red light running, predicting pedestrian conflicts, and modeling static or real-time crash risks, emphasizing high-resolution data's role in enhancing predictive accuracy and traffic safety management. Future research should aim to standardize methods across diverse detector configurations and expand datasets with safety features such as approaching vehicle's headway and surrogate safety measures for comprehensive traffic safety improvements.

3.3. Best Practices for Operational Countermeasures at Intersections

This research proposes improvements in traffic signalization based on Automated Traffic Signal Performance Measures (ATSPM). An essential step involves reviewing established practices as recommended in technical manuals. This section outlines key aspects underscored in the existing manuals and suggests enhancements. The review primarily focuses on six strategic implementations:

a) No Right Turn on Red

b) Leading Pedestrian Interval (LPI)

c) Protected and Permitted Left turn

d) Yellow time adjustment

e) Red time adjustment

f) Pedestrian recall

Relevant manuals such as the FDOT Design Manual (FDM), Federal Highway Administration Signalized Intersections Informational Guide (FHWA SIIG), Highway Capacity Manual (HCM), Manual on Uniform Traffic Control Devices (MUTCD), and Traffic Engineering Manual (TEM) were reviewed, specifically their latest versions. This review concentrates on actionable insights from ATSPM's traffic signal and detector event data, focusing on the existence of clear criteria to implement. Detailed explanations and excerpts are presented in APPENDIX.

3.3.1. Traffic Signal Strategies

3.3.1.1. No Right Turn on Red (RTOR)

Table 3-5 shows that different traffic manuals provide varied guidance on RTOR.

Table 3-5. Summary of Best Practices for NRTR

Source (Year)	Best Practices
MUTCD (2009)	• No RTOR when sight distance is insufficient for safe maneuvering. • Restrict RTOR at intersections where vehicles may unexpectedly conflict with other road users, including pedestrians and cyclists. • No RTOR during exclusive pedestrian phases to protect pedestrians.
FHWA SIIG (2013)	• No RTOR is suggested where sight distance is inadequate for safe turning movements, which can lead to crashes. • RTOR is commonly restricted at intersections with high pedestrian traffic to avoid pedestrian-vehicle conflicts. • Certain vehicles like school buses are prohibited from turning right on red for safety reasons.
HCM (2022)	• Consider RTOR where right turns are critical to intersection operations. • Evaluate lane allocation to determine if prohibiting RTOR would benefit traffic flow and safety. • Factors such as right-turn flow rate, sight distance, and conflicting movements should be considered to determine the feasibility of RTOR. • Analyze the volume-to-capacity ratio for conflicting movements to assess whether prohibiting RTOR would reduce congestion or improve safety.
FDM (2023)	• RTOR is prohibited in the intersection bicycle box and two-stage bicycle turn box. • No right turn signs are required at specific intersections, including diverging diamond intersections
TEM (2024)	• Use static or dynamic “No Turn On Red” sign to prohibit turns on red. • Display dynamic signs during the LPI interval and the preceding yellow and red intervals.

The MUTCD emphasizes safety, recommending No RTOR where sight distance is limited or conflicts with pedestrians/cyclists are likely during exclusive pedestrian phases. FHWA SIIG echoes these concerns, suggesting NRTR restrictions where sight distance is inadequate or pedestrian traffic is high and for specific vehicles like school buses. In contrast, the HCM takes a more operational approach, advocating for careful evaluation of RTOR based on factors like lane allocation, right-turn flow rate, sight distance, and conflicting movements. The FDM focuses on specific scenarios, prohibiting RTOR in bicycle boxes and certain intersections. Lastly, the TEM provides practical guidance on using static or dynamic "No Turn On Red' signs to effectively implement these restrictions. While safety remains a common concern, the manuals differ in their emphasis on operational considerations and the level of detail in their recommendations.

3.3.1.2. Leading Pedestrian Interval

Leading Pedestrian Interval (LPI) implementation guidance varies across traffic signal manuals, as shown in **Table 3-6**. The MUTCD recommends LPIs at intersections with high pedestrian and conflicting turning vehicle volumes, advising a minimum 3-second duration to ensure pedestrians cross at least one lane. The FHWA SIIG similarly recommends LPIs, where pedestrian traffic is moderate to heavy, or pedestrian-vehicle interactions are frequent. The HCM provides broader guidance on timing walk intervals but lacks specific LPI criteria. The FDM does not mention LPIs. Lastly, the TEM offers a comprehensive approach, suggesting LPI reviews based on sight distance, geometry, and signal timing while providing maximum durations (10 seconds for actuated, 7 seconds for automatic recall) and suggesting a 3-second duration for busy intersections. The TEM also includes a formula to calculate LPI duration based on various factors.

Overall, while the manuals generally agree on the benefits of LPIs, they differ in the specificity of their recommendations and the factors considered for implementation.

Table 3-6. Summary of Best Practices for LPI

Source (Year)	Best Practices
MUTCD (2009)	• Consider LPI at intersections with high pedestrian and conflicting turning vehicle volumes. • Use at least 3 seconds of LPI to allow pedestrians to begin crossing and establish their presence in the crosswalk, ensuring they cross at least one traffic lane.
FHWA SIIG (2013)	• LPI are recommended where there is moderate to heavy pedestrian traffic to enhance pedestrian safety by allowing them to start crossing before vehicles get a green signal. • LPIs are encouraged in areas with frequent pedestrian-vehicle interactions to reduce conflicts and improve pedestrian safety.
HCM (2022)	• The manual describes how walk intervals should be timed with traffic signals, including leading pedestrian intervals, but does not specify exact criteria for their implementation.
FDM (2023)	• There is no specific mention of LPI or related strategies.
TEM (2024)	• Reviewed LPI implementation based on sight distance concerns, geometric updates, and suitability for exclusive pedestrian phases or concurrent but protected signal timing. • Maximum LPI duration is 10 seconds for actuated pedestrian phase and 7 seconds for automatic pedestrian recall. • Suggest a 3-second LPI duration for intersections operating close to capacity to balance pedestrian safety with traffic flow efficiency. • The manual also includes a formula (Formula 3.11.5.2-1) to calculate LPI duration based on crosswalk width, detector location, walking speed, and start-up lost time.

3.3.1.3. Protected or Permitted Left Turn

Table 3-7 shows the guidance for protected or permitted left turns is more precise than other implementations using various factors and thresholds. While the MUTCD lacks specific mention of these turn types, the FHWA SIIG provides comprehensive criteria for protected-permissive phasing, recommending it based on left-turn volume, the number of opposing lanes, opposing traffic speed, crash history, sight distance, road layout, opposing left-turn signals, and engineering studies. The HCM primarily focuses on volume thresholds, suggesting protected operation when the left-turn volume is high or combined with opposing through volume. The FDM outlines implementation details, such as using flashing yellow arrows for single-turn lanes and separate signals for dual lanes and discusses split phasing options. The TEM allows both leading and lagging protected/permissive left turns, favoring lagging, and permits concurrent LPIs except with flashing yellow arrows. While the manuals generally acknowledge the importance of protected and permitted left turns, their recommendations differ in their specificity and the factors considered for implementation, ranging from volume-based thresholds to broader considerations like safety and traffic flow.

Table 3-7. Summary of Best Practices for Protected or Permitted Left Turn

Source (Year)	Best Practices
MUTCD (2009)	• There is no specific mention of protected or permitted left turn
FHWA SIIG (2013)	• Protected-permissive left-turn phasing is recommended if a minimum of 2 left-turning vehicles per cycle is observed. • This phasing is suggested when left turns cross three or more opposing lanes. • It is advised for situations where opposing traffic speeds exceed 45 mph. • A minimum of five left-turn collisions within a 12-month period suggests the need for protected/permissive phasing. • When sight distances are below the minimum requirements, this phasing should be considered. • Implement protected/permissive phasing in areas with atypical road layouts. • If the opposing left-turn approach has a left-turn signal, use protected/permissive phasing. • Any engineering study indicating the necessity for protected/permissive phasing should be followed.
HCM (2022)	• Protected operation is assumed when the left-turn volume reaches or exceeds 240 vehicles per hour. • The product of left-turn volume and opposing through volume must exceed certain thresholds based on the number of opposing lanes. The thresholds are 50,000 for one opposing lane, 90,000 for two lanes, and 110,000 for three or more lanes. These thresholds ensure that the intersection can handle the traffic flow efficiently. • If there is more than one left-turn lane on the approach, protected phasing is recommended.
FDM (2023)	• Both protected or permissive phasing with flashing yellow arrow signal are available at single turn lane. • Only protected phasing implemented with a separate signal head at dual turn lanes. • Split phasing based on offset opposing approaches, heavy left-turn volumes, or left turns from multiple lanes.

TEM (2024)	• Both leading and lagging protected/permissive left turns are allowed, with lagging preferred. • LPIs can be implemented concurrently with protected/permissive left turns, except when using flashing yellow arrow (FYA) signal heads, which prohibit permissive left turns during the LPI for safety.

3.3.1.4. Yellow Time Adjustment

The MUTCD recommends that the duration of yellow time should be determined by engineering practice, particularly referring to the ITE's Handbook. It suggests a yellow change interval between 3 to 6 seconds, with a longer interval for approaches with higher speeds. The FHWA SIIG supports a similar interval range, with a commonly employed maximum of 5 seconds. It also suggests that local practices, including ITE's standards, should dictate the length of the interval and recommend modifications in scenarios with high numbers of collisions and red-light violations. The HCM reiterates the 3 to 6 seconds interval, emphasizing longer durations for higher speed approaches. The FDM mandates that signal timings for the yellow change must align with the TEM. The TEM specifies a yellow change interval between 3 to 6 seconds, using the ITE formula for calculations. **Table 3-8** summarizes the best practices for yellow time adjustment as presented in each manual.

Table 3-8. Summary of Best Practices for Yellow Time Adjustment

Source (Year)	Best Practices
MUTCD (2009)	• Duration of yellow time to be determined by engineering practice: ITE's Handbook. • Yellow change interval between 3 and maximum 6 sec. • Longer interval for approaches with higher speeds
FHWA SIIG (2013)	• Yellow change interval between 3 and maximum 6 sec. • A maximum of 5 seconds is commonly employed. • Longer interval for approaches with higher speeds. • Local practice dictates the length of interval, including ITE's standard. • Modifying the yellow may be considered where: high number of angle/left turn and rear-end collisions, and high number of red-light violations.
HCM (2022)	• Yellow change interval between 3 and maximum 6 sec. • Longer interval for approaches with higher speeds
FDM (2023)	• Signal timings for the yellow change must be in accordance with the TEM.
TEM (2024)	• Yellow change interval between 3 and maximum 6 sec. • To calculate the yellow change interval, the formula from the ITE is to be used.

3.3.1.5. Red Time Adjustment

The MUTCD advises determining the red clearance interval duration using engineering practice from the ITE's Handbook, allowing for extension if a vehicle is predicted to violate red, with a maximum of 6 seconds. The FHWA SIIG typically sets the interval by local policy or calculation, recommending increases for wider intersections and adjustments for high collision and red-light violation areas. The HCM specifies a red clearance interval of 1 or 2 seconds. The FDM mandates alignment with the TEM, which specifies an interval between 2 and 6 seconds, calculated

using the ITE formula, with longer durations for complex intersections or those with safety concerns. **Table 3-9** summarizes these best practices for red time adjustment.

Table 3-9. Summary of Best Practices for Red Time Adjustment

Source (Year)	**Best Practices**
MUTCD (2009)	• Duration of red clearance interval time to be determined by *engineering practice*: ITE's Handbook • Red clearance interval may be extended from its predetermined value if a vehicle is predicted to violate red. • Interval should have a duration not exceeding 6 seconds, with *exception*.
FHWA SIIG (2013)	• Red clearance interval is typically either set by local policy or calculated using an equation. • Interval should be increased as intersections are widened. • Modifying the red clearance interval may be considered where: high number of angle/left turn and rear-end collisions, and high number of red-light violations.
HCM (2022)	• The red clearance interval is typically 1 or 2 s.
FDM (2023)	• Signal timings for the red clearance interval must be in accordance with the TEM.
TEM (2024)	• Interval should have a duration not exceeding 6 seconds. • To calculate the red clearance interval, use the formula from the ITE. • The red clearance interval must be between 2 and 6 seconds long. • Longer red clearance intervals may be appropriate for wide or complex intersections or those with a crash history or limited sight distance.

3.3.1.6. Pedestrian Recall

The MUTCD suggests a walk interval of at least 7 seconds, reducing to 4 seconds for low pedestrian volumes. It evaluates pedestrian clearance time at speeds of 4 ft/s (extended pushbutton press), 3.5 ft/s (normal), and below 3.5 ft/s for areas with slower pedestrians. Pedestrian signals are recommended for safe crossing assistance, engineering judgment, partial street crossing, and where vehicular signals are not visible to pedestrians. The FHWA SIIG advises setting the walk interval based on local policy, recommending a minimum of 7 seconds, but allowing as low as 4 seconds if conditions permit. Longer walk times are recommended in downtown areas, school zones, and areas with many elderly pedestrians. The HCM specifies a minimum walk time of 7 seconds for actuated phases, allowing shorter times if appropriate, and suggests setting intervals based on vehicle and pedestrian needs for pretimed and coordinated phases. The FDM highlights the need for longer walk times in school crossings or areas of high pedestrian activity. The TEM eliminates the need for a push button or passive detection and ensures that pedestrian walk and clearance intervals are provided in each cycle. **Table 3-10** summarizes these best practices for pedestrian recall.

Table 3-10. Summary of Best Practices for Pedestrian Recall

Source (Year)	Best Practices
MUTCD (2009)	• In normal scenario, the *walk* interval should be at least 7 sec in length. However, for low pedestrian volume the interval is 4 sec. • To evaluate the sufficiency of the pedestrian clearance time: 4 ft/s (extended pushbutton press), 3.5 ft/s (normal condition), <3.5 ft/s (slower pedestrians) • Pedestrian signals should be used under the following conditions: requires assistance for safe crossing, engineering judgement, permitted to cross a portion of the street, no vehicular signal indications are visible to pedestrians.
FHWA SIIG (2013)	• The *walk* interval varies based upon local agency policy. • A minimum *walk* time of 7 seconds, although *walk* times as low as 4 seconds may be used if pedestrian volumes do not require a 7-second interval. • In downtown areas, longer *walk* times are often appropriate to promote walking and serve pedestrian demand. • School zones and areas with large numbers of elderly pedestrians also warrant consideration and the display of *walk* times more than the minimum *walk* time. • FHWA pedestrian design guidance recommends a lower speed if needed to accommodate users who require additional time to cross the roadway, and in particular a lower speed where there are concentrations of children/elderly.
HCM (2022)	• For an actuated or non-coordinated phase, minimum *walk* time of 7 seconds, although *walk* times as low as 4 seconds may be used if pedestrian volumes and characteristics do not require a 7-second interval. • For pretimed phase, ***walk* intervals should be set to the amount of time vehicles need the green light minus the time pedestrians need to clear the intersection.** • For a coordinated phase, the controller is sometimes set to use a coordination mode that extends the walk interval for most of the green interval duration.
FDM (2023)	• Longer walk time in school crossings or other areas of high pedestrian activity.
TEM (2024)	• The pedestrian recall mode eliminates the need for a push button or passive detection and ensures that pedestrian *walk,* and clearance intervals are provided in each cycle.

3.3.2. Summary of Best Practices

While generally aimed at improving traffic flow and pedestrian safety, the six traffic signal strategies vary in the specificity and detail of their implementation guidelines across different traffic manuals. No Right Turn on Red (NRTR) guidelines range from prioritizing safety concerns (limited sight distance, pedestrian conflicts) to operational considerations (lane allocation, right-turn flow rate). The Leading Pedestrian Interval (LPI) recommendations also vary, with some manuals focusing on pedestrian volume and vehicle-pedestrian interactions, while others provide broader guidance on timing walk intervals. Protected or Permitted Left Turn implementation is the most complex, with factors ranging from left-turn volume and opposing traffic to sight distance and crash history.

Yellow Time Adjustment and Red Time Adjustment have the most consistent guidelines across manuals, with specific recommendations for the duration (3-6 seconds for yellow, 1-6 seconds for red) and adjustments for higher speeds or specific intersection conditions. These strategies prioritize safety by ensuring sufficient time for vehicles to clear the intersection or stop safely. Pedestrian Recall guidelines are also diverse, with recommendations for minimum walk times (4-7 seconds), adjustments for pedestrian speed, and considerations for specific areas (school zones, downtown areas). Overall, while the manuals generally agree on the benefits of these strategies, the variations in their recommendations highlight the need for careful consideration of local conditions, traffic patterns, and safety concerns when implementing these strategies.

CHAPTER 4: Data Collection

4.1. Data Collection

In this report, we acquired two types of data: detector configuration and controller event log data. The data were collected at ATSPM-equipped intersections in Brevard, Lake, Orange, Osceola, Seminole, Marion, Volusia, Flagler, and Sumter counties in District 5, Florida, USA. However, the scope of this project is limited to the intersections in Orange and Seminole counties. This chapter describes the data collection process implemented in this report.

4.1.1. Detector Configuration Data

The detector configuration data was collected from the NOEMI. NOEMI provides a snapshot of the current status of the signal system. In the form of reports, NOEMI offers detailed data on detector configuration[5].

Prior to acquiring the detector configuration data, we identified all intersections in the concerned counties in District 5, Florida, USA, from NOEMI. Specifically, we gathered information on all ATSPM-equipped intersections linked to the Signalized Intersection Inventory Application (SIIA). The selection based on SIIA aligns with the scope of this project. In total, 2092 intersections were identified, although not all are active[6].

The detector configuration data of all ATSPM intersections were collected using an open API from NOEMI. The API is: 'https://noemi.cflsmartroads.com/ssv/report.html?id={siiaID}'

---

[5] NOEMI - Smart Signal View

[6] NOEMI - ATSPM availability

Abnormality in Detector Configuration Data

Given the absence of other sources, we relied on detector configuration data from NOEMI. To verify the reliability of this data, we conducted a preliminary manual review of this data for a sample of ATSPM equipped intersections. We found logging errors in the detector configuration data, specifically in phase numbering (the identifier of phases along an approach), detector length, detector distance from the stop bar, and possibly channel numbering (the identifier of unique detectors on a phase). **Figure 4-1** provides an example of the problem with phase numbering. As shown in the figure, there is an inconsistency in phase numbering in the 'Phase' column, indicating an abnormality.

ID	Approach	Lane Type	Width	Length	Lane No. from Left	Type	Channel	Phase	Stopbar Distance	Slot Number	Length
1	1 US-17-92 NEB	Left	12	275	1	Inductive Loop	1	1	0	1	40
2	1 US-17-92 NEB	Left	12	320	2	Inductive Loop	2	1	0	1	40
3	1 US-17-92 NEB	Through	12	null	3	Inductive Loop	16	6	150	8	6
3	1 US-17-92 NEB	Through	12	null	3	Inductive Loop	19	6	330	10	6
4	1 US-17-92 NEB	Through	12	null	4	Inductive Loop	17	6	150	9	6
4	1 US-17-92 NEB	Through	12	null	4	Inductive Loop	20	5	330	10	6
5	1 US-17-92 NEB	Through Right	12	null	5	Inductive Loop	18	6	150	9	6
5	1 US-17-92 NEB	Through Right	12	null	5	Inductive Loop	21	6	330	11	6
6	2 SEMINOLA BLVD SEB	Left	12	205	1	Inductive Loop	9	3	0	5	40
7	2 SEMINOLA BLVD SEB	Left	12	205	2	Inductive Loop	10	3	0	5	40
8	2 SEMINOLA BLVD SEB	Through	12	null	3	Inductive Loop	24	8	0	12	40
9	2 SEMINOLA BLVD SEB	Through	12	null	4	Inductive Loop	25	8	0	13	40
10	2 SEMINOLA BLVD SEB	Right	12	null	5	Inductive Loop	26	8	0	13	40

Figure 4-1. Abnormality in Detector Configuration

Based on our review of the phase numbering, we identified 1817 intersections without abnormality in phase numbering. The frequency distribution of the normal and abnormal intersections based on abnormalities in phase numbering is shown in **Figure 4-2**. As indicated in the figure, Orange County has the highest number of intersections without abnormality in phase numbering. Moreover, the only intersection in Flagler County was identified as abnormal.

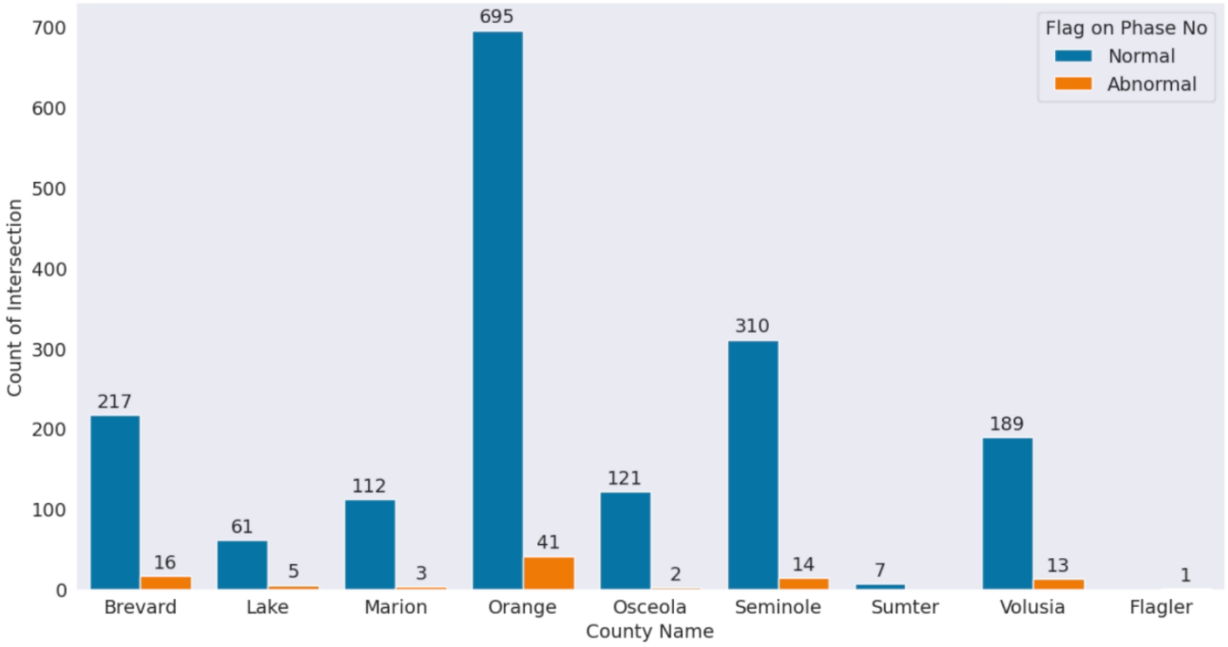

Figure 4-2. Distribution of Intersections Based on Abnormalities in Phase Numbering

It should be noted that our preliminary analysis was solely based on abnormalities in phase numbering, and our conclusions may be inaccurate pending more investigation and scrutiny in latter efforts. As such, we recommend a thorough review of the detector configuration data for all ATSPM-equipped intersections in the NOEMI system, focusing on detector length, detector distance from the stop bar, and channel numbering.

4.1.2. Controller Event Log Data

The controller event log data is openly archived in SunStore as CSV staged files for each day of the current running month and as ZIP staged files for every month since January 2018.

We directly accessed the ZIP staged files from SunStore. This report primarily focuses on selecting ATSPM-equipped intersections in Orange and Seminole counties rather than any in-depth data processing and feature extraction. Hence, we only collected data for May 2024. This data included controller event logs for all intersections in concerned counties in District 5, Florida, USA, though the scope is limited to the intersections in Orange and Seminole counties.

The descriptive summary of the detector configuration and controller event log data collected for this report is shown in **Table 4-1**[7].

Table 4-1. Descriptive Summary of Collected Data

Data Type	**Source**	**Month/Year**	**Counties Covered**
Detector Configuration	NOEMI	-	Brevard, Lake, Orange*, Osceola, Seminole*, Marion, Volusia, and Sumter
Controller Event Log	SunStore	May/2024	

[7] *Counties within the scope of this project. Initially, Orange County was not within the scope. However, this county was added later by the Florida Department of Transportation (FDOT) by recommending intersections.

4.2. Grouping Detector Configuration and Data Quality Check

Detector configurations in ATSPM-equipped intersections exhibit variance, and not all detectors at these intersections produce high-quality event data. In this chapter, we analyze the collected data on detector configurations and controller event logs to identify and group unique detector configurations and develop a pipeline to assess the data quality.

4.2.1. Grouping Detector Configuration

Variability in detector configuration is common at ATSPM-equipped intersections. The detector configuration may vary per intersection, per type of approach (e.g., major or minor roads) and type of phase (e.g., left-turn, through, and right-turn). This variability can affect consistency and uniformity in data transformation and decision-making for future tasks in this project. Therefore, it is crucial to identify and group unique detector configurations.

The most advanced configurations exist in the form of count detectors, stop bars, and setbacks, as illustrated in **Figure 4-3**. However, detector configurations in the 1817 ATSPM equipped intersections in Brevard, Lake, Orange, Osceola, Seminole, Marion, Volusia, and Sumter counties in District 5, Florida, USA, feature only stop bars and setbacks. Therefore, in this report, the configuration including a ‘count detector’ is disregarded when identifying and grouping detector configuration.

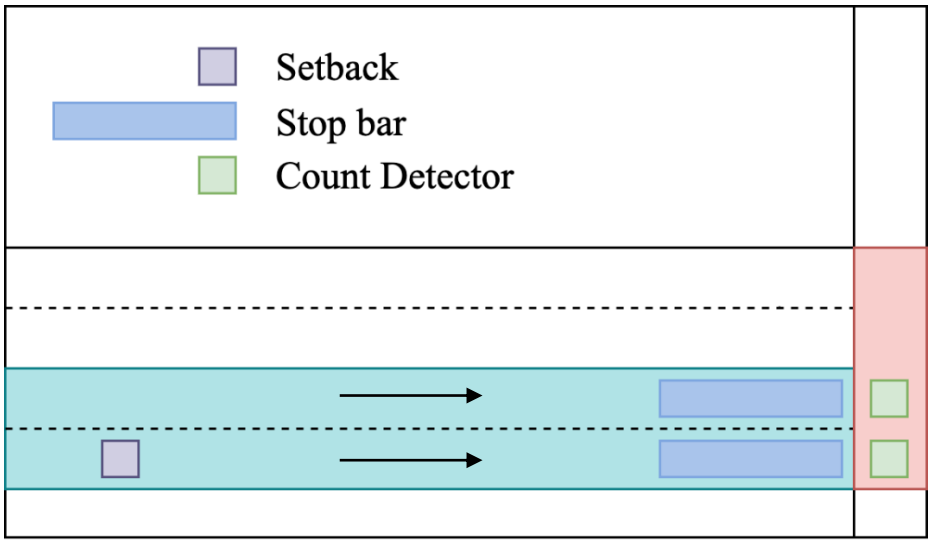

Figure 4-3. Advanced Detector Configuration

Simply knowing the existence of stop bars and setbacks is not enough to identify and group detector configurations. More precise metrics are needed. Therefore, we defined four reference metrics for this purpose, including:

a) Whether more than two lanes exist in a phase.

b) Whether a setback detector exists in a phase.

c) Whether multiple setback detectors exist in a phase.

d) Whether a stop bar exists in a phase.

Based on the metrics, we identified and grouped detector combinations in three different ways, which are described in the following sections.

4.2.1.1. Grouping by Intersection

In this method, we grouped detector configurations by evaluating the entire intersection's configuration. This process involved first identifying all unique detector configurations based on

the entire intersection layout and then grouping them accordingly. This method resulted in over 500 distinct detector combinations.

4.2.1.2. Grouping by Type of Approach

In ATSPM equipped intersections, there are two types of approaches: major and minor. Typically, major approaches are part of arterial roads, but they can also be part of collector roads. However, minor approaches are usually part of collector roads. Therefore, major approaches generally have more advanced detector configuration systems compared to minor approaches, marking a distinction in configurations.

In this method, we grouped detector configurations by considering the layout per the approach type. This method resulted in 218 unique detector configurations for major approaches and 119 for minor approaches.

4.2.1.3. Grouping by Type of Phase

Types of phases at intersections can include left-turn, through movement, and right-turn phases. Additionally, there can be shared lanes that serve multiple phases. In this method, prior to grouping detector configurations, we defined the types of phase into four groups: left-turn, through, right-turn, and shared. The shared phase refers to a lane that can accommodate multiple phases simultaneously.

This method resulted in a significantly lower frequency of unique detector configurations based on the type of approach, making it a more practical choice for grouping. In contrast, the frequency of unique detector configurations by intersection and by type of approach is extremely high. Since our upcoming tasks involve data transformation that relies on detector configuration, a less frequent grouping is preferred to facilitate transformation and enhance generalizability,

making grouping with high frequency unfeasible. Therefore, we selected grouping by phase type and will use this method for future tasks in this project. The frequency distribution of unique detector configurations by the type of phase is shown in **Figure 4-4**.

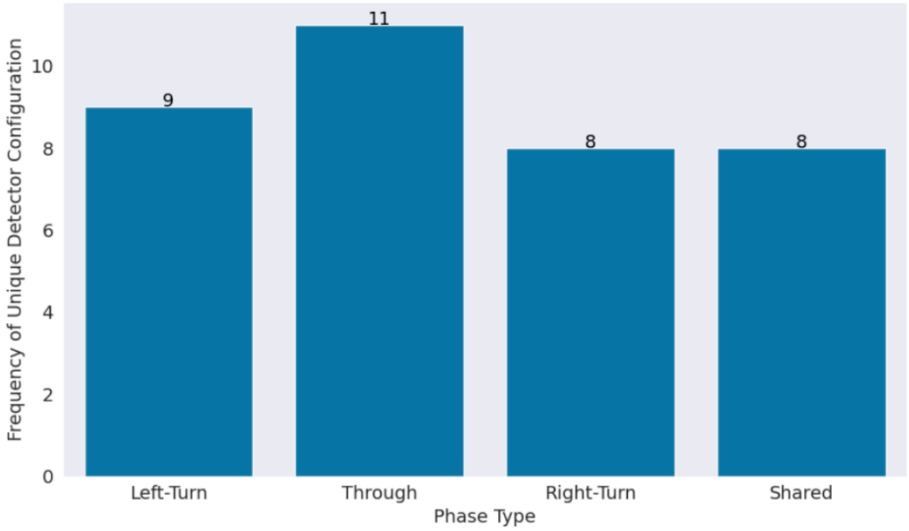

Figure 4-4. Frequency Distribution of Unique Detector Configurations by Type of Phase

The schematic diagram of the unique detector configurations per type of phase is shown in Figure 4-5. The “L,” “T,” “R,” and “S” denoting left turn, through movement, right turn, and shared lane, respectively. For every phase, ‘Type 1’ represents the configuration with no detector. The algorithm that calculates the performance measure does not change based on the presence or absence of a channel number. Also, If we Including this would make the number of possible configuration types too large. Therefore, this configuration classification system does not consider channel numbers, only the type and location of the detector. If the channel number does not exist and the detector is tied to all across the lanes, it is assigned a type based on the type and location of the detector.

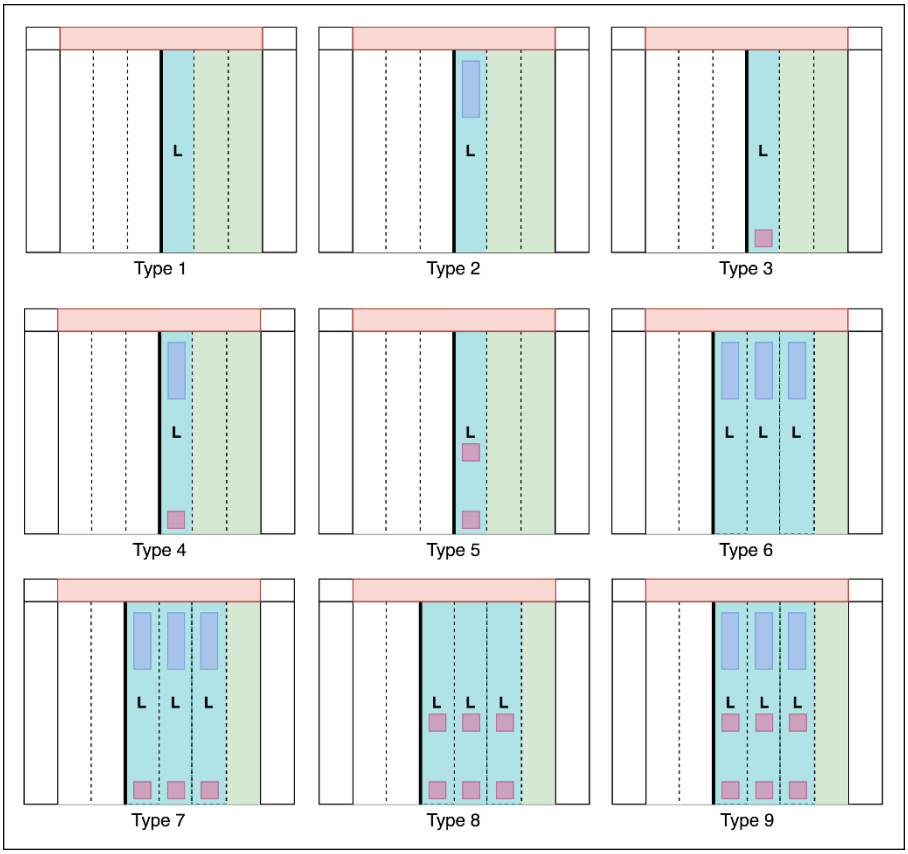

(a) Left-Turn Phase

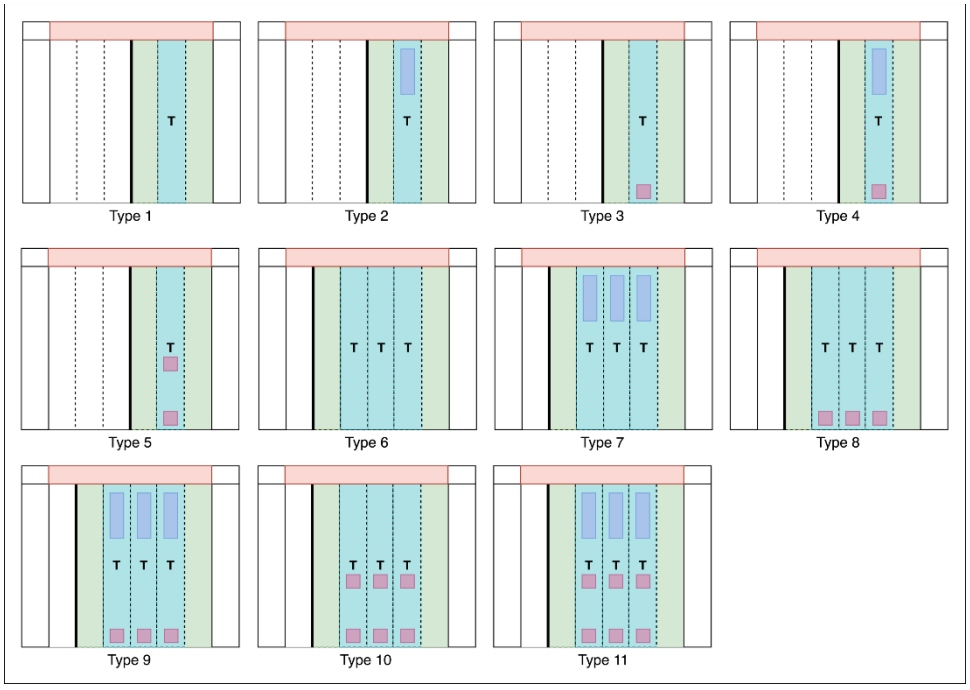

(b) Through Phase

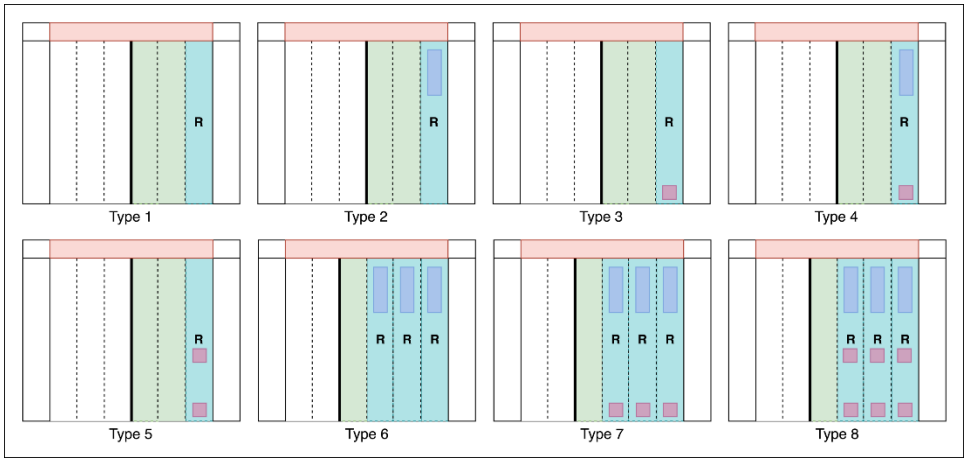

(c) Right-Turn Phase

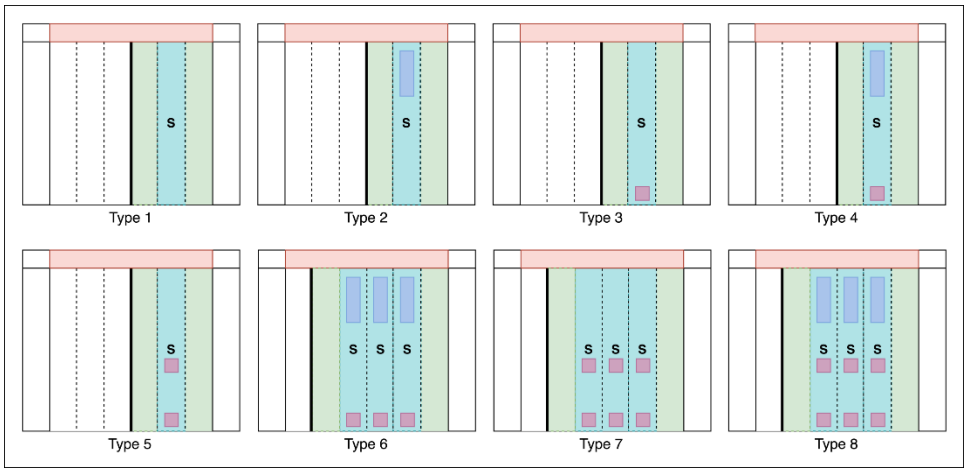

(d) Shared Phase

Figure 4-5. Schematic Diagram of the Unique Detector Configurations by Type of Phase

The descriptive summary of the detector configurations by type of phase (based on the defined reference metrics) is presented in **Table 4-2.** The optimal detector configurations are 'Types 4, 7, 9' for the left-turn phase, 'Types 4, 9, 11' for the through phase, 'Types 4, 7, 8' for the right-turn phase, and 'Types 4, 6, 8' for the shared phase. These configurations are preferred because they minimize restrictions on determining performance measures using controller event log data, which will be addressed in future tasks of this project. However, not every intersection is

equipped with the most optimal detector configurations per type of phase. Specifically, for the left-turn phase, 46, 23, and 12 intersections have ‘Types 4, 7, and 9,’ respectively. For the through phase, 75, 199, and 95 intersections have ‘Types 4, 9, and 11,’ respectively. For the right-turn phase, 26, 3, and 5 intersections have ‘Types 4, 7, and 8,’ respectively. And for the shared phase, 153, 1, and 44 intersections have ‘Types 4, 6, and 8,’ respectively.

Table 4-2. Descriptive Summary of Detector Configurations by Type of Phase

Type of Configuration	Type of Phase			
	Left-Turn	Through	Right-Turn	Shared
1	<= 2 lane(s)*			
2	<= 2 lane(s)*, stop bar exists			
3	<= 2 lane(s)*, setback exists			
4	<= 2 lane(s)*, stop bar exists, setback exists			
5	<= 2 lane(s)*, multiple setbacks exist			
6	> 2 lanes**, stop bar exists	> 2 lanes**	> 2 lanes**, stop bar exists	> 2 lanes**, stop bar exists, setback exists
7	> 2 lanes**, stop bar exists, setback exists	> 2 lanes**, stop bar exists	> 2 lanes**, stop bar exists, setback exists	> 2 lanes**, multiple setbacks
8	> 2 lanes**, multiple setbacks	> 2 lanes**, setback exists	> 2 lanes**, stop bar exists, multiple setbacks exist	
9	> 2 lanes**, stop bar exists, multiple setbacks	> 2 lanes**, stop bar exists, setback exists	-	-
10	-	> 2 lanes**, multiple setbacks	-	-
11	-	> 2 lanes**, stop bar exists, multiple setbacks	-	-

In the schematic diagrams (Figure 4-5(a)-Figure 4-5(d)),

* The only lane, identified as L, T, R, or S, represents <= 2 lane(s).

** The triple lanes, identified as L, T, R, or S, represent > 2 lanes.

The frequency distribution of all ATSPM equipped intersections in the District 5, Florida, USA, per unique detector configuration by phase type is presented in **Figure 4-6**.

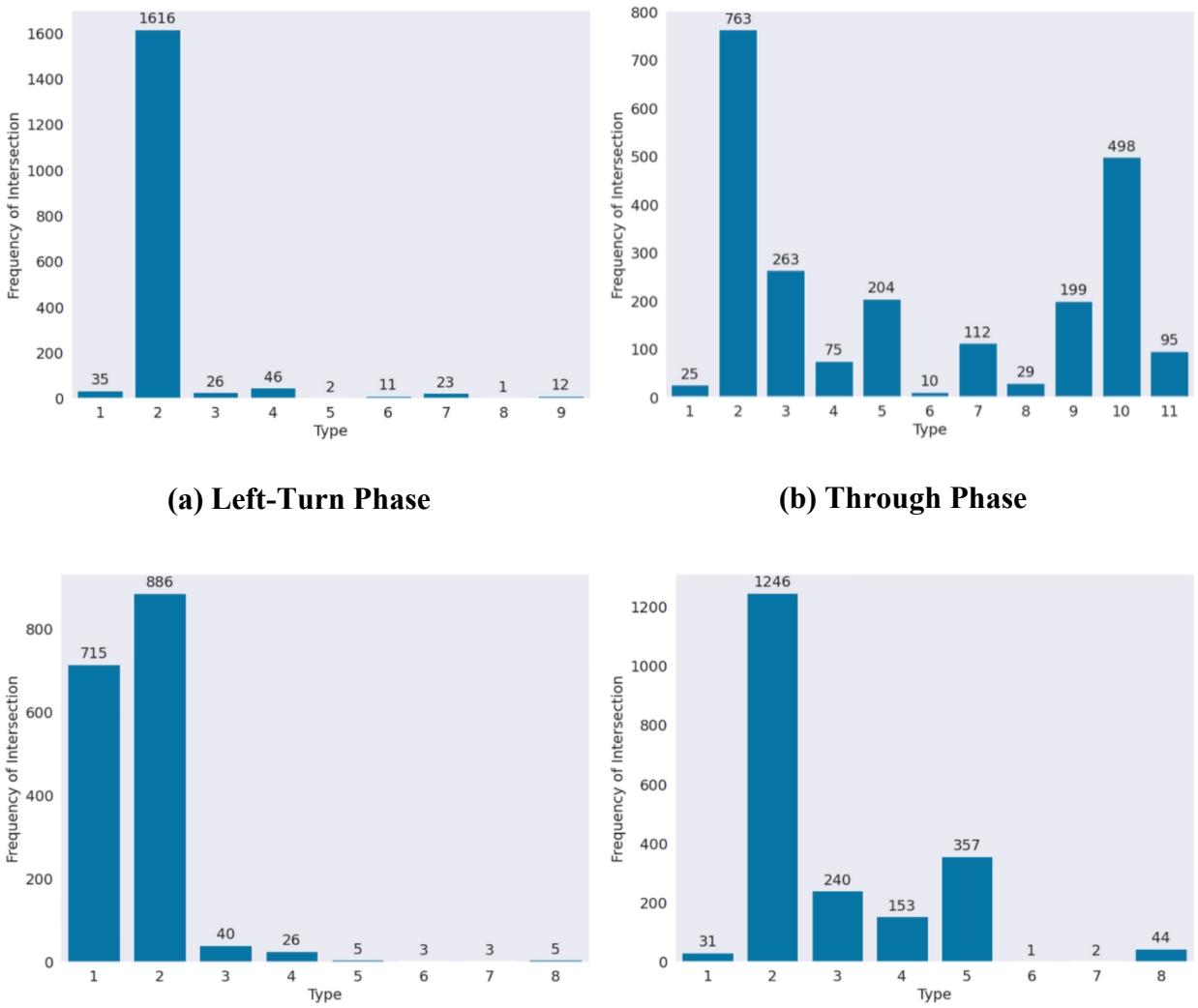

(a) Left-Turn Phase

(b) Through Phase

(c) Right-Turn Phase

(d) Shared Phase

Figure 4-6. Frequency Distribution of ATSPM equipped Intersections per Unique Detector Configuration by Type of Phase

Figure 4-6 indicates that 'Type 2' is the most common detector configuration found in ATSPM equipped intersections in the counties concerned in District 5, Florida, USA, for all types of phases. **Figure 4-6(b)** also shows that a significant number of intersections have detector

configurations ‘Types 4, 9, and 11’ along through phase. Further, **Figure 4-6(c)** reveals that many intersections with a dedicated right-turn phase lack detectors on them, classified as ‘Type 1’.

A descriptive summary of the most common and optimal detector configuration per type of phase is presented in **Table 4-3**.

Table 4-3. Descriptive Summary of Most Common and Optimal Detector Configuration

Type of Phase	**Most Common Configuration**	**Optimal Configuration**
Left-Turn	Type 2	Type 4, Type 7, Type 9
Through	Type 2	Type 4, Type 9, Type 11
Right-Turn	Type 2	Type 4, Type 7, Type 8
Shared	Type 2	Type 4, Type 6, Type 8

4.2.2. Data Quality Check

A critical challenge for this project is the quality of controller event log data produced by detectors in ATSPM-equipped intersections. The logging process involves timestamping events, such as changes in signal outputs and detector states, with a resolution of a tenth of a second. Several factors can negatively impact this logging, including lack of regular maintenance of detectors, electrical and mechanical failures, communication failures, outdated configurations, and adverse environmental conditions (Day et al., 2016). As a result, not every intersection in Brevard, Lake, **Orange**, Osceola, **Seminole**, Marion, Volusia, and Sumter counties in District 5, Florida, USA, provides reliable detectors that produce high-quality data. Therefore, it is essential to develop a pipeline to identify which detectors generate good data and which do not. This pipeline assists in selecting sample intersections in Orange and Seminole counties, ensuring that only intersections with detectors that consistently produce quality data are included.

Signal timing and detector on-off sequences are crucial event logs produced by detectors in ATSPM equipped intersections. As such, they serve as critical indicators for verifying the quality of controller event log data. The signal timing sequence follows a distinct pattern: ‘start of green - start of yellow - start of red clearance - start of red’ for every phase at the intersection (Day et al., 2014). The detector on-off sequence is ‘detector on - detector off’ (Day et al., 2014). If any sequence in the controller event log data does not adhere to these patterns, it can be considered anomalous. Based on this principle, we devised a framework named the Event Sequence Quality Checker (ESQC) to assess the quality of data produced by detectors in ATSPM equipped intersections.

4.2.2.1. Event Sequence Quality Checker (ESQC)

Our framework, ESQC, operates using a dual-step logic, as illustrated in **Figure 4-7**. In the first step, ESQC checks if the detectors at the input intersections are producing any controller event log data. If they are not producing any data, then ESQC moves to the next input. However, if they are producing data, then in the second step, ESQC verifies all possible event sequences in the data, matching them against the patterns 'start of green - start of yellow - start of red clearance - start of red' and 'detector on - detector off.' The output of the ESQC is a report indicating whether the detectors at ATSPM-equipped intersections are producing data and, if so, the percentage of anomalous sequences in the data.

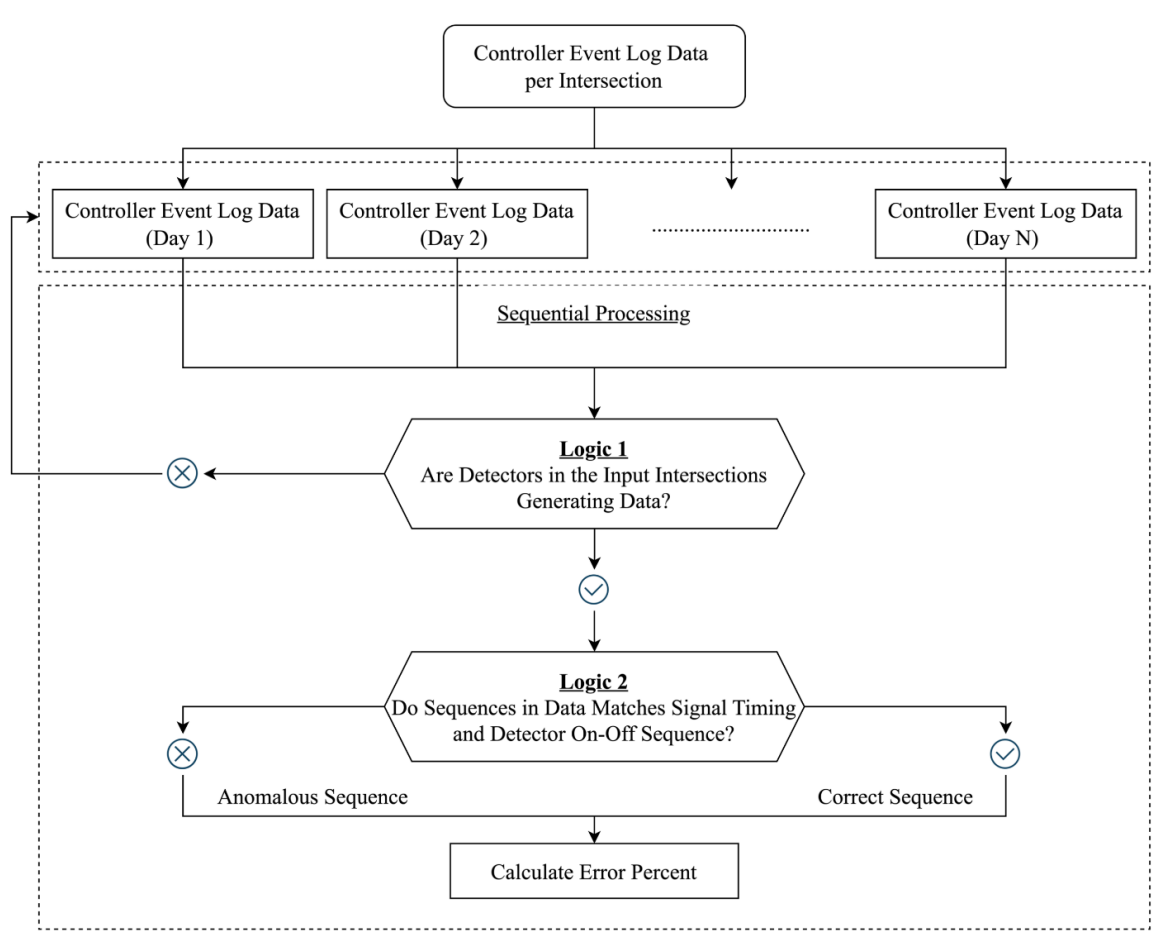

Figure 4-7. Event Sequence Quality Checker (ESQC)

It is important to note that ESQC processes each data set on a daily basis (i.e., sequential processing). Therefore, if a month of data is analyzed for any intersection, it will generate daily reports showing the temporal variation in the quality of the data for all the days in the month.

4.2.2.2. Data Quality Check Results

We tested our framework on the controller event data produced by detectors in ATSPM-equipped intersections in the concerned counties in District 5, Florida, USA, for May 2024. However, in this subsection, we are only presenting the results of Orange and Seminole counties.

Figure 4-8 presents the results of the first step of ESQC. **Figure 4-8(a)** shows that out of 695 intersections in Orange County (see **Figure 4-2**), detectors in nearly 600 intersections, on average, produced data for 23 days in May 2024. **Figure 4-8(b)** indicates that for the same month, out of 310 intersections in Seminole County (see **Figure 4-2**), detectors in nearly 300 intersections, on average, produced data for 22 days in May 2024.

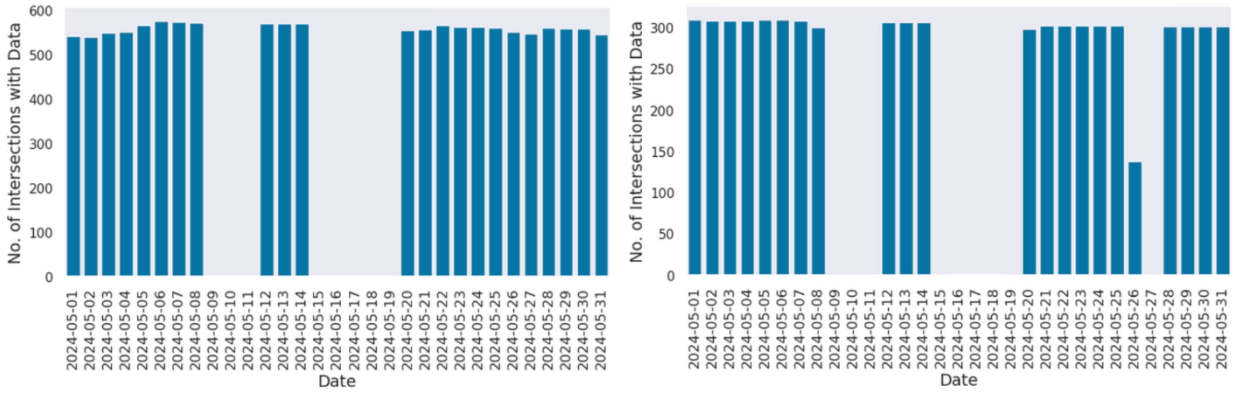

(a) Orange County **(b) Seminole County**

Figure 4-8. Daily Frequency Distribution of Intersections with Detectors Producing Controller Event Log Data in May 2024

Figure 4-9 presents the results of the second and final step of ESQC. **Figure 4-9 (a)** and **Figure 4-9(b)** show that for both Orange and Seminole counties, detectors in nearly every intersection produced very poor-quality data until May 20, 2024. Each line in the figure represents different intersections. Given that all intersections failed on specific days, it is probable that the cause was a system-wide outage or maintenance activity rather than an issue at each individual intersection. The quality began to improve after this date across all the intersections. The figures also indicate that detectors in Seminole County intersections were more consistent in producing high-quality data compared to those in Orange County.

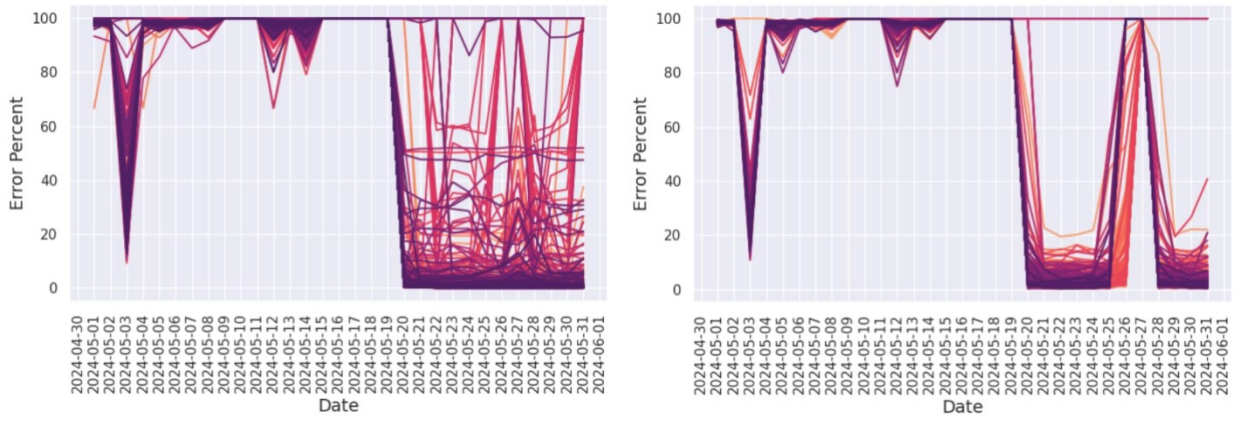

(a) Orange County **(b) Seminole County**

Figure 4-9. Daily Error Percent Distribution of Intersections with Detectors Producing Controller Event Log Data in May 2024

4.3. Intersection Selection

4.3.1. Intersection Selection

In selecting the intersections, our primary focus was to maximize the inclusion of ATSPM-equipped intersections with the optimal detector configurations (see Section 4.1.3 and **Figure 4-5**), especially for through phases. We selected the intersections in two different ways. They are:

e) Direct recommendation from Florida Department of Transportation (FDOT).
f) Randomly sampling ATSPM-equipped intersections with the optimal detector configurations for the through phase (see **Section 4.1.3**, **Figure 4-5(b),** and **Table 4-3**) that produce high-quality controller event log data (see **Section 4.2** and **Figure 4-7**).

4.3.1.1. Direct Recommendation from FDOT

FDOT recommended 13 ATSPM equipped intersections. Out of the 13, one was from Orange County, and 12 were from Seminole County. **Figure 4-10** presents the recommended intersections along with their unique signal identifiers. Experts from FDOT selected these intersections by analyzing variations in detector configurations and geometries, controller event log data, channel (i.e., detector) activation status and more.

It is important to note that the initial project scope only included ATSPM-equipped intersections from Seminole County. However, as FDOT recommended one intersection from Orange County, we are now also considering ATSPM-equipped intersections from Orange County within the scope of this project.

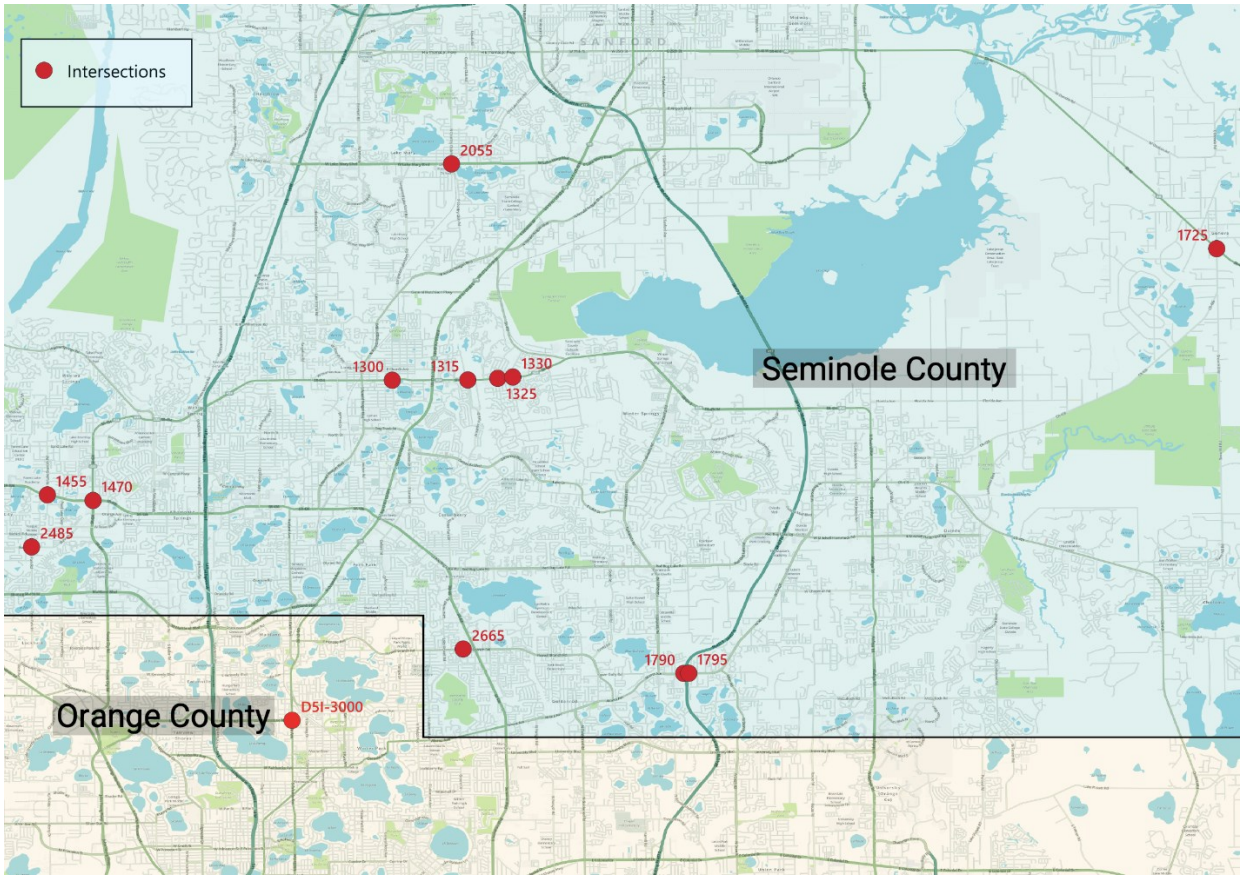

Figure 4-10. Recommended Intersections from FDOT

Checking Detector Configuration Groups and Data Quality

We analyzed the intersections recommended by FDOT using the available data. Specifically, we identified the detector configuration groups (by phase type, as defined in **Figure 4-5**) for the recommended intersections. Also, we applied our proposed ESQC to verify whether the detectors at these intersections produced any high-quality data in May 2024.

Figure 4-11 presents the results of our analysis on detector configuration groups. **Figure 4-11(a)** shows that the left-turn phase detector configuration of all recommended intersections from FDOT is 'Type 2.' **Figure 4-11(b)** reveals the infrequency of the optimal detector configurations (i.e., 'Types 4, 9, 11') for the through phase. **Figure 4-11(c)** indicates that there are five intersections with a dedicated right-turn phase that have no detectors.

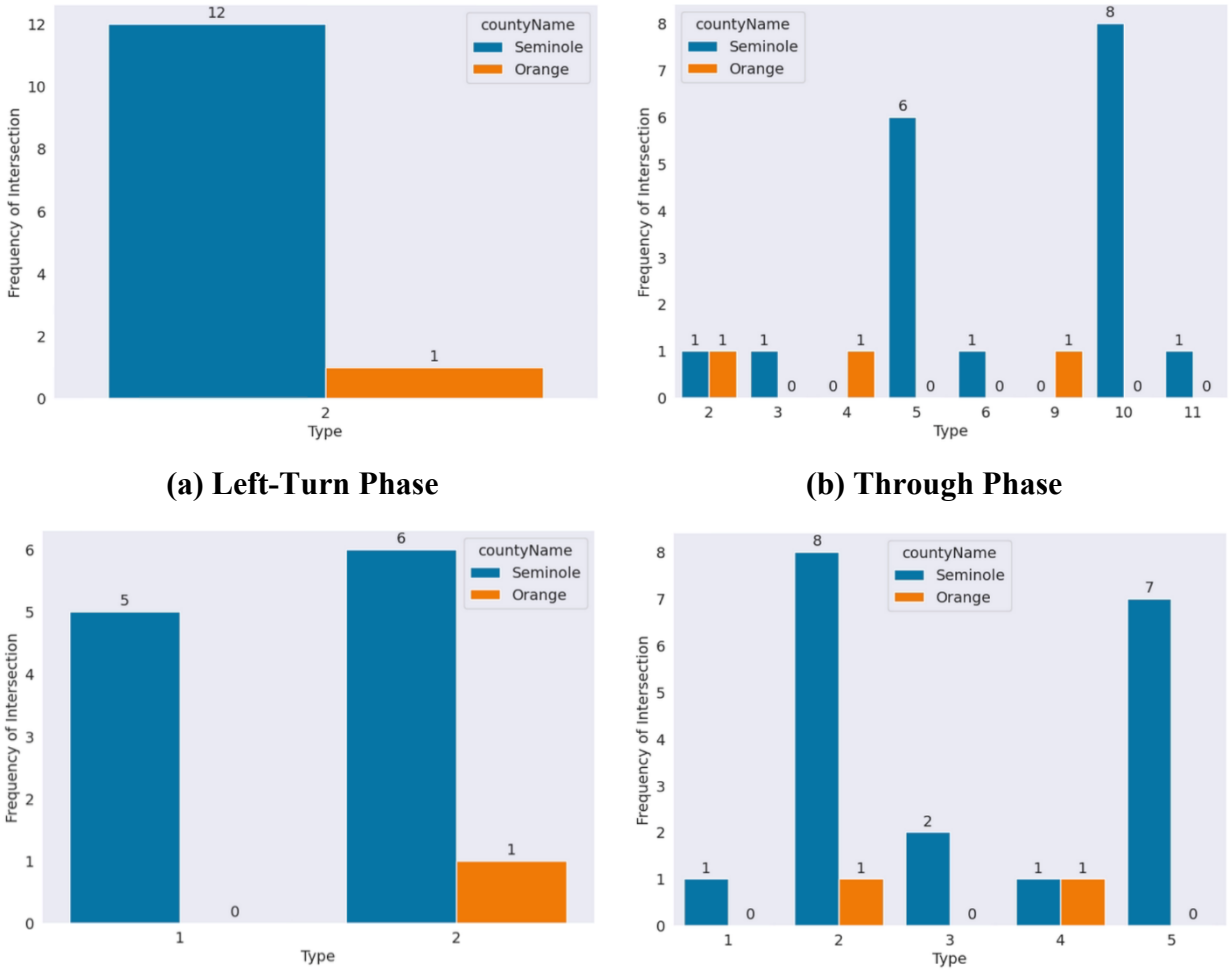

(a) Left-Turn Phase

(b) Through Phase

(c) Right-Turn Phase

(d) Shared Phase

Figure 4-11. Frequency Distribution of the Recommended ATSPM equipped Intersections per Unique Detector Configuration by Type of Phase

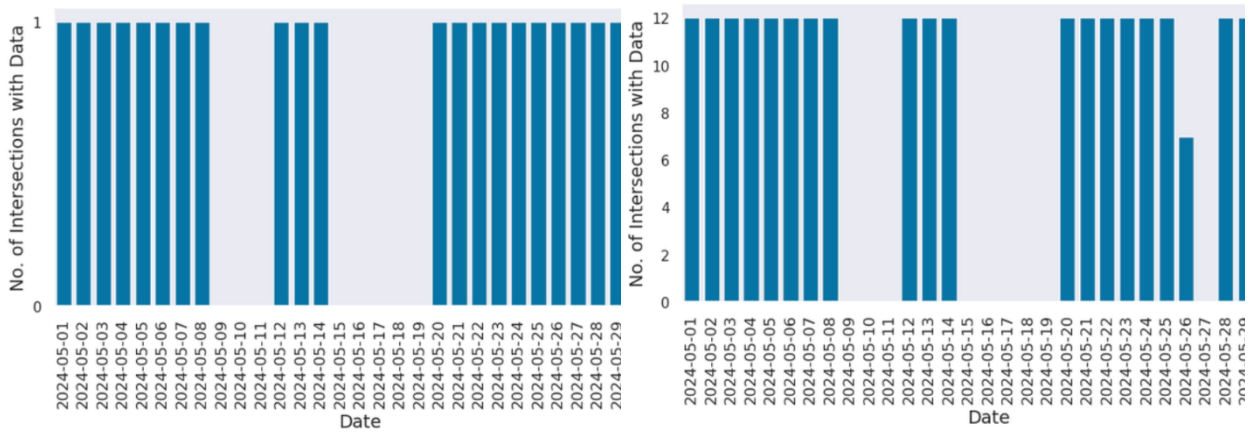

(a) Orange County **(b) Seminole County**

Figure 4-12. Daily Frequency Distribution of the Recommended Intersections with Detectors Producing Controller Event Log Data in May 2024

Figure 4-12 and **Figure 4-13** show that detectors in all the recommended intersections are producing high-quality data after May 20, 2024. Each line in figures 5-4(a) and 5-4(b) represents different intersections. However, detectors in the intersections in Seminole County exhibited some anomalies on May 26-27.

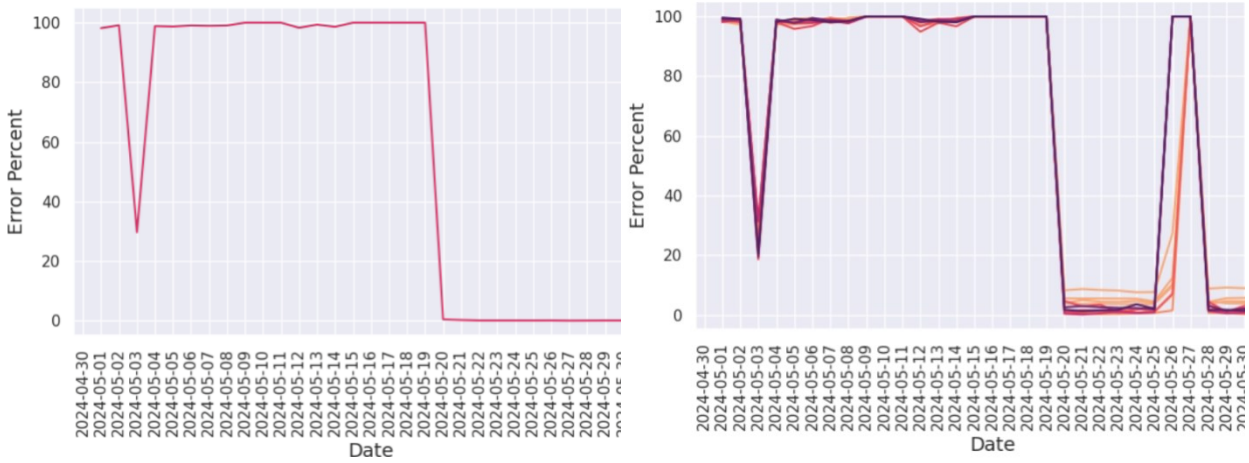

(a) Orange County **(b) Seminole County**

Figure 4-13. Daily Error Percent Distribution of the Recommended Intersections with Detectors Producing Controller Event Log Data in May 2024

From our analysis of the recommended intersections, we concluded that more intersections with detectors producing high-quality data are needed, particularly those with 'Types 4, 9, 11' detector configurations along through phase.

4.3.1.2. Sampling Intersections with Optimal Detector Configuration

In Orange and Seminole counties, 373 intersections have optimal detector configuration along through phase (i.e., 'Types 4, 9, 11'). To select a sample of these intersections, we implemented a stratified random sampling technique, focusing on intersections with optimal detector configurations along through phase. The intersections were divided into 11 strata based on unique detector configurations along through phase (see **Figure 4-5(b)**). Our strata of interest were 'Types 4, 9, 11.' Moreover, we limited our selection to Seminole County and sampled 7 ATSPM-equipped intersections from this area, as shown in **Figure 4-14**.

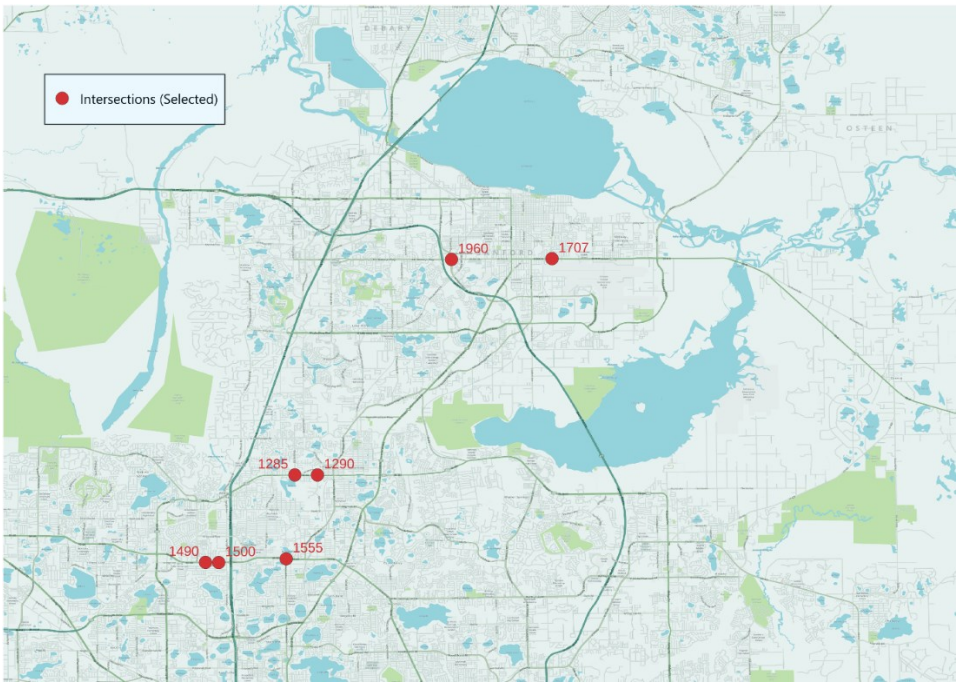

Figure 4-14. Selected Intersections (Seminole County) through Stratified Sampling

The frequency distribution of the selected intersections per unique detector configuration by type of phase is depicted in **Figure 4-15**. We selected the intersections exclusively from Seminole County. **Figure 4-15(b)** shows that our selection resulted in a higher number of optimal detector configurations (i.e., 'Types 4, 9, 11') along through phase compared to those recommended by FDOT. Moreover, the variation in detector configuration types for the left-turn phase also increased with our selection using the stratified sampling technique.

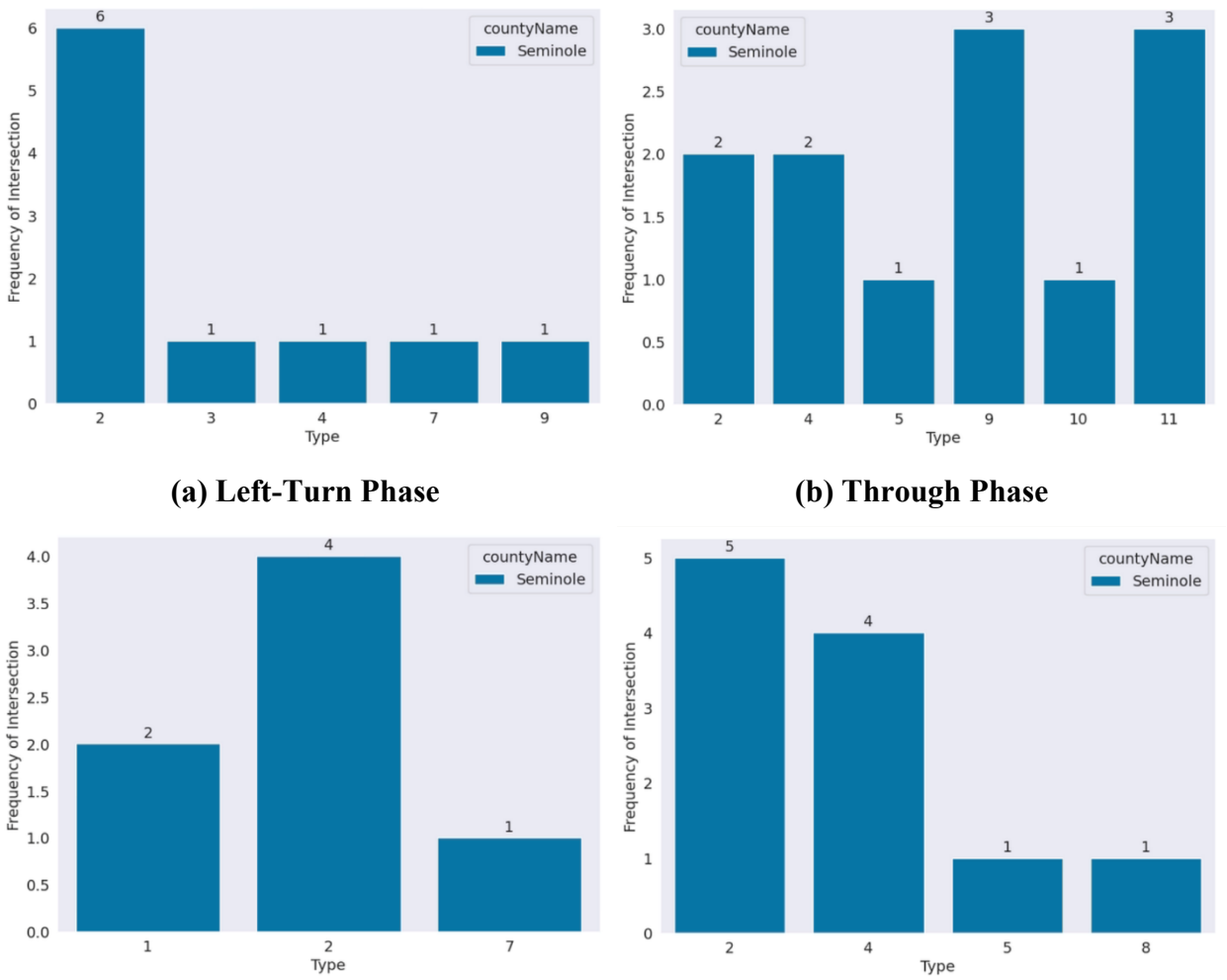

(a) Left-Turn Phase **(b) Through Phase**

(c) Right-Turn Phase **(d) Shared Phase**

Figure 4-15. Frequency Distribution of the Selected ATSPM equipped Intersections

We also ensured that our selected intersections were not only generating data (**Figure 4-16(a)**) but that the data was of high quality (**Figure 4-16(b)**), especially after May 20, 2024, by applying ESQC. Each line in the figure 4-5(b) represents different intersections.

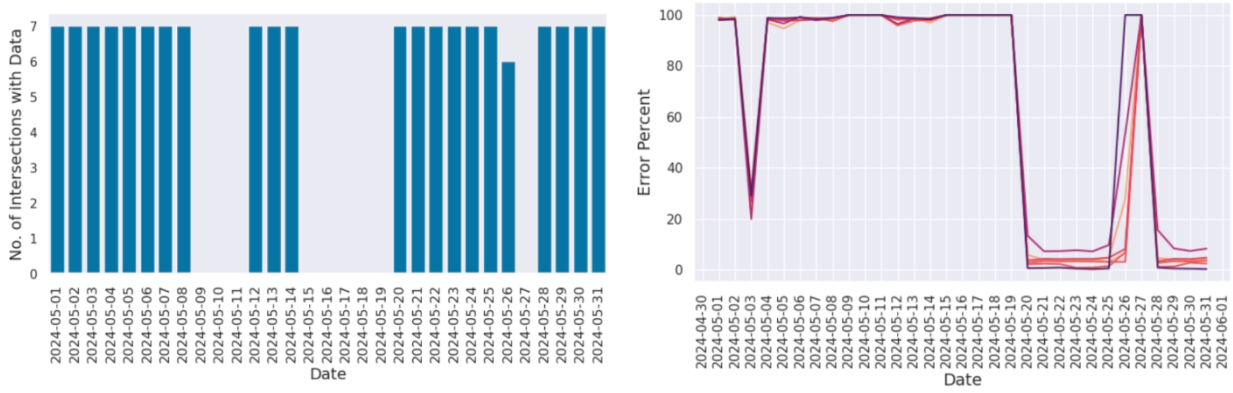

(a) Step 1 of ESQC (Figure 4-7

(b) Step 1 of ESQC (Figure 4-7)

Figure 4-16. Applying ESQC on the Selected Intersections

4.3.2. Summary of Selected Intersections

Table 4-4 presents a descriptive summary of the ATSPM equipped intersections recommended and selected for future tasks.

Table 4-4. Descriptive Summary of Recommended and Selected Intersections

Signal ID	SIIA ID	Intersection Name	Latitude	Longitude	Type of Intersection	Nos. of Lane in Through Phase** (maj1, maj2) / (min1, min2)*	County	Remarks
1300	44	SR-434 at Grant St	28.69785	-81.33809	4-Legged	(2, 2) / (1, 1)	Seminole	Recommend by FDOT
1315	1178	SR 434 at North Winter Park Dr	28.69792	-81.31766	3-Legged	(2, 2) / (0, 0)		
1325	1188	SR 434 at Edgemon Ave	28.69835	-81.30957	4-Legged	(2, 2) / (1, 1)		
1330	1190	SR 434 at Moss Rd	28.6987	-81.30548	4-Legged	(2, 2) / (1, 1)		
1455	1225	SR 436 & Academy Dr / Lake Brantley Rd	28.66686	-81.43134	4-Legged	(3, 3) / (1, 1)		
1470	620	SR 436 @ SR 434	28.66535	-81.419	4-Legged	(3, 3) / (3, 3)		
1725	1397	SR 46 & CR 426 (1st St)	28.73339	-81.11515	4-Legged	(1, 1) / (1, 1)		
1790	1421	SR 426 & SR 417 SB Ramp	28.61863	-81.25926	3-Legged	(2, 3) / (0, 0)		
1795	1426	SR 426 & SR 417 NB Ramp	28.61866	-81.25791	3-Legged	(3, 2) / (0, 0)		
2055	234	Lake Mary Blvd & Country Club Rd	28.75629	-81.32206	4-Legged	(2, 2) / (1, 1)		
2485	4122	Bunnel Rd @ Eden Park	28.6528	-81.43563	4-Legged	(1, 1) / (1, 1)		

2665	4175	Howell Branch Rd at Plaza Entrance (Butler)	28.62521	-81.31892	4-Legged	(2, 2) / (1, 1)		
D5I-3000	515	US 17/92 at SR423/Lee Rd	28.60595	-81.36518	4-Legged	(2, 2) / (2, 1)	Orange	
1285	53	SR-434 @ Range Line Rd	28.69786	-81.36221	4-Legged	(2, 3) / (1, 1)	Seminole	Selected by UCFSST
1290	42	SR-434 at Florida Central Pkwy	28.69783	-81.35289	4-Legged	(2, 2) / (1, 1)		
1707	4197	SR 46 & Mellonville Ave	28.7868	-81.2562	4-Legged	(2, 2) / (1, 1)		
1500	794	SR436 @ Westmonte dr	28.66183	-81.39358	4-Legged	(4, 4) / (1, 1)		
1490	72	SR-436 at Lynchfield Ave / Frances Dr	28.66189	-81.39902	4-Legged	(4, 3) / (1, 1)		
1555	65	SR-436 / Semoran Blvd / Altamonte Dr at CR-427 / Maitland Ave	28.66335	-81.36578	4-Legged	(3, 3) / (1, 1)		
1960	254	HE Thomas Jr Pkwy @ Airport Blvd	28.78647	-81.29763	4-Legged	(2, 2) / (2, 2)		

* Each major and minor road can have multiple approaches. For instance, at a four-legged intersection, there can be two approaches along the major roads (maj1 and maj2) and two approaches along the minor roads (min1 and min2).

** An approach along a road may not have any through phase.

The quality of data was checked using our Event Sequence Quality Checker (ESQC). In particular, we checked signal timing ('start of green - start of yellow - start of red clearance - start of red') and detector on-off ('detector on - detector off') sequence. The check results of the 19 intersections in Seminole County are depicted in **Figures 2-1** and **2-2**.

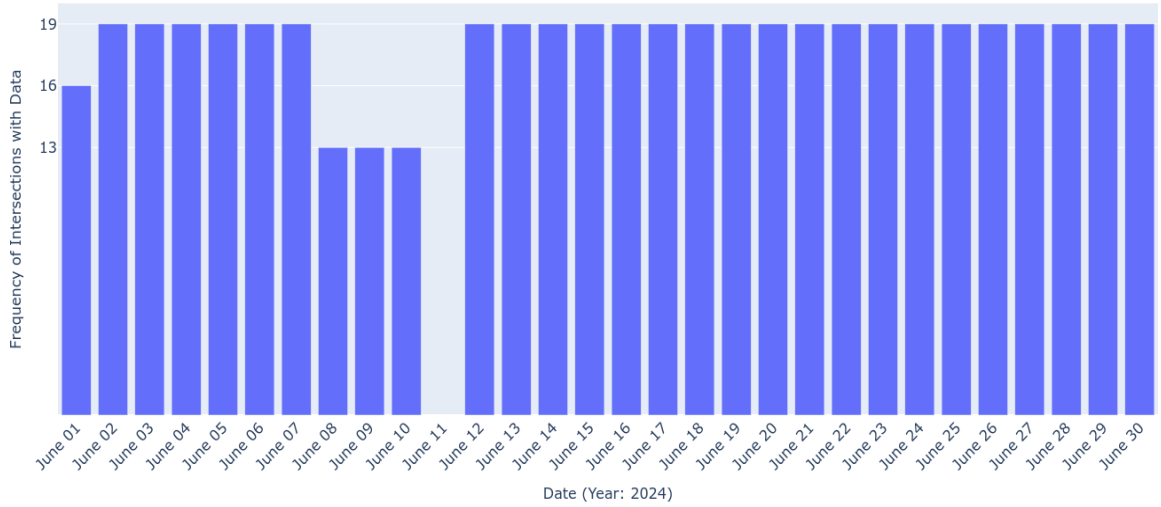

Figure 4-17. Daily Frequency Distribution of Intersections with Detectors Producing Controller Event Log Data in June 2024

Figure 4-17 shows that, on average, detectors at the selected 19 intersections reported data for 29 days in June 2024. Detector activity at a few intersections exhibited slight fluctuations until June 10. However, the activity became stable and consistent from June 12 through the end of the month.

The daily error percentage trend depicted in **Figure 4-18** indicates that detectors at most intersections produced data with an average error percentage below 10% throughout June 2024, demonstrating the reliability of the data used for Task 2. The only exception was the detectors at the intersection of SR 436 and SR 434 (Signal ID: 1470), which produced data with error

percentages exceeding 10% but remaining below 20%. In the analysis, all 19 intersections were retained after removing the erroneous sequences.

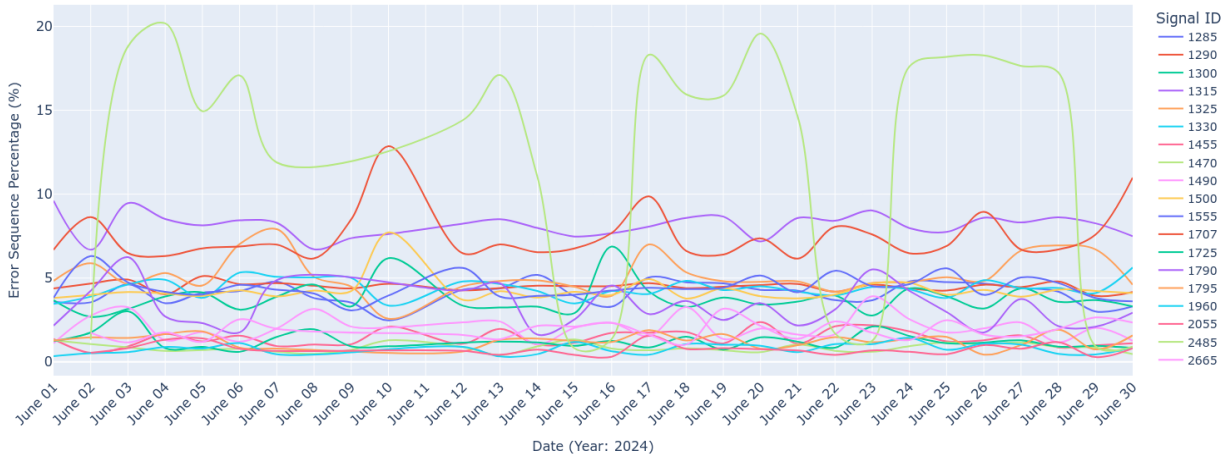

Figure 4-18. Daily Error Percent Distribution of Intersections with Detectors Producing Controller Event Log Data in June 2024

CHAPTER 5: Algorithm Development

We selected 20 intersections in Seminole and Orange counties in District 5, Florida, USA, by analyzing detector configuration and checking the quality of controller event log data. This chapter overviews the process of transforming accurate controller event log data into meaningful performance measures. The term "intersections" in this report specifically refers to those equipped with the Automated Traffic Signal Performance Measures (ATSPM) system.

5.1. Performance Measure Calculation

5.1.1. Detector Configuration (Simplified)

The controller event log data produced by detectors installed at intersections can be processed to derive various performance measures, such as volume, occupancy, headway, red-light running, and more. However, this transformation heavily relies on the detector configuration at the intersections.

Detector configurations at intersections can vary significantly. Not all approaches (major or minor roads) to an intersection may have the necessary detector configuration. Again, variations in configuration are common across different phases, such as left-turn movements or through movements (which may include right-turns). In some cases, differences in configuration can also occur between lanes within the same phase.

In this chapter, a summary of the detector configurations for the selected 19 intersections, as shown in **Figure 5-1**, is provided in simplified layouts. At the lowest spatial resolution (per lane

per phase per approach), the detector configuration of the selected intersections can be structured into 6 types, as illustrated in **Figure 5-1**.

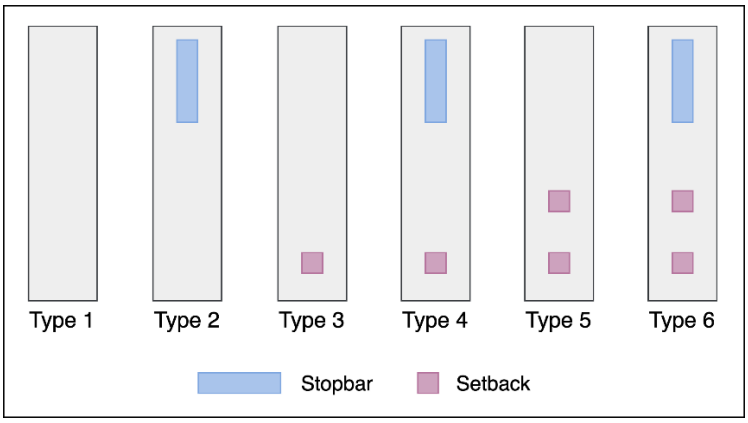

Figure 5-1. Schematic Diagram of the Detector Configurations by Lane

The phase and lane are two distinct concepts for the configuration taxonomy. A phase (left-turn, or through (+right-turn) movements) can consist of different lane types, such as left-turn, through, right-turn, or shared lanes.

Table 5-1. Phase-Lane Relation

Phase Type	**Related Lane Type**
Left-Turn	Left-Turn, Shared (Left-Turn + Right-Turn)
Through (+Right-Turn)	Through, Right-Turn, Shared (Left-Turn + Through + Right-Turn, Left-Turn + Through, Through + Right-Turn)

Given the lane-level detector configuration across the selected intersections is not consistent, deriving performance measures at the lowest spatial resolution (per lane per phase per approach) is not always achievable. This limitation was considered in calculating performance measures from controller event log data.

Table A-1 in **A. Appendix** provides a summary of the detector configurations for each intersection, including details on approach type, phase type, and lane type.

5.1.2. Transformation

When processed correctly, controller event log data can be transformed into various Signal Phasing and Timing (SPaT) and traffic-related performance measures. Our objective was to derive these measures at the lowest possible temporal resolution (i.e., cycle-level) and, where feasible, at the lowest spatial resolution (i.e., per lane per phase per approach). In cases where lane-level measures could not be calculated, we opted for the next higher spatial resolution (e.g., per phase per approach).

The transformation generated performance measures that primarily include SPaT, volume, occupancy time, headway, conflicts, red-light running, pedestrian activity indicator, pedestrian delay, and shockwave properties.

5.1.2.1. Signal Phasing and Timing (SPaT)-Related Measures

The SPaT-related measures include the duration of different signal types (i.e., green, yellow, red clearance, and red) as well as the cycle length. These measures were derived using event codes corresponding to the start of green, yellow, and red clearance phases, and the end of red clearance (Anik et al., 2025). The start and end of all cycles were determined using the 'dual-ring, eight-phase' framework. According to this framework, a complete traffic cycle is defined as the duration between successive crossings of the "Barrier" (Day et al., 2014). Cycle length simply represents the length of each distinct complete cycle.

5.1.2.2. Vehicle Traffic-Related Measures

Vehicle traffic-related measures primarily include volume, occupancy, headway, traffic conflicts, and red-light running. These measures were derived by transforming vehicle detection

event log data generated by controllers in ATSPM systems. Figure 5-2 illustrates the vehicle detection mechanism. The detector (stop bar or setback) is activated when the front of a vehicle enters the detection zone (t_{on}) and deactivates when the rear exits the zone (t_{off}). We assumed that a valid detection event for a vehicle (n) requires a "detector on" event to always precede a "detector off" event. Instances where only one of these events was recorded were considered detection errors and were excluded from the analysis.

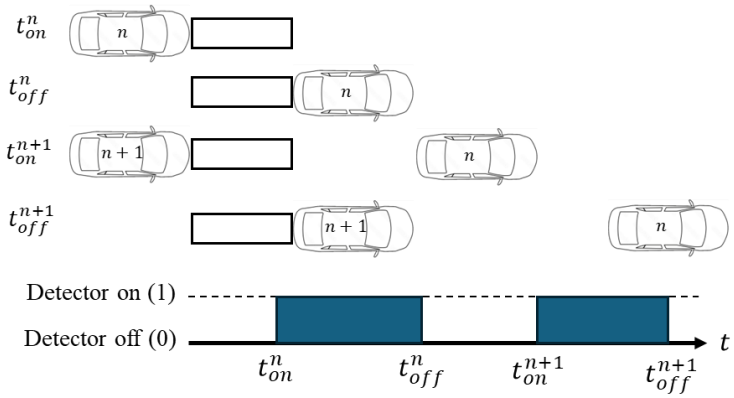

Figure 5-2. Vehicle Detection Mechanism

The **volume** of vehicles was calculated using the vehicle detection event log data from back detectors (i.e., setbacks). Setbacks are typically very short in length (6–10 feet), enabling them to distinctly capture the "detector on" and "detector off" events for each vehicle. Vehicle volume was calculated by counting all valid "detector on-off" sequences, as shown in **Equation 5-1.**

$$\text{Volume} = \sum \text{Detection}_{(on-off)}^{n} \quad (5\text{-}1)$$

where n represents the sequence of a valid detection event.

Invalid sequences, such as isolated "detector on" events without a corresponding "detector off" or isolated "detector off" events without a preceding "detector on," occasionally occurred due to sensor malfunctions or data transmission errors**.** These incomplete sequences typically do not represent valid vehicle detections and were generally discarded during data processing. However, in certain cases, when the pattern of events and traffic flow suggested that an isolated "on" or "off" event was likely part of a missed detection, imputation was applied to estimate the presence of a vehicle. Specifically, if an isolated "on" or "off" event occurred within a short time window of a valid detection sequence, it was inferred that the corresponding "off" or "on" event was likely missed, and the isolated event was treated as a valid detection, contributing one vehicle to the volume count. The time window threshold for identifying these likely missed detections was not fixed arbitrarily. Instead, it was determined hourly based on the average gap between valid "detector on-off" sequences for each hour of the day.

A platoon refers to a group of vehicles traveling together, often due to coordinated signal timing or natural traffic flow dynamics. Platoon ratio quantifies the quality of progression on an approach. The platoon ratio represents the ratio of the number of vehicles arriving during the green phase to the proportion of the green interval of the total cycle. This can be expressed as (**Equation 2-2**):

$$\text{Platoon Ratio}, R_p = \frac{\text{Volume}_G}{\text{Volume}_{\text{Total}}} \times \frac{C}{\text{Signal Duration}_G} \quad (2\text{-}2)$$

where Volume_G represents volume of vehicle arriving during green signal. C and Signal Duration_G represent cycle length (in sec), and duration (in sec) of green signal, respectively.

The arrival type is a qualitative measure of how well vehicles are grouped into platoons when reaching an intersection. It ranges from 1 (worst platoon condition) to 6 (best platoon condition). A higher platoon ratio typically corresponds to a better arrival type, reflecting improved traffic progression. The relationship between platoon ratio and arrival type, suggested by HCM (2000), is summarized in **Table 5-2**.

Table 5-2. Relationship Between Platoon Ratio and Arrival Type

Arrival Type	Range of Platoon Ratio	Default Value	Progression Quality
1	$R_p \leq 0.50$	0.333	Very poor
2	$0.50 < R_p \leq 0.85$	0.667	Unfavorable
3	$0.85 < R_p \leq 1.15$	1.000	Random arrivals
4	$1.15 < R_p \leq 1.50$	1.333	Favorable
5	$1.50 < R_p \leq 2.00$	1.667	Highly favorable
6	$R_p > 2.00$	2.000	Exceptional

Occupancy time is defined as the duration during which the presence zone (denoted by the stop bar) is occupied by vehicles approaching an intersection. This is calculated as the interval between the "detector on" (t_{on}^n) and "detector off" (t_{off}^n) events recorded by the stop bar detector (**Equation 2-3**).

$$\text{Occupancy Time}^n = t_{off}^n - t_{on}^n \quad (2\text{-}3)$$

A split failure occurs when a phase cannot serve all its demand within one cycle, i.e., if it takes a vehicle two or more cycles to execute its movement at an intersection, a split failure has occurred. As per Purdue, when both green occupancy ratio (GOR) (**Equation 2-4**), and red

occupancy ratio in the first five seconds of red (ROR_5) (**Equation 2-4**) are high (typically 80 percent or higher), a split failure occurs (**Equation 2-5**).

$$GOR = \frac{\text{Occupancy Time}_G}{\text{Signal Duration}_G};\ ROR_5 = \frac{\text{Occupancy Time}_{R-5}}{5} \tag{2-4}$$

$$\text{Split Failure} = \begin{cases} 1, & if\ (GOR \geq 80\%\ \&\ ROR_5 \geq 80\%) \\ 0, & else \end{cases} \tag{2-5}$$

where Occupancy Time_G and Signal Duration_G represent occupancy (in sec) during green signal, and duration (in sec) of green signal, respectively. $\text{Occupancy Time}_{R-5}$ represents occupancy (in sec) during the first five seconds of red signal.

Headway refers to the time interval between two consecutive vehicles approaching an intersection from the same direction. It was calculated as the time difference between the current "detector on" event (t_{on}^{n}) and the previous "detector on" event (t_{on}^{n-1}) recorded by the setback, as shown in Figure 5-3. Mathematically, headway (also called time headway) can be calculated as follows (**Equation 2-6**)

$$\text{Headway}^n = t_{on}^{n} - t_{on}^{n-1} \tag{2-6}$$

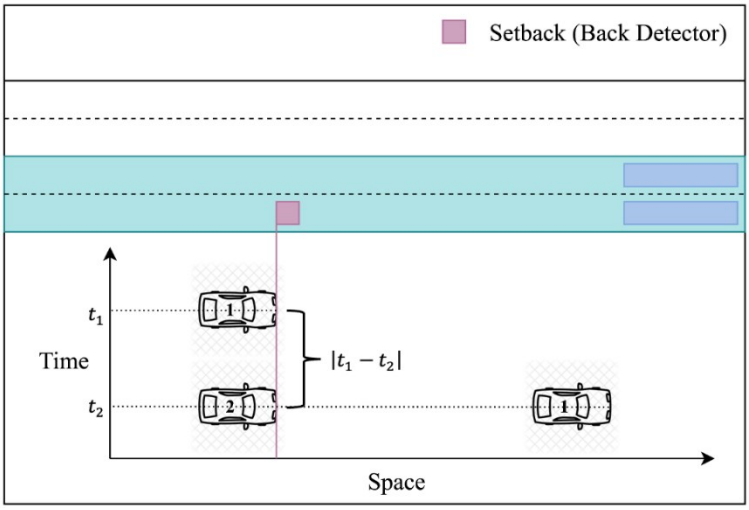

Figure 5-3. Time Headway

Speed-dependent conflict metrics, such as time-to-collision (TTC) and deceleration rate to avoid collision (DRAC), are commonly used to quantify traffic conflicts. However, these metrics require vehicle speed, which cannot be estimated at the selected intersections or any other intersections in Seminole County due to the detector configuration (detectors do not measure vehicle length). To address this limitation, headway was used as an alternative metric for identifying traffic conflicts. A traffic conflict is defined as an event where the headway falls below a specified threshold. While there is no universally accepted threshold for defining traffic conflicts, values between 1 and 3 seconds are commonly used. For instance, U.S. driver training programs indicate that maintaining a headway of less than 2 seconds is unsafe (Michael et al., 2000), while Swedish police use a threshold of 1 second (Vogel, 2003).

In this report, the threshold was set to 2 second, as it is generally considered the most critical and dangerous point in the spectrum. Traffic conflict is defined as (**Equation 2-7**):

$$\text{Conflict} = \begin{cases} 1, & if\ \text{Headway} \leq 2\ \text{sec} \\ 0, & else \end{cases} \quad (2\text{-}8)$$

A Red Light Running (RLR) event occurs when a vehicle enters an intersection after the traffic signal has turned red, thereby violating the red signal. Calculating RLR events using ATSPM systems requires detectors to be placed at the edge of the approach to the intersection. While stop bar detectors are typically installed at this location, they present a challenge for accurately identifying RLR events due to their large detection length (typically greater than 50 feet). Because stop bar detectors can accommodate more than one vehicle at a time, they do not reliably indicate whether a vehicle has violated the red signal. For instance, if one vehicle violates the red signal while another vehicle is already on the stop bar, the detector will remain activated,

making it difficult to distinguish RLR events. To address this limitation, we propose an algorithm to estimate RLR events using only "detector off" events recorded by stop bar detectors. Specifically, if a "detector off" event is recorded during the red clearance or red, the event is flagged as RLR, regardless of whether the corresponding "detector on" event occurred during the green, yellow, red clearance, or red.

It is important to note that this method provides a close approximation rather than a precise estimation, as there may be situations where an RLR event occurs, but the "detector on" event persists due to multiple vehicles occupying the stop bar. Therefore, instead of estimating the frequency of RLR events, we focused on flagging red clearance or red signal with potential RLR occurrences, using an indicator of 0 (no RLR) and 1 (RLR). The RLR flagging scenario is illustrated in **Figure 5-4**.

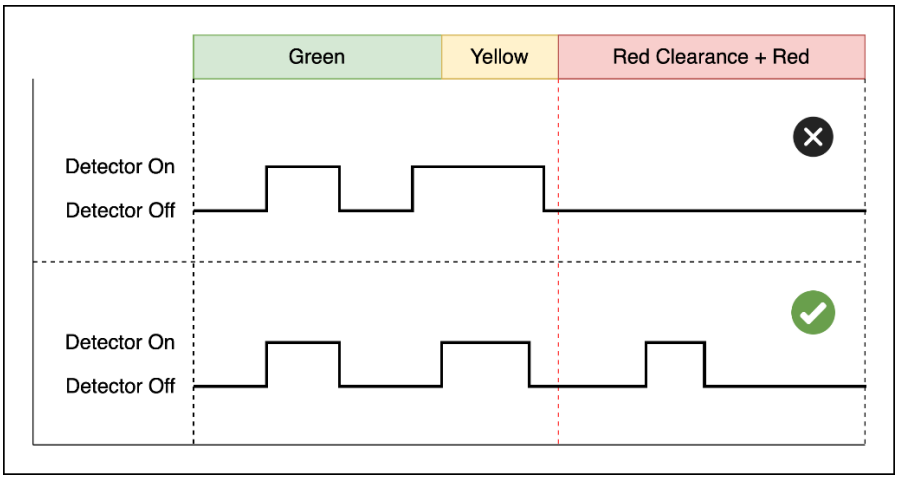

Figure 5-4. Red Light Running Flag Using "Stop Bar"

RLR is defined as (**Equation 2-9**):

$$\mathrm{RLR} = \begin{cases} 1, & if\ \mathrm{Any}\left(\mathrm{Detector}_{off(RC,R)} \middle| \mathrm{Detector}_{on(G,Y,RC,R)}\right) \\ 0, & else \end{cases} \tag{2-9}$$

where $G, Y, RC,$ and R represent the different signal types namely green, yellow, red clearance, and red, respectively.

All vehicle traffic-related performance measures were calculated at a cycle-level temporal resolution, with spatial resolution varying between lane-, phase-, and approach-level depending on the measure. Variations in the measures across different signal types were also recorded. A detailed descriptive summary of these measures is provided in **Table 5-3**.

5.1.2.3. Pedestrian Traffic-Related Measures

Pedestrian activity indicator and delay are pedestrian traffic-related measures that can be calculated using pedestrian detection event log data. At the selected intersections in Seminole County, the ATSPM systems detect pedestrians via push buttons. Specifically, the pedestrian detector is activated ($t_{p,on}$) when a pedestrian presses the button and is automatically deactivated ($t_{p,off}$) after a short duration. We assumed that a valid pedestrian detection event requires a "pedestrian detector on" event to precede a "pedestrian detector off" event. Any instance where only one of these events was recorded was considered a detection error and excluded from the analysis.

One limitation of pedestrian detectors in ATSPM systems is that they are not fully compatible with quantifying pedestrian volume. For example, if multiple pedestrians intend to cross an intersection, only those who press the button are recorded, while others are not. As a result, the detectors cannot provide an accurate count of the total number of pedestrians. However, this limitation does not diminish the utility of pedestrian detectors.

Pedestrian activity indicator was calculated to determine the presence of pedestrians using the "pedestrian detector on" and "pedestrian detector off" events. This indicator represents a binary

variable with values 0 (no pedestrian present) and 1 (pedestrian present), that can be mathematically expressed as (**Equation 2-10**):

$$\text{Pedestrian Activity Indicator} = \begin{cases} 1, & if\ \text{Detection}_{p,(on-off)} \\ 0, & else \end{cases} \quad (2\text{-}10)$$

Pedestrian delay is defined as the time a pedestrian waits after pressing the button until the pedestrian signal begins (start of the "Walk" signal). This wait time was calculated as the difference between the timestamp of the first button press and the start of the pedestrian signal. Mathematically, pedestrian delay is expressed as (**Equation 2-11**):

$$\text{Pedestrian Delay} = t_{p,\text{Walk Begin}} - \left(t_{p,on} \middle| \text{First Press}\right) \quad (2\text{-}11)$$

All pedestrian traffic-related performance measures were calculated at a cycle-level temporal resolution, and phase-level spatial resolution. A detailed descriptive summary of these measures is provided in **Table 5-3**.

Table 5-3. Descriptive Summary of Performance Measures

Task Group	Performance Measures	Unit	Detector Configuration	Temporal Resolution	Spatial Resolution	Variation by Signal Type
Counting	Vehicle Volume	Count	Types 3, 4, 5, 6	Cycle-Level	Approach-Level*	✓
	Pedestrian Activity Indicator	Binary Count (0 / 1)	-		Phase-Level	-
Progression	Percent Arrival on Green	%	Types 3, 4, 5, 6		Approach-Level*	-
	Platoon Ratio	-	Types 3, 4, 5, 6		Approach-Level*	-
	Occupancy Time	Seconds	Types 2, 4, 6		Lane-Level	✓
	Split Failure	Count	Types 2, 4, 6		Lane-Level	-
	Pedestrian Delay	Seconds	-		Phase-Level	-
Safety	(Time) Headway	Seconds	Types 3, 4, 5, 6		Approach-Level*	✓
	Conflict (Vehicle-Vehicle)	Count	Types 3, 4, 5, 6		Approach-Level*	✓
	Red Light Running (Flag)**	Binary Count (0 / 1)	Types 2, 4, 6		Lane-Level	-
	Pedestrian-Vehicle Conflict Propensity***	Numeric (0-1)	Types 2, 4, 6		Phase-Level	-

*Resolution at the phase and lane levels is feasible; however, approach-level resolution offers the highest accuracy.

**Approximate estimation.

***Determined using pedestrian exposure and vehicle exposure during pedestrian activity duration

5.2. Exploratory Data Analysis and Safety Scoring

In this chapter, we provide an overview of the exploratory analysis carried out on the performance measures to gain insights necessary for making recommendations on the six metrics for the selected intersections.

5.2.1. Data Aggregation

The performance measures were calculated from controller event log data at a cycle-level temporal resolution. While this resolution is highly effective for capturing the nuances of Signal Phasing and Timing (SPaT) and traffic conditions at intersections, understanding broader temporal patterns requires data aggregation over longer intervals. To gain insights into these patterns, the data was aggregated at 15, 30, 45, and 60-minute intervals.

5.2.2. Data Analysis

In Task 3, we primarily relied on performance measures aggregated at 60-minute intervals (i.e., hourly temporal resolution) to provide hourly recommendations on the six metrics. Therefore, this section mainly focuses on presenting the hourly trends and distributions of the various calculated measures. Along with the trends, 95% confidence intervals are shown to account for the variability in the data. The confidence intervals are calculated under the assumption that the sampling distribution of the mean is approximately normal. This assumption is valid given our sufficiently large sample size (n > 30), which allows the application of the Central Limit Theorem. The intervals were computed using **Equation 3-1**.

$$\mathrm{CI} = \bar{x} \pm z\left(\frac{s}{\sqrt{n}}\right) \tag{2-10}$$

where $\bar{x}$ is the sample mean, z is 1.96 for a **95% confidence level** (assuming normal distribution), s is the sample standard deviation, and n is the sample size.

Although all intersections were analyzed, for clarity, the hourly trends and distributions are illustrated for only one study intersection. The intersection at SR436 and Westmonte Drive (Signal ID: 1500), as shown in **Figure 5-5**, were chosen for the presentation of our analysis, as it had the most comprehensive detector configuration (see **Table A-1**), allowing the calculation of almost all performance measures, including measures for right-turn lanes.

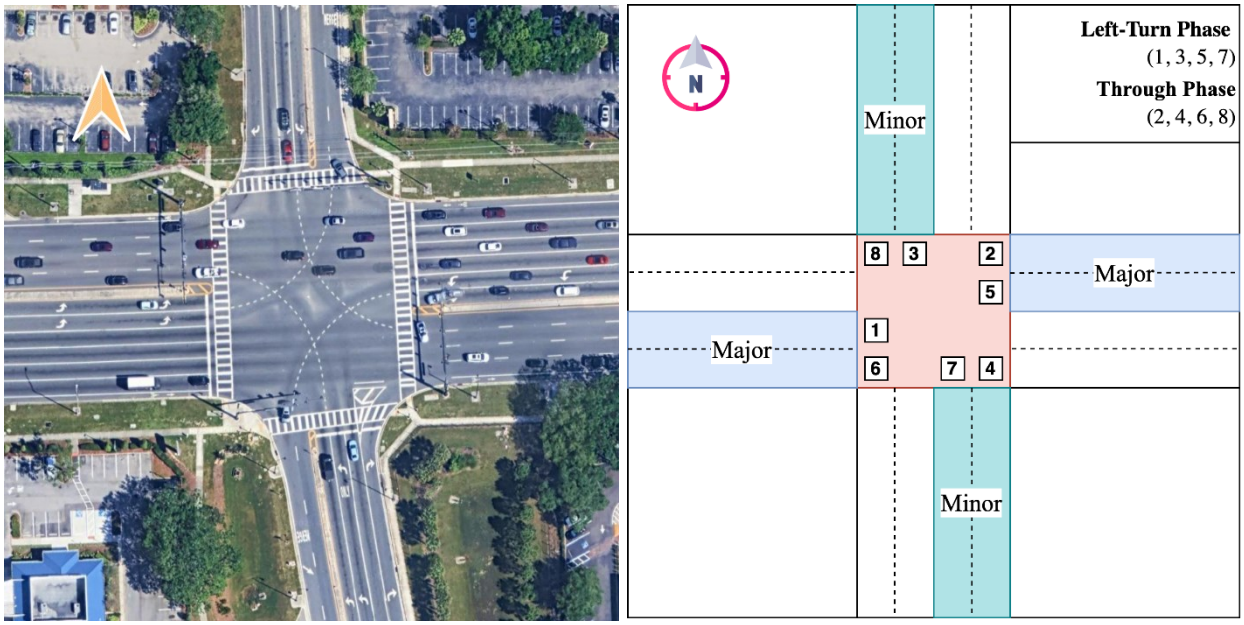

(a) **(b)**

Figure 5-5. Intersection at SR436 and Westmonte Drive (Signal ID: 1500)

It is important to note that while the temporal resolution for trends and distributions is hourly, the spatial resolution follows the phase-specific resolutions outlined in **Table 5-3**.

5.2.2.1. Signal Phasing and Timing (SPaT)-Related Measures

Figure 5-6 illustrates the hourly variation in cycle length at the intersection of SR436 and Westmonte Drive, along with the 95% confidence interval (CI) to capture variability in cycle length throughout the day.

- Between midnight and early morning (12:00 AM – 3:00 AM), cycle lengths are significantly high, likely due to low traffic volumes and signal control strategies that allocate longer cycles when fewer vehicles are present.
- A steep increase is observed during the morning peak hours (6:00 AM – 9:00 AM), coinciding with increased traffic demand as commuters travel to work.
- The afternoon and evening period (4:00 PM – 8:00 PM) exhibits relatively stable cycle lengths, likely due to consistent traffic demand. However, after 8:00 PM, cycle lengths begin to decline, reflecting reduced vehicle volumes and potentially shorter green phases.
- The confidence interval remains wide during both midnight and morning peak hours, indicating greater variability in cycle lengths during these times. This could be attributed to irregular traffic patterns, signal control adjustments, or fluctuating vehicle arrivals, particularly in low-traffic conditions.

Overall, this analysis highlights the dynamic nature of traffic signal operations throughout the day, with cycle lengths adapting based on time-of-day traffic conditions and operational strategies.

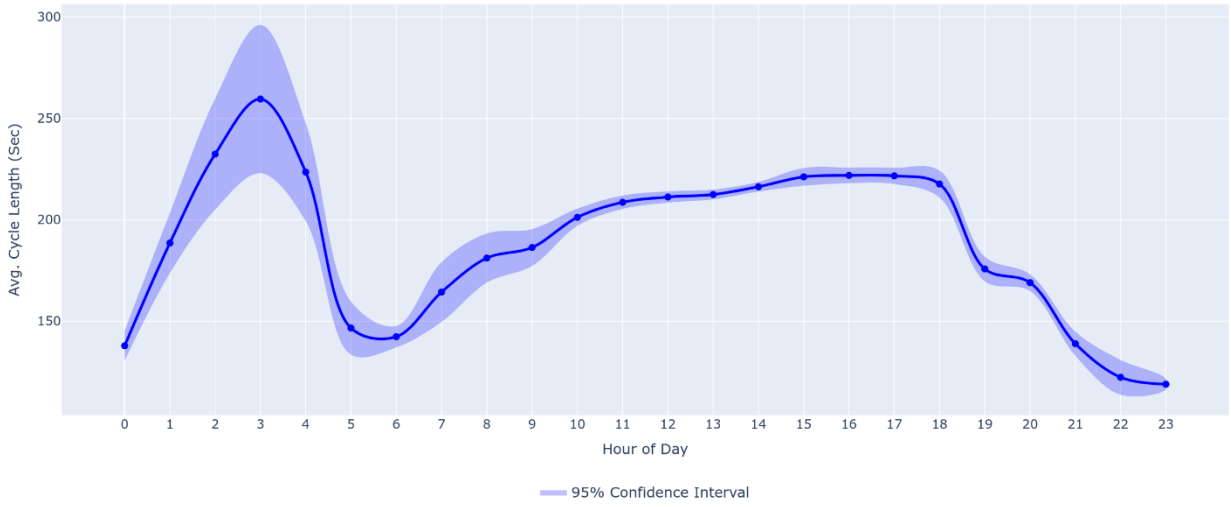

Figure 5-6. Hourly Trend of Cycle Length

Figure 5-7 presents the hourly variations in signal durations for green, yellow, red clearance, and red signals across left-turn (Phases 1, 3, 5, 7) and through phases (Phases 2, 4, 6, 8). These trends illustrate how signal timings adjust throughout the day to accommodate varying traffic conditions.

Green Signal Duration:

Through phases (Phases 2, 4, 6, 8) generally have longer green times than left-turn phases due to higher traffic volumes in the through movement. Among them, Phase 2 exhibits the longest green duration, remaining consistently high throughout the day. Phase 5 (left-turn movement) shows notable peaks from noon to evening (12:00 PM – 7:00 PM), indicating periods of high left-turn demand. Phases 4 and 8 (through movements on minor road (refer to Figure 5-5)) show relatively low and stable green durations throughout the day.

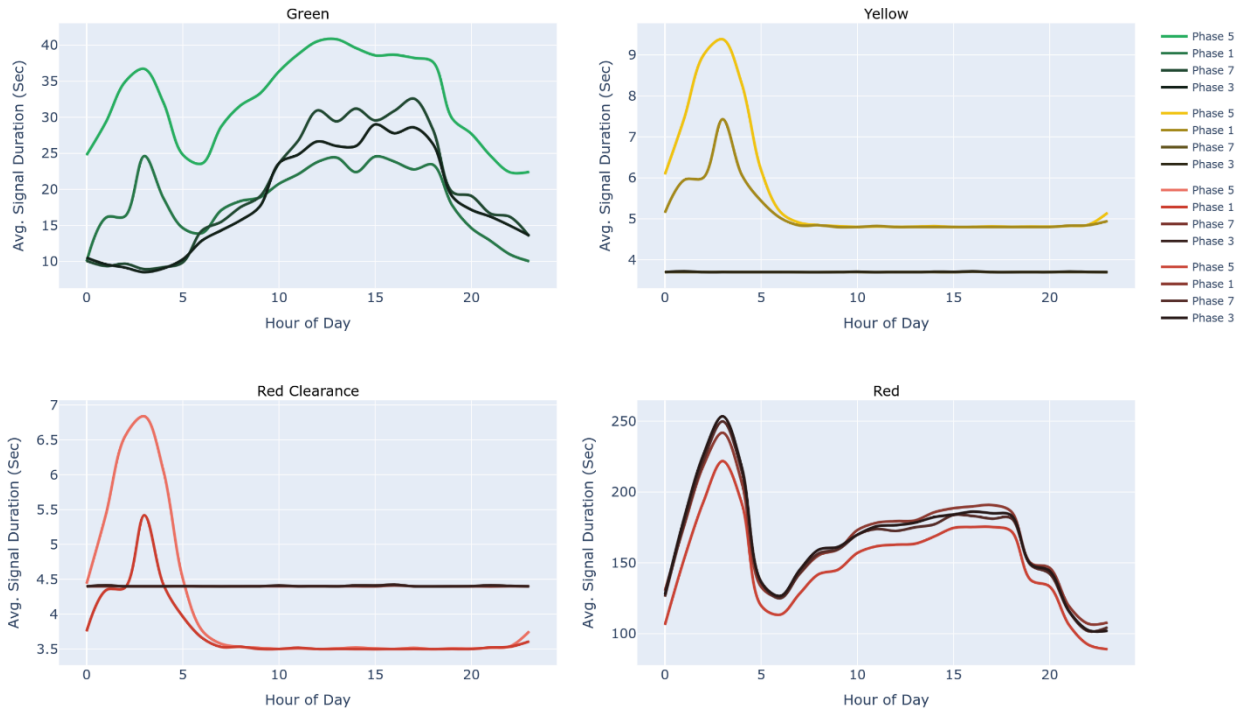

(a) Left-Turn Phases

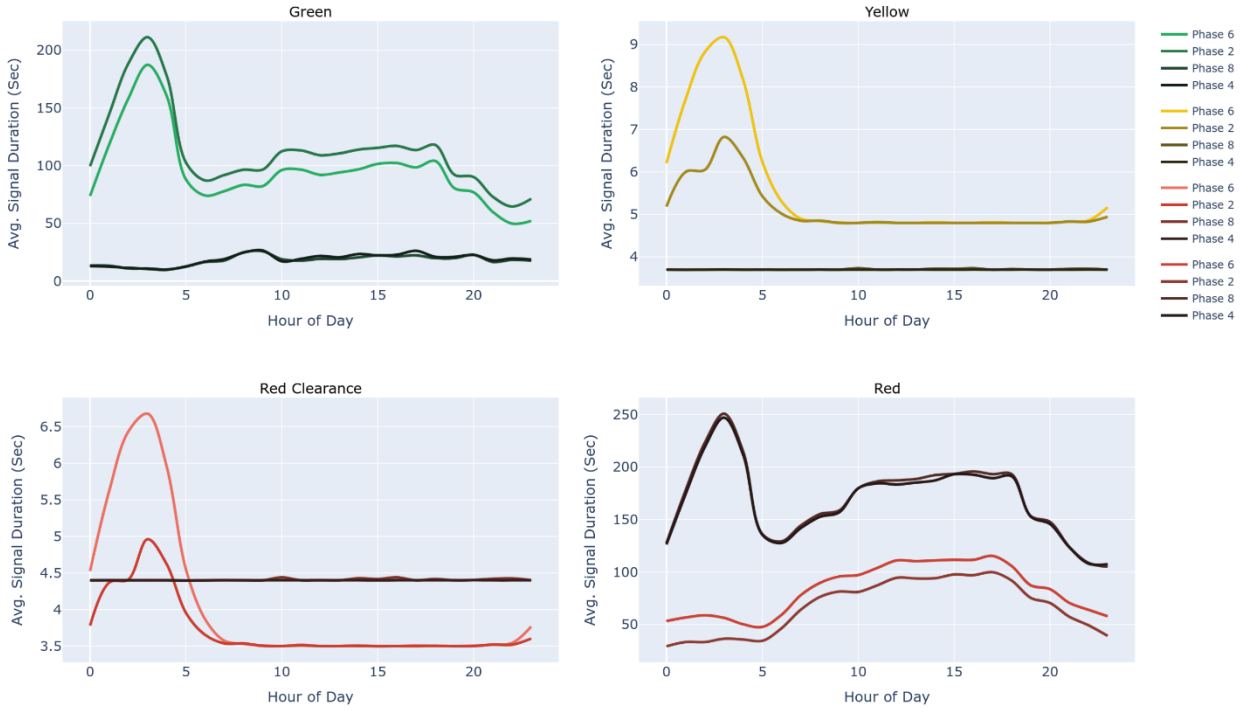

(b) Through Phases

Figure 5-7. Hourly Trend of the Duration of Different Signal Types

Yellow Signal Duration:

- Yellow durations typically range between 3–6 seconds for most phases, except between midnight and early morning (12:00 AM – 3:00 AM) on major road (Phases 1, 6, 5, and 2).
- Phases on minor road (Phases 3, 8, 7, and 4) remain constant, showing no variations throughout the day.

Red Clearance Duration:

- Red clearance durations mostly fall within the expected range of 2–6 seconds, ensuring adequate clearance time for vehicles exiting the intersection.
- After 8:00 AM, red clearance durations for phases on major roads are shorter compared to those on minor roadways.

Red Signal Duration:

- Left-turn phases (Phases 1, 5, 3, and 7) consistently have longer red durations throughout the day, indicating signal priority for through movements.
- Through phases (Phases 2 and 6) on major roads have the shortest red durations compared to all other phases.

5.2.2.2. Vehicle Traffic-Related Measure

Figure 5-8 presents the hourly trends of vehicle volumes observed during green and red signals for each approach at the intersection of SR436 and Westmonte Drive. The figure highlights the differences in traffic demand between major (westbound and eastbound) and minor (northbound and southbound) road approaches, showing how signal control prioritizes major road traffic while minor road movements experience longer red durations.

Major Road Approaches (Westbound & Eastbound):

- The westbound and eastbound approaches, which belong to the major road, exhibit significantly higher vehicle volumes, particularly during morning peak hours (7:00 AM – 9:00 AM) and evening peak hours (4:00 PM – 6:00 PM).
- Vehicle volumes remain consistently high during green signals, reflecting their priority in signal phasing.

Figure 5-8. Hourly Trend of Approach-Level Vehicle Volume

Minor Road Approaches (Northbound & Southbound):

- The northbound and southbound approaches, representing minor roads, show lower overall vehicle volumes compared to the major road approaches.
- These approaches experience moderate peaks during mid-afternoon hours (3:00 PM – 5:00 PM).

- Unlike the major roads, red signal durations dominate minor road traffic, indicating that priority is given to the major road movements.
- The confidence intervals for red signal volumes in minor road approaches are wider during peak hours, suggesting greater variability in waiting vehicles.

Figure 5-9 illustrates the hourly variations in platoon ratio for all approaches at the intersection of SR436 and Westmonte Drive, providing insights into traffic flow efficiency and signal coordination. The platoon ratio is a measure of traffic progression, where values closer to 1.0 indicate well-coordinated movement, and values significantly above 1.0 suggest favorable conditions with well-formed platoons (refer to **Table 5-2**).

Major Road Approaches (Westbound & Eastbound):

- The westbound and eastbound approaches (major roads) consistently exhibit platoon ratios between 1.15 and 1.50 during peak hours (7:00 AM – 9:00 AM and 4:00 PM – 6:00 PM), indicating favorable progression and efficient signal coordination.
- Confidence intervals are narrow, reinforcing that traffic progression remains predictable and well-regulated on these approaches.

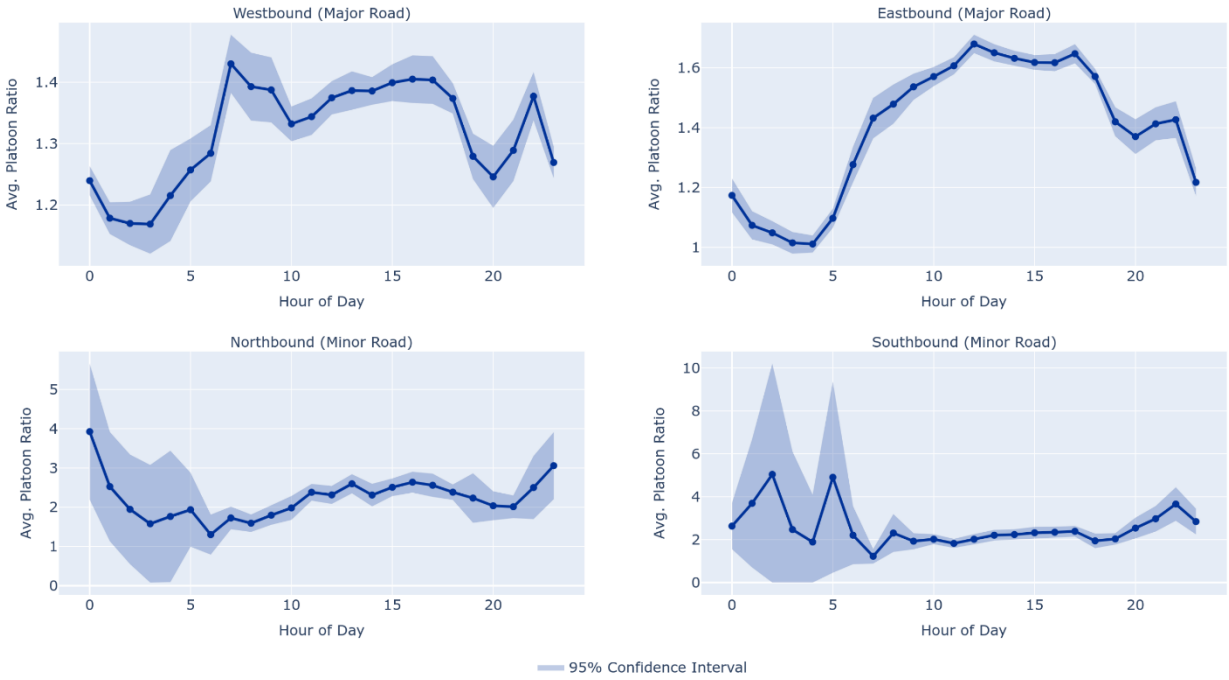

Figure 5-9. Hourly Trend of Approach-Level Platoon Ratio

Minor Road Approaches (Northbound & Southbound):

- The northbound and southbound approaches (minor roads) frequently exhibit platoon ratios exceeding 1.50, indicating persistent platoon formations rather than occasional occurrences.
- Variability in platoon ratio is more distinct during midnight hours, as indicated by the wider confidence intervals, likely due to inconsistent vehicle arrivals and lower traffic volumes.

Figure 5-10 illustrates the hourly variations in phase-level occupancy time during the red signal for all approaches at the intersection of SR436 and Westmonte Drive. The occupancy time in the figure represents the average of the hourly mean occupancy across all lanes within a given phase, providing a comprehensive measure of vehicle presence and queuing during red signal periods.

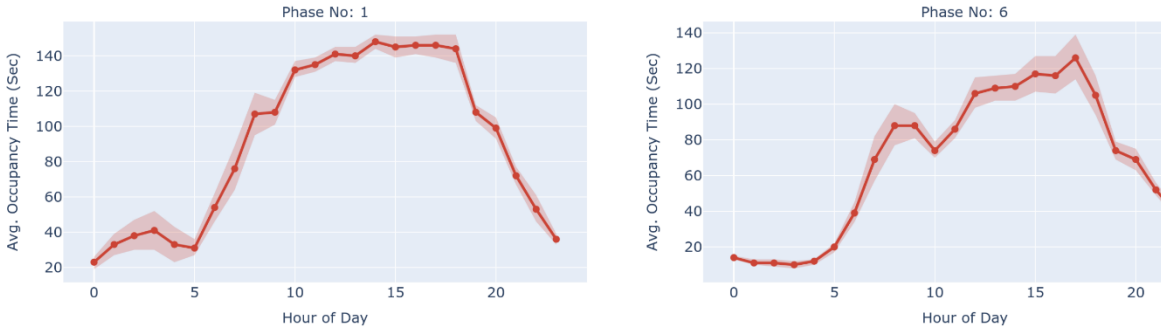

(a) Eastbound Approach (Major Road)

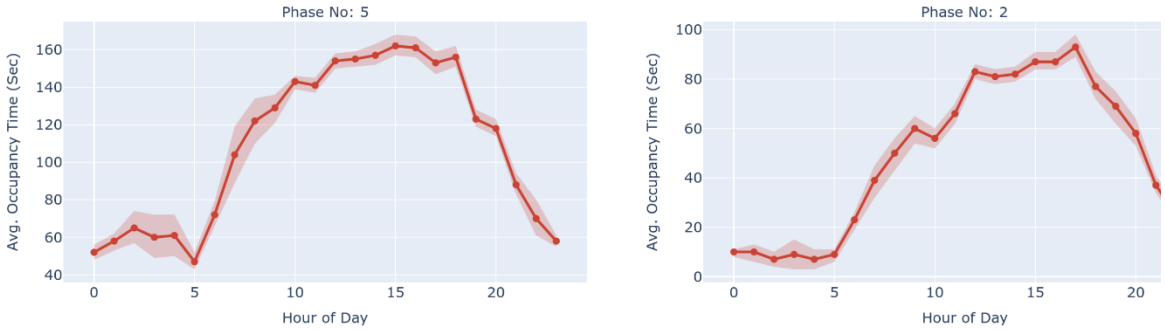

(b) Westbound Approach (Major Road)

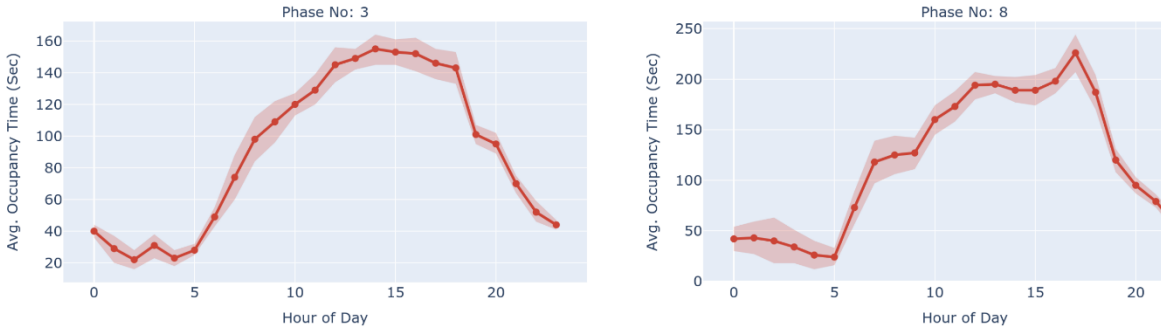

(c) Southbound Approach (Minor Road)

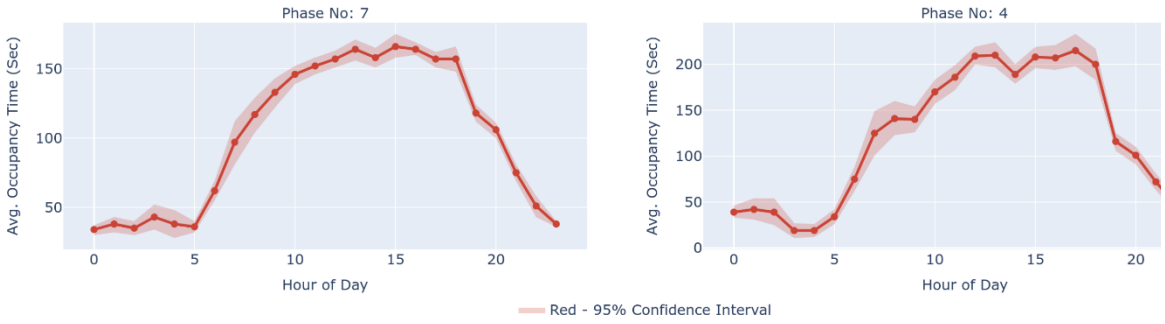

(d) Northbound Approach (Minor Road)

Figure 5-10. Hourly Trend of the Phase-Level Occupancy Time During Red

Major Road Approaches (Eastbound & Westbound):

- The eastbound and westbound approaches (major roads) exhibit higher occupancy times during the morning (7:00 AM – 9:00 AM) and evening (4:00 PM – 6:00 PM) peak hours, indicating increased vehicle accumulation while waiting for the green signal.
- Occupancy time trends remain elevated throughout the day, reinforcing the impact of sustained traffic demand on major road approaches.

Minor Road Approaches (Northbound & Southbound):

- In the northbound and southbound approaches (minor roads), left-turn phases (Phases 3, and 7) display slightly lower occupancy times compared to through phases (Phases 8, and 4).

While occupancy time was calculated at lane-level resolution (refer to **Table 5-3**), it is presented at phase-level resolution for better clarity and interpretation. All remaining lane-level features are also represented at phase-level resolution.

Figure 5-11 illustrates the hourly variations in split failure across all approaches at the intersection of SR436 and Westmonte Drive. Split failure occurs when the allocated green time is insufficient to clear the queued vehicles within a phase, leading to unmet demand and potential congestion. The figure highlights phase-specific and time-dependent patterns in split failures, indicating differences in traffic demand and signal performance across approaches.

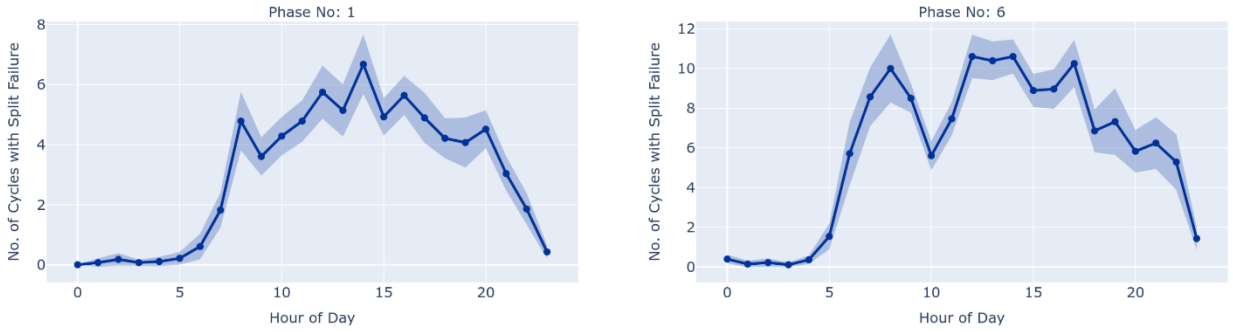

(a) Eastbound Approach (Major Road)

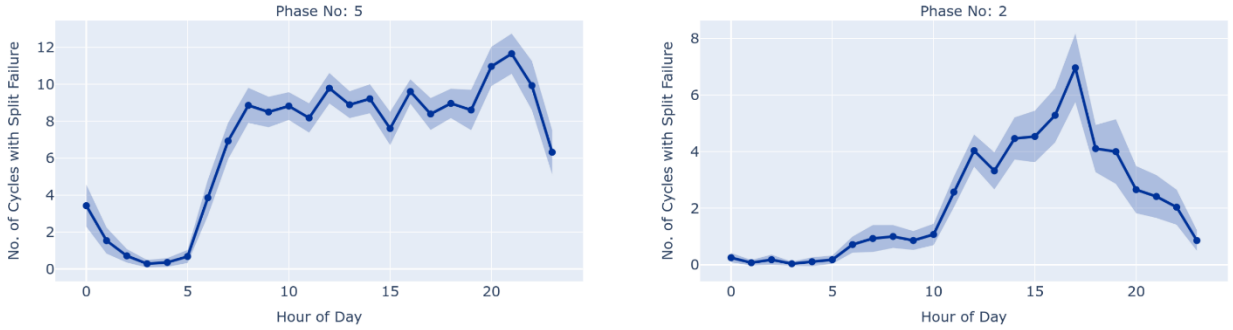

(b) Westbound Approach (Major Road)

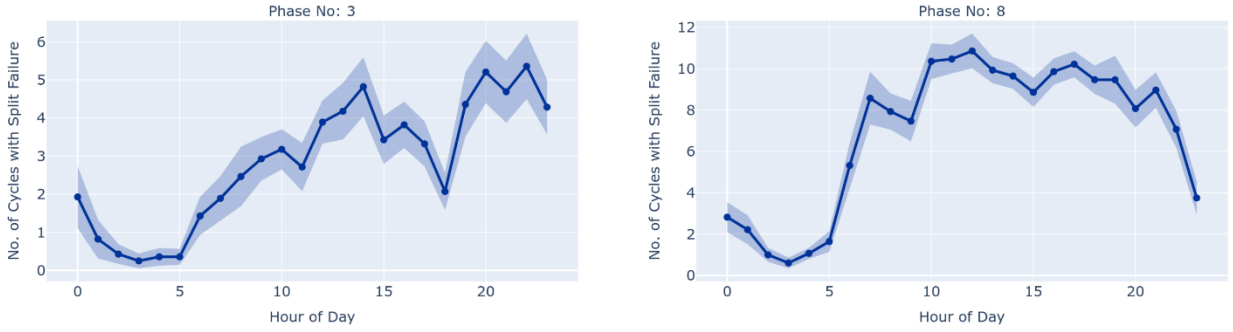

(c) Southbound Approach (Minor Road)

(d) Northbound Approach (Minor Road)

Figure 5-11. Hourly Trend of the Phase-Level Split Failure (Purdue Standard)

Major Road Approaches (Eastbound & Westbound):

- Phases 1 and 5 (eastbound major road) and Phases 2 and 6 (westbound major road) experience the highest split failures, particularly during afternoon and evening peak periods.
- Split failures in Phase 5 remain elevated throughout the day, indicating consistent traffic demand exceeding the allocated green time.
- Phase 2 exhibits a sharp increase in split failures between 3:00 PM and 6:00 PM, reflecting congestion buildup.

Minor Road Approaches (Northbound & Southbound):

- Phases 4 and 8 exhibit moderate split failures in the afternoon and evening, likely due to left-turn demand exceeding available green time.
- Phase 3 and 7 show steady but comparatively less frequent split failures.

Figure 5-12 presents the hourly variations in headway during green and red signals for through-moving vehicles at Phase Nos. 2, 4, 6, and 8. Headway, defined as the time interval between consecutive vehicles approaching the intersection, serves as an indicator of traffic flow efficiency and vehicle interaction patterns across different phases and time of the day.

Major Road Phases (Phases 2 & 6):

- Phases 2 and 6, representing major road approaches, exhibit shorter headways during peak hours (6:00 AM – 9:00 AM and 4:00 PM – 6:00 PM), indicating higher traffic demand and reduced spacing between vehicles.
- The shorter headways during peak periods suggest a well-utilized green signal, as vehicles arrive in denser formations, minimizing gaps between consecutive vehicles.
- Between midnight and early morning (12:00 AM – 3:00 AM), headways during green are very high, reflecting lower demand and more dispersed vehicle arrivals.

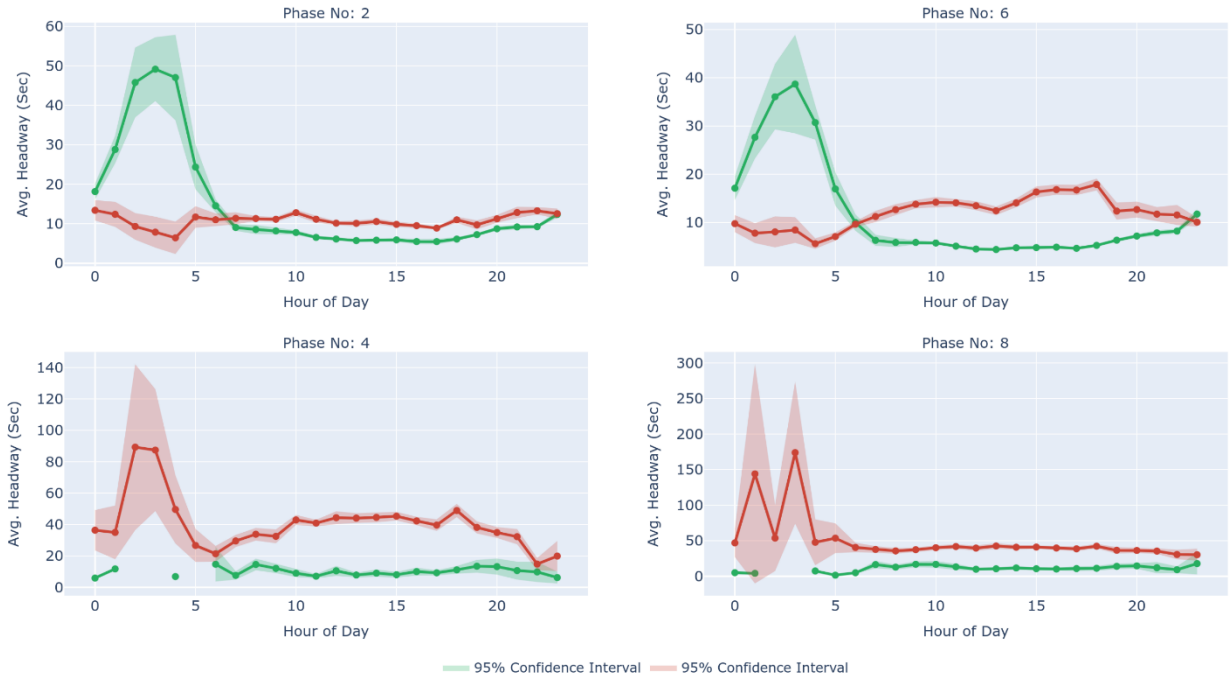

Figure 5-12. Hourly Trend of the Phase-Level Headway

Minor Road Phases (Phases 4 & 8):

- Phases 4 and 8, representing minor road approaches, consistently exhibit higher headways than major road phases throughout the day, reflecting lower traffic volumes, less frequent vehicle interactions, and larger gaps between consecutive arrivals.
- Headway variations during midnight and early morning hours are more distinct, as indicated by wider confidence intervals, likely due to irregular vehicle arrivals in low-demand conditions.
- Headway variations during midnight and early morning hours are more distinct, as indicated by wider confidence intervals, likely due to irregular vehicle arrivals in low-demand conditions.

Figure 5-13 illustrates the hourly variations in traffic conflicts occurring during green and red signals across different phases. The trends highlight temporal and phase-specific differences in conflict occurrences throughout the day.

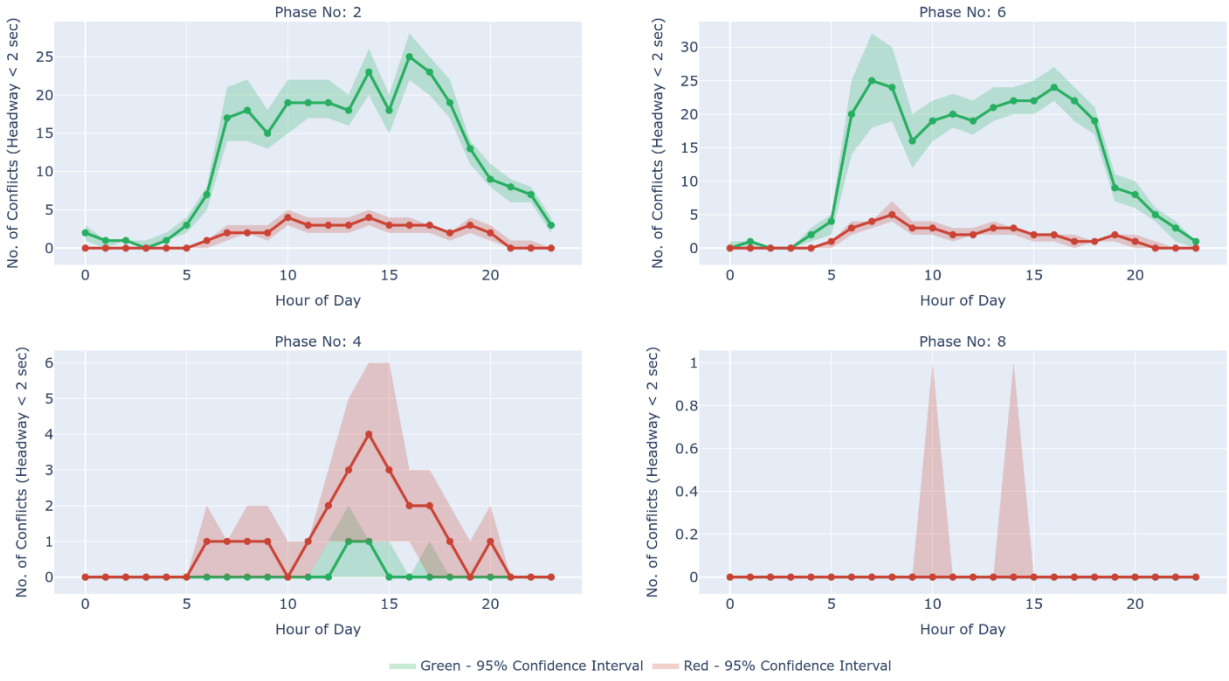

Figure 5-13. Hourly Trend of the Phase-Level Conflict

Major Road Phases (Phases 2 & 6):

- Phases 2 and 6 (major road approaches) experience the highest number of conflicts during, particularly between 6:00 AM and 9:00 AM, and 4:00 PM and 7:00 PM, suggesting increased interaction among vehicles during the morning and evening peak periods.
- No. conflict during red remain low throughout the day.

Minor Road Phases (Phases 4 & 8):

- Conflicts during red signals are relatively infrequent, but Phase 4 exhibits a gradual increase during midday, followed by a subsequent decline.

Figure 5-14 illustrates the hourly variations in red light running (RLR) flags, which represent the number of signal cycles with red light violations across different approaches. The trends reveal temporal and directional variations in RLR activity, highlighting peak periods and potential safety concerns.

Eastbound Approach (Major Road):

- Significant RLR activity is observed for Phase 1 in the afternoon hours, peaking between 3:00 PM and 5:00 PM.
- For Phase 6, RLR activity peaks in the morning around 8:00 AM, indicating potential morning rush-hour congestion or aggressive driver behavior during peak commuting times. Following this peak, RLR occurrences decline but gradually rise again in the evening, though at a lower intensity compared to the morning.

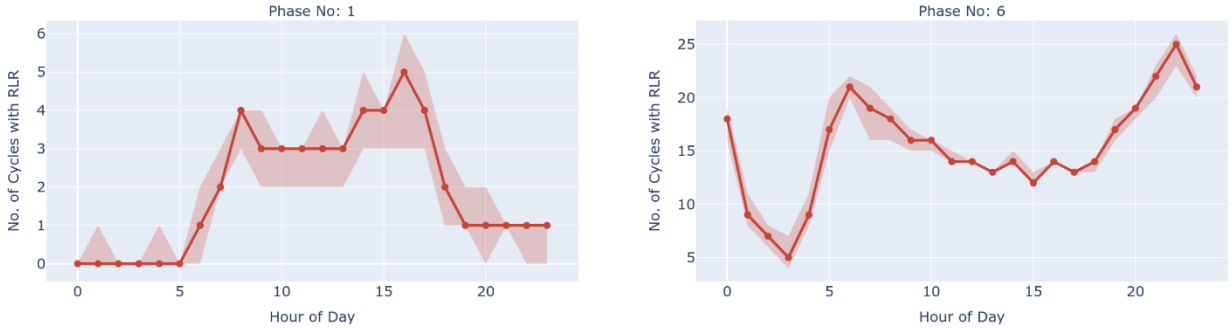

(a) Eastbound Approach (Major Road)

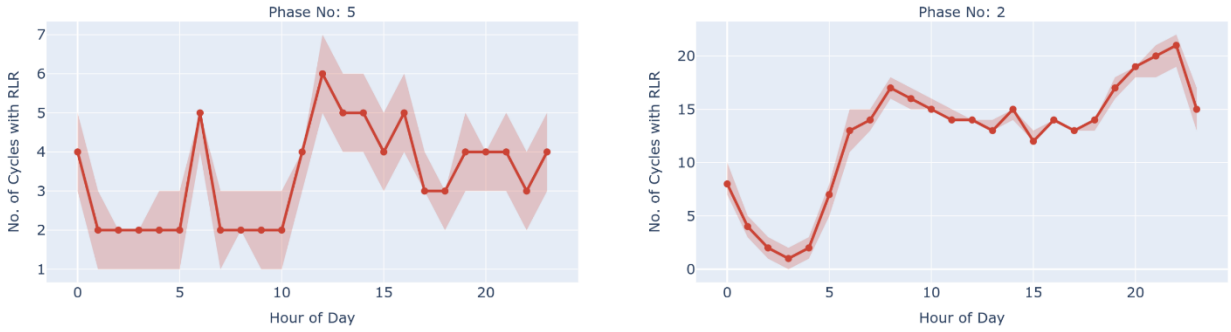

(b) Westbound Approach (Major Road)

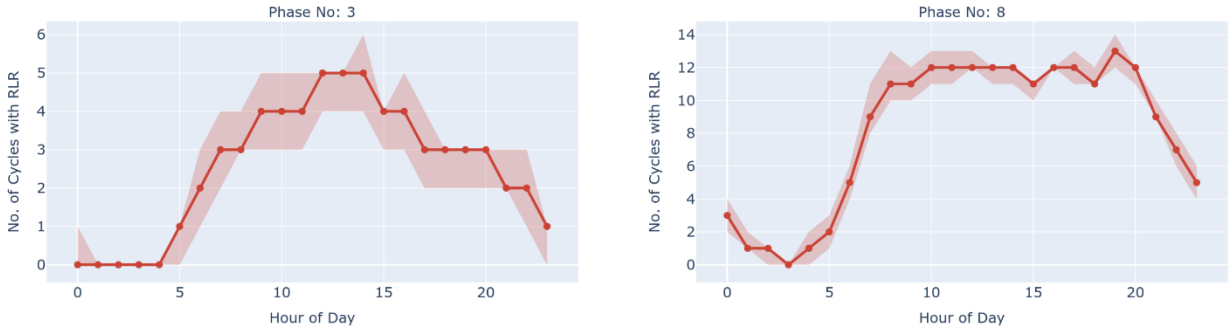

(c) Southbound Approach (Minor Road)

(d) Northbound Approach (Minor Road)

Figure 5-14. Hourly Trend of the Phase-Level Red Light Running Flag

Southbound Approach (Minor Road):

- For Phase 3, RLR occurrences gradually increase from 5:00 AM to 10:00 PM, indicating a steady rise in violations throughout the day.
- Phase 8 exhibits persistent RLR trends throughout the day, indicating frequent violations, possibly due to long red signal durations or turning movement conflicts.

5.2.2.3. Pedestrian Traffic-Related Measures

Figure 5-15 illustrates the hourly variations in pedestrian activity indicator across all pedestrian phases at the intersection of SR436 and Westmonte Drive. The pedestrian activity indicator is represented as a binary measure (0 or 1) per signal cycle, where 1 indicates pedestrian presence and 0 indicates no pedestrian presence. This method serves as a proxy for pedestrian

activity, as ATSPM detectors only capture whether an actuation (e.g., a push button press) occurred, rather than the actual number of pedestrians crossing. The key observations are:

- Morning Peak (7:00 AM – 9:00 AM): Pedestrian activity increases steadily for Phases 4 and 8, indicating higher pedestrian demand during early commuting hours.
- Evening Peak (5:00 PM – 8:00 PM): A second significant increase in pedestrian presence is observed across all phases, aligning with commute times and recreational movement.
- Late Night (After 9:00 PM): Pedestrian activity gradually declines, suggesting minimal pedestrian demand during late-night hours.

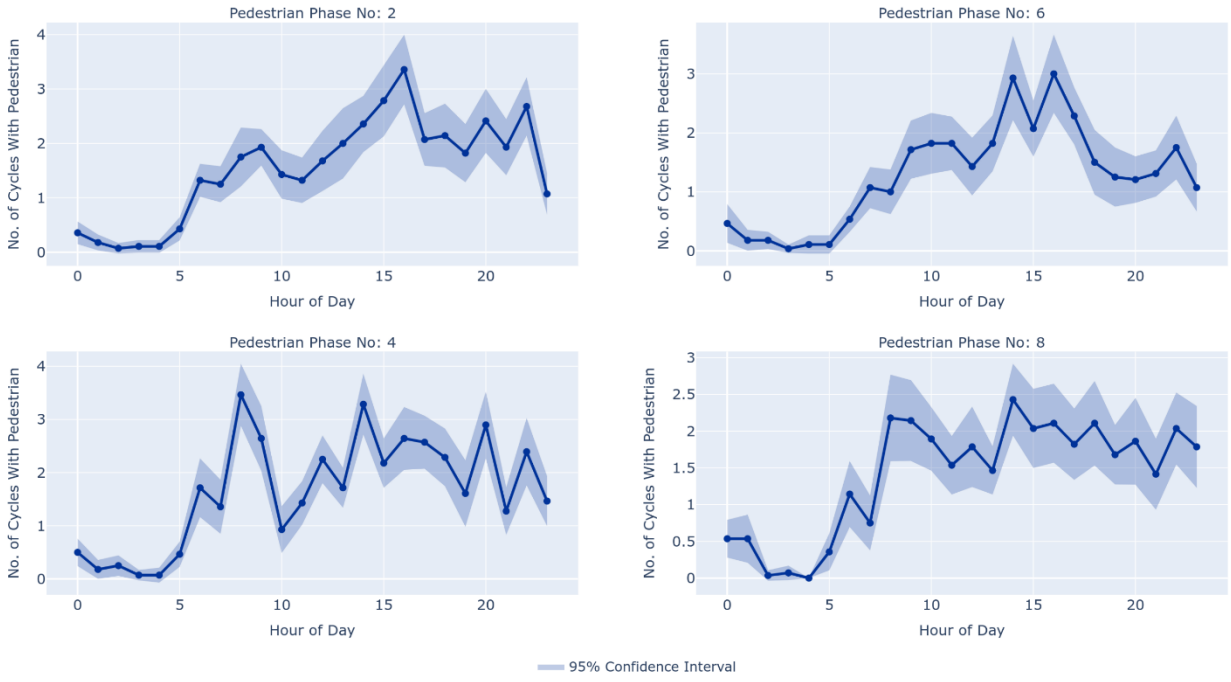

Figure 5-15. Hourly Trend of the Phase-Level Pedestrian Activity Indicator

Figure 5-16 illustrates the hourly variations in pedestrian delay across all pedestrian phases at the intersection of SR436 and Westmonte Drive. Pedestrian delay represents the waiting time experienced by pedestrians before receiving a walk signal, which is influenced by signal phasing, vehicle demand, and pedestrian actuation requirements. The key observations are:

- Morning Hours (6:00 AM – 10:00 AM): Pedestrian delays remain relatively low, with gradual increases observed as traffic demand builds.
- Midday Period (11:00 AM – 2:00 PM): Phase 6 experiences its highest pedestrian delay around 1:00 PM, suggesting possible delays due to signal timing prioritization for vehicular movements.
- Afternoon and Evening Peak (3:00 PM – 7:00 PM):Phases 2 and 4 exhibit increasing pedestrian delays, peaking around 5:00 PM, reflecting higher vehicle demand and extended pedestrian waiting times. Phase 8 shows relatively stable pedestrian delay throughout the day, with moderate peaks observed in the evening hours.

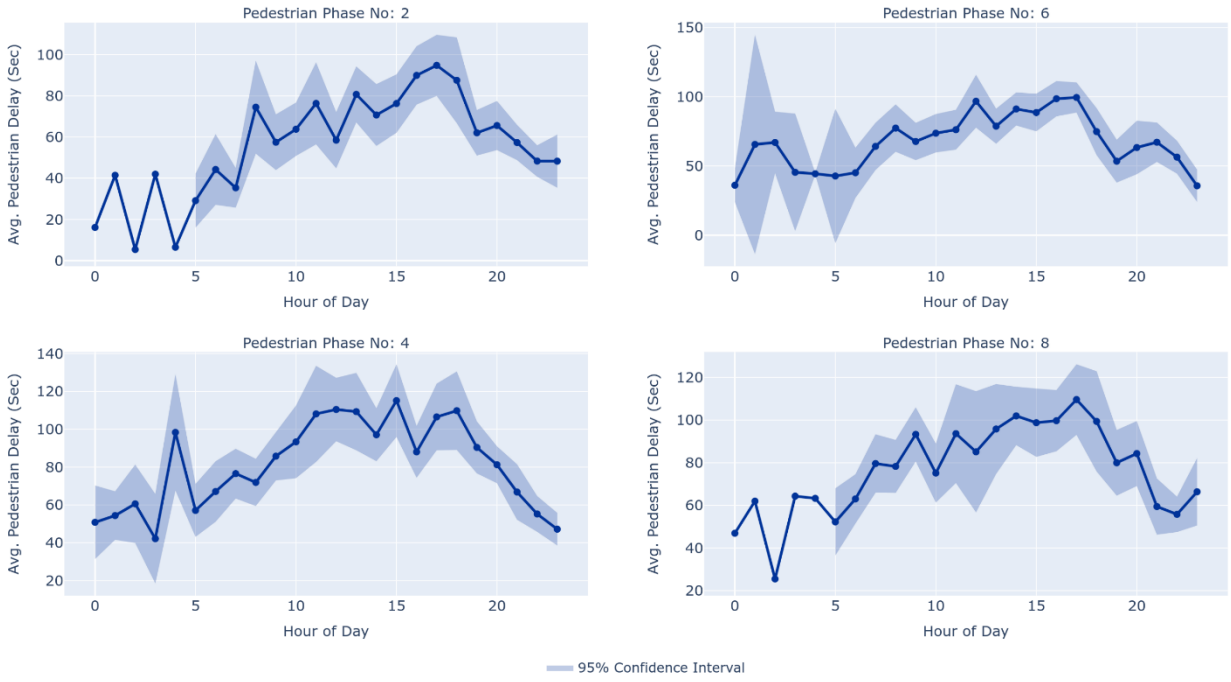

Figure 5-16. Hourly Trend of the Phase-Level Pedestrian Delay

5.3. Yellow and Red Clearance Time Adjustment

5.3.1. Current Standard and Background

Yellow and Red Clearance phases are typically timed using kinematic equations reliant on assumed driver behaviors, such as reaction time and approach speed, as outlined in the FDOT TEM. **Equations 4-1** and **4-2** define the yellow and red clearance signal duration.

$$Y = t + \frac{1.47v}{2(a + Gg)} \quad (4\text{-}1)$$

$$R = \frac{W + L}{1.47v} \quad (4\text{-}2)$$

Notions & Definitions:

- Y = yellow signal duration (seconds),
- t = perception-reaction time (1.4 seconds),
- v = approach speed of the vehicle (mph),
- a = deceleration rate in response to the yellow signal (10 ft/sec²),
- g= acceleration due to gravity (32.2 ft/sec²),
- G= grade percentage (positive for uphill, negative for downhill).
- R = red clearance signal duration (seconds),
- W = intersection width (feet), measured from the near-side stop line to the far edge of the conflicting traffic lane along the actual vehicle path,
- L = vehicle length (20 feet),

Signal length is primarily determined by approach speed and intersection width, as default values are unavailable, and most roads in Florida have no grade. This study obtained speed limit

data from the FDOT Sunstore and manually measured intersection width using Google satellite imagery to assess whether current red clearance durations meet the standard. **Appendix A-2** presents the FDOT TEM recommendations for yellow and red clearance phase durations alongside the observed distribution. The analysis revealed that while most intersections adhered to the yellow time standard, red clearance durations frequently did not meet the recommended values.

Meanwhile, assumptions on those parameters, such as approach speed as speed limit and fixed reaction time across drivers, often diverge from real-world conditions, sometimes leading to poorly calibrated signals that either sacrifice efficiency for safety or vice versa (Jerome et al., 2022). Also, these parameters are not available in the current study site's detector configuration. With growing urban traffic volumes, optimizing the duration of these transition phases demands a paradigm shift from integrating high-resolution behavioral data to replacing assumptions.

This study bridges this gap by applying causal forest to isolate the impact of signal adjustments while controlling for variables like traffic volume and platoon ratio. Although dynamic yellow time is neither feasible nor permitted in Florida, this study evaluates the potential effects of implementing dynamic yellow time on intersection safety. Results reveal an adaptive signal adjustment technique for the yellow and red clearance phases that reduces conflict rates at these phases by up to 6% and 7%, respectively. By aligning signal timing with observed driver behavior rather than idealized assumptions, this work provides a scalable framework for FDOT to enhance intersection safety through a data-driven approach.

5.3.2. Algorithm

5.3.2.1. Calculation of Conflict Rate Per Vehicle

We assumed that signal adjustments only affects the yellow and red clearance signals since adjusting the yellow and red clearance signals is unlikely to have an effect on the green and red times because the effect dilutes over time. For yellow we only tested increasing the phase, while for red clearance time we tested both an increase or decrease. The frequency of conflicts during the yellow and red clearance phase is influenced by factors such as yellow duration, traffic volume, and the number of lanes. However, monitoring only the frequency of conflicts for signal adjustment has several drawbacks. For example, extending the yellow duration tends to increase conflicts, often falsely rendering the increasing signal duration less effective at most intersections. Likewise, reducing the yellow duration decreases conflicts, primarily due to a shorter time window for conflicts to occur. An analysis based solely on conflict frequency indicates that risks are concentrated during peak traffic hours, and it largely ignores nighttime. Therefore, it is essential to account for exposure when analyzing these patterns.

This study addressed this issue by calculating the conflict rate per vehicle ($CRPV$), referred to as the conflict rate for simplicity. This metric represents the proportion of vehicles involved in conflicts relative to the total number of vehicles passing through during yellow signal phases. Accordingly, the traffic conflict rate per vehicle at a particular phase i ($CRPV^i$) is defined via **Equation 4-1**:

$$CRPV^i = \frac{TC^i}{V^i} = \frac{\sum_{j \in P_i} 1\left(TH_j \leq 2\right)}{\sum_{j \in P_i} 1\left(t_{on}^j < t_{off}^j\right)} \tag{4-1}$$

where P_i represents the set of time headway instances during phase i. The indicator function $1(TH_j \leq \delta)$ equals 1 if the condition $TH_j \leq \delta$ is satisfied, and 0 otherwise. V^i denotes the traffic volume during phase i. Here, this study used 2 seconds as the threshold to obtain enough observations for modeling and inference. Also, the time headway is calculated using the setback detector, meaning it only considers conflicts that occur on one approach. As a result, this study monitors the conflict rate per vehicle at the yellow and red clearance phases that occurred downstream of the intersection for signal adjustment.

5.3.2.2. Conflict Rate Estimation Models

This study employed three tree-based machine learning algorithms—Random Forest (RF), Adaptive Boosting (AdaBoost), and Extreme Gradient Boosting (XGBoost)—to estimate traffic conflict rates. These models were selected for their ability to capture non-linear relationships inherent in traffic dynamics while addressing challenges such as overfitting and data sparsity.

Random Forest, a bagging ensemble method, constructs multiple decision trees using bootstrapped subsets of the data and aggregates predictions through majority voting. This approach reduces overfitting by diversifying errors across individual trees, rendering RF robust to noise and suitable for high-dimensional datasets. In contrast, AdaBoost, a boosting technique, iteratively trains weak learners such as shallow decision trees by reweighting misclassified instances. While computationally efficient for simpler datasets, AdaBoost's sensitivity to noisy data and lack of regularization limit its applicability to complex tasks. Extreme Gradient Boosting (XGBoost), a state-of-the-art boosting framework, optimizes loss functions via gradient descent and incorporates L1/L2 regularization to penalize model complexity. XGBoost leverages parallel processing to

handle missing values effectively, though its performance depends heavily on careful hyperparameter tuning.

Tree-based algorithms were chosen for their capacity to model non-linear interactions, such as the combined effect of traffic volume and yellow signal duration while accommodating mixed data types. Their inherent interpretability, when augmented with explainability techniques, aligns with the study's dual objectives of predictive accuracy and acquisition of insight for using causal forest.

To address the black-box problem of machine learning models, Shapley Additive exPlanations (SHAP) were applied to quantify feature contributions using principles from cooperative game theory. SHAP values reveal the directionality (positive or negative influence) and magnitude of variables such as yellow duration or lane count, while also revealing non-linear interactions. A cumulative feature importance threshold of 70% was adopted to mitigate overfitting, discarding noise-prone covariates.

Figure 5-17 presents the top 10 features that significantly influence the estimation of conflict rate per vehicle during the yellow phase. The bar graph shows the percentage of total feature importance. The label format was "Phase_Feature_Direction_Movement(Lane)". For example, "Yellow_Volume_Forward_Through(T)" represents the Volume of forward direction in the through movement during the yellow phase recorded at the through (T) lane. The shared lane with the through and right-turn lane is recorded as TR. As a result, conflict rates per vehicle during the yellow and red clearance period were most correlated to the volume of vehicles passing through the intersection during the yellow phase.

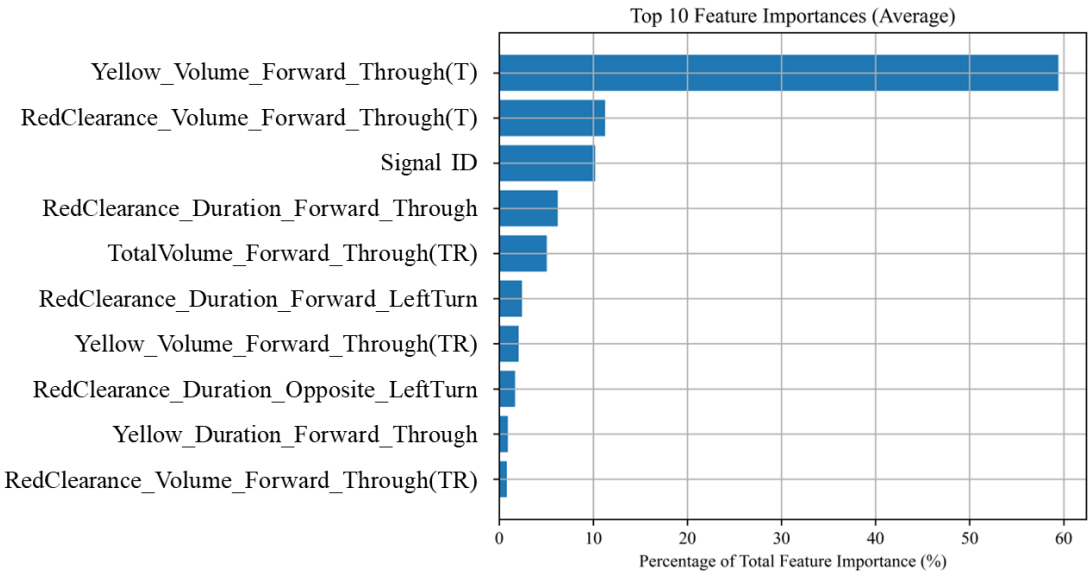

Figure 5-17. Top 10 Feature Importance

The dataset was partitioned into training and testing subsets at an 80:20 ratio to ensure robust validation. Hyperparameter optimization was conducted via grid search, which systematically evaluated predefined parameter spaces to identify combinations maximizing model performance on test data. Key hyperparameters included the number of estimators, maximum tree depth, and learning rate. **Table 5-4** presents the grid search results, displaying alternatives, with the selected value shown in bold.

Table 5-4. Hyperparameter Options and Selected Parameters

Model	Parameter		
	No. of estimators	**Max Tree Depth**	**Learning Rate**
AdaBoost	50, 100, 200	-	0.001, 0.01
RF	50, 100, 200	5, 10	-
XGBoost	50, 100, 200	5, 10	-

Table 5-5 presents a comparison of models estimating the conflict rate per vehicle occurring during the yellow and red clearance phase of through movements. To ensure comparability, consistent hyperparameter search procedures and feature sets were applied across all models. Among these, XGBoost exhibited the best performance, achieving an R-squared value of 0.457. Consequently, the subsequent analysis uses XGBoost to estimate the baseline and treatment effect of the causal forest, as it provided the highest accuracy.

Table 5-5. Model Performance of Different Models

Performance measure	Models		
	Random Forest	**AdaBoost**	**XGBoost**
R-square	0.453	0.366	**0.457**
MAE (%)	**1.45**	1.64	1.50
RMSE (%)	5.70	6.14	**5.68**

5.3.2.3. Causal Forest

This study employs the causal forest algorithm to estimate heterogeneous treatment effects (HTEs) across multiple signalized intersections. The causal forest partitions the feature space by selecting splits that maximize treatment effect heterogeneity while simultaneously promoting a covariate balance between treatment and control groups. To reduce overfitting and enhance credibility, this study uses the "honesty" approach, which involves using separate samples for tree construction and effect estimation. This dual-sample approach ensures that splits are selected based on one part of the data and treatment effects are estimated on an independent subset. The HTE (τ) represents the impact of a treatment T' on an outcome y and is defined as **Equation 4-2**:

$$\tau = y(T') - y(T_0) \tag{4-2}$$

where $y(T_0)$ and $y(T')$ denote the outcomes under control and treatment conditions, respectively. In this study, T_0 represents the initial treatment level. To simulate signal timing adjustments, a treatment adjustment factor ΔT is introduced, modifying the treatment level (T') as shown in **Equation 4-3**.

$$T' = T_0 + \Delta T \tag{4-3}$$

The adjustment of treatment is determined by the observed signal durations, with the objective being to enhance the reliability of the treatment effect and to ensure that durations remain within the permitted range. In certain cases, The causal forest's treatment effect makes a conflict ratio fall below zero (i.e., $\tau + y(T_0) < 0$). This often occurs when the predictive model extrapolates to unobserved values, which is not feasible and requires correction. To address this, the treatment effect is adjusted by setting $\tau = -y(T_0)$ in such instances, as expressed in **Equation 4-4**.

$$\hat{\tau} = \max(\tau, -y(T_0)) \quad (4\text{-}4)$$

This adjustment ensures that the conflict rate remains non-negative after the treatment is applied. By incorporating this post-processing step, the analysis avoids overestimating the treatment's impact, thereby providing a more conservative estimate of the recommendation's effectiveness. The Conditional Average Treatment Effect (CATE), given a set of features x is expressed as **Equation 4-5**.

$$\tau(x) = E(\hat{\tau}|x) \quad (4\text{-}5)$$

This formulation enables the causal forest to estimate treatment effects that are specific to varying conditions, capturing the interactions between features and outcomes. Additionally, the CATE was adjusted to ensure that the conditional average conflict rate after treatment remains non-negative, preventing any overestimation of the CATE. This adjustment are presented in **Equation 4-6**.

$$\hat{\tau}(x) = \max(\tau(x), -E(y(T_0)|x) \quad (4\text{-}6)$$

The framework explicitly models the shift from T_0 to T_1', enabling the estimation of outcome changes under hypothetical interventions. This estimation approach is grounded in the ignorability assumption, which posits that treatment assignment is independent of potential outcomes, given the observed covariates. In addition, the Causal Forest relies on variability in the data to produce reliable estimates of treatment effects. The method assumes a sufficient level of data variability and covariate balance between treatment and control groups. A lack of these conditions can undermine the accuracy and reliability of the estimated treatment effects. Intersections with fixed signal durations typically lack the necessary variation for meaningful analysis. In this study, however, variability is introduced through occasional deviations in signal

timing, such as those caused by vehicle detection system activations. These fluctuations provide the variability required for the Causal Forest to estimate the effects of signal timing adjustments effectively. Therefore, the selection of signal adjustment candidates is informed by observed signal durations.

5.3.2.4. Signal Adjustment Recommendation

Figure 5-18 shows the proposed recommendation system for yellow and red clearance signal duration adjustment based on the causal forest. The algorithm begins by calculating various performance measures from raw high-resolution event-based data and aggregates them by phase level. The data is then split into training and test sets. The training set is fed into a modeling process to learn key relationships between conflict ratio per vehicle and signal duration. Multiple models are explored, with model selection performed by comparing performance metrics on the test set. Once the best model is chosen, a causal forest is trained to understand how proposed signal adjustments (treatments) would affect different intersections at different times. Causal forests provide heterogeneous treatment effect estimates, indicating how each intersection is likely to respond to each candidate signal duration. This approach captures variations across traffic signal IDs, times of day, and whether it is a weekend or weekday, rather than relying on a one-size-fits-all timing plan.

Signal adjustment candidates are identified by analyzing the distribution of yellow and red clearance phases to enable accurate treatment estimation. Each candidate is assessed using a causal forest, which provides estimates of HTEs. In this study, these effects were calculated by varying the duration within specified ranges in 0.1-second increments. The results were averaged to

compute the CATE for each subgroup. The CATE for a given subgroup determines the recommended signal duration.

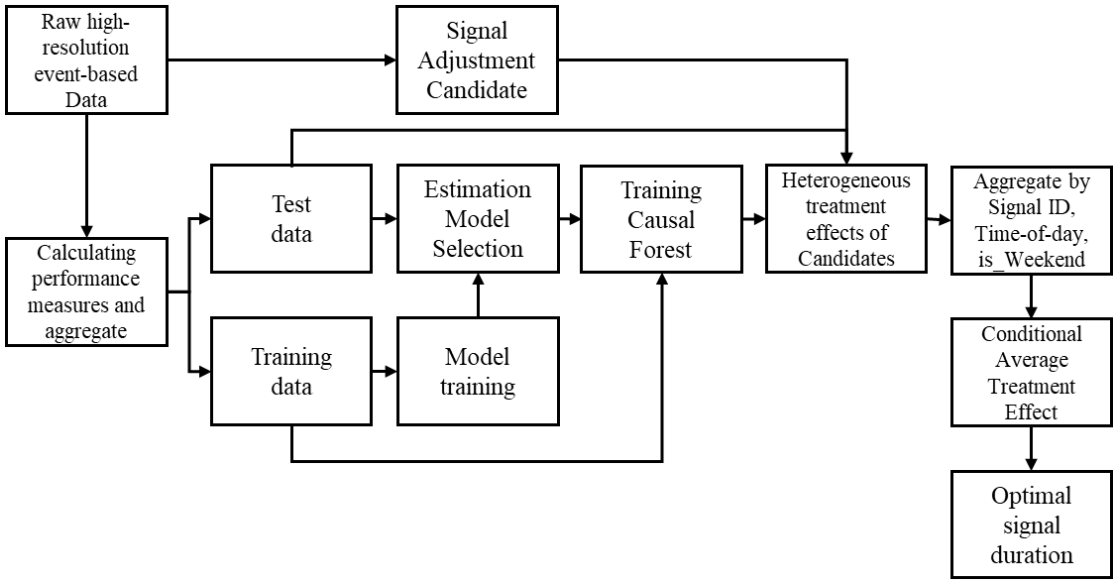

Figure 5-18. Recommendation System for Yellow and Red Clearance Signal Duration

The reliability of these estimates depends on subgroup size. Small subgroups may produce unreliable averages, while large subgroups may overlook critical environmental variations, such as changes in traffic conditions. To address this, CATE values were calculated for each intersection, for every hour, and separately for weekdays and weekends. This ensures adequate sample sizes while accounting for temporal variations, intersection-specific characteristics, and weekday/weekend differences. The optimal signal duration is identified by selecting the candidate with the lowest conflict rate per vehicle during the transition phase. Finally, the algorithm set the recommended adjustments for the yellow signal duration to 0 if the systems recommend reducing it, which is in line with current FDOT standards. This method integrates data-driven modeling, hypothesis testing, and causal inference to enable iterative refinement of traffic signal control strategies.

5.3.3. Recommendation Results

5.3.3.1. Yellow and Red Clearance Duration Candidates

The proposed algorithm requires a reasonable number of observations for reliable estimation, so the candidates should be investigated based on the observed frequency. **Figure 5-19** shows the duration of yellow and red clearance times observed in the collected data. The figure shows that most cycles are operated with 4-6 seconds for yellow and 2-4 seconds for red clearance. This range ensures that recommended durations do not deviate excessively from existing guidelines. Therefore, this study chose this range as a candidate for recommendation.

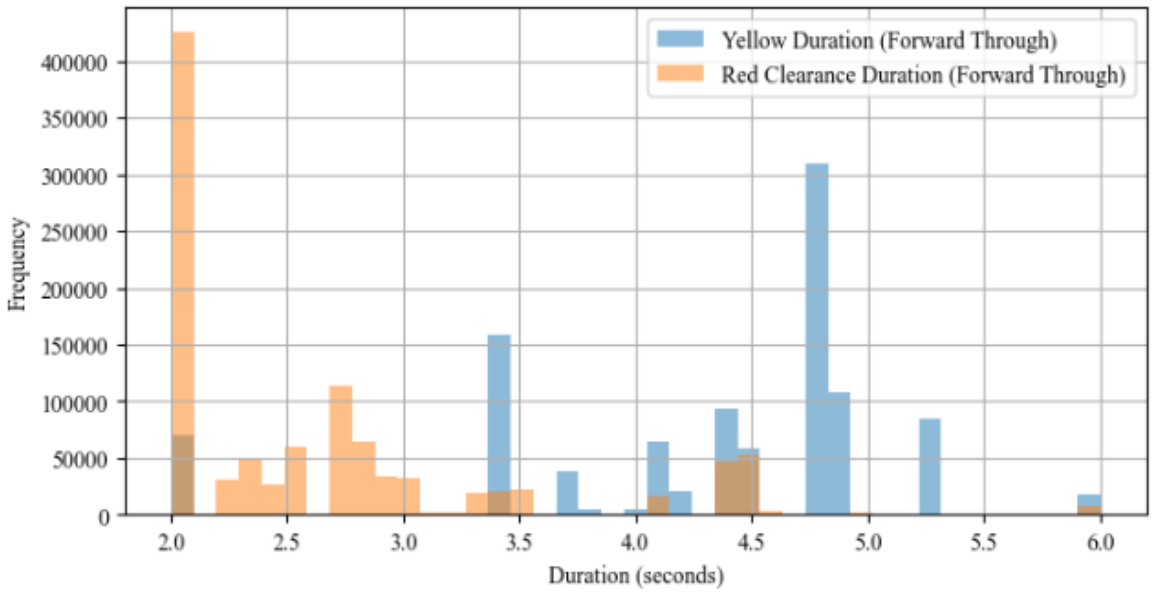

Figure 5-19. Observed Yellow and Red Clearance Durations.

5.3.3.2. Conditional Average Treatment Effect

In this study, CATE denotes the average conflict rate that changes when all observations of a given condition (intersection, time of day, weekend or not) are fixed to a certain duration. **Figure 5-20** presents the CATE of adjustments to yellow and red clearance signal duration, evaluated for different times of the day and weekends.

The effect of adjustments was identified in increments of 0.1 seconds within the specified phase duration ranges. Blue regions represent conditions where the adjustments are expected to reduce conflicts per vehicle during the transition phase, while red regions denote an anticipated increase. The duration with the lowest value in this contour will have the lowest conflict rate per vehicle among the candidate durations and is therefore recommended. At the study sites, adjusting signal duration to a fixed duration typically increased the conflict rate per vehicle in the transition phase, as the smallest durations are found around the average observed duration. This can be attributed to the flexibility of the signal's internal algorithm to adjust the signal based on the vehicle's detection information. In such situations, signal adjustments are not only unnecessary but, as demonstrated by the analysis, may inadvertently contribute to a rise in the conflict rate.

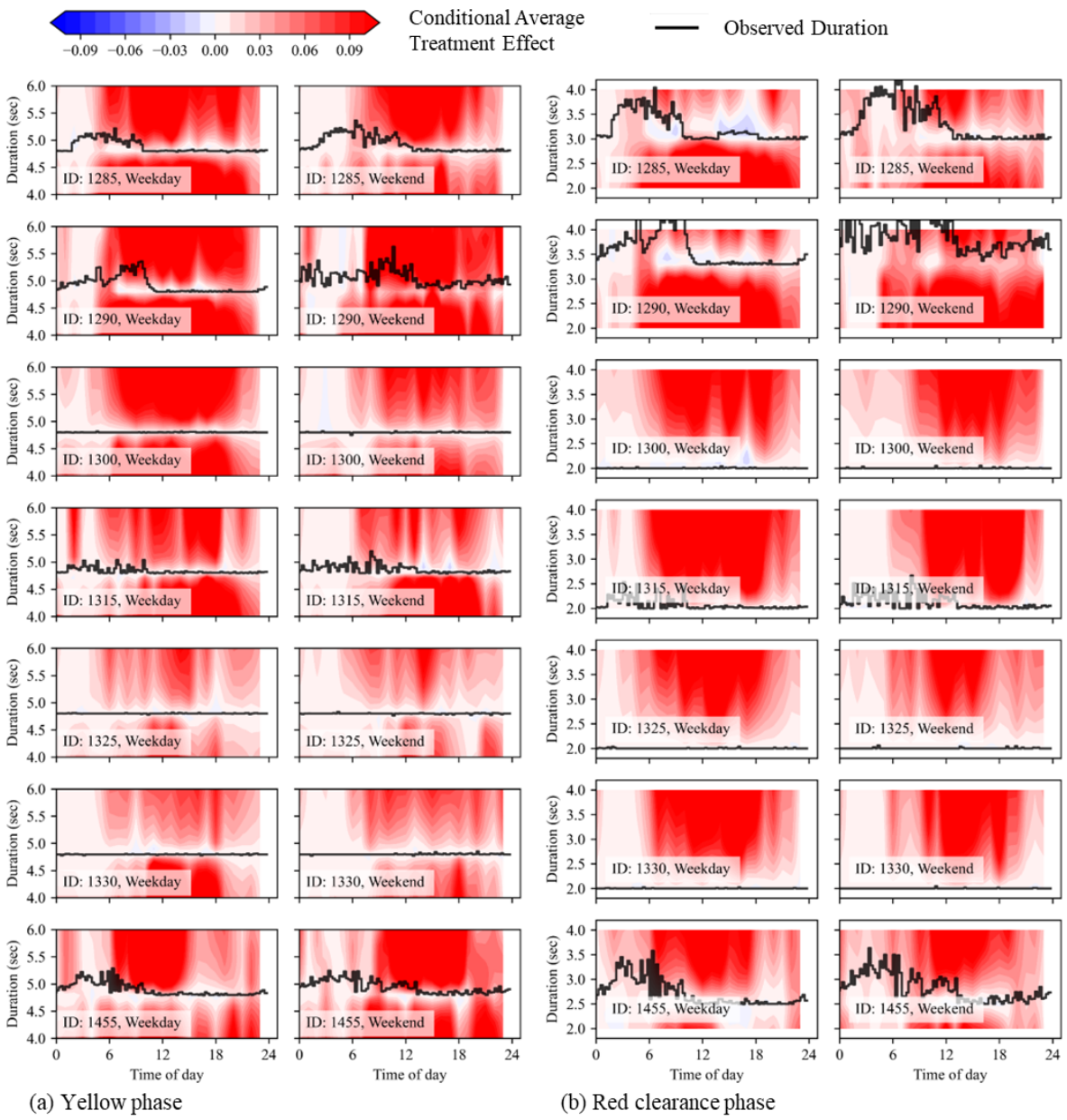

Figure 5-20. Conditional Average Treatment Effect of Yellow (a) and Red Clearance (b)

Figure 5-21(a) presents the recommended durations for yellow and red clearance signals at each intersection, differentiated by time of day and weekday versus weekend, based on the contour data shown in Figure 4-4. For most intersections, the current duration was recommended because adjusting signal lengths was projected to increase conflict rates in the majority of cases. This duration scheme is recommended as the default setting for intersections, with the possibility of incorporating variability based on their internal algorithms. Introducing variability allows for observing driver responses to different signal lengths, which can aid in refining future algorithms by providing diverse data. This approach supports the estimation of treatment effects for subsequent signal adjustments. As additional data on similar signal durations is collected, the reliability of the adjustment algorithm is expected to improve.

Figure 5-21**(b)** shows the effect of the recommendation system, comparing the CATE of the current average duration and that of the minimum duration. It shows the expected percentage reduction in the conflict rate compared to the traditional system. It was estimated that the reduction in conflict rate would be mainly concentrated during the daytime when traffic is high and conflicts are common. The CATE of the proposed recommendation system is expected to be negative because the recommendation system selects the duration that results in the lowest conflict rate from a range of candidates. This feature ensures that the algorithm continuously improves safety with each update.

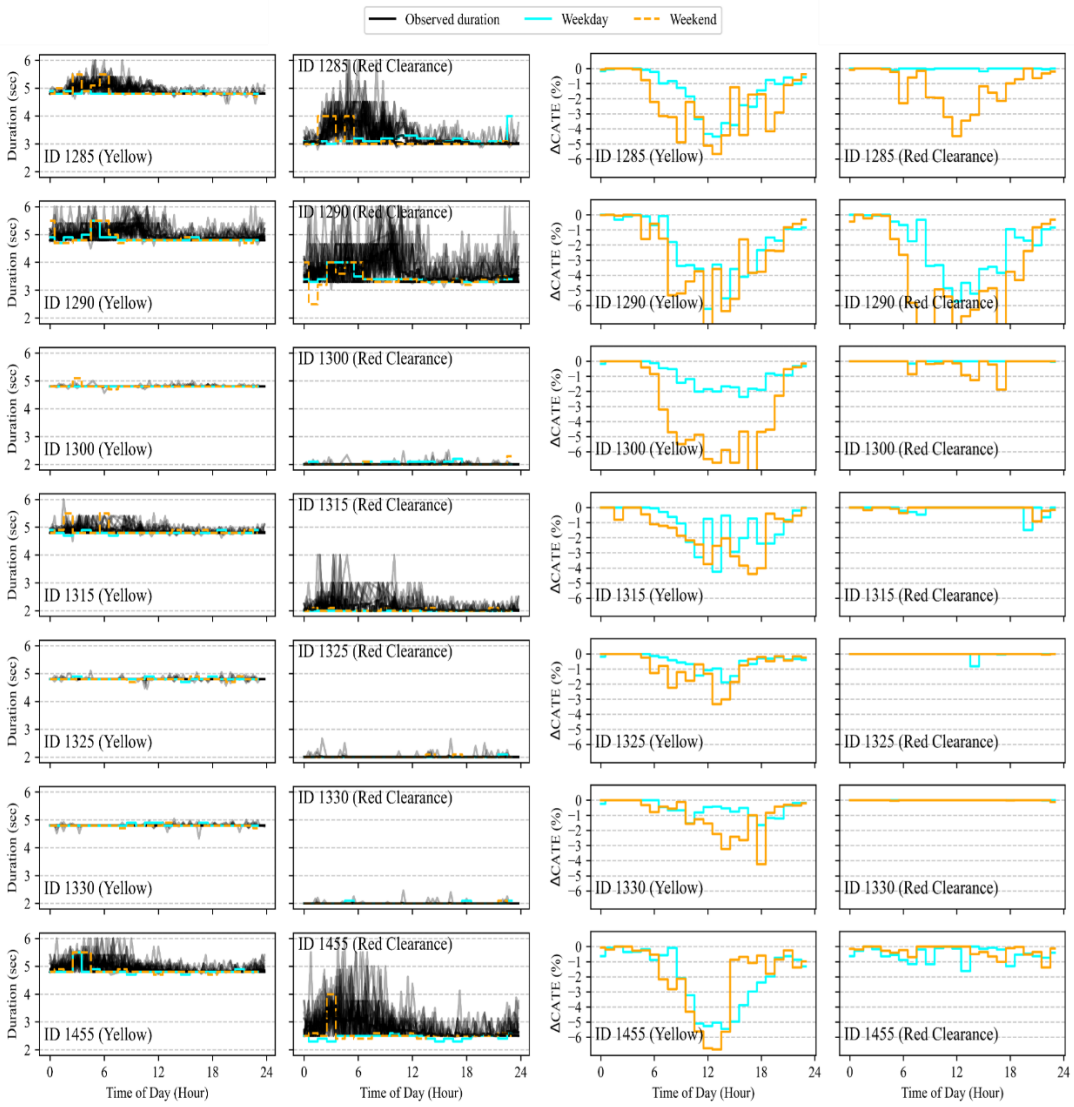

Figure 5-21. Recommended Duration (a) and Corresponding Conditional Average Treatment Effect (b)

As these recommendations are data-driven and based on a complicated framework, the specific factors influencing these values remain uncertain. Thus, signal adjustments should be limited to a small set of candidate durations, including the existing range of duration. Gradual adjustments to the yellow signal are particularly critical to ensure drivers have adequate time to adapt. This study provides recommendations based on individual intersections and specific hours of the day. When signal timing

varies between weekdays and weekends, the average value is recommended. In addition, the yellow and red clearance duration for opposing intersections is set to be the same when the recommendation is provided. Detailed recommended durations by intersection are attached in **Table A-3** and **Table A-4**.

Tables A-2 and **A-3** present the recommended adjustments to the current duration values. However, optimizing each signal timing must comply with the constraints outlined in local traffic signal manuals, which may vary based on vehicle actuation events. If the recommended duration falls outside this range, it must be adjusted accordingly. For instance, Florida specifies that yellow and red clearance durations should not exceed six seconds. Therefore, if an intersection's current yellow signal length is 5.9 seconds and an addition of 0.3 seconds is recommended, it should be adjusted to six seconds to remain within the specified limits.

5.4. Choice of Protected vs Permitted Left turn

5.4.1. Algorithm

5.4.1.1. Calculation of Gap from Stopbar Detector

The Signalized Intersections Informational Guide (2013) and the Highway Capacity Manual (HCM) 2022 provide detailed criteria for determining when left-turn phasing is appropriate at intersections using the volume of left-turn and through movements. However, this study recommends the protected left turn using a gap-based method to focus on safety. FDOT TEM standards utilize critical gap values to determine the need for a protected left-turn phase. Critical gap estimation requires the observation of both accepted and rejected gaps, which cannot be directly obtained in this study. Instead, the gap between opposing through movements is used to assess left-turn safety and recommend a protected left-turn. **Figure 5-22** illustrates a scenario involving two consecutive vehicle detections.

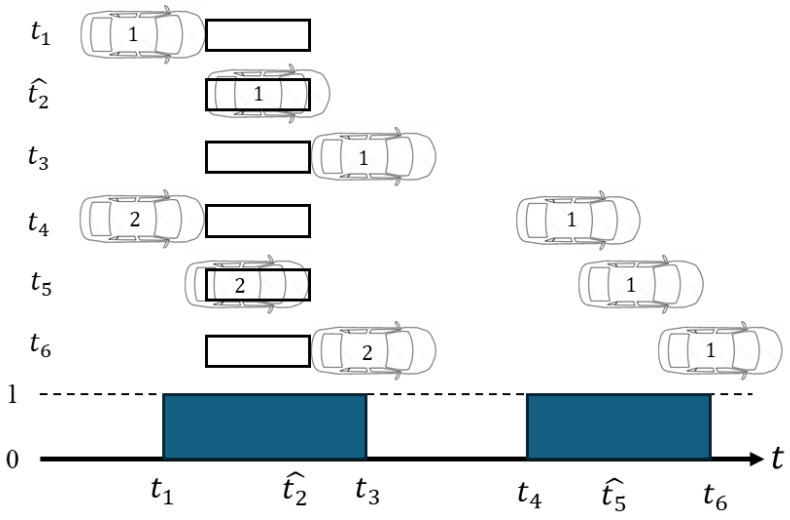

Figure 5-22. Gap Calculation Method

A gap is defined as the time interval between the exit of the first vehicle's rear from the detector ($\widehat{t_2}$) and the entry of the second vehicle. $\widehat{t_2}$ is not directly observable, as it depends on detector length and vehicle speed. (**Equation 5-1)** defines the gap in this scenario**.**

$$Gap = t_4 - \widehat{t_2} = t_4 - \left(t_3 - \frac{L_{detector}}{v_1}\right) \quad (5\text{-}1)$$

While the effect of detector length is negligible when detector length ($L_{detector}$) is short, and speed is fast, but a short detector near the stop line is unavailable in Seminole County. If the detector length is 40 feet, which is the typical length of a stopbar detector, and the vehicle speed is 25 mph, the difference is approximately 1.1 seconds. Therefore, this study considered detectors and approach speeds, which are assumed to be speed limits.

Gaps detected by individual detectors should not be used because left-turning vehicles interact with vehicles across all conflicting lanes. When multiple detection channels span multiple lanes, they are synchronized within a single detector. Specifically, only the first and last detection events from the vehicle platoon are considered, even if the vehicles are in different lanes. This approach is equivalent to using a single detector covering multiple lanes. **Figure 5-23** illustrates an example of a synchronized channel.

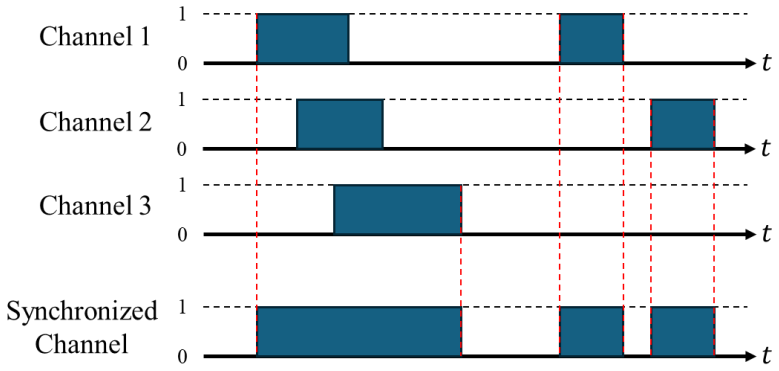

Figure 5-23. Example of Synchronized Channel

5.4.1.2. Left-turn Volume Estimation using Stopbar Detector

Protected left-turn recommendations depend on accurate left-turn traffic measurements, which typically require short detectors at the near stop lines. Since these detectors are not available in Seminole County, we developed an alternative approach to estimate traffic volume using occupancy data from stopbar detectors. The stopbar-based method enables more scalable estimates of left-turn volume since most intersections with ATSPM systems have stopbar detectors installed on a lane-by-lane basis. Estimating left-turn volume requires an assumed saturation flow rate and effective green time because stopbar detectors do not directly measure vehicle counts. Additionally, this method is applicable only to intersections with protected left-turn phases.. The left-turn volume at phase i (V_i^{left}) is determined via (**Equation 5-2)**:

$$V_i^{left} = Q \cdot \text{Occupancy Ratio}_i \cdot \text{Effective green}_i \cdot \text{No. of lane}$$
$$\approx Q \cdot (\sum_{\ell_{left}} \text{Occupancy}_{G,\ell_{left}} + \text{Occupancy}_{Y,\ell_{left}} - T^l) \quad (5\text{-}2)$$

In this equation, Q represents the saturation flow rate for left-turning vehicles (veh/sec). $\text{Occupancy}_{G,\ell_{left}}$ and $\text{Occupancy}_{Y,\ell_{left}}$ denote the occupancy duration during the green and yellow phases at the left-turn lane (ℓ_{left}), respectively. T^l refers to the lost time.

For validation of this approach, this study uses manually collected turning movement data managed by FDOT. The data records traffic volumes for left-turn, through, right-turn, and U-turn movements over eight hours, including peak hours, to support signal phase and timing decisions at most intersections. This study multiplies hourly traffic volume by the cycle length to calculate the left-turn volume per cycle. This study linearly interpolates missing hours due to recorder breaks and excludes unobserved hours. We compared this traffic with the traffic obtained through **Equation 5-1**

to find the optimal saturation flow rate and lost time. **Figure 5-24** shows optimization results using observed turning movement data collected by FDOT. This study uses a total of 70,616 cycles for optimization and observed an RMSE of 6.45 veh per cycle. As a result, this study uses 1,160 veh/hr for saturation flow rate and 0 sec for loss time.

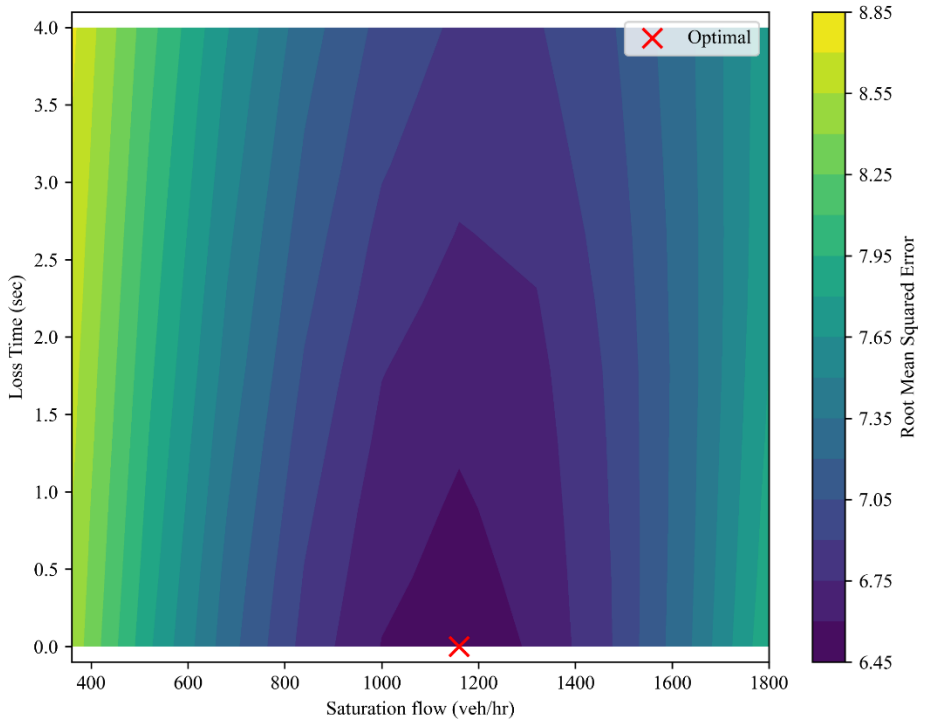

Figure 5-24. Optimization Results of Saturation Flow and Lost Time.

5.4.1.3. Recommended algorithm

The critical gap and follow-up gap determine the number of vehicles that can safely complete a left turn, referred to as the allowable left-turn volume (ALV). Let P_i^{gap} represent the set of gaps during phase i, where $P_i^{gap} = \{g_1, g_2, \ldots, g_k\}$, the ALV of the opposing left-turn approach is defined by (**Equation 5-3).**

$$ALV = \sum_{g \in P_i^{gap}}^{k} \left\lfloor \frac{g - gap^{critical}}{gap^{followup}} + 1 \right\rfloor \quad (5\text{-}3)$$

where $\lfloor x \rfloor$ is the floor function, which returns the largest integer less than or equal to x. The critical gap ($gap^{critical}$) and follow-up gap ($gap^{followup}$) are set to 4.5 and 2.5 sec, based on the default values in the HCM 2022. **Figure 5-25** shows examples of average ALV per cycle, aggregated on an hourly basis.

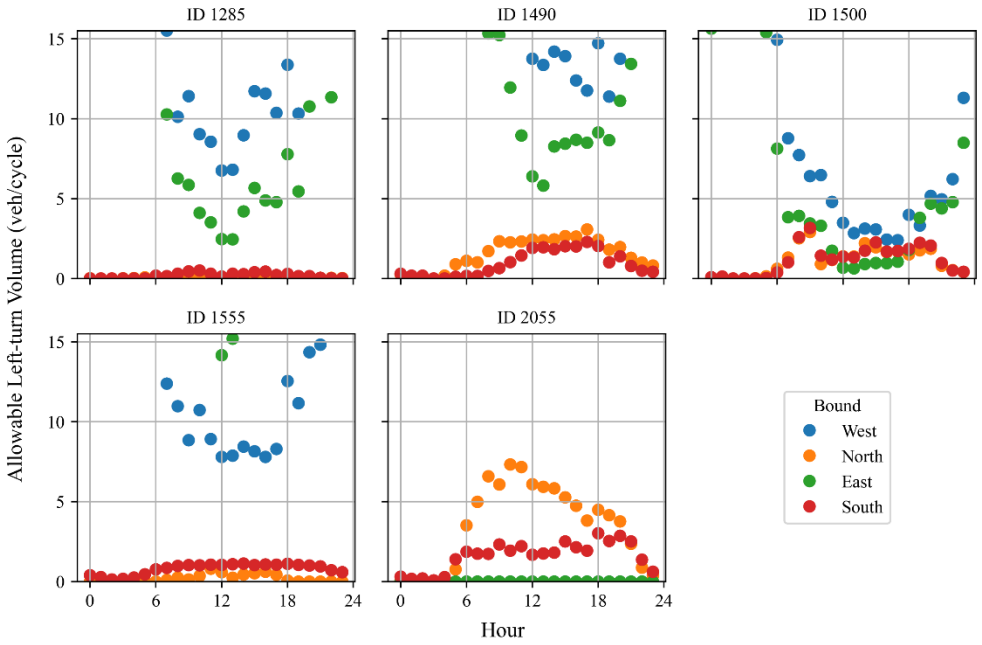

Figure 5-25. Examples of Allowable Left-turn Volume

When the ALV is lower than the left-turn demand, vehicles are exposed to unsafe left-turn movements, and therefore, the permissive phase should be avoided. This study recommends a protected left-turn phase when the probability of hours where the ALV falls below the left-turn demand exceeds 20% within the observed period. The 20% threshold is the sole parameter used in the algorithm, though practitioners may adjust it based on specific requirements and contextual factors. **Figure 5-26** shows examples of average hourly ALV and left-turn volume of westbound (WB) and eastbound (EB) of intersection 1500 and 1555. For example, both intersections 1500 and 1555 have higher ALVs than left turn demand during the early morning hours, practitioner may consider switching to permissive during these hours.

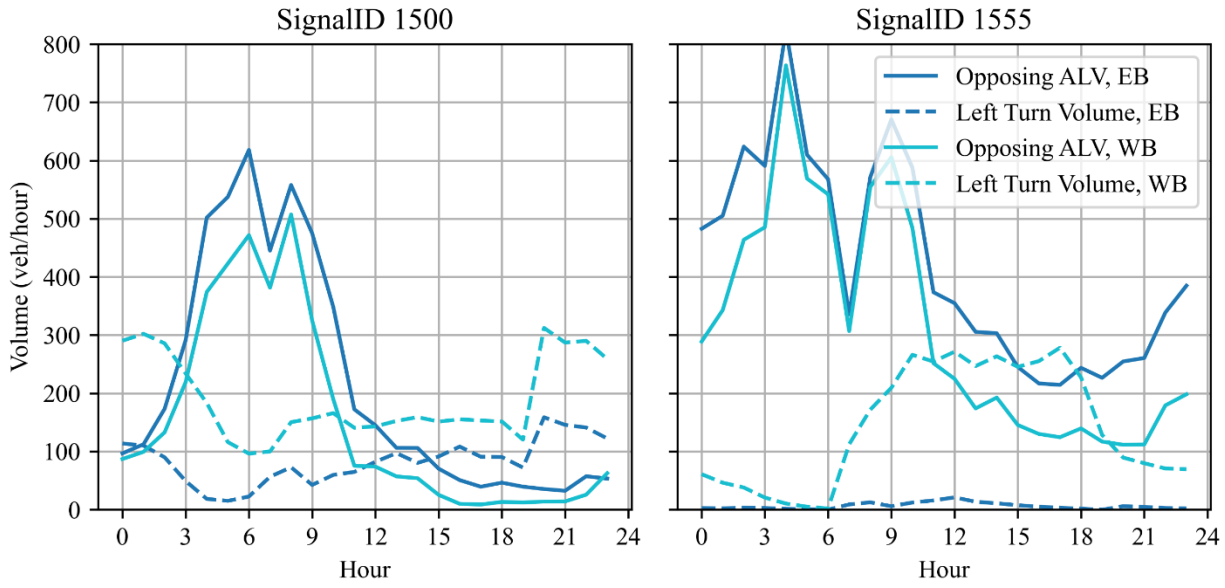

Figure 5-26. Hourly ALV and Left-turn Volume

5.4.2. Recommendation Results

Recommendations are made at intersections and times of day when left-turning traffic is available, and stopbar detectors are available in the opposing approach. In this study, we used data from turning movement data where they existed, and data from ATSPM where they did not. **Figure 5-27** shows examples of ALV probability of hours where the ALV falls below the left-turn demand. As turning movement observations were conducted from 7:00 to 19:00, the variation in probability differences by observation time is not significantly different for each intersection. Recommendation results for other intersections are attached in **Table A-4.**

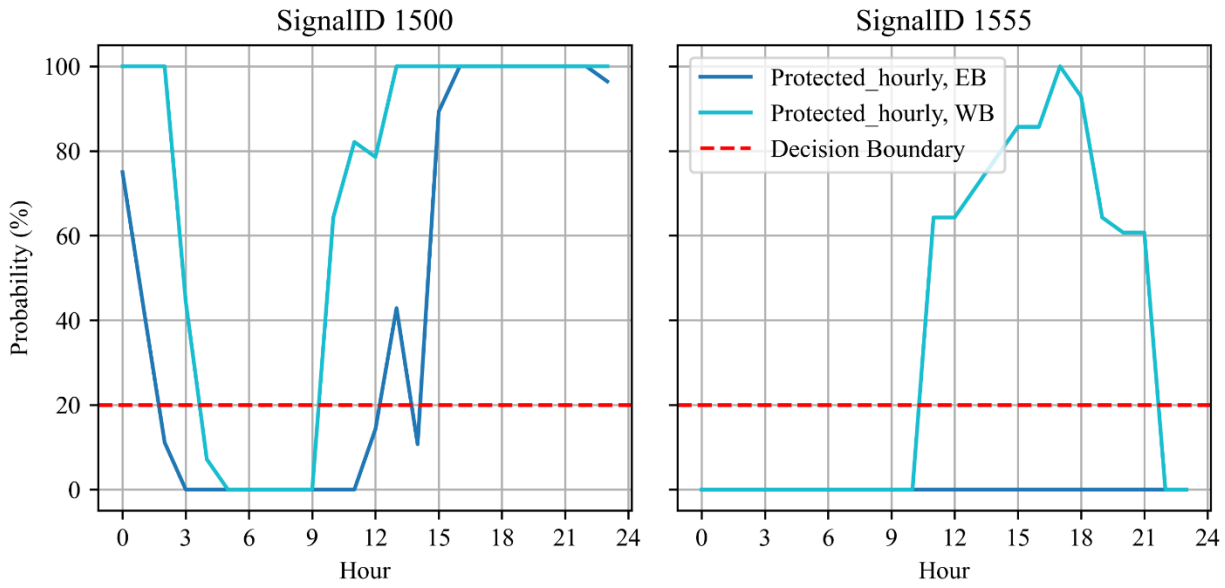

Figure 5-27. Protected Recommendation Examples

Although the configuration of detectors in the intersections examined did not support this capability, the ATSPM system can estimate accurate left-turn volume when left-lane counting is available. Alternatively, a cross-product approach leveraging third-party trajectory data can be used to estimate hourly left-turn volume. These approaches will make these recommendations available to a wider range of intersections.

5.5. Pedestrian Recall

At signalized intersections, pedestrian phases can be configured as either recall or push-button actuated. Pedestrian recall (PR) is a signal control strategy where pedestrian phases are automatically activated during every cycle without requiring push-button activation. This chapter presents the algorithm and results for recommending PR at the selected signalized intersections based on performance measures.

5.5.1. Algorithm

Pedestrian recall (PR) is often implemented during periods of high pedestrian demand. We analyze pedestrian presence probability at intersections to develop an algorithm that identifies the most critical hours for each pedestrian phase necessitating PR implementation at selected signalized intersections. The algorithm applies a three-step process:

- **Calculation of Pedestrian Presence Probability**: Calculate pedestrian presence probability using pedestrian activity indicator.
- **Identification of Critical Hours**: Determine the critical hours for PR implementation based on calculated pedestrian presence probability.
- **Pedestrian Recall (PR) Recommendation**: Recommend PR implementation for the identified critical hours of each pedestrian phase.

5.5.1.1. Calculation of Pedestrian Presence Probability

Pedestrian presence probability (P_{PP}) represents the likelihood that a given signal cycle will have pedestrian presence. In other words, P_{PP} is the probability that at least one pedestrian actuation (button press or detector activation) occurs within a cycle, making it a key measure for

determining pedestrian demand at intersections. A straightforward method to estimate P_{PP} is using the observed proportion of cycles with pedestrian presence (Equation 6-1):

$$P_{PP} = \frac{\sum \text{Cycles with Pedestrian Presence per Hour}}{\sum \text{Cycles per Hour}} \quad (6\text{-}1)$$

While this method provides a direct estimate, it does not account for variability in pedestrian arrivals across different days or under low pedestrian demand conditions.

To better capture day-to-day variability and overdispersion in pedestrian arrivals, a Beta-Binomial model was used instead of a simple proportion. The Beta-Binomial approach models pedestrian presence as a stochastic process, allowing for fluctuations in pedestrian activity across different time periods. The probability of pedestrian presence per cycle is estimated using the Beta-Binomial likelihood function (**Equation 6-2**):

$$P_{PP} = \frac{\alpha + X}{\alpha + \beta + N} \quad (6\text{-}2)$$

where X is the number of cycles with pedestrian presence in a given period, N is the total number of cycles in that period, and (α, β) are the shape parameters of the Beta prior, learned from the data. This formulation ensures that pedestrian presence probability is adjusted for data sparsity and provides a more robust and reliable estimate.

The pedestrian presence probability was calculated at an hourly level. Morever, to quantify variability, the 95% confidence intervals were determined using bootstrapping, which involved resampling the dataset multiple times.

5.5.1.2. Identification of Critical Hours

The critical hours for PR implementation correspond to periods with high pedestrian presence probability. However, no predefined threshold exists to differentiate between low and high pedestrian presence probability. To address this, k-means clustering was applied to the hourly aggregated pedestrian presence probability data for all the study intersections, naturally grouping the data into two categories: low probability and high probability.

Critical hours for PR were determined by comparing pedestrian presence probability values against the centroid of the high-probability cluster. The decision rule is as follows:

- If, for a given hour, the lower bound of the pedestrian presence probability exceeds the centroid of the high-probability cluster, that hour is considered statistically critical for PR implementation.

It is important to note that, the threshold will dynamically change as more data and intersections are added.

5.5.1.3. Pedestrian Recall (PR) Recommendation

PR was recommended for a pedestrian phase during hours identified as critical by comparing pedestrian presence probability with the centroid of the high-probability cluster.

5.5.2. Recommendation Results

Our algorithm was applied to recommend PR across all selected intersections. The identification of critical hours for a sample intersection, SR436 and Westmonte Drive (Signal ID: 1500), based on pedestrian presence probability (P_{PP}), are illustrated in Figure 5-28**.**

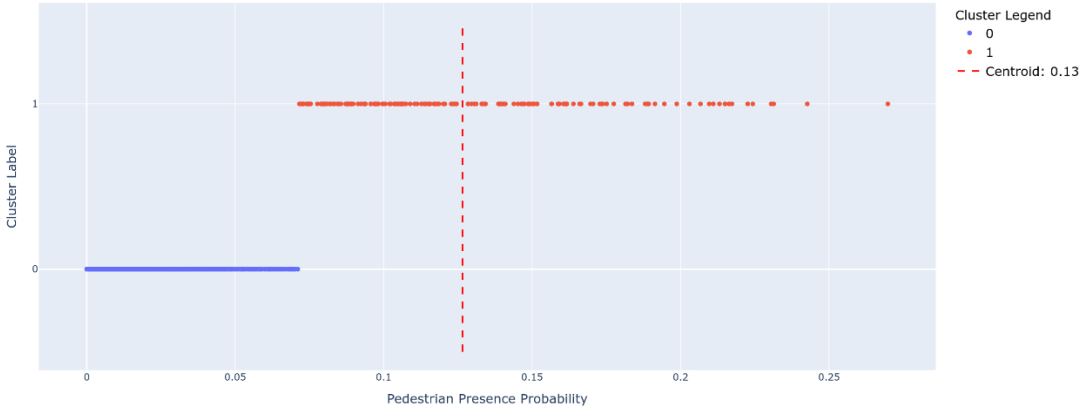

(a) Identification of Cluster Centroids

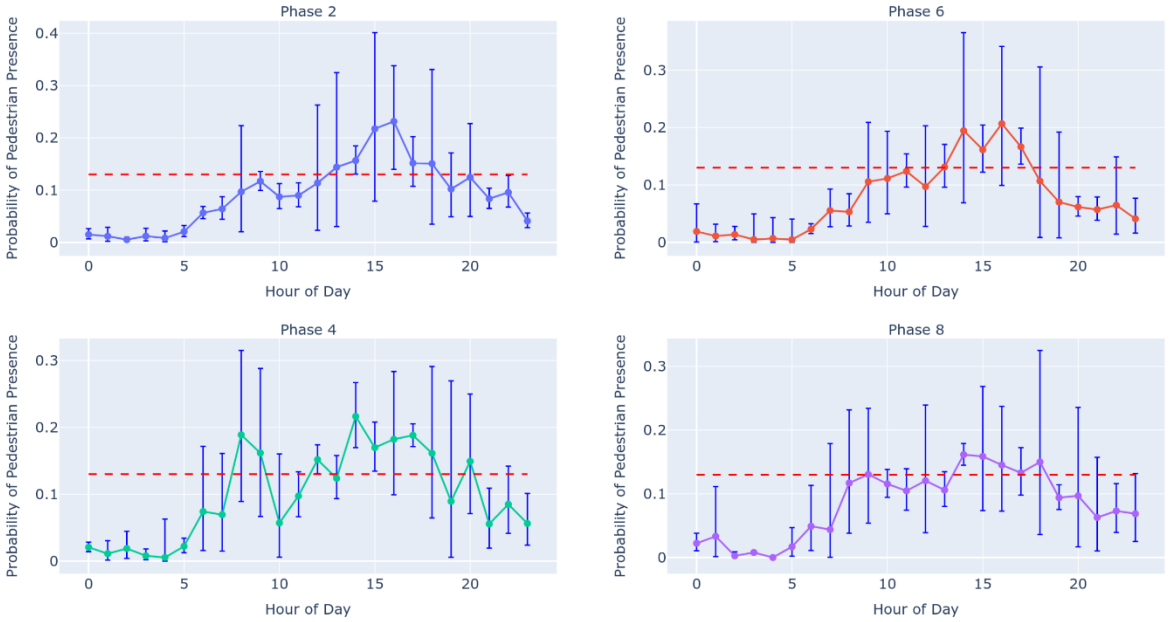

(b) Hourly Average Pedestrian Presence Probability with 95% Confidence Interval

Figure 5-28. Identification of Critical Hours to Recommend PR (Signal ID: 1500)

Figure 5-28(a) presents the clustering results of hourly aggregated pedestrian presence probability data for all study intersections. The identified threshold for selecting critical hours is **0.13**, which corresponds to the centroid of the high-probability cluster. This threshold indicates that a **13% probability** of at least one pedestrian actuation (button press or detector activation)

within a cycle is considered critical for PR recommendation. Figure 5-28**(b)** displays the most critical hours for all pedestrian phases at the SR436 and Westmonte Drive intersection (Signal ID: 1500). PR implementation is required for each phase during its identified critical hours at this intersection.

The PR recommendations for the intersection at SR436 and Westmonte Drive (Signal ID: 1500) are shown in **Figure 5-29.**

Figure 5-29. Pedestrian Recall (PR) Recommendations for the Intersection at SR436 and Westmonte Drive (Signal ID: 1500)

Comprehensive PR recommendations for all selected intersections are summarized in **Table A-6** in **A.** Appendix.

5.6. Leading Pedestrian Interval and No Right Turn on Red

A **Leading Pedestrian Interval (LPI)** is a signal control strategy that provides pedestrians with a short head start (3-7 seconds) to enter the crosswalk and cross the street before a parallel green signal for vehicles. This approach reduces potential conflicts between pedestrians and turning vehicles by allowing pedestrians to establish their presence in the crosswalk before vehicles begin turning. A No Right Turn on Red (NRTOR) restriction complements an LPI by prohibiting vehicles from making right-turns during a red light.

LPI and NRTOR primarily aim to enhance pedestrian safety at intersections by minimizing the risk of pedestrian-vehicle conflicts. In this chapter, we present the algorithm and results for recommending LPI and NRTOR at the selected signalized intersections based on performance measures.

5.6.1. Algorithm

Leading Pedestrian Interval (LPI) and No Right Turn on Red (NRTOR) are strategies aimed at reducing pedestrian-vehicle conflicts, particularly at intersections, by mitigating the risk of collisions involving right-turn vehicles and pedestrians. To recommend LPI and NRTOR effectively, it is crucial to have a comprehensive understanding of pedestrian-vehicle conflict risks at intersections.

We propose a three-step framework for recommending LPI and NRTOR at the selected intersections:

- **Calculation of Pedestrian-Vehicle (Right-Turn) Conflict Propensity**: Calculate conflict propensity between pedestrian and right-turn vehicles.

- **Identification of Critical Hours:** Identify the most critical hours for LPI and NRTOR implementation using cluster-based thresholding of conflict risk levels.
- **LPI and NRTOR Recommendation:** Recommend LPI and NRTOR for the identified critical hours specific to each pedestrian phase.

5.6.1.1. Calculation of Pedestrian-Vehicle (Right-Turn) Conflict Propensity

To calculate pedestrian-vehicle conflict propensity, we analyzed the interaction between pedestrian and vehicle presence in concurrent pedestrian and vehicle phases at intersections. Our approach considers pedestrian exposure (duration of pedestrian activity period), and right-turn vehicle exposure (duration of right-turn vehicle presence within pedestrian activity period). The pedestrian activity period is defined as the time from the first push-button activation to the end of the pedestrian "Clearance" interval. Our algorithm for calculating pedestrian-vehicle conflict propensity can be mathematically expressed as (**Equation 7-1**):

$$CP_{P-V} = \sum_{\ell} W_{\ell}^{Adj} \times \left(1 - e^{-k \times H\left(P_{exp}, V_{exp,\ell}\right)}\right) \tag{7-1}$$

Notions & Definitions:

- CP_{P-V}: Represents the pedestrian-vehicle (right-turn) conflict propensity for a given concurrent pedestrian phase P and vehicle phase V. The propensity score ranges between 0 and 1, where values closer to 1 indicate a higher propensity of conflict, while values closer to 0 represent a lower propensity.
- ℓ: Denotes each lane within vehicle phase V that has right-turn vehicles.
- W_{ℓ}: Assumed lane-specific weights based on the contribution of right-turn vehicles:

  $W_{\ell} = 1$: Lanes dedicated to right-turns.

  $W_{\ell} = 0.5$: Lanes shared between right-turn and either through or left-turn vehicles.

$W_\ell = 0.33$: Lanes shared between right-turn and two other movements (e.g., left and through).

- $W_\ell^{Adj}\left(= W_\ell \times \frac{W_\ell}{\sum_\ell W_\ell}\right)$: Adjusted lane weight, ensuring each lane maintains its intrinsic weight while being distributed proportionally across multiple lanes.
- P_{exp}: Pedestrian exposure in pedestrian phase P is defined as the time interval from the first push-button activation to the end of the pedestrian "Clearance" interval.
- $V_{exp,\ell}$: Vehicle exposure in lane ℓ of vehicle phase V (concurrent to pedestrian phase P), defined as the duration a vehicle remains at the stopbar in lane ℓ during the pedestrian activity period $\left(P_{exp}\right)$.
- $H\left(P_{exp}, V_{exp,\ell}\right)$: The harmonic mean of pedestrian exposure P_{exp} and vehicle exposure $V_{exp,\ell}$, ensuring a balanced contribution:
- $H\left(P_{exp}, V_{exp,\ell}\right) = \begin{cases} \frac{2\times\left(P_{exp}\times V_{exp,\ell}\right)}{P_{exp}+V_{exp,\ell}}, & if\ P_{exp} > 0\ or\ V_{exp,\ell} > 0 \\ 0, & else \end{cases}$
- k: A constant decay controlling the diminishing returns applied to the interaction between pedestrian and vehicle presence. Higher values of k result in faster diminishing returns. Diminishing returns were used to account for the decreasing marginal impact of high pedestrian and vehicle exposure levels on conflict propensity, ensuring that extreme activity values do not disproportionately inflate the calculated propensity.

The pedestrian-vehicle conflict propensity was calculated at an hourly level. Morever, to quantify variability, the 95% confidence intervals were determined using bootstrapping, which involved resampling the dataset multiple times.

5.6.1.2. Identification of Critical Hour

LPI and NRTOR are complementary strategies designed to reduce pedestrian-vehicle conflicts, and are often implemented simultaneously. However, there is no universally defined threshold of conflict propensity for determining the critical hours requiring their implementation. To establish a practical and simple decision criterion, we assume a 50th percentile threshold for pedestrian-vehicle conflict propensity. The decision rule is:

- A specific hour is classified as statistically critical for LPI and NRTOR implementation if the lower bound of its pedestrian-vehicle conflict propensity score exceeds the 50th percentile.

It is important to note that practitioners can adjust this threshold based on specific requirements and contextual considerations.

5.6.2. Recommendation Results

Due to limitations in detector configurations, our algorithm for recommending LPI and NRTOR was applied exclusively to intersections with Type 2 and Type 4 configurations (see **Table A-1**). Phases with right-turn lanes lacking detectors were excluded from the analysis.

The pedestrian-vehicle conflict propensity and clustering results for the intersection at SR436 and Westmonte Drive (Signal ID: 1500) are shown in **Figure 5-30**. This intersection includes Type 4 detector configurations on dedicated right-turn lanes for Phase 4 and Phase 8, as well as on shared right-turn lanes for Phase 2 and Phase 6. The conflict propensity was calculated using $k = 0.01$ and compared against a threshold score of 0.5 to identify critical hours.

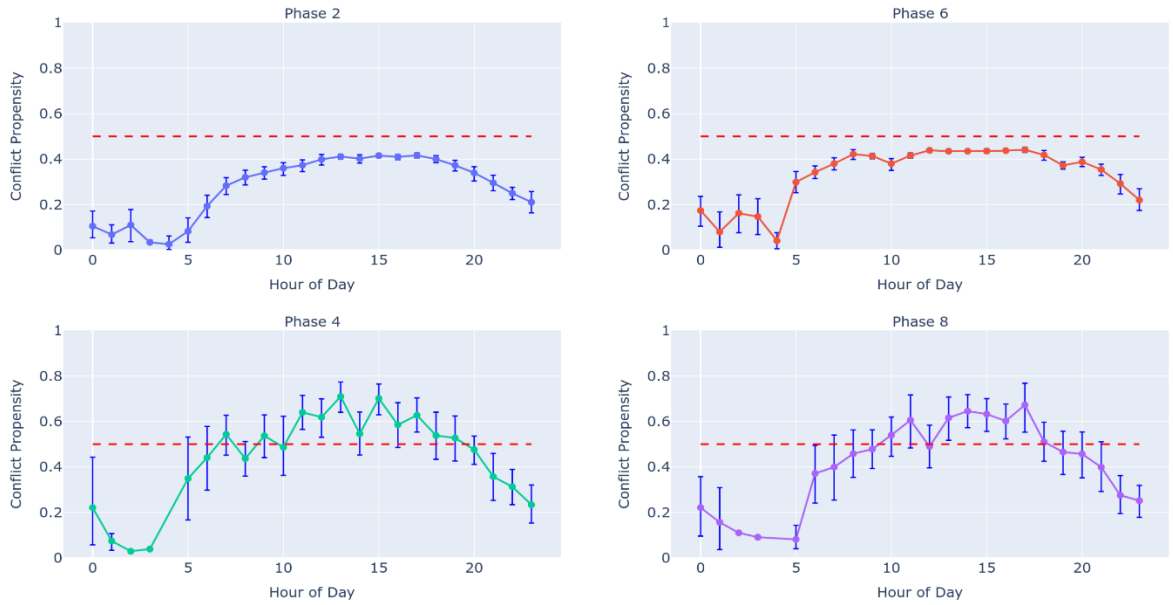

Hourly Average Pedestrian-Vehicle (Right-Turn) Conflict Propensity

Figure 5-30. Identification of Critical Hours to Recommend LPI and NRTOR (Signal ID: 1500)

We recommend LPI and NRTOR based on the analysis of identified critical hours. The recommendations for the intersection at SR436 and Westmonte Drive (Signal ID: 1500) are presented in **Figure 5-31(a)** displays the LPI recommendation status, while **Figure 5-31(b)** highlights the NRTOR recommendations.

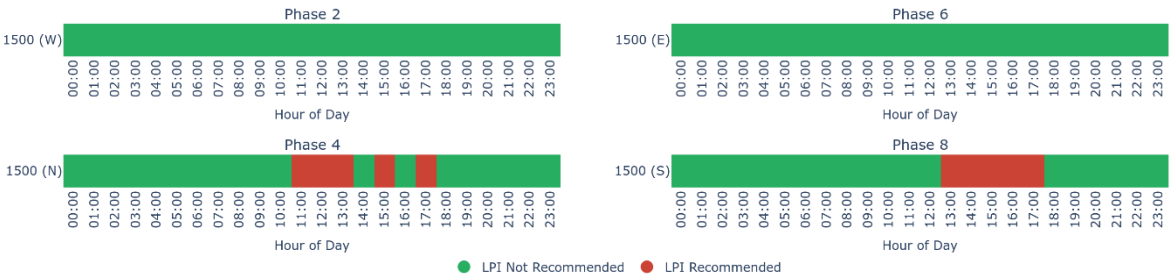

(a) LPI Recommendation

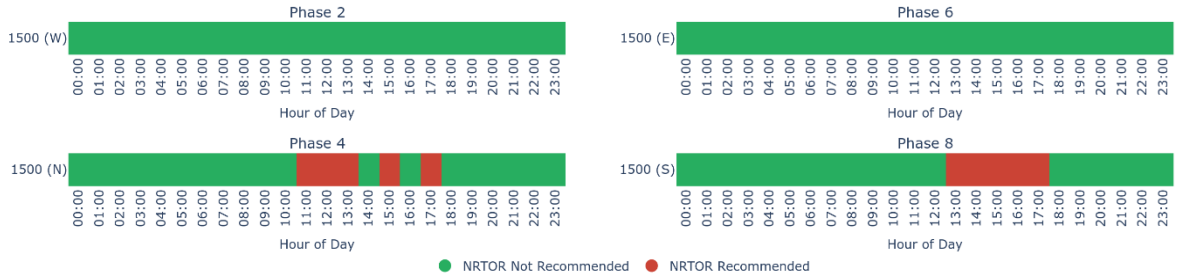

(b) NRTOR Recommendation

Figure 5-31. LPI and NRTOR Recommendations for the Intersection at SR436 and Westmonte Drive (Signal ID: 1500)

A comprehensive summary of LPI and NRTOR recommendations for all selected intersections with Type 2 and Type 4 configurations (**Figure 4-5**; **Table A-1**) can be found in **Table A-7** and **Table A-8** in **A.** Appendix, respectively. The pedestrian-vehicle conflict propensity, which served as the basis for the recommendations across all intersections, was calculated using **k = 0.01**.

It is important to note that adjusting the value of k will impact the conflict propensity scores: increasing k will lead to higher scores, whereas decreasing k will result in lower scores. The final dashboard will have the option to tweak this parameter.

LPI and NRTOR were recommended simultaneously during the critical hours of high pedestrian-vehicle conflict propensity, i.e., when lower bound of propensity exceeds 50th percentile.

CHAPTER 6: System Architecture

In this chapter, we present the development of the Smart Signal Performance Monitor (SSPM) system. The SSPM system integrates three key components: the Transform–Recommend–Rank (TRR) server, the database server, and the frontend server. A high-level overview of the architecture of the SSPM system is depicted in **Figure 6-1**. This chapter details the role and architecture of each component, emphasizing how they work together to deliver accurate and efficient safety recommendations for traffic signal operations.

The system architecture described in this chapter was developed and tested using ATSPM data collected from 19 study intersections in Seminole County, Florida, for June 2024 (refer to the Task 3 report for additional details). Once fully deployed, the system is expected to automatically scrape, process, and analyze SunStore data and deliver actionable safety recommendations to FDOT operators to support safer and more efficient traffic operations at intersections throughout Seminole County, Florida.

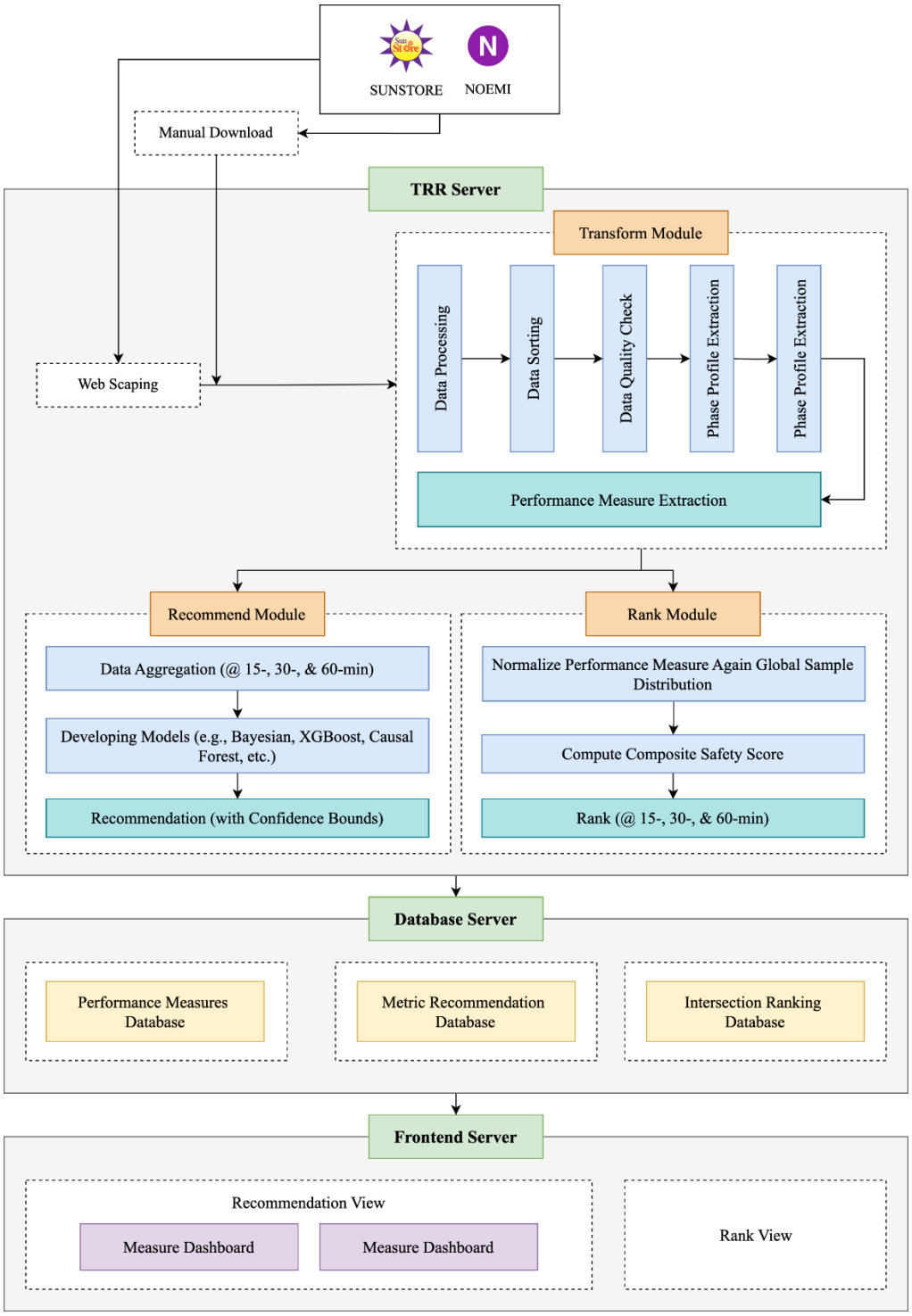

Figure 6-1. The architecture of the SSPM System

6.1. Transform–Recommend–Rank (TRR) Server

As the name suggests, the TRR server comprises three core modules, as shown in **Figure 6-2**: (1) the transform module, (2) the recommend module, and (3) the rank module.

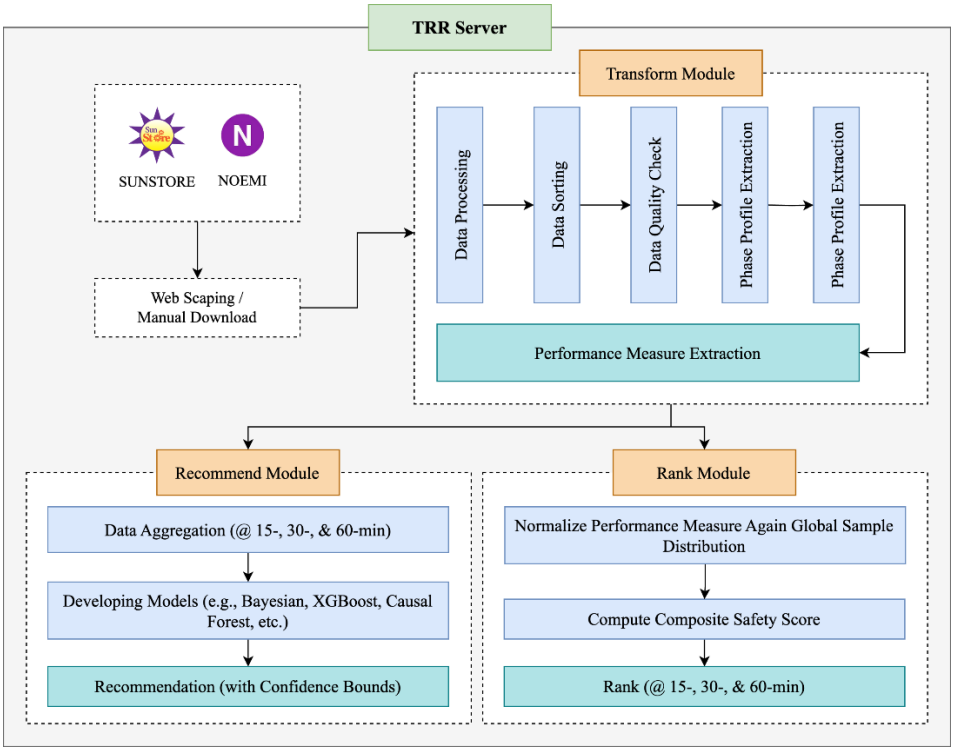

Figure 6-2. Architecture of the Transform–Recommend–Rank (TRR) Server

6.1.1. Transform Module

The transform module is the central component of the TRR server, as the accuracy and reliability of the recommend and rank modules depend heavily on it. This module processes raw ATSPM data, performs data quality checks, and transforms clean, error-free data into cycle-level performance measures, including Signal Phasing and Timing (SPaT), volume, occupancy, headway, split failures, vehicle-vehicle conflicts, red-light violations, pedestrian activity indicators, pedestrian delay, and pedestrian-vehicle conflict propensity.

6.1.2. Recommend Module

The recommend module applies the signal safety enhancement algorithms developed in Task 3. Using statistical and machine learning models, such as the Beta-Binomial model, Causal Forest, and XGBoost, this module processes performance measures produced by the transform module to generate specific safety recommendations. These include interventions like Yellow and Red Clearance Time Adjustment, Protected/Permitted Left Turn, Pedestrian Recall, Leading Pedestrian Intervals (LPI), and No Right Turn on Red, as specified in the project scope.

Most recommendations are generated using a binary classification framework (0 or 1) to indicate whether a specific safety treatment is warranted. However, the module provides a quantitative duration recommendation instead of a binary output for Yellow and Red Clearance Time Adjustments. A summary of the performance measures used, the analytical methods applied, and the corresponding type of recommendation is provided in **Table 6-1**. All recommendations are computed at three temporal resolutions (15-minute, 30-minute, and 1-hour) for each study intersection. Since real-time ATSPM data was not available during development, this module performed batch-level analysis on historical data over a defined period. This ensured the statistical validity and reliability of the generated recommendations.

6.1.3. Rank Module

The rank module ranks all study intersections based on a unified safety score derived from multiple standardized performance measures (vehicle-vehicle conflicts, red light violations, and pedestrian delay) at the cycle-level resolution. Given that intersections may have varying numbers of phases (left-turn or through movements), the module applies a normalization and aggregation strategy to ensure fair and meaningful comparisons.

Table 6-1. Summary of Performance Measures, Methods, and Recommendation Types in the Recommend Module

Safety Metric	Key Performance Measures	Method	Recommendation Type
Yellow Time Adjustment	Volume, Occupancy, Gap, Split Failure, Red Light Running, Pedestrian Delay	Causal Forest + XGBoost	Continuous (Duration in Sec)
Red Clearance Time Adjustment			Continuous (Duration in Sec)
Protected/Permitted Left Turn	Occupancy, Gap		Binary (0 = Not Recommended, 1 = Recommend)
Pedestrian Recall	Pedestrian Activity	Bayesian Beta-Binomial	Binary (0 = Not Recommended, 1 = Recommend)
Leading Pedestrian Interval (LPI)	Occupancy, Pedestrian Activity	Bootstrapping + Threshold-Based	Binary (0 = Not Recommended, 1 = Recommend)
No Right Turn on Red			

Safety Score Computation Steps:

To ensure fair comparison across intersections, especially when they have varying numbers of approaches and phases, raw performance measure values are normalized using a robust, distribution-based method. The normalization approach differs based on the type of performance measures: continuous-valued or binary indicator.

Continuous-Valued Features (e.g., Conflicts, Pedestrian Delay)

For continuous measures such as vehicle-vehicle conflicts and pedestrian delay, a global reference distribution is constructed using values collected from all study intersections across all signal cycles. In the current implementation, this reference distribution is derived from the transformed features generated by the transform module for June 2024. As more data becomes available, the global distribution is dynamically updated to reflect the expanded dataset, ensuring long-term consistency and fairness in scoring.

From this global distribution, the 95th percentile (P_{95}) is computed for each measure m. This value serves as a robust threshold that limits the influence of outliers and ensures that all normalized values fall within the$[0, 1]$ range. The normalization rule is:

$$x_{\text{norm}}^{(m)}(i,j,c) = \begin{cases} \dfrac{x^{(m)}(i,j,c)}{P_{95}^{(m)}}, & if\ x(i,j,c) < P_{95}^{(m)} \\ 1, & else \end{cases} \tag{2-1}$$

where $x^{(m)}(i,j,c)$ is the raw value for measure m, intersection i, phase j, and cycle c. $P_{95}^{(m)}$ is the global 95th percentile for measure m. This method avoids local biases (e.g., cycle-based normalization) and creates a globally fair, outlier-resistant safety scale.

Binary Indicator Features (e.g., `Red Light Running Flag`)

For binary-valued features such as red-light running, percentile-based normalization is not applicable. Since values are already bounded in $\{0, 1\}$, they are already normalized by definition, and are passed directly to the aggregation step (Step 2) without any transformation.

Aggregation Across Phases per Cycle: After normalization, normalized scores across all phases within each intersection and cycle was aggregated to obtain a single per-measure score for each intersection per cycle. The default aggregation function is the arithmetic mean:

$$M_i^{(m)}(c) = \frac{1}{N_i} \sum_{j=1}^{N_i} x_{\text{norm}}^{(m)}(i, j, c) \quad (2\text{-}2)$$

where $M_i^{(m)}(c)$ is the score for measure m at intersection i, cycle c, and N_i is the number of active phases at intersection i.

Composite Safety Score Calculation**:** A composite safety score was computed for each intersection and cycle as a weighted sum of the individual per-measure scores. The weights are derived from expert judgment and reflect the relative importance of each safety indicator:

$$S_i(c) = w_1 \cdot C_i(c) + w_2 \cdot R_i(c) + w_3 \cdot P_i(c) \quad (2\text{-}3)$$

where C_i is the normalized vehicle-vehicle conflict score, R_i is the normalized red-light violation score, and P_i is normalized the pedestrian delay score. w_1, w_2, and w_3 are the weights derived from expert judgment ($w_1 = 0.5$, $w_2 = 0.3$, $w_3 = 0.2$).

Time Interval-Based Aggregation and Ranking: To provide dynamic, time-aware safety assessments, cycle-level composite scores are aggregated over rolling time intervals of 15 minutes, 30 minutes, and 60 minutes:

$$S_i^{(T)} = \frac{1}{N_T} \sum_{c \in T} S_i(c) \quad (2\text{-}4)$$

where T is the aggregation interval (e.g., 15-min window). N_T is the number of cycles within interval T. These interval-based scores are used by the Rank module to continuously rank intersections based on their safety performance, enabling proactive safety monitoring and targeted interventions.

6.2. Database Server

The architecture of the database server is illustrated in **Figure 6-3**. This server is responsible for storing the transformed performance measures, safety recommendations, and intersection rankings (based on safety scores) generated by the various modules of the TRR server. By centralizing these outputs, the database ensures that all system results are readily accessible for both immediate use and in-depth analysis.

The database server maintains a comprehensive archive of TRR server outputs for June 2024 on data collected from 19 study intersections (refer to the Task 3 report for details). This dataset was used to demonstrate performance measure trends, visualize the six safety recommendations in **Table 6-1**, and generate intersection rankings in the frontend server.

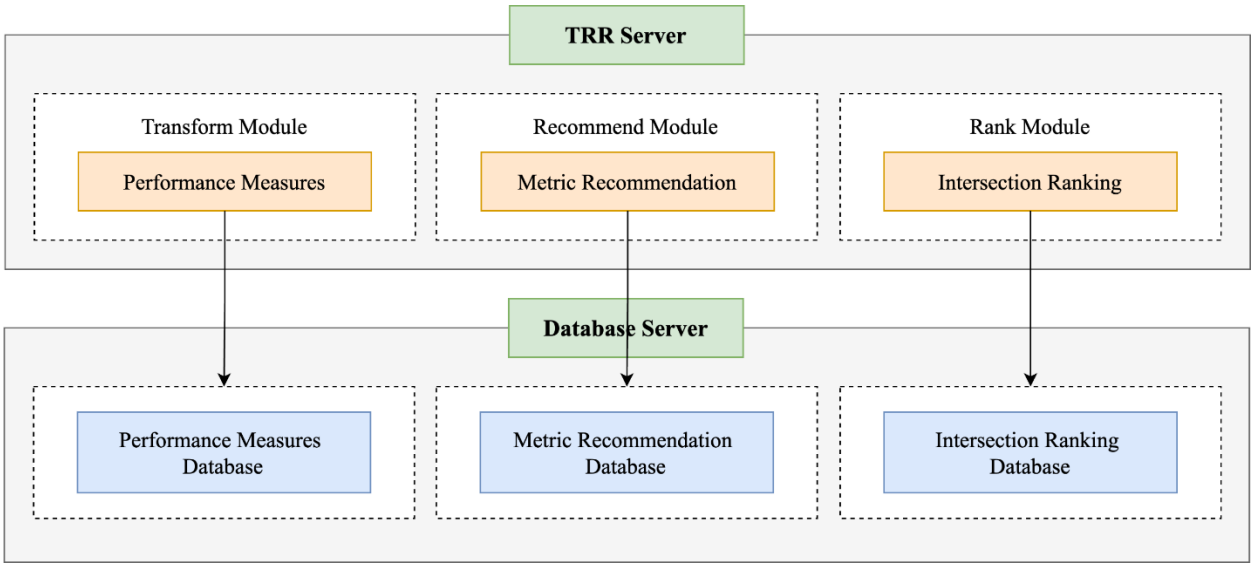

Figure 6-3. The architecture of Database Server

6.2.1. API Endpoints and Data Access

To enable seamless communication between the backend system and the operator-facing dashboard, a modular set of RESTful Application Programming Interfaces (APIs) has been implemented. These APIs support dynamic querying of data aggregated at different temporal resolutions (e.g., cycle, 15-min, 30-min, 60-min) and filtered by signal, feature type, and other relevant metadata. The current API endpoints are organized into three categories:

- Performance Measure APIs
- Safety Metric Recommendation APIs
- Safety Ranking APIs

All API endpoints are organized under three primary namespaces: `/api/measures`, `/api/recommendation`, and `/api/ranking`.

Performance Measures API: /api/measures

This endpoint retrieves performance measure data for a specified intersection (`signalID`) at a user-selected aggregation level. Aggregations supported include: `"Cycle"`, `"15 min"`, `"30 min"`, and `"60 min"`.

(1) Required Query Parameters:

Parameter	Type	Description
`signalID`	String	ID of the signalized intersection (e.g., "1500")
`featureName`	String	Feature name (e.g., "volume," "conflict," "gap")
`aggregation`	String	Temporal aggregation level (e.g., "Cycle," "15 min," "30 min")
`startDate`	String	ISO 8601 format timestamp (e.g., "2024-06-01T10:00:00Z")
`endDate`	String	ISO 8601 format timestamp (e.g., "2024-06-01T11:00:00Z")

Timestamps must be in ISO 8601 format (`YYYY-MM-DDTHH:mm:ssZ`) and should match UTC (Z = Zulu time). Internally, timestamps are stored in UTC.

(2) Example Request:

`/api/measure?signalID=1500&featureName=volume&interval=15min&startDate=2024-06-01T10:00:00Z&endDate=2024-06-01T11:00:00Z`

(3) Sample Response (JSON):


```
[
  {
    "_id": "67f5182565da982782157479",
    "signalID": "1500",
    "feature": "greenVolumePhase1L",
    "featureName": "volume",
    "cycleLength": 194.36,
```

```
    "value": 5,
    "signalType": "green",
    "laneType": "L",
    "phaseNo": 1,
    "timeStamp": "2024-06-01T10:00:00.000Z",
    "day": 1,
    "month": 6,
    "year": 2024
  }
]
```


(4) Response Attribute:

Field	Type	Description
_id	String	MongoDB object ID
signalID	String	ID of the intersection
feature	String	Internally generated feature key
featureName	String	Human-readable feature label (e.g., "volume")
cycleLength	Number	Cycle duration (only for "Cycle" level)
value	Number	Extracted metric value for cycle-level data only. If value is present, min, max, mean, and std will not be available.
min	Number	Minimum, maximum, average, and standard deviation of the metric across the aggregation window. If min, max, mean, and std are present, value will not be available.
max	Number	
mean	Number	
std	Number	
signalType	String	Signal phase type ("green", "yellow", etc.)
laneType	String	Lane identifier ("L" for left, "T" for through, etc.)
phaseNo	Integer	Signal phase number
timeStamp	ISO Date	UTC timestamp for the observation
day/month/year	Integer	Redundant date components for indexing and filtering

Safety Metric Recommendation API: /api/recommendation

This endpoint retrieves safety metric recommendation data for a given intersection (signalID) and safety metric (Yellow and Red Clearance Time Adjustment, Protected/Permitted Left Turn, Pedestrin Recall, Leading Pedestrian Intervals (LPI), and No Right Turn on Red) at a selected aggregation level. Supported aggregations include: “15 min”, “30 min”, and “60 min”. This API returns probability-based outputs, statistical bounds, and binary recommendation flags for safety interventions.

(1) Required Query Parameters:

Parameter	**Type**	**Description**
`signalID`	String	ID of the signalized intersection (e.g., “1500”)
`featureName`	String	Name of the safety feature (e.g., “pedestrianPresenceProbability”, “conflictPropensity”)
`aggregation`	String	Aggregation level: “15”, “30”, or “60”
`year`	Number	Year of data (e.g., 2024)
`month`	Number	Month of data (e.g., 6 for June)

The system currently uses month-level batch recommendations. All entries retrieved will correspond to the selected signalID, featureName, aggregation, year, and month.

(2) Example Request:

/api/recommendation?signalID=1500&featureName=pedestrianPresenceProbability&interval=15&year=2024&month=6

(3) Sample Response (JSON):


```
[
  {
    "_id": "6678ba6c2f7d938f4f5e12cc",
    “signalID”: “1500”,
    “feature”: “pedestrianPresenceProbability”,
    “phaseNo”: 3,
    “year”: 2024,
    “month”: 6,
    “time”: “10:00”,
    “alpha”: 3.12,
    “beta”: 5.88,
    “probability”: 0.348,
    “lowerBound”: 0.21,
    “upperBound”: 0.51,
    “threshold”: 0.30,
    “recommend”: 1,
  }
]
```

(4) Response Attributes:

Field	Type	Description
`_id`	String	MongoDB object ID
`signalID`	String	ID of the intersection
`feature`	String	Internal name of the feature used for modeling (e.g., pedestrianPresenceProbability)
`phaseNo`	Integer	Signal phase number
`year`	Integer	Year of the recommendation data
`month`	Integer	Month of the recommendation data
`time`	String	Time in HH:mm format representing the hour block (e.g., “10:00”)
`alpha`	Number	Estimated α parameter (for Beta model) or statistical posterior
`beta`	Number	Estimated β parameter (for Beta model) or statistical posterior
`probability`	Number	Estimated probability of safety event (e.g., pedestrian presence, conflict occurrence)
`lowerBound`	Number	Lower bound of the confidence interval (e.g., 95%)
`upperBound`	Number	Upper bound of the confidence interval
`threshold`	Number	Decision threshold used to determine recommendation
`recommend`	Integer	Binary recommendation (1 = treatment warranted, 0 = no treatment)
`k`	Number	Optional decay constant (used in conflictPropensity-related features only); null otherwise

Safety Ranking API: /api/ranking

This endpoint retrieves intersection-level safety rankings derived from aggregated performance measures. The ranking algorithm integrates multiple indicators (e.g., vehicle-vehicle conflicts, red-light violations, and pedestrian delay) to generate a unified safety score for each intersection over a specified time frame.

(1) Required Query Parameters:

Parameter	Type	Description
`aggregation`	String	Aggregation level (e.g., `"15"`, `"30"`, `"60"`). Determines the resolution of score computation
`startDate`	String	ISO 8601 formatted timestamp indicating the beginning of the time window (e.g., `"2024-06-01T00:00:00Z"`)
`endDate`	String	ISO 8601 formatted timestamp indicating the end of the time window (e.g., `"2024-06-30T23:59:59Z"`)
`weightLabel`	String	Dash-separated weights for conflict, red-light running, and pedestrian delay (e.g., `"0.5-0.3-0.2"`). The weights must sum to 1.

(2) Example Request:

`api/rank?interval=60&startDate=2024-06-01T00:00:00Z&endDate=2024-06-30T23:59:59Z&weightLabel=0.5-0.3-0.2`

(3) Sample Response (JSON):


```
[
  {
    "_id": "6817a854261e032aa67b4683",
    "weightLabel": "0.5-0.3-0.2",
    "timeStamp": "2024-06-01T00:00:00.000Z",
    "signalID": "1707",
    "conflictScore": 0.27314814814814814,
    "runningFlagScore": 0.09523809523809523,
    "pedestrianDelayScore": 1,
    "conflictWeight": 0.5,
    "runningFlagWeight": 0.3,
    "pedestrianDelayWeight": 0.2,
    "safetyScore": 0.36514550264550266,
```

```
    "year": 2024,
    "month": 6,
    "day": 1,
    "rank": 1
  }
]
```

(4) Response Attributes:

Field	Type	Description
`_id`	String	MongoDB object ID
`signalID`	String	ID of the signalized intersection
`weightLabel`	String	Combination of weights used for computing safetyScore
`conflictScore`	Number	Normalized conflict score (e.g., vehicle-vehicle conflicts)
`runningFlagScore`	Number	Score based on red-light running frequency or severity
`pedestrianDelayScore`	Number	Normalized pedestrian delay score
`conflictWeight`	Number	Weight applied to the conflict score
`runningFlagWeight`	Number	Weight applied to the red-light running score
`pedestrianDelayWeight`	Number	Weight applied to the pedestrian delay score
`safetyScore`	Number	Final weighted safety score computed as: `(conflictWeight × conflictScore) + (runningFlagWeight × runningFlagScore) + (pedestrianDelayWeight × pedestrianDelayScore)`
`rank`	Integer	Rank among all intersections (1 = highest safety score)
`timeStamp`	ISO Date	UTC timestamp for the record
`year`, `month`, `day`	Integer	Redundant date fields for filtering and indexing

6.2.2. API Endpoints Accessibility

The current setup is hosted on a local development server, and the API endpoints are accessible only from the host machine (e.g., `http://127.0.0.1:2500`).

When the backend is deployed on a cloud environment (e.g., an AWS EC2 instance) or an external server (e.g., FDOT infrastructure), the base IP address (or domain) in all API requests should be updated accordingly. The table below provides examples:

Environment	**API Base URL Example**
Local Testing	http://127.0.0.1:2500/api/...
AWS Deployment	http://<aws-ec2-ip>:2500/api/...
FDOT Server	http://<fdot-server-ip>:2500/api/...

6.3. Frontend Server

The frontend server is carefully designed to facilitate interaction between FDOT operators and the safety analytics system. Built with a modern component-based architecture in React, the interface enables seamless querying and visualization of data for safety interventions and intersection rankings. The interface is organized into two main webpages to support its dual function: 1) Recommendation View and 2) Rank View, each aligned with a specific backend module. These pages integrate intuitive selectors, visual displays, and responsive elements to deliver a highly usable and analytically powerful dashboard experience.

The frontend server is designed with a user-friendly interface that allows operators to effectively monitor intersection performance and identify critical locations. It supports decision-making on whether safety interventions are needed. The interface is divided into two main views:

(1) Recommendation View and (2) Rank View, each serving a distinct purpose aligned with the scope of this project.

6.3.1. Recommendation View

The Recommendation View serves as an interactive and analytical interface where users can examine safety-related performance trends and system-generated recommendations for improving traffic signal operations. Designed to support data-driven decision-making, this view combines high-resolution performance metrics and model-informed recommendations into an accessible dashboard framework. The Recommendation View is composed of two main components: Measure Dashboard and Recommendation Dashboard.

Interface Overview and Signal Selection

Upon entering the Recommendation View, users are first prompted to select a signalized intersection of interest. This can be done in one of two ways:

Signal Map View: A spatial interface displays all monitored signal locations on an interactive map (**Figure 6-4(a)**). Each cluster of intersections is marked by a green circle containing the number of signals in that cluster. Users can zoom into a cluster and click on specific signal markers, indicated by black pins, to load the corresponding dashboards. This spatial layout is intuitive for users who prefer geographic selection based on area familiarity or regional analysis.

Signal List View: Alternatively, users can view a tabulated list of signals sorted by `Signal ID`, `SIIA ID`, and `Intersection Name` (**Figure 6-4(b)**). This is useful for quick access to known intersections or when working with specific IDs.

These dual-selection mechanisms enhance usability, allowing both spatial and ID-based entry points into the analysis. Users can either click on marker (Signal Map View), or row (Signal List View) or manually enter a `Signal ID` in the input field at the bottom and press “Go” to proceed.

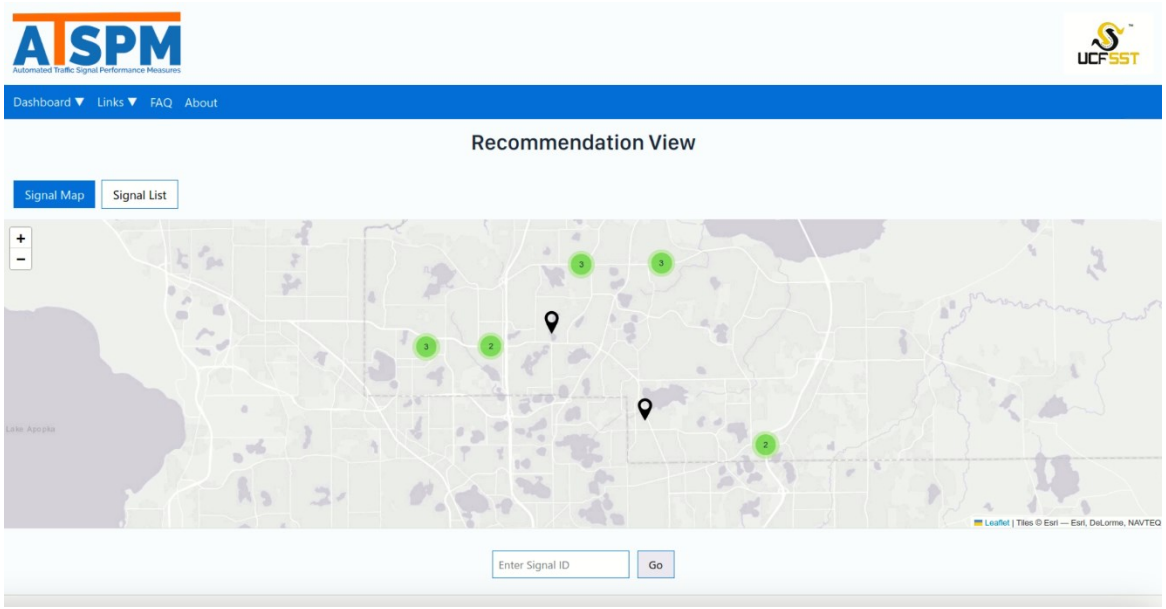

(a)

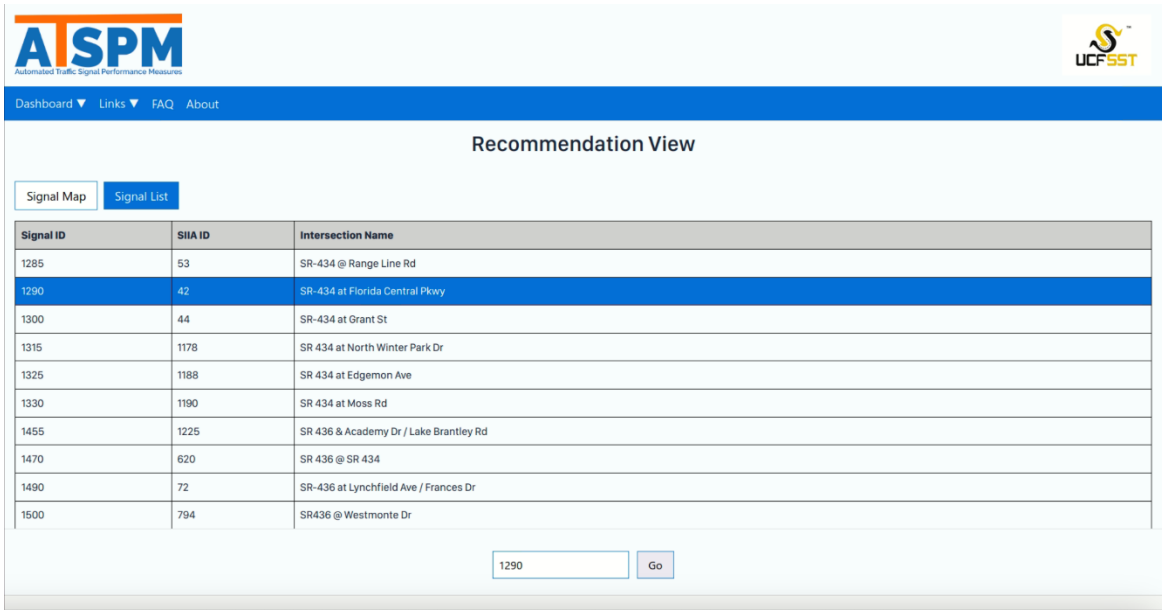

(b)

Figure 6-4. Top Interface of Recommendation View: Signal Map and Signal List Selection

6.3.1.1. Measure Dashboard

The Measure Dashboard is one of the major component of the Recommendation View, purpose-built to support exploratory analysis of signal performance at a fine temporal and spatial resolution. It offers a comprehensive set of tools that enable transportation engineers, analysts, and agency staff to investigate traffic patterns, diagnose operational issues, and uncover contributing factors to signal-level safety concerns. The dashboard is interactive and highly customizable, supporting various layers of filtering and visual exploration.

After selecting a signalized intersection, users can directly interact with Measure Dashboard, where they can perform the following actions:

1) Performance Measure Selection (Left Panel)

Displayed on the left sidebar, the system offers a list of Automated Traffic Signal Performance Measures (ATSPM), covering both traditional traffic operations and advanced surrogate safety metrics. These include duration**, v**olume**, o**ccupancy, split failure**,** gap, headway, conflict**,** red light running**,** pedestrian activity indicator**,** pedestrian delay**,** and pedestrian-vehicle (right-turn) conflict propensity. These measures can be individually selected depending on the user's objective. For instance, to analyze recurring pedestrian delays or frequent near-misses.

2) Date and Time Range Selection

In the center panel (**Figure 6-5**), users are presented with date-time pickers to define a specific analysis window. Start and End fields allow minute-level granularity, supporting both short-term (e.g., peak hour) and long-term (e.g., full day, week) analysis. This flexibility enables:

- Focused investigation during complaint periods or special events

- Comparison of before-and-after conditions due to signal timing changes
- Routine monitoring of daily performance

3) Time Interval Level Selection

To support varying levels of detail, the dashboard offers four interval intervals**:** cycle (most granular), 15-minute, 30-minute, and 60-minute **(Figure 6-5).** Once selected, users must press the "Confirm" button to proceed. This step ensures that the backend appropriately aggregates raw data before visual rendering.

Interval level significantly impacts trend clarity. For example: cycle-level is ideal for observing short-term volatility or event-triggered behaviors. Whereas, hourly or 30-minute levels are more suited to identifying broad operational trends and daily patterns.

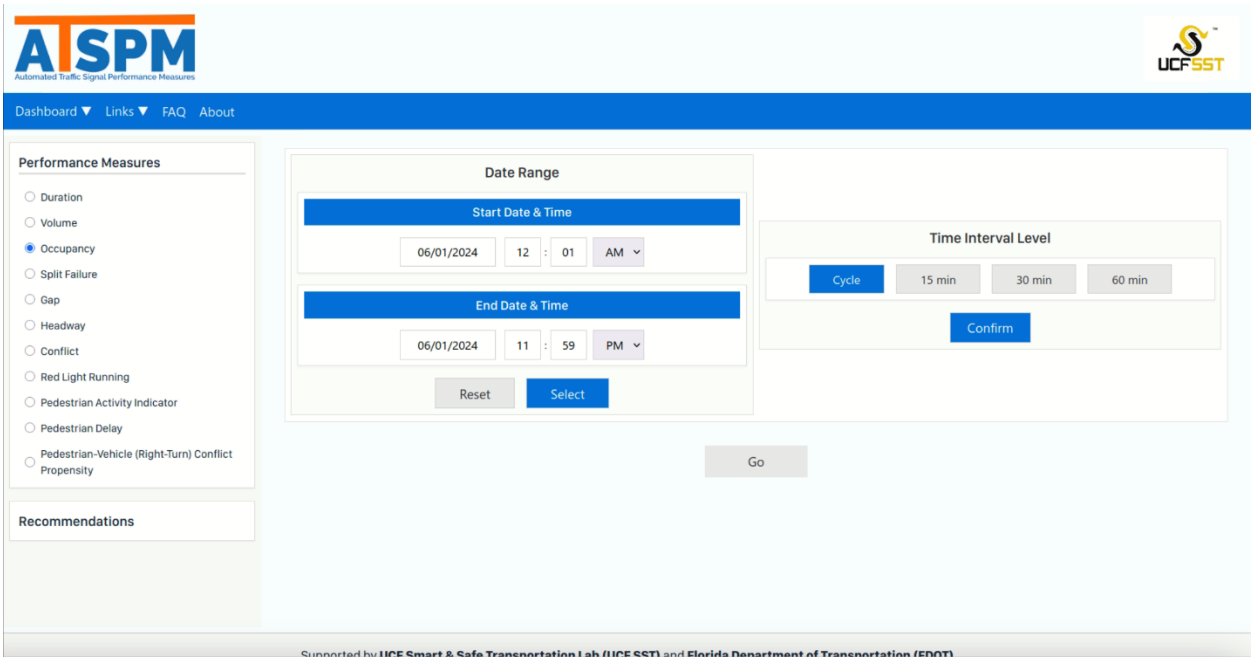

Figure 6-5. Date Range and Time Interval Selection Panel in Measure Dashboard

4) Contextual Filters: Signal Type, Lane Type, and Phase Number

To refine the analysis, users are required to specify the signal type, lane type, and phase number (**Figure 6-6**). These contextual filters ensure the trendline reflects the exact operating conditions under analysis. For example, observing occupancy on through lanes during green signal of phase 2.

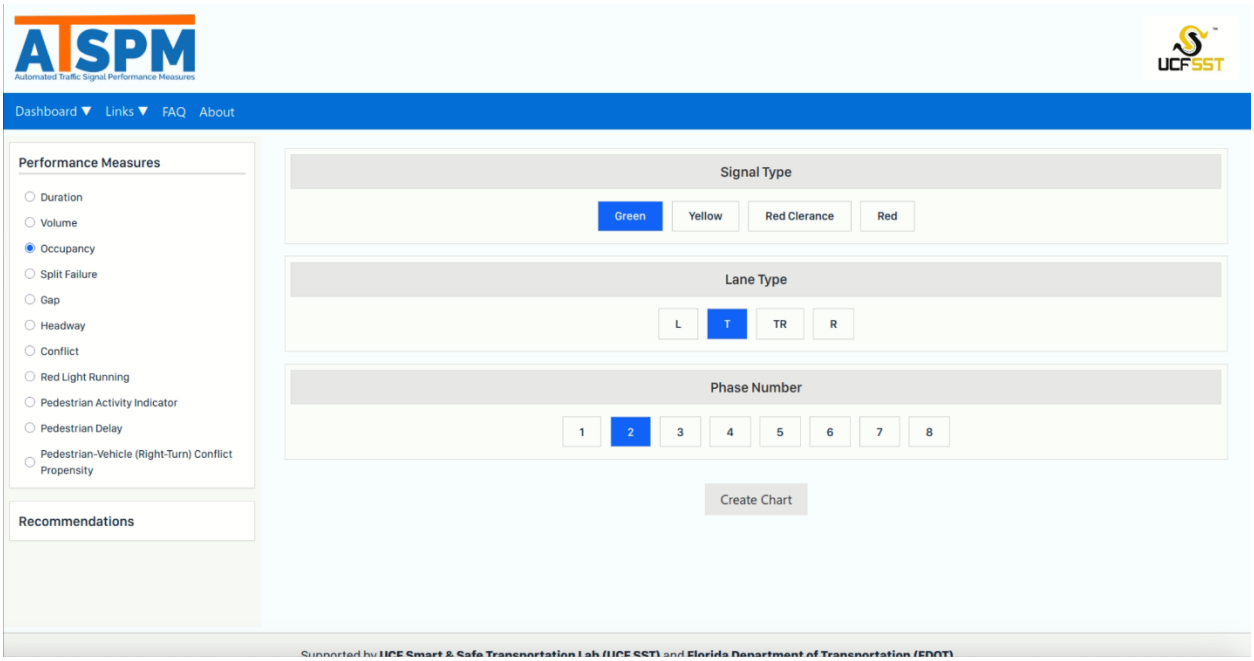

Figure 6-6. Signal Type, Lane Type, and Phase Number Filter Panel in Measure Dashboard

The availability of the options depends on the selected performance measure and the detectors' configuration. For instance, if the user selects the 'Duration' measure, the 'Lane Type' option will either be disabled or default to 'N/A,' which, while still selectable, does not influence the filtering process in this context.

5) Chart Generation and Visualization

Upon configuring all parameters, the user clicks the "Create Chart" button, triggering dynamic chart rendering on the lower portion of the page. The generated chart provides a time-series trendline of the selected performance measure (e.g., occupancy) (**Figure 6-7**). Key visualization components include:

- **Y-axis**: Represents the metric's value (e.g., seconds of occupancy, vehicle count).
- **X-axis**: Represents the time progression, labeled with timestamps reflecting the selected aggregation level and date range.
- **Chart Tools**: A control panel located in the top-right of the graph offers:
  - **Zoom In/Out**: Allows users to focus on specific time windows.
  - **Reset View**: Resets the chart to the full date range.
  - **Download Icon**: Enables exporting the chart in image format (PNG/SVG) for documentation or presentation.

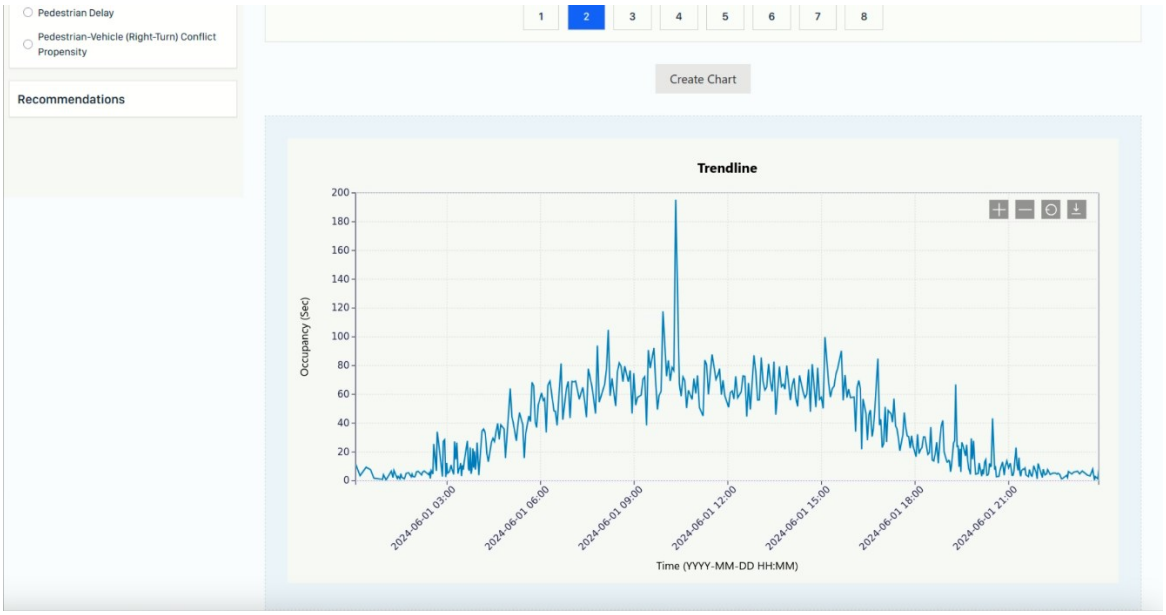

Figure 6-7. Time-Series Trendline of Occupancy (sec) Across Selected Date Range

The chart is responsive and adjusts its layout based on selected filters. High peaks in the chart may signal traffic congestion, high pedestrian activity, or safety-critical events such as frequent phase violations. The flow diagram of Measure Dashboard is depicted in **Figure 6-8**.

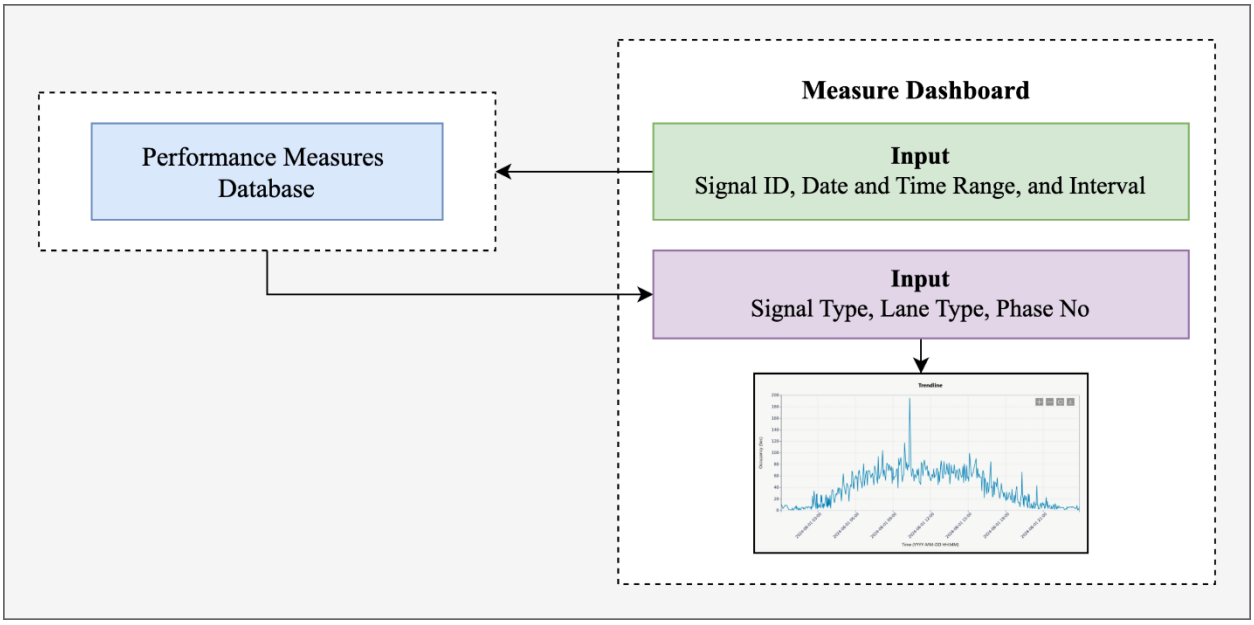

Figure 6-8. Workflow of Measure Dashboard

6.3.1.2. Recommendation Dashboard

The *Recommendation Dashboard* offers a comprehensive and interactive interface for visualizing safety treatment recommendations derived from statistical and machine learning models. This module enables transportation operators and analysts to assess when and where specific interventions are warranted based on underlying traffic and safety conditions. The design supports side-by-side exploration of multiple treatments, offering both temporal granularity and operational clarity.

1) Recommendation Type Selection (Left Panel):

On the left side of the interface, users are presented with a list of six key safety metrics/treatments. One or more of these options can be selected for visualization: signal adjustment, protected/permitted left-turn, pedestrian recall, leading pedestrian interval, and no right-turn on red. This flexible selection feature allows users to focus on a single intervention or compare multiple treatments concurrently (**Figure 6-9**).

2) Temporal Controls:

To ensure statistically valid and temporally consistent insights, the dashboard requires the user to set time-specific parameters (**Figure 6-9**):

- **Month and Year:** Selected from dropdowns to define the data batch for analysis.
- **Time Aggregation Interval:** Options include 15-minute, 30-minute, and 60-minute resolutions. Once an interval is selected, users must press the Confirm button to proceed.

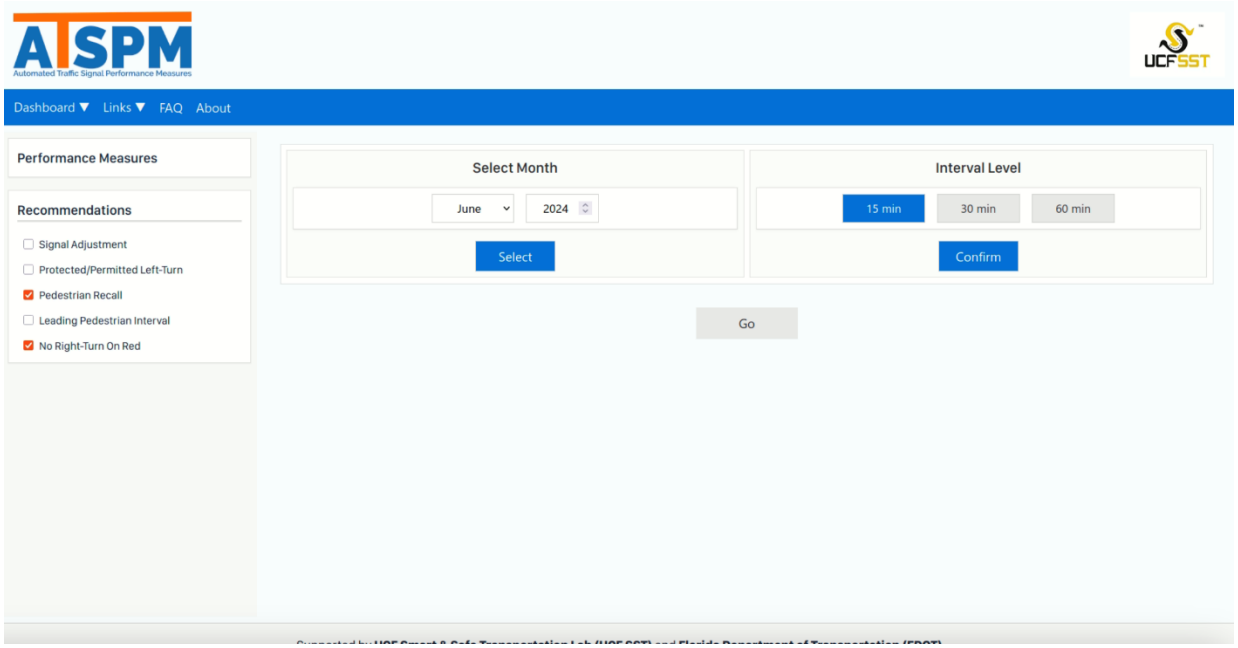

Figure 6-9. Month and Time Interval Selection Panel (with Multi-Treatment) in Recommendation Dashboard

After confirming the interval, a second panel becomes active, allowing users to select signal phase simultaneously. This is especially useful for intersections with complex signal configurations. Once these selections are finalized, the "Create Chart" button triggers the generation of binary timeline visualizations for each selected recommendation.

3) Treatment Visualization

Each selected recommendation, except "*Signal Adjustment*," is visualized as a time-series binary bar chart (**Figure 6-10**), designed to highlight temporal patterns in treatment necessity. The structure of the binary charts includes:

- **X-axis:** Represents the 24-hour daily timeline, segmented according to the selected interval level (e.g., 15-minute blocks).
- **Y-axis:** Lists the selected phase numbers.
- **Color-coded Segments:**
  - **Red:** Indicates that a recommendation is *active* for that phase and time interval, meaning the treatment is advised.
  - **Green:** Denotes that no recommendation is necessary for that phase and time period.

This binary visualization approach provides an intuitive and efficient way for users to identify critical time windows during which interventions are most needed. For example, consistent "*Pedestrian Recall"* recommendations during morning hours may signal heavy pedestrian activity, whereas frequent "*No Right-Turn on Red"* suggestions during evening periods may point to vehicular-pedestrian conflict risks at those times.

Figure 6-10. Binary Timeline Chart Displaying Safety Treatment Recommendations by Phase and Time Interval

Each chart includes advanced interaction tools similar to those in the *MeasureDashboard*:

- **Zoom:** Enables users to focus on a particular time window, such as a critical two-hour interval during peak traffic.
- **Reset View:** Returns the chart to the full daily timeline.
- **Download:** Allows users to export the current chart as a PNG or SVG image for reporting or documentation purposes.

These controls enhance usability, ensuring that users can explore the data dynamically while also generating static visuals for analysis and communication.

4) Multi-Recommendation Display

The interface supports simultaneous visualization of multiple selected recommendation types. Each selected treatment appears as an individual plot stacked vertically on the dashboard. This layout facilitates a comparative review of safety interventions across time and signal phases.

For instance, analysts can observe whether "*Protected/Permitted Left Turn"* and "*Leading Pedestrian Interval"* are advised at overlapping intervals, providing insight into phase-level risk correlations and operational conflicts. The flow diagram of the Recommendation Dashboard is depicted in **Figure 6-11**.

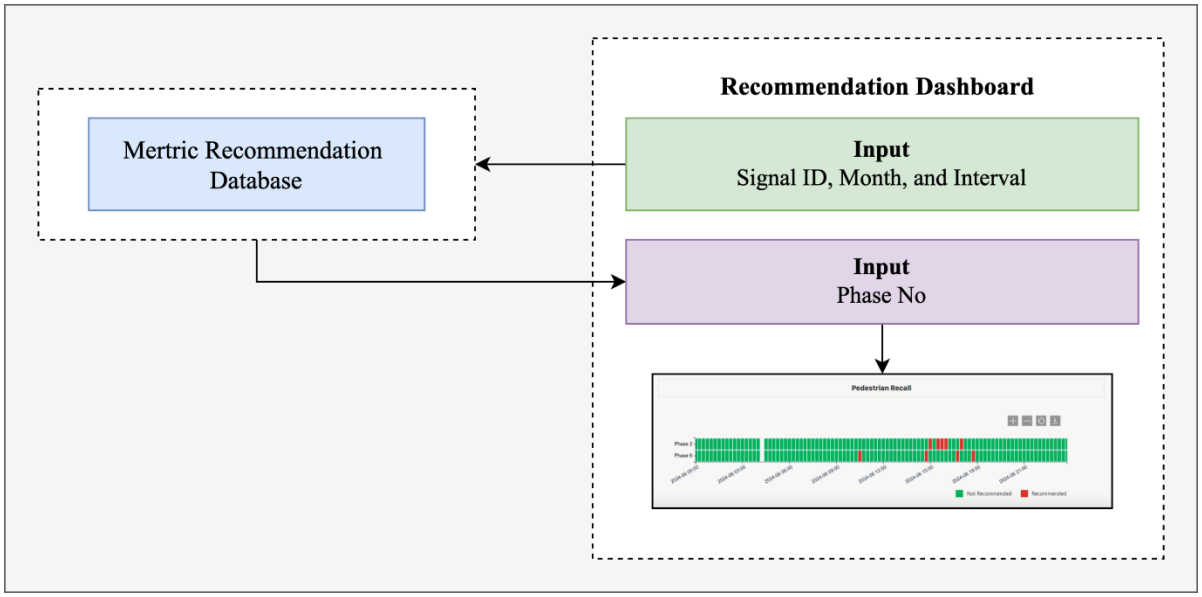

Figure 6-11. Workflow of Recommendation Dashboard

6.3.2. Rank View

The Rank View is a comprehensive evaluation interface within the ATSPM dashboard that enables stakeholders, such as traffic engineers and safety analysts, to assess and prioritize signalized intersections based on their safety performance. This view integrates several filtering, scoring, and visualization layers to deliver a dynamically ranked list of intersections, reflecting their safety risk level for a specified time frame. It is particularly useful for identifying high-risk intersections where interventions might be necessary.

6.3.2.1. Key Functional Components of Rank View

1) Date and Time Filtering (Figure 6-12)

The Rank View begins with a dual-panel configuration interface that allows users to define the scope of analysis through temporal filters. The Date Range section includes two fields: Start Date & Time, and End Date & Time. These fields allow users to focus on a specific timeframe. For instance, one hour, a single day, or a particular operational window (e.g., peak hours).

2) Time Interval Level (Figure 6-12)

Alongside the date filters, users must choose the interval level for safety scoring and ranking. The available intervals are: 15 minutes, 30 minutes, and 60 minutes. This selection determines the granularity at which safety scores will be computed and ranked. For example, if "30 min" is selected and the date range covers two hours, then the dashboard will return four separate ranking tables, one for each half-hour block. Users can confirm the interval to finalize their settings.

3) Weight Customization for Safety Scoring (Figure 6-12)

An essential feature of the Rank View is the ability to assign custom weights to each of the three performance components that feed into the safety score: vehicle-vehicle conflict score, red light running (rlr) score, and pedestrian delay score.

The weight sliders allow users to dynamically adjust the relative importance of each safety metric. For instance, if pedestrian safety is a higher concern for a particular study, the analyst can assign a higher weight to Pedestrian Delay. A validation mechanism ensures that the weights sum

to exactly 1.0 before allowing further progression. This flexible weighting system supports a broad spectrum of use cases, including:

- Prioritizing vehicle conflicts in high-volume corridors
- Targeting pedestrian safety in school zones
- Assessing red-light violations at signalized intersections

Once the user confirms the weights, the safety score is calculated using a weighted average of the three metrics, and the dashboard is ready to generate rankings.

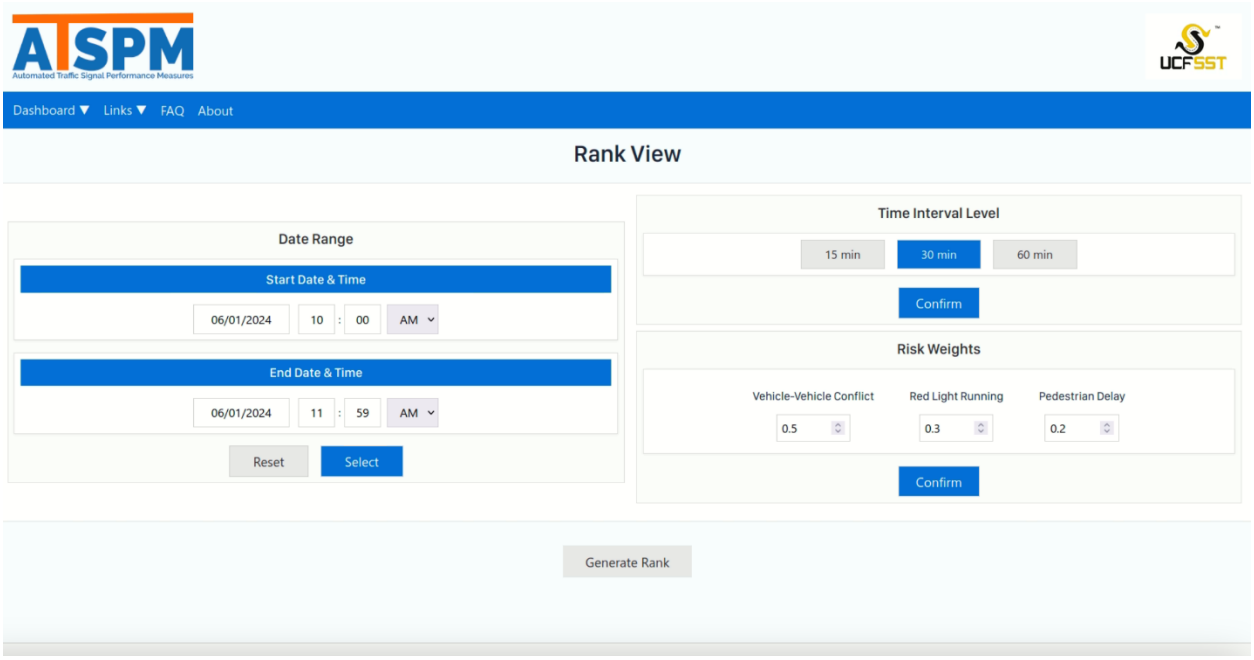

Figure 6-12. Rank View Configuration Panel

4) Generating and Viewing Safety Rankings (Figure 6-13)

Upon pressing the "Generate Rank" button, the dashboard fetches safety score data and displays the output in the form of a ranked table. Each table corresponds to a single time interval and is structured as follows:

Rank	Signal ID	Intersection Name	Conflict Score	RLR Score	Ped Delay Score	Safety Score

Each intersection is assigned a rank based on its overall safety score: the higher the score, the higher the risk, and thus the lower (better) the rank number. Rank 1 indicates the highest-risk intersection.

5) Color-Coded Risk Categories (Figure 6-13)

To enhance interpretability, the rows in the table are color-coded based on the safety score:

- **Red (≥ 0.6):** High-risk intersections
- **Yellow (0.4–0.6):** Moderate-risk intersections
- **Green (< 0.4):** Safe intersections

This visual encoding allows users to immediately identify locations that require urgent attention. For example, an intersection ranked first with a score of 0.65 would be highlighted in red, drawing attention to its critical safety need.

6) Pagination for Multi-Interval Visualization (Figure 6-13)

If the selected time window includes multiple time intervals, each interval is scored and visualized independently, and separate tables are generated for each. The user can toggle between intervals using pagination controls at the bottom of the page:

- Previous and Next buttons
- An indication of the current interval position, such as “Interval 1 of 4”

This design ensures that safety trends are not averaged across long timeframes, which can obscure short-duration risks. Instead, each interval gets a dedicated table that maintains temporal resolution and makes it easy to pinpoint when certain intersections pose the highest risk.

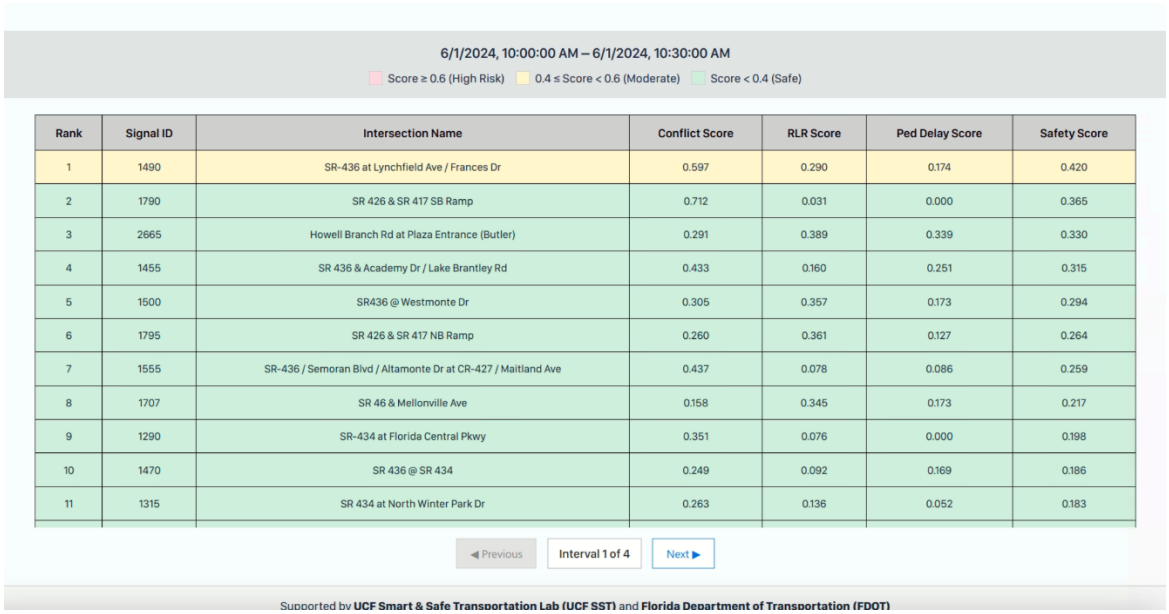

Figure 6-13. Interval-Based Safety Ranking Table with Color-coded Risk Classifications

The flow diagram of Rank View is presented in **Figure 6-14**.

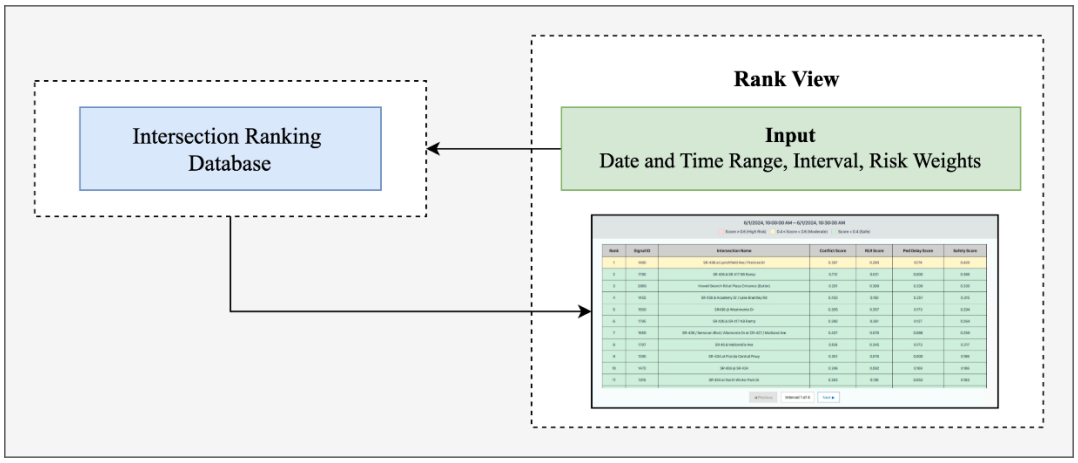

Figure 6-14. Workflow of Rank View

The current version of the dashboard was developed in alignment with the project's original scope, which specifically required the implementation of recommendation visualizations and intersection risk-based rankings. Performance measure trend analysis was added as a value-added feature to support exploratory insights. Additional modules, such as the Purdue Coordination Diagram, Purdue Split Failure Diagram, distribution plots of performance measures, and a comprehensive summary of all measures and metrics, will be incorporated before the final project submission to FDOT.

6.4. Summary

The prototype demonstrates a data pipeline by combining the Transform–Recommend–Rank server, the database server, and the React-based dashboard. It moves from raw ATSPM ingestion and quality verification through statistical modeling to a composite safety score that ranks intersections by risk. This end-to-end pipeline was tested using data from June 2024 at 19 locations. It can deliver recommendations at 15-minute, 30-minute, and 60-minute intervals. The system offers a roadmap for pilot and full-scale deployment. FDOT practitioners can test the prototype at 19 intersections to compare suggestions between intersections using various recommendation parameters.

A few limitations remain that need to be resolved before the broad application. The prototype relies on historical batch data rather than live feeds. Moving to live ATSPM feeds and migrating processing to AWS will support much larger data volumes in a secure, scalable environment. The composite risk-score weights reflect expert judgment and may require calibration for different regions. In addition, additional features may be required in the dashboard to make it more user-friendly. The next steps involve migrating the prototype to AWS and setting up ongoing performance checks with regular recalibration of the scoring weights. Integrating this safety-performance platform into the statewide traffic operations framework will enable fully automated signal calibrations and decision support that maintain proactive safety management rather than reactive.

CHAPTER 7: Conclusion

This report outlines the development of the Smart Signal Performance Monitor (SSPM) system, a comprehensive tool that predicts safety opportunities and provides actionable recommendations for traffic signal operations by leveraging Automated Traffic Signal Performance Measures (ATSPM). The primary objective of the SSPM system is to enhance safety at signalized intersections in Florida's District 5 through proactive traffic management.

The system's foundation is based on the utilization of ATSPM data, which encompasses detector configuration from the Normalized Operational Equipment Management Initiative (NOEMI) and controller event logs from SunStore. A critical aspect of the development involved meticulous data collection, processing, and quality assurance, including the implementation of an Event Sequence Quality Checker (ESQC) to ensure data reliability and accuracy. Raw ATSPM data were transformed into cycle-level performance measures, including Signal Phasing and Timing (SPaT), vehicle volume, occupancy, headway, traffic conflicts, red-light running (RLR) incidents, and pedestrian activity and delay.

Building upon these performance measures, sophisticated algorithms were developed to generate specific safety recommendations. These include adjustments to yellow and red clearance times, informed by causal forest models, which demonstrated a potential reduction in conflict rates of up to 7%. The determination of protected versus permitted left-turn phasing was based on gap analysis and estimations of left-turn volume. Pedestrian recall strategies were recommended using pedestrian presence probability calculated via a Beta-Binomial model. Furthermore, recommendations for Leading Pedestrian Intervals (LPI) and No Right Turn on Red (NRTOR) were derived from assessments of pedestrian-vehicle conflict propensity. The SSPM system

architecture integrates a Transform–Recommend–Rank (TRR) server, a database server, and a user-friendly frontend server, enabling FDOT operators to utilize the system's outputs effectively.

Key findings from this work include the successful development of a prototype system that not only processes and analyzes ATSPM data but also provides ranked intersection safety scores and specific intervention strategies. The study also identified and addressed challenges, including abnormalities in detector configuration data from NOEMI and initial data quality issues.

Despite the significant advancements, the current study has limitations. The prototype relies on historical batch data from June 2024 for 19 selected intersections in Seminole County rather than live ATSPM feeds. Additionally, the weights used for the composite safety scores are currently based on expert judgment and may require calibration for broader applicability.

Future work will focus on migrating the SSPM prototype to a cloud environment to enhance scalability and enable the processing of live ATSPM data. This will involve establishing ongoing performance checks and implementing regular recalibration of the safety scoring weights. Further enhancements to the dashboard are also envisioned to improve user-friendliness and incorporate additional analytical modules, such as the Purdue Coordination Diagram and Purdue Split Failure Diagram.

In essence, the SSPM system represents a significant step towards data-driven, proactive traffic safety management. By providing robust analytical capabilities and actionable insights, the system empowers traffic operators to make more informed decisions, ultimately contributing to safer and more efficient traffic operations at signalized intersections across Florida.

REFERENCES

Journal Articles or Conference Papers

1. Abdelrahman, A., Abdel-Aty, M., Lee, J., Yue, L., Al-Omari, M.M.A., 2020. Evaluation of displaced left-turn intersections. Transportation Engineering 1, 100006. doi:10.1016/j.treng.2020.100006
2. Ahmad, S., Ali, A., Ahmed, H.U., Huang, Y., Lu, P., 2023. Evaluating Traffic Operation Conditions during Wildfire Evacuation Using Connected Vehicles Data. Fire 6 5, 184. doi:10.3390/fire6050184
3. Alshayeb, S., Stevanovic, A., Stevanovic, J., Dobrota, N., 2023. Optimizing of Traffic-Signal Timing Based on the FCIC-PI—A Surrogate Measure for Fuel Consumption. Future Transportation 3 2 , 663–683. doi:10.3390/futuretransp3020039
4. Anik, B.M.T.H., Abdel-Aty, M., Islam, Z., 2025. Can we realize seamless traffic safety at smart intersections by predicting and preventing impending crashes? Accident Analysis & Prevention 211, 107908. doi:10.1016/j.aap.2024.107908
5. Bassett, D., Burbidge, S.K., Azra, N., Lunt, C., 2023. Evaluation of Methods for Left-Turn Gap Analysis Using High-Resolution Signal Data. Transportation Research Record2677 3, 1097–1109. doi:10.1177/03611981221121265
6. Cvijovic, Z., Zlatkovic, M., Stevanovic, A., Song, Y., 2022. Conditional Transit Signal Priority for Connected Transit Vehicles. Transportation Research Record 2676 2, 490–503. doi:10.1177/03611981211044459
7. Day, C.M., Bullock, D.M., 2020. Optimization of Traffic Signal Offsets with High Resolution Event Data. J. Transp. Eng., Part A: Systems 146 3, 04019076. doi:10.1061/JTEPBS.0000309
8. Day, C.M., Li, H., Sturdevant, J.R., Bullock, D.M., 2018. Data-Driven Ranking of Coordinated Traffic Signal Systems for Maintenance and Retiming. Transportation Research Record 2672 18, 167–178. doi:10.1177/0361198118794042
9. Dobrota, N., Cesme, B., Gault, S., Warchol, S., Rahman, R., Rouphail, N., 2024. Traffic Signal Systems Solutions Toolbox: A Case Study from Pennsylvania. Transportation Research Record03611981241230507. doi:10.1177/03611981241230507
10. Dobrota, N., Stevanovic, A., Mitrovic, N., Alshayeb, S., Zlatkovic, M., 2023. Development and Evaluation of Performance Measures for Capacity Utilization of Traffic Signals. Transportation Research Record2677 1 , 1337–1355. doi:10.1177/03611981221104460

11. Emtenan, A.M.T., Day, C.M., 2022. Correlation Analysis for Exploring the Relationship Between Probe Vehicle Data and Event-Based Traffic Signal Performance Measures. Transportation Research Record 2676 8, 587–600. doi:10.1177/03611981221084684

12. Emtenan, A.M.T., Day, C.M., 2020. Impact of Detector Configuration on Performance Measurement and Signal Operations. Transportation Research Record 2674 4, 300–313. doi:10.1177/0361198120912244

13. Gayen, S., Saldivar-Carranza, E.D., Bullock, D.M., 2023. Comparison of Estimated Cycle Split Failures from High-Resolution Controller Event and Connected Vehicle Trajectory Data. JTTs 13 04 , 689–707. doi:10.4236/jtts.2023.134032

14. Gong, Y., Abdel-Aty, M., Yuan, J., Cai, Q., 2020. Multi-Objective reinforcement learning approach for improving safety at intersections with adaptive traffic signal control. Accident Analysis & Prevention 144, 105655. doi:10.1016/j.aap.2020.105655

15. Huang, T., Poddar, S., Aguilar, C., Sharma, A., Smaglik, E., Kothuri, S., Koonce, P., 2018. Building Intelligence in Automated Traffic Signal Performance Measures with Advanced Data Analytics. Transportation Research Record 2672 18, 154–166. doi:10.1177/0361198118791380

16. Islam, Z., Abdel-Aty, M., Mahmoud, N., 2022. Using CNN-LSTM to predict signal phasing and timing aided by High-Resolution detector data. Transportation Research Part C: Emerging Technologies 141, 103742. doi:10.1016/j.trc.2022.103742

17. Islam, Z., Abdel-Aty, M., Ugan, J., 2024. Signal Phasing and Timing Prediction Using Connected Vehicle Data. Transportation Research Record2678 1 , 662–673. doi:10.1177/03611981231171909

18. Jackson, J., Huang, R., Koonce, P., Burkman, E., 2023. Use of High-Resolution Signal Controller Data to Measure Transit Signal Priority Performance: A Case Study in the Boston Region. Transportation Research Record03611981231194345. doi:10.1177/03611981231194345

19. Jerome, Z., Wang, X., Shen, S., Liu, H.X., 2022. Determining Yellow Change and Clearance Intervals for Left-Turning Phases: Evaluation of the Current Guidelines with Connected Vehicle Data. Transportation Research Record2676 11 , 1–14. doi:10.1177/03611981221091557

20. Karapetrovic, J., Martin, P.T., 2021. The Turning Movement Estimation in Real Time (TMERT) Model: Lower Bound Constraint Calibration. Procedia Computer Science 184, 76–83. doi:10.1016/j.procs.2021.03.020

21. Karimpour, A., Anderson, J.C., Kothuri, S., Wu, Y.-J., 2022. Estimating pedestrian delay at signalized intersections using high-resolution event-based data: a finite mixture modeling method. Journal of Intelligent Transportation Systems 26 5, 511–528. doi:10.1080/15472450.2021.1926246

22. Karnati, Y., Sengupta, R., Rangarajan, A., Ranka, S., 2022. Subcycle Waveform Modeling of Traffic Intersections Using Recurrent Attention Networks. IEEE Trans. Intell. Transport. Syst. 23 3 , 2538–2548. doi:10.1109/TITS.2021.3121250

23. Karnati, Y., Sengupta, R., Ranka, S., 2021. InterTwin: Deep Learning Approaches for Computing Measures of Effectiveness for Traffic Intersections. Applied Sciences 11 24 , 11637. doi:10.3390/app112411637

24. Kazenmayer, L., Ford, G., Zhang, J., Rahman, R., Cimen, F., Turgut, D., Hasan, S., 2022. Traffic Volume Prediction with Automated Signal Performance Measures (ATSPM) Data, in: 2022 IEEE Symposium on Computers and Communications (ISCC). Presented at the 2022 IEEE Symposium on Computers and Communications (ISCC), IEEE, Rhodes, Greece, pp. 1–6. doi:10.1109/ISCC55528.2022.9912469

25. Kidando, E., Kitali, A.E., Kutela, B., Ghorbanzadeh, M., Karaer, A., Koloushani, M., Moses, R., Ozguven, E.E., Sando, T., 2021. Prediction of vehicle occupants injury at signalized intersections using real-time traffic and signal data. Accident Analysis & Prevention 149, 105869. doi:10.1016/j.aap.2020.105869

26. Kidando, E., Kitali, A.E., Kutela, B., Karaer, A., Ghorbanzadeh, M., Koloushani, M., Ozguven, E.E., 2022. Use of Real-Time Traffic and Signal Timing Data in Modeling Occupant Injury Severity at Signalized Intersections. Transportation Research Record 2676 2 , 825–839. doi:10.1177/03611981211047836

27. Lau, S.K., Schultz, G.G., Shoaf, M., Bassett, D., Eggett, D.L., 2024. Evaluating Signal Preemption Requests in Utah Using Vehicle-to-Everything Dedicated Short-Range Communication Equipped Snowplows. Transportation Research Record03611981231216976. doi:10.1177/03611981231216976

28. Lee, J., Abdel-Aty, M., Xu, P., Gong, Y., 2019. Is the safety-in-numbers effect still observed in areas with low pedestrian activities? A case study of a suburban area in the United States. Accident Analysis & Prevention 125, 116–123. doi:10.1016/j.aap.2019.01.037

29. Leonard, B.D., Mackey, J., Sheffield, M., Bassett, D., Larson, S., Hooper, I., 2019. Demonstrating Transit Schedule Benefits with a Dedicated Short-Range Communication-Based Connected Vehicle System. Transportation Research Record 2673 12 , 215–224. doi:10.1177/0361198119859321

30. Li, H., Platte, T., Mathew, J., Smith, W.B., Saldivar-Carranza, E., Bullock, D.M., 2020. Using Connected Vehicle Data to Reassess Dilemma Zone Performance of Heavy Vehicles. Transportation Research Record 2674 5 , 305–314. doi:10.1177/0361198120914606

31. Mahajan, D., Banerjee, T., Karnati, Y., Rangarajan, An., Ranka, S., 2020. A Data Driven Approach to Derive Traffic Intersection Geography using High Resolution Controller Logs:, in: Proceedings of the 6th International Conference on Vehicle Technology and Intelligent Transport Systems. Presented at the 6th International Conference on Vehicle Technology

and Intelligent Transport Systems, SCITEPRESS - Science and Technology Publications, Prague, Czech Republic, pp. 203–210. doi:10.5220/0009355402030210

32. Mahajan, D., Banerjee, T., Rangarajan, A., Agarwal, N., Dilmore, J., Posadas, E., Ranka, S., 2019. Analyzing Traffic Signal Performance Measures to Automatically Classify Signalized Intersections:, in: Proceedings of the 5th International Conference on Vehicle Technology and Intelligent Transport Systems. Presented at the 5th International Conference on Vehicle Technology and Intelligent Transport Systems, SCITEPRESS - Science and Technology Publications, Heraklion, Crete, Greece, pp. 138–147. doi:10.5220/0007714701380147

33. Mahmoud, N., Abdel-Aty, M., Cai, Q., Yuan, J., 2021. Predicting cycle-level traffic movements at signalized intersections using machine learning models. Transportation Research Part C: Emerging Technologies 124, 102930. doi:10.1016/j.trc.2020.102930

34. Michael, P.G., Leeming, F.C., Dwyer, W.O., 2000. Headway on urban streets: observational data and an intervention to decrease tailgating. Transportation Research Part F: Traffic Psychology and Behaviour 3 2 , 55–64. doi:10.1016/S1369-8478(00)00015-2

35. Mitrovic, N., Dobrota, N., Pereira, M.B., Espino, E., Stevanovic, A., 2023. Data-Driven Decision Support Platform for Selection of Intersections for Adaptive Traffic Signal Control. Transportation Research Record2677 9 , 567–581. doi:10.1177/03611981231159872

36. Park, K., Singleton, P.A., Brewer, S., Zuban, J., 2023. Pedestrians and the Built Environment during the COVID-19 Pandemic: Changing Relationships by the Pandemic Phases in Salt Lake County, Utah, U.S.A. Transportation Research Record2677 4 , 448–462. doi:10.1177/03611981221083606

37. Parks-Young, A., Sharon, G., 2022. Intersection Management Protocol for Mixed Autonomous and Human-Operated Vehicles. IEEE Trans. Intell. Transport. Syst. 23 10 , 18315–18325. doi:10.1109/TITS.2022.3169658

38. Rahman, R., Zhang, J., Tirtha, S.D., Bhowmik, T., Jahan, I., Eluru, N., Hasan, S., 2022. A Data-Driven Network Model for Traffic Volume Prediction at Signalized Intersections. J. Big Data Anal. Transp. 4 2–3 , 135–152. doi:10.1007/s42421-022-00059-2

39. Runa, F., Guler, S.I., Gayah, V.V., 2024. Do existing split failure metrics accurately reflect pedestrian operation at signalized intersections? International Journal of Transportation Science and Technology 13, 270–283. doi:10.1016/j.ijtst.2023.02.006

40. Runa, F., Singleton, P.A., 2023. Impacts of the COVID-19 Pandemic on Pedestrian Push-Button Utilization and Pedestrian Volume Model Accuracy in Utah. Transportation Research Record2677 4 , 494–502. doi:10.1177/03611981221089935

41. Runa, F., Singleton, P.A., 2021. Assessing the Impacts of Weather on Pedestrian Signal Activity at 49 Signalized Intersections in Northern Utah. Transportation Research Record 2675 6 , 406–419. doi:10.1177/0361198121994111

42. Saldivar-Carranza, E., Li, H., Mathew, J., Hunter, M., Sturdevant, J., Bullock, D.M., 2021. Deriving Operational Traffic Signal Performance Measures from Vehicle Trajectory Data. Transportation Research Record 2675 9 , 1250–1264. doi:10.1177/03611981211006725

43. Saldivar-Carranza, E.D., Gayen, S., Li, H., Bullock, D.M., 2024. Comparison at Scale of Traffic Signal Cycle Split Failure Identification from High-Resolution Controller and Connected Vehicle Trajectory Data. Future Transportation 4 1 , 236–256. doi:10.3390/futuretransp4010012

44. Saldivar-Carranza, E.D., Li, H., Gayen, S., Taylor, M., Sturdevant, J., Bullock, D.M., 2023. Comparison of Arrivals on Green Estimations from Vehicle Detection and Connected Vehicle Data. Transportation Research Record2677 12 , 328–342. doi:10.1177/03611981231168116

45. Sengupta, R., Reddy, R.R.K., Shah, P., Dika, J., Huang, X., Rangarajan, A., Ranka, S., 2023. Computing Arterial Travel Time Distributions From Loop Detector and Probe Datasets. IEEE Trans. Intell. Transport. Syst. 24 11 , 11607–11622. doi:10.1109/TITS.2023.3298345

46. Sheffield, M.H., Schultz, G.G., Bassett, D., Eggett, D.L., 2021. Sensitivity Analysis of the Transit Signal Priority Requesting Threshold and the Impact on Bus Performance and General Traffic. Transportation Research Record 2675 5, 149–163. doi:10.1177/0361198120985853

47. Singleton, P.A., Park, K., Lee, D.H., 2021. Varying influences of the built environment on daily and hourly pedestrian crossing volumes at signalized intersections estimated from traffic signal controller event data. Journal of Transport Geography 93, 103067. doi:10.1016/j.jtrangeo.2021.103067

48. Singleton, P.A., Runa, F., 2021. Pedestrian Traffic Signal Data Accurately Estimates Pedestrian Crossing Volumes. Transportation Research Record 2675 6, 429–440. doi:10.1177/0361198121994126

49. Singleton, P.A., Taylor, M., Day, C., Poddar, S., Kothuri, S., Sharma, A., 2023. Impact of COVID-19 on Traffic Signal Systems: Survey of Agency Interventions and Observed Changes in Pedestrian Activity. Transportation Research Record2677 4, 192–203. doi:10.1177/03611981211026303

50. Talukder, M.A.S., Tedla, E.G., Hainen, A.M., Atkison, T., 2022. Analytical and Empirical Evaluation of Freight Priority System in Connected Vehicle Environment. J. Transp. Eng., Part A: Systems 148 6 , 04022029. doi:10.1061/JTEPBS.0000673

51. Tariq, M.T., Hadi, M., Saha, R., 2021. Using High-Resolution Signal Controller Data in the Calibration of Signalized Arterial Simulation Models. Transportation Research Record 2675 12 , 1043–1055. doi:10.1177/03611981211031882

52. Vogel, K., 2003. A comparison of headway and time to collision as safety indicators. Accident Analysis & Prevention 35 3 , 427–433. doi:10.1016/S0001-4575(02)00022-2

53. Waddell, J.M., Remias, S.M., Kirsch, J.N., 2020a. Characterizing Traffic-Signal Performance and Corridor Reliability Using Crowd-Sourced Probe Vehicle Trajectories. J. Transp. Eng., Part A: Systems 146 7 , 04020053. doi:10.1061/JTEPBS.0000378

54. Waddell, J.M., Remias, S.M., Kirsch, J.N., Kamyab, M., 2020b. Replicating Advanced Detection using Low Ping Frequency Probe Vehicle Trajectory Data to Optimize Signal Progression. Transportation Research Record 2674 7, 528–539. doi:10.1177/0361198120923654

55. Wang, B., Schultz, G.G., Macfarlane, G.S., Eggett, D.L., Davis, M.C., 2023. A Methodology to Detect Traffic Data Anomalies in Automated Traffic Signal Performance Measures. Future Transportation 3 4 , 1175–1194. doi:10.3390/futuretransp3040064

56. Wang, B., Schultz, G.G., Macfarlane, G.S., McCuen, S., 2022. Evaluating Signal Systems Using Automated Traffic Signal Performance Measures. Future Transportation 2 3, 659–674. doi:10.3390/futuretransp2030036

57. Wang, Q., Gong, Y., Yang, X., 2022. Connected automated vehicle trajectory optimization along signalized arterial: A decentralized approach under mixed traffic environment. Transportation Research Part C: Emerging Technologies 145, 103918. doi:10.1016/j.trc.2022.103918

58. Wang, Q., Yang, X. (Terry), Leonard, B.D., Mackey, J., 2020. Field Evaluation of Connected Vehicle-Based Transit Signal Priority Control under Two Different Signal Plans. Transportation Research Record 2674 7 , 172–180. doi:10.1177/0361198120921161

59. Wang, Q., Yuan, Y., Yang, X. (Terry), Huang, Z., 2021. Adaptive and multi-path progression signal control under connected vehicle environment. Transportation Research Part C: Emerging Technologies 124, 102965. doi:10.1016/j.trc.2021.102965

60. Xu, P., Li, X., Wu, Y.-J., Noh, H., 2023. Network-level turning movement counts estimation using traffic controller event-based data. Journal of Intelligent Transportation Systems 27 5 , 677–691. doi:10.1080/15472450.2022.2075701

61. Yuan, J., Abdel-Aty, M., Gong, Y., Cai, Q., 2019. Real-Time Crash Risk Prediction using Long Short-Term Memory Recurrent Neural Network. Transportation Research Record 2673 4 , 314–326. doi:10.1177/0361198119840611

62. Yuan, J., Abdel-Aty, M.A., Yue, L., Cai, Q., 2021. Modeling Real-Time Cycle-Level Crash Risk at Signalized Intersections Based on High-Resolution Event-Based Data. IEEE Trans. Intell. Transport. Syst. 22 11 , 6700–6715. doi:10.1109/TITS.2020.2994126

63. Zarindast, A., Huang, T., Sharma, A., Day, C.M., 2024. Data-Driven Approach to Reverse Engineer Detector Metadata at Signalized Intersections with Unknown Control Plans. Data Sci. Transp. 6 2 , 7. doi:10.1007/s42421-024-00093-2

64. Zhang, T.T., Jin, P.J., Brennan, T.M., McVeigh, K., Jalayer, M., Patel, D., 2023. Arterial Vehicle Trajectory Reconstruction Based on Stopbar Video Sensor for Automated Traffic Signal Performance Measures. J. Transp. Eng., Part A: Systems 149 4, 04023014. doi:10.1061/JTEPBS.0000749

65. Zhang, Y., Cheng, L.-C., Qiao, F., Patel, A., 2019. Automated Traffic Signal Performance Measures: Features and Applications, in: 2019 6th International Conference on Systems and Informatics (ICSAI). Presented at the 2019 6th International Conference on Systems and Informatics (ICSAI), IEEE, Shanghai, China, pp. 70–75. doi:10.1109/ICSAI48974.2019.9010269

Research Reports

1. Chamberlin R. and Fayyaz K. Using Atspm Data For Traffic Data Analytics, Resource Systems Group, Salt Lake City, Utah, Sponsored by the Utah. Department of Transportation. 2019.

2. Charles R. Lattimer, Automated Traffic Signals Performance Measures. Atkins, Orlando, Florida, Sponsored by the U.S. Department of Transportation, Federal Highway Administration. 2020.

3. Day, C. M., D. M. Bullock, H. Li, S. M. Remias, A. M. Hainen, R. S. Freije, A. L. Stevens, J. R. Sturdevant, and T. M. Brennan. Performance Measures for Traffic Signal Systems: An Outcome-Oriented Approach. Purdue University, West Lafayette, Indiana, Sponsored by the Utah Department of Transportation. 2014.

4. Day, C. M., D. M. Bullock, H. Li, S. M. Lavrenz, W. B. Smith, and J. R. Sturdevant. Integrating Traffic Signal Performance Measures into Agency Business Processes. Purdue University, West Lafayette, Indiana, Sponsored by the Indiana Department of Transportation. 2015.

5. Day, C., O'Brien, P., Stevanovic, A., Hale, D., Matout, N., A Methodology and Case Study: Evaluating the Benefits and Costs of Implementing Automated Traffic Signal Performance. Leidos, Reston, Virginia, Sponsored by the Indiana Department of Transportation. 2020.

6. National Academies of Sciences, Engineering, and Medicine. Performance-Based Management of Traffic Signals. Washington, DC: The National Academies Press. Sponsored by the American Association of State Highway and Transportation Officials and Federal Highway Administration. 2020.

Manuals

1. Florida Department of Transportation. (2024). Traffic engineering manual (Publication No. 750-000-005). https://www.fdot.gov/traffic/TrafficServices/Studies/TEM/TEM.shtm
2. Florida Department of Transportation. (2023). FDOT design manual (Publication No. 625-000-002). https://www.fdot.gov/roadway/fdm/default.shtm
3. Federal Highway Administration. (2013). Signalized intersections informational guide (Publication No. FHWA-SA-13-027). U.S. Department of Transportation. https://safety.fhwa.dot.gov/intersection/signal/fhwasa13027.pdf
4. Transportation Research Board. (2022). Highway capacity manual (Publication No. LP-674C). National Research Council.
5. Federal Highway Administration. (2009). Manual on Uniform Traffic Control Devices for Streets and Highways, 2009 Edition including Revision 1 and 2 dated May 2012. U.S. Department of Transportation. https://mutcd.fhwa.dot.gov

A. Appendix

Table A-1. Summary of Detector Configuration Per Intersection

Signal ID	Approach Type	Approach Direction	Detector Configuration Type (per Figure 4-5)				
			'Through' Phase			'Left-Turn' Phase	
			'Through' Lane	'Right-Turn' Lane	'Shared' Lane	'Left-Turn' Lane	'Shared' Lane
1285	Major	E	6	2		2	
		W	4, 6	2		2	
	Minor	N	2	2		2	
		S		2	2	2	
1290	Major	E	6	1		2	
		W	6	1		2	
	Minor	N			2	2	
		S	2	2		2	
1300	Major	E	3		3	2	
		W	5		5	2	
	Minor	N		2	2		
		S			2		
1315	Major	E	5		5		
		W	5			2	
	Minor	N		2		2	
1325	Major	E	5		5	2	
		W	5		5	2	
	Minor	N			2		
		S			2		
1330	Major	E	5	1		2	
		W	5		5	2	
	Minor	N		2			2
		S		2	2		
1455	Major	E	5		5	2	
		W	5		5	2	

	Minor	N			2		
		S			2	2	
1470	Major	E	1	1		2	
		W	1	1		2	
	Minor	N	5	1		2	
		S	5, 4, 2	1		2	
1490	Major	E	4	2		4	
		W	4		4	2	
	Minor	N			2	2	
		S			2		
1500	Major	E	6		6	4	
		W	6		6	4	
	Minor	N	4	4		4	
		S	4	4		4	
1555	Major	NW	4		4	2	
		SE	4		4	2	
	Minor	NE		2	2	2	
		SW		2	2		
1707	Major	E	4		4	3	
		W	4		4	2	
	Minor	N			2		
		S			2		
1725	Major	NW			5	2	
		SE			5	2	
	Minor	N			4	2	
		S			2	2	
1790	Major	E	3, 5	1			
		W	5			2	
	Minor	S		1	2		
1795	Major	E	5			2	
		W	3, 5	1			
	Minor	N		2		2	
1960	Major	E	5	1		2	
		W	5		5	2	
	Minor	N	4		4	2	

		S	4		4	2	
2055	Major	E	5	1		2	
		W	5		5	2	
	Minor	N	2	2		2	
		S	2	2		2	
2485	Major	E			3	2	
		W			3	2	
	Minor	N			2	2	
		S			2	2	
2665	Major	E	5			2	
		W	3			2	
	Minor	N		2			2
		S			1	2	

Table A-2. Summary of Yellow and Red Clearance Phase Duration of Through Phase

Signal ID	Approach Type	Approach Direction	Speed limit (mph)	Intersection width(ft)	Yellow Phase Duration				Red Clearance Phase Duration			
					TEM	Observed*			TEM	Observed*		
						Mean	Percentile			Mean	Percentile	
							5%	95%			5%	95%
1285	Major	E	45	110	4.8	4.93	4.8	6	2.0	3.32	3	6
		W	45	102	4.8	4.82	4.8	4.8	2.0	3.1	3	3.2
	Minor	N	20	130	3.0	3.88	2	4.1	5.2	2.36	2	2.4
		S	35	121	4.0	3.22	2	3.7	2.8	2.36	2	2.5
1290	Major	E	45	127	4.8	4.94	4.8	6	2.3	3.62	3.3	6
		W	45	130	4.8	4.89	4.8	6	2.3	3.51	3.3	6
	Minor	N	35	127	4.0	3.93	2	4.1	2.9	2.92	2	3
		S	20	124	3.0	2.88	2	3.8	4.9	2.24	2	2.5
1300	Major	E	45	70	4.8	4.8	4.8	4.8	2.0	2	2	2
		W	45	60	4.8	4.8	4.8	4.8	2.0	2	2	2
	Minor	N	20	85	3.0	3.4	3.4	3.4	3.6	2	2	2
		S	25	81	3.4	3.4	3.4	3.4	2.8	2	2	2
1315	Major	E	45	80	4.8	4.8	4.8	4.8	2.0	2	2	2
		W	45	93	4.8	4.86	4.8	6	2.0	2.12	2	4
	Minor	N	25	-								
1325	Major	E	45	61	4.8	4.8	4.8	4.8	2.0	2	2	2
		W	45	65	4.8	4.8	4.8	4.8	2.0	2	2	2
	Minor	N	25	92	3.4	3.4	3.4	3.4	3.1	2.7	2.7	2.7
		S	25	86	3.4	3.4	3.4	3.4	2.9	2.7	2.7	2.7
1330	Major	E	45	83	4.8	4.8	4.8	4.8	2.0	2	2	2
		W	45	87	4.8	4.8	4.8	4.8	2.0	2	2	2
	Minor	N	25	82	3.4	2.9	2	3.4	2.8	2.32	2	2.5
		S	25	104	3.4	3.39	3.4	3.4	3.4	2.5	2.5	2.5
1455	Major	E	45	85	4.8	4.86	4.8	4.8	2.0	2.63	2.5	2.5
		W	45	97	4.8	4.92	4.8	6	2.0	2.76	2.5	5
	Minor	N	25	117	3.4	2.91	2	4	3.8	2.36	2	2.8
		S	35	130	4.0	3.31	2	3.4	3.0	2.84	2	2.9
1470	Major	E	45	154	4.8	4.92	4.9	4.9	2.7	4.53	4.5	4.5
		W	45	165	4.8	4.92	4.9	4.9	2.8	4.52	4.5	4.5

	Minor	N	45	147	4.8	4.55	2	4.9	2.6	4.11	2	4.4
		S	45	148	4.8	4.49	2	4.9	2.6	4.06	2	4.4
1490	Major	E	45	78	4.8	5	4.8	6	2.0	2.75	2.3	6
		W	45	68	4.8	4.93	4.8	6	2.0	2.57	2.3	4.6
	Minor	N	25	152	3.4	3.4	3.4	3.4	4.7	4.1	4.1	4.1
		S	25	163	3.4	3.4	3.4	3.4	5.0	4.1	4.1	4.1
1500	Major	E	45	133	4.8	4.89	4.8	6	2.4	3.7	3.5	6
		W	45	124	4.8	4.84	4.8	4.8	2.2	3.59	3.5	3.5
	Minor	N	30	165	3.7	3.23	2	3.7	4.2	3.73	2	4.4
		S	30	164	3.7	3.14	2	3.7	4.2	3.6	2	4.4
1555	Major	SE	40	143	4.4	4.42	4.4	4.4	2.8	2.94	2.9	2.9
		NW	40	84	4.4	4.5	4.4	6	2.0	3.08	2.9	5.8
	Minor	NE	40	116	4.4	2.35	2	3.4	2.4	2.22	2	2.9
		SW	40	116	4.4	4.39	4.4	4.4	2.4	2.3	2.3	2.3
1707	Major	E	40	58	4.4	4.4	4.4	4.4	2.0	2.01	2	2
		W	40	76	4.4	4.43	4.4	4.4	2.0	2.03	2	2
	Minor	N	30	80	3.7	3.7	3.7	3.7	2.3	2	2	2
		S	25	86	3.4	3.7	3.7	3.7	2.9	2	2	2
1725	Major	SE	45	109	4.8	5.3	5.3	5.3	2.0	2	2	2
		NW	45	109	4.8	5.3	5.3	5.3	2.0	2	2	2
	Minor	N	45	130	4.8	5.3	5.3	5.3	2.3	3.8	2	4.5
		S	30	122	3.7	3.58	2	4.2	3.3	3.01	2	3.4
1790	Major	E	45	56	4.8	4.8	4.8	4.8	2.0	2.9	2.3	6
		W	45	56	4.8	4.9	4.9	4.9	2.0	2.3	2.3	2.3
	Minor	S	25	-					-			
1795	Major	E	45	67	4.8	4.9	4.9	4.9	2.0	2.7	2.7	2.7
		W	45	105	4.8	4.91	4.9	4.9	2.0	2.78	2.7	2.8
	Minor	N	25	-					-			
1960	Major	E	45	116	4.8	4.82	4.8	4.8	2.1	2.86	2.8	2.8
		W	45	106	4.8	4.85	4.8	4.8	2.0	2.91	2.8	2.8
	Minor	N	45	112	4.8	4.52	2	4.8	2.0	2.63	2	2.7
		S	45	131	4.8	4.57	2	4.8	2.3	2.64	2	2.7
2055	Major	E	45	86	4.8	4.45	4.5	4.5	2.0	2.23	2	3
		W	45	81	4.8	4.55	4.5	6	2.0	2.38	2.2	4.4
	Minor	N	35	127	4.0	4.26	2	4.5	2.9	2.02	2	2

		S	35	159	4.0	4.19	2	4.5	3.5	2.02	2	2
2485	Major	E	35	78	4.0	4.1	4.1	4.1	2.0	2	2	2
		W	35	75	4.0	4.1	4.1	4.1	2.0	2	2	2
	Minor	N	25	76	3.4	3.28	2	4.4	2.7	2	2	2
		S	40	74	4.4	4.34	4.4	4.4	2.0	2	2	2
2665	Major	E	40	128	4.4	4.57	4.4	6	2.6	2.66	2.3	4.7
		W	40	100	4.4	4.46	4.4	4.4	2.1	2.52	2.4	2.5
	Minor	N	25	80	3.4	3.4	3.4	3.4	2.8	2	2	2
		S	25	77	3.4	3.4	3.4	3.4	2.7	2	2	2

*Observations were considered errors and excluded if they were less than 2 seconds or more than 6 seconds.

Table A-3. Summary of Yellow Time Adjustment Recommendations

Signal ID	Approach Type	Approach Direction	Hour-of-day																							
			0	1	2	3	4	5	6	7	8	9	10	11	12	13	14	15	16	17	18	19	20	21	22	23
1285	Major	W	0.1	0	0.1	0.1	0.2	0.2	0.2	0.2	0.2	0.2	0.2	0.2	0.2	0.2	0.2	0.2	0.2	0.2	0	0	0	0	0	0
		E	0.1	0	0.1	0.1	0.2	0.2	0.2	0.2	0.2	0.2	0.2	0.2	0.2	0.2	0.2	0.2	0.2	0.2	0	0	0	0	0	0
	Minor	N																								
		S																								
1290	Major	W	0	0	0	0.1	0.1	0.1	0.2	0.1	0.2	0.2	0.2	0.1	0.1	0.1	0.1	0.1	0.1	0	0	0	0	0	0	0
		E	0	0	0	0.1	0.1	0.1	0.2	0.1	0.2	0.2	0.2	0.1	0.1	0.1	0.1	0.1	0.1	0	0	0	0	0	0	0
	Minor	N																								
		S																								
1300	Major	W	0.2	0.2	0.2	0.2	0.2	0.2	0.2	0.2	0.2	0.2	0.2	0.2	0.2	0.2	0.2	0.2	0.2	0.2	0.2	0.2	0.2	0.2	0.2	0.2
		E	0.2	0.2	0.2	0.2	0.2	0.2	0.2	0.2	0.2	0.2	0.2	0.2	0.2	0.2	0.2	0.2	0.2	0.2	0.2	0.2	0.2	0.2	0.2	0.2
	Minor	N																								
		S																								
1315	Major	W	0.1	0.1	0.1	0.2	0.2	0.2	0.2	0.2	0.2	0.2	0.2	0.2	0.2	0.2	0.2	0.2	0.2	0.1	0.1	0.1	0.1	0.2	0.1	0.1
		E	0.1	0.1	0.1	0.2	0.2	0.2	0.2	0.2	0.2	0.2	0.2	0.2	0.2	0.2	0.2	0.2	0.2	0.1	0.1	0.1	0.1	0.2	0.1	0.1
	Minor	N																								
1325	Major	W	0.2	0.2	0.2	0.2	0.2	0.2	0.2	0.2	0.2	0.2	0.2	0.2	0.2	0.2	0.2	0.2	0.2	0.2	0.2	0.2	0.2	0.2	0.2	0.2
		E	0.2	0.2	0.2	0.2	0.2	0.2	0.2	0.2	0.2	0.2	0.2	0.2	0.2	0.2	0.2	0.2	0.2	0.2	0.2	0.2	0.2	0.2	0.2	0.2
	Minor	N																								
		S																								
1330	Major	W	0.2	0.2	0.2	0.2	0.2	0.2	0.2	0.2	0.2	0.2	0.2	0.2	0.2	0.2	0.2	0.2	0.2	0.2	0.2	0.2	0.2	0.2	0.2	0.2
		E	0.2	0.2	0.2	0.2	0.2	0.2	0.2	0.2	0.2	0.2	0.2	0.2	0.2	0.2	0.2	0.2	0.2	0.2	0.2	0.2	0.2	0.2	0.2	0.2
	Minor	N																								
		S																								
1455	Major	W	0	0.1	0.1	0.1	0.1	0.2	0.2	0.2	0.2	0.2	0.2	0.2	0.2	0.2	0.2	0.1	0.1	0	0	0	0	0	0	0
		E	0	0.1	0.1	0.1	0.1	0.2	0.2	0.2	0.2	0.2	0.2	0.2	0.2	0.2	0.2	0.1	0.1	0	0	0	0	0	0	0
	Minor	N																								
		S																								
1470	Major	W	0	0.1	0.1	0.1	0.1	0.1	0.1	0.1	0.1	0.1	0.1	0.1	0.1	0.1	0.1	0.1	0.1	0.1	0.1	0.1	0.1	0	0	0
		E	0	0.1	0.1	0.1	0.1	0.1	0.1	0.1	0.1	0.1	0.1	0.1	0.1	0.1	0.1	0.1	0.1	0.1	0.1	0.1	0.1	0	0	0
	Minor	N																								
		S																								

1490	Major	W	0	0	0	0	0	0	0.1	0.1	0.2	0.2	0.2	0.2	0.2	0.2	0.2	0.1	0.1	0	0	0	0	0	0	0
		E	0	0	0	0	0	0	0.1	0.1	0.2	0.2	0.2	0.2	0.2	0.2	0.2	0.1	0.1	0	0	0	0	0	0	0
	Minor	N																								
		S																								
1500	Major	W	0	0	0.1	0.2	0.2	0.2	0.2	0.2	0.2	0.2	0.2	0.2	0.2	0.2	0.2	0.2	0.2	0.2	0.2	0.2	0.1	0	0	0	0
		E	0	0	0.1	0.2	0.2	0.2	0.2	0.2	0.2	0.2	0.2	0.2	0.2	0.2	0.2	0.2	0.2	0.2	0.2	0.2	0.1	0	0	0	0
	Minor	N																								
		S																								
1555	Major	W	0.4	0.5	0.5	0.6	0.6	0.6	0.6	0.6	0.6	0.6	0.6	0.6	0.6	0.6	0.6	0.6	0.6	0.6	0.5	0.5	0.4	0.4	0.5	0.3
		E	0.4	0.5	0.5	0.6	0.6	0.6	0.6	0.6	0.6	0.6	0.6	0.6	0.6	0.6	0.6	0.6	0.6	0.6	0.5	0.5	0.4	0.4	0.5	0.3
	Minor	N																								
		S																								
1707	Major	W	0.6	0.6	0.6	0.6	0.6	0.6	0.6	0.6	0.6	0.6	0.6	0.6	0.6	0.6	0.6	0.6	0.6	0.6	0.6	0.6	0.6	0.6	0.6	0.6
		E	0.6	0.6	0.6	0.6	0.6	0.6	0.6	0.6	0.6	0.6	0.6	0.6	0.6	0.6	0.6	0.6	0.6	0.6	0.6	0.6	0.6	0.6	0.6	0.6
	Minor	N																								
		S																								
1725	Major	NW	0	0	0	0	0	0	0	0	0	0	0	0	0	0	0	0	0	0	0	0	0	0	0	0
		SE	0	0	0	0	0	0	0	0	0	0	0	0	0	0	0	0	0	0	0	0	0	0	0	0
	Minor	N																								
		S																								
1790	Major	W	0.1	0	0	0	0.1	0.1	0	0	0	0	0.1	0.1	0.1	0.1	0.1	0.1	0.1	0.1	0.1	0.1	0.1	0.2	0.2	0.2
		E	0.1	0	0	0	0.1	0.1	0	0	0	0	0.1	0.1	0.1	0.1	0.1	0.1	0.1	0.1	0.1	0.1	0.1	0.2	0.2	0.2
	Minor	N																								
1795	Major	W	0.1	0.1	0.1	0.1	0.1	0.1	0.1	0.1	0.1	0.1	0.1	0.1	0.1	0.1	0.1	0.1	0.1	0.1	0.1	0.1	0.1	0.1	0.1	0.1
		E	0.1	0.1	0.1	0.1	0.1	0.1	0.1	0.1	0.1	0.1	0.1	0.1	0.1	0.1	0.1	0.1	0.1	0.1	0.1	0.1	0.1	0.1	0.1	0.1
	Minor	N																								
1960	Major	W	0.1	0.2	0.2	0.2	0.2	0.2	0.2	0.2	0.2	0.2	0.2	0.2	0.2	0.2	0.2	0.2	0.2	0.2	0.2	0.2	0.1	0.1	0.1	0.1
		E	0.1	0.2	0.2	0.2	0.2	0.2	0.2	0.2	0.2	0.2	0.2	0.2	0.2	0.2	0.2	0.2	0.2	0.2	0.2	0.2	0.1	0.1	0.1	0.1
	Minor	N																								
		S																								
2055	Major	W	0.4	0.4	0.6	0.7	0.6	0.6	0.7	0.6	0.6	0.6	0.5	0.7	0.7	0.7	0.5	0.6	0.6	0.4	0.4	0.3	0.3	0.2	0.3	0.3
		E	0.4	0.4	0.6	0.7	0.6	0.6	0.7	0.6	0.6	0.6	0.5	0.7	0.7	0.7	0.5	0.6	0.6	0.4	0.4	0.3	0.3	0.2	0.3	0.3
	Minor	N																								
		S																								
2485	Major	W	0.9	0.9	0.9	0.9	0.9	0.9	0.9	0.9	0.9	0.9	0.9	0.9	0.9	0.9	0.9	0.9	0.9	0.9	0.9	0.9	0.9	0.9	0.9	0.9

		E	0.9	0.9	0.9	0.9	0.9	0.9	0.9	0.9	0.9	0.9	0.9	0.9	0.9	0.9	0.9	0.9	0.9	0.9	0.9	0.9	0.9	0.9	0.9	0.9
	Minor	N																								
		S																								
2665	Major	W	0.4	0.4	0.3	0.4	0.5	0.6	0.5	0.5	0.5	0.6	0.6	0.6	0.6	0.6	0.6	0.6	0.5	0.4	0.2	0.3	0.3	0.4	0.5	0.4
		E	0.4	0.4	0.3	0.4	0.5	0.6	0.5	0.5	0.5	0.6	0.6	0.6	0.6	0.6	0.6	0.6	0.5	0.4	0.2	0.3	0.3	0.4	0.5	0.4
	Minor	N																								
		S																								

Table A-4. Summary of Red Clearance Time Adjustment Recommendations

Signal ID	Approach Type	Approach Direction	Hour-of-day (Local Time)																							
			0		1	2	3	4	5	6	7	8	9	10	11	12	13	14	15	16	17	18	19	20	21	22	23
1285	Major	W	-0.5	-0.4	-0.2	-0.2	-0.1	0	-0.1	-0.1	-0.1	-0.1	0	0	0	0	0	0	-0.1	-0.1	-0.4	-0.7	-0.7	-0.7	-0.8	-0.5	
		E	-0.5	-0.4	-0.2	-0.2	-0.1	0	-0.1	-0.1	-0.1	-0.1	0	0	0	0	0	0	-0.1	-0.1	-0.4	-0.7	-0.7	-0.7	-0.8	-0.5	
	Minor	N																									
		S																									
1290	Major	W	-1.2	-1.3	-1.1	-0.6	-0.6	-0.4	-0.4	-0.4	-0.4	-0.4	-0.4	-0.4	-0.4	-0.5	-0.4	-0.5	-0.6	-0.7	-0.7	-0.7	-0.9	-0.8	-0.8	-1.1	
		E	-1.2	-1.3	-1.1	-0.6	-0.6	-0.4	-0.4	-0.4	-0.4	-0.4	-0.4	-0.4	-0.4	-0.5	-0.4	-0.5	-0.6	-0.7	-0.7	-0.7	-0.9	-0.8	-0.8	-1.1	
	Minor	N																									
		S																									
1300	Major	W	0	0	0	0	0	0	0	0	0	0	0	0	0	0	0	0	0	0	0	0	0	0	0	0	
		E	0	0	0	0	0	0	0	0	0	0	0	0	0	0	0	0	0	0	0	0	0	0	0	0	
	Minor	N																									
		S																									
1315	Major	W	0	0	0	0	0	0	0	0	0	0	0	0	0	0	0	0	0	0	-0.1	-0.1	0	0	-0.1		
		E	0	0	0	0	0	0	0	0	0	0	0	0	0	0	0	0	0	0	-0.1	-0.1	0	0	-0.1		
	Minor	N																									
1325	Major	W	0	0	0	0	0	0	0	0	0	0	0	0	0	0	0	0	0	0	0	0	0	0	0		
		E	0	0	0	0	0	0	0	0	0	0	0	0	0	0	0	0	0	0	0	0	0	0	0		
	Minor	N																									
		S																									
1330	Major	W	0	0	0	0	0	0	0	0	0	0	0	0	0	0	0	0	0	0	0	0	0	0	0		
		E	0	0	0	0	0	0	0	0	0	0	0	0	0	0	0	0	0	0	0	0	0	0	0		
	Minor	N																									
		S																									
1455	Major	W	0	0	0	0.1	0	0	0	0	0	0	0	0	0	0	0	0	0	0	-0.1	-0.3	-0.1	-0.1	0	-0.1	
		E	0	0	0	0.1	0	0	0	0	0	0	0	0	0	0	0	0	0	0	-0.1	-0.3	-0.1	-0.1	0	-0.1	
	Minor	N																									
		S																									
1470	Major	W	-1.6	-1.5	-1.5	-1.5	-1.5	-1.5	-1.5	-1.5	-1.5	-1.5	-1.5	-1.5	-1.5	-1.5	-1.5	-1.5	-1.5	-1.5	-1.5	-1.5	-1.5	-1.6	-1.6	-1.6	
		E	-1.6	-1.5	-1.5	-1.5	-1.5	-1.5	-1.5	-1.5	-1.5	-1.5	-1.5	-1.5	-1.5	-1.5	-1.5	-1.5	-1.5	-1.5	-1.5	-1.5	-1.5	-1.6	-1.6	-1.6	
	Minor	N																									
		S																									

1490	Major	W	-0.2	-0.2	-0.2	-0.1	0	0	0	0	0	0	0	0	0	0	0	0	0	0	-0.1	-0.5	-0.7	-0.5	-0.8	-0.2
		E	-0.2	-0.2	-0.2	-0.1	0	0	0	0	0	0	0	0	0	0	0	0	0	0	-0.1	-0.5	-0.7	-0.5	-0.8	-0.2
	Minor	N																								
		S																								
1500	Major	W	-1.3	-0.9	-0.7	-0.5	-0.5	-0.5	-0.5	-0.5	-0.5	-0.5	-0.5	-0.5	-0.5	-0.5	-0.5	-0.5	-0.5	-0.5	-0.5	-0.6	-0.9	-1.3	-1.3	-1.4
		E	-1.3	-0.9	-0.7	-0.5	-0.5	-0.5	-0.5	-0.5	-0.5	-0.5	-0.5	-0.5	-0.5	-0.5	-0.5	-0.5	-0.5	-0.5	-0.5	-0.6	-0.9	-1.3	-1.3	-1.4
	Minor	N																								
		S																								
1555	Major	W	-0.2	-0.2	-0.1	0	0	0	0	0	0	0	0	0	0	0	0	0	0	0	-0.1	-0.2	-0.2	-0.3	-0.2	-0.4
		E	-0.2	-0.2	-0.1	0	0	0	0	0	0	0	0	0	0	0	0	0	0	0	-0.1	-0.2	-0.2	-0.3	-0.2	-0.4
	Minor	N																								
		S																								
1707	Major	W	0	0	0	0	0	0	0	0	0	0	0	0	0	0	0	0	0	0	0	0	0	0	0	0.4
		E	0	0	0	0	0	0	0	0	0	0	0	0	0	0	0	0	0	0	0	0	0	0	0	0.4
	Minor	N																								
		S																								
1725	Major	NW	0	0	0	0	0	0	0	0	0	0	0	0	0	0	0	0	0	0	0	0	0	0	0	0
		SE	0	0	0	0	0	0	0	0	0	0	0	0	0	0	0	0	0	0	0	0	0	0	0	0
	Minor	N																								
		S																								
1790	Major	W	-0.1	0	-0.2	0	0.1	0.1	-0.1	-0.1	-0.1	0	0	0	0	0	0	0	0	0	0	0	0	0	0	0
		E	-0.1	0	-0.2	0	0.1	0.1	-0.1	-0.1	-0.1	0	0	0	0	0	0	0	0	0	0	0	0	0	0	0
	Minor	N																								
1795	Major	W	0	0	0	0	0	0	0	0	0	0	0	0	0	0	0	0	0	0	0	0	0	0	0	0
		E	0	0	0	0	0	0	0	0	0	0	0	0	0	0	0	0	0	0	0	0	0	0	0	0
	Minor	N																								
1960	Major	W	0	0	0	0	0	0	0	0	0	0	0	0	0	0	0	0	0	0	0	0	0	-0.1	-0.1	0
		E	0	0	0	0	0	0	0	0	0	0	0	0	0	0	0	0	0	0	0	0	0	-0.1	-0.1	0
	Minor	N																								
		S																								
2055	Major	W	0	0	0.1	0	0	0	0	0	0	0	0	0	0	0	0	0	0	0	0	0	0	-0.1	0	0.1
		E	0	0	0.1	0	0	0	0	0	0	0	0	0	0	0	0	0	0	0	0	0	0	-0.1	0	0.1
	Minor	N																								
		S																								
2485	Major	W	0	0	0	0	0	0	0	0	0	0	0	0	0	0	0	0	0	0	0	0	0	0	0	0

		E	0	0	0	0	0	0	0	0	0	0	0	0	0	0	0	0	0	0	0	0	0	0	0	0
	Minor	N																								
		S																								
2665	Major	W	0	-0.2	0	0.1	0.1	0	-0.1	0	-0.1	0	0	0	0	0	0	0	0	0	0	0	0	-0.1	0	-0.1	0
		E	0	-0.2	0	0.1	0.1	0	-0.1	0	-0.1	0	0	0	0	0	0	0	0	0	0	0	0	-0.1	0	-0.1	0
	Minor	N																								
		S																								

Table A-5. Summary of Protected Left-Turn Recommendation*

Signal ID	Approach Type	Approach Direction	Hour of Day (Local Time)																							
			0	1	2	3	4	5	6	7	8	9	10	11	12	13	14	15	16	17	18	19	20	21	22	23
1285	Major	E	0	0	0	0	0	0	0	0	0	0	0	1	1	1	1	1	1	1	1	1	1	1	0	1
		W	0	0	0	0	0	0	0	0	0	0	0	0	0	0	0	0	0	0	0	0	0	0	0	0
	Minor	N								1	1	1	1	1	1	1	1	1	1	1	1	1				
		S								1	1	1	1	1	1	1	1	1	1	1	1	1				
1290	Major	E	1	1	1	1	1	1	1	1	1	1	1	1	1	1	1	1	1	1	1	1	1	1	1	1
		W	1	1	1	1	1	1	1	1	1	1	1	1	1	1	1	1	1	1	1	1	1	1	1	1
	Minor	N								1	1	1	1	1	1	1	1	1	1	1	1	1				
		S								1	1	1	1	1	1	1	1	1	1	1	1	1				
1300	Major	E																								
		W																								
	Minor	N								1	1	1	1	1	1	1	0	1	1	1	1	1				
		S								1	1	1	1	1	1	1	1	1	1	1	1	1				
1315	Major	E																								
		W																								
	Minor	N																								
1325	Major	E																								
		W																								
	Minor	N								1	1	1	1	1	1	1	1	1	1	1	1	1	0			
		S								1	1	1	1	1	1	1	1	1	1	1	1	1	0			
1330	Major	E																								
		W																								
	Minor	N								1	1	1	1	1	1	1	1	1	1	1	1	1	1			
		S								1	1	1	1	1	1	1	1	1	1	1	1	1	0			
1455	Major	E																								
		W																								
	Minor	N								1	1	1	1	1	1	1	1	1	1	1	1	1				
		S								1	1	1	1	1	1	1	1	1	1	1	1	1				
1470	Major	E																								
		W																								
	Minor	N								1	1	1	1	1	1	1	1	1	1	1	1	1				
		S																								

1490	Major	E	0	0	0	0	0	0	0	0	0	0	0	0	0	0	0	0	0	0	0	0	0	0	0	0
		W	0	0	0	0	0	0	0	0	0	0	0	0	0	0	0	0	0	0	0	0	0	0	0	0
	Minor	N																								
		S																								
1500	Major	E	1	1	0	0	0	0	0	0	0	0	0	0	0	1	0	1	1	1	1	1	1	1	1	1
		W	1	1	1	1	0	0	0	0	0	0	1	1	1	1	1	1	1	1	1	1	1	1	1	1
	Minor	N	1	1	1	1	1	1	1	1	1	1	1	1	1	1	1	1	1	1	1	1	1	1	1	1
		S	1	1	1	1	1	1	1	1	1	1	1	1	1	1	1	1	1	1	1	1	1	1	1	1
1555	Major	SE	0	0	0	0	0	0	0	0	0	0	0	0	0	0	0	0	0	0	0	0	0	0	0	0
		NW	0	0	0	0	0	0	0	0	0	0	0	1	1	1	1	1	1	1	1	1	1	1	0	0
	Minor	NE																								
		SW																								
1707	Major	E																								
		W	0	0	0	0	0	0	0	0	0	0	0	0	0	0	0	0	0	0	0	0	0	0	0	0
	Minor	N																								
		S																								
1725	Major	SE																								
		NW																								
	Minor	N	1	1	1	1	1	1	1	1	1	1	1	1	1	1	1	1	1	1	1	1	1	1	1	1
		S																								
1790	Major	E																								
		W																								
	Minor	S																								
1795	Major	E																								
		W																								
	Minor	N																								
1960	Major	E																								
		W																								
	Minor	N	1	1	1	1	1	1	1	1	1	1	1	1	1	1	1	1	1	1	1	1	1	1	1	1
		S	1	1	1	1	1	1	1	1	1	1	1	1	1	1	1	1	1	1	1	1	1	1	1	1
2055	Major	E																								
		W																								
	Minor	N	1	0	0	1	1	1	1	1	1	1	1	1	1	1	1	1	1	1	1	1	1	1	1	1
		S																								
2485	Major	E																								

		W																									
	Minor	N	1	1	1	1	1	1	1	1	1	1	1	1	1	1	1	1	1	1	1	1	1	1	1	1	1
		S	0	0	0	0	0	0	0	0	0	0	0	0	0	0	0	0	0	0	0	0	0	0	0	0	0
2665	Major	E																									
		W																									
	Minor	N																									
		S																									

* :1 indicate a protected left turn recommendation.

Table A-6. Summary of Pedestrian Recall

Signal ID	Approach Type	Approach Direction	Hour of Day (Local Time)																							
			0	1	2	3	4	5	6	7	8	9	10	11	12	13	14	15	16	17	18	19	20	21	22	23
1285	Major	E	0	0	0	0	0	0	0	0	0	0	0	0	0	0	0	0	0	0	0	0	0	0	0	0
		W	0	0	0	0	0	0	0	0	0	0	0	0	0	0	0	0	0	0	0	0	0	0	0	0
	Minor	S	0	0	0	0	0	0	0	0	0	0	0	0	0	0	0	0	0	0	0	0	0	0	0	0
		N	0	0	0	0	0	0	0	0	0	0	0	0	0	0	0	0	0	0	0	0	0	0	0	0
1290	Major	W	0	0	0	0	0	0	0	0	0	0	0	0	0	0	0	0	0	0	0	0	0	0	0	0
		E	0	0	0	0	0	0	0	0	0	0	0	0	0	0	0	0	0	0	0	0	0	0	0	0
	Minor	N	0	0	0	0	0	0	0	0	0	0	0	0	0	0	0	0	0	0	0	0	0	0	0	0
		S	0	0	0	0	0	0	0	0	0	0	0	0	0	0	0	0	0	0	0	0	0	0	0	0
1300	Major	E	0	0	0	0	0	0	0	0	0	0	0	0	0	0	0	0	0	0	0	0	0	0	0	0
		W	0	0	0	0	0	0	0	0	0	0	0	0	0	0	0	0	0	0	0	0	0	0	0	0
	Minor	S	0	0	0	0	0	0	0	0	0	0	0	0	0	0	0	0	0	0	0	0	0	0	0	0
		N	0	0	0	0	0	0	0	0	0	0	0	0	0	0	0	0	0	0	0	0	0	0	0	0
1315	Major	E	0	0	0	0	0	0	0	0	0	0	0	0	0	0	0	0	0	0	0	0	0	0	0	0
		W																								
	Minor	N	0	0	0	0	0	0	0	0	0	0	0	0	0	0	0	0	0	0	0	0	0	0	0	0
1325	Major	E	0	0	0	0	0	0	0	0	0	0	0	0	0	0	0	0	0	0	0	0	0	0	0	0
		W	0	0	0	0	0	0	0	0	0	0	0	0	0	0	0	0	0	0	0	0	0	0	0	0
	Minor	S	0	0	0	0	0	0	0	0	0	0	0	0	0	0	0	0	0	0	0	0	0	0	0	0
		N	0	0	0	0	0	0	0	0	0	0	0	0	0	0	0	0	0	0	0	0	0	0	0	0
1330	Major	E	0	0	0	0	0	0	0	0	0	0	0	0	0	0	0	0	0	0	0	0	0	0	0	0
		W	0	0	0	0	0	0	0	0	0	0	0	0	0	0	0	0	0	0	0	0	0	0	0	0
	Minor	S	0	0	0	0	0	0	0	0	0	0	0	0	0	0	0	0	0	0	0	0	0	0	0	0
		N	0	0	0	0	0	0	0	0	0	0	0	0	0	0	0	0	0	0	0	0	0	0	0	0
1455	Major	W	0	0	0	0	0	0	0	0	0	0	0	0	0	0	0	0	0	0	0	0	0	0	0	0
		E	0	0	0	0	0	0	0	0	0	0	0	0	0	0	0	0	0	0	0	0	0	0	0	0
	Minor	N	0	0	0	0	0	0	0	0	0	0	0	0	0	0	0	0	0	0	0	0	0	0	0	0
		S	0	0	0	0	0	0	0	0	0	0	0	0	0	0	0	0	0	0	0	0	0	0	0	0
1470	Major	E	0	0	0	0	0	0	0	0	0	0	0	0	0	0	0	0	0	0	0	0	0	0	0	0
		W	0	0	0	0	0	0	0	0	0	0	0	0	0	1	1	1	0	1	1	0	0	0	0	0
	Minor	S	0	0	0	0	0	0	0	0	0	0	1	0	0	0	0	1	0	0	1	0	0	0	0	0
		N	0	0	0	0	0	0	0	0	0	0	0	0	0	0	1	0	0	0	0	0	0	0	0	0

1490	Major	W	0	0	0	0	0	0	0	0	0	0	0	0	0	0	0	0	0	0	0	0	0	0	0
		E	0	0	0	0	0	0	0	0	0	0	0	0	0	0	0	0	0	0	0	0	0	0	0
	Minor	N	0	0	0	0	0	0	0	0	0	0	0	0	0	0	0	0	0	0	0	0	0	0	0
		S	0	0	0	0	0	0	0	0	0	0	0	0	0	0	0	0	0	0	0	0	0	0	0
1500	Major	W	0	0	0	0	0	0	0	0	0	0	0	0	0	1	0	1	0	0	0	0	0	0	0
		E	0	0	0	0	0	0	0	0	0	0	0	0	0	0	0	0	1	0	0	0	0	0	0
	Minor	N	0	0	0	0	0	0	0	0	0	0	0	0	1	0	1	1	0	1	0	0	0	0	0
		S	0	0	0	0	0	0	0	0	0	0	0	0	0	0	1	0	0	0	0	0	0	0	0
1555	Major	SE	0	0	0	0	0	0	0	0	0	0	0	0	0	0	0	0	0	0	0	0	0	0	0
		NW	0	0	0	0	0	0	0	0	0	0	0	0	0	0	0	0	0	0	0	0	0	0	0
	Minor	SW	0	0	0	0	0	0	0	0	0	0	0	0	0	0	0	0	0	0	0	0	0	0	0
		NE																							
1707	Major	W	0	0	0	0	0	0	0	0	0	0	0	0	0	0	0	0	0	0	0	0	0	0	0
		E	0	0	0	0	0	0	0	0	0	0	0	0	0	0	0	0	0	0	0	0	0	0	0
	Minor	N																							
		S																							
1725	Major	SE																							
		NW																							
	Minor	S																							
		N																							
1790	Major	W	0	0	0	0	0	0	0	0	0	0	0	0	0	0	0	0	0	0	0	0	0	0	0
		E	0	0	0	0	0	0	0	0	0	0	0	0	0	0	0	0	0	0	0	0	0	0	0
	Minor	S																							
1795	Major	W	0	0	0	0	0	0	0	0	0	0	0	0	0	0	0	0	0	0	0	0	0	0	0
		E	0	0	0	0	0	0	0	0	0	0	0	0	0	0	0	0	0	0	0	0	0	0	0
	Minor	N																							
1960	Major	W	0	0	0	0	0	0	0	0	0	0	0	0	0	0	0	0	0	0	0	0	0	0	0
		E	0	0	0	0	0	0	0	0	0	0	0	0	0	0	0	0	0	0	0	0	0	0	0
	Minor	N	0	0	0	0	0	0	0	0	0	0	0	0	0	0	0	0	0	0	0	0	0	0	0
		S	0	0	0	0	0	0	0	0	0	0	0	0	0	0	0	0	0	0	0	0	0	0	0
2055	Major	W	0	0	0	0	0	0	0	0	0	0	0	0	0	0	0	0	0	0	0	0	0	0	0
		E	0	0	0	0	0	0	0	0	0	0	0	0	0	0	0	0	0	0	0	0	0	0	0
	Minor	N	0	0	0	0	0	0	0	0	0	0	0	0	0	0	0	0	0	0	0	0	0	0	0
		S	0	0	0	0	0	0	0	0	0	0	0	0	0	0	0	0	0	0	0	0	0	0	0
2485	Major	E	0	0	0	0	0	0	0	0	0	0	0	0	0	0	0	0	0	0	0	0	0	0	0

		W	0	0	0	0	0	0	0	0	0	0	0	0	0	0	0	0	0	0	0	0	0	0	0
	Minor	S	0	0	0	0	0	0	0	0	0	0	0	0	0	0	0	0	0	0	0	0	0	0	0
		N	0	0	0	0	0	0	0	0	0	0	0	0	0	0	0	0	0	0	0	0	0	0	0
2665	Major	W	0	0	0	0	0	0	0	0	0	0	0	0	0	0	0	0	0	0	0	0	0	0	0
		E	0	0	0	0	0	0	0	0	0	0	0	0	0	0	0	0	0	0	0	0	0	0	0
	Minor	N	0	0	0	0	0	0	0	0	0	0	0	0	0	0	0	0	0	0	0	0	0	0	0
		S	0	0	0	0	0	0	0	0	0	0	0	0	0	0	0	0	1	0	0	0	0	0	0

Table A-7. Summary of Leading Pedestrian Interval (k = 0.01)

Signal ID	Approach Type	Approach Direction	Hour of Day (Local Time)																							
			0	1	2	3	4	5	6	7	8	9	10	11	12	13	14	15	16	17	18	19	20	21	22	23
1285	Major	E	0	0	0	0	0	0	0	0	0	0	0	0	0	0	0	0	0	0	0	0	0	0	0	0
		W	0	0	0	0	0	0	0	0	0	0	0	0	0	0	0	0	0	0	0	0	0	0	0	0
	Minor	S	0	0	0	0	0	0	0	0	0	0	0	0	0	0	0	0	0	1	0	0	0	0	0	0
		N	0	0	0	0	0	0	0	0	0	0	0	0	0	0	0	0	0	0	0	0	0	0	0	0
1290	Major	W	0	0	0	0	0	0	0	0	0	0	0	0	0	0	0	0	0	0	0	0	0	0	0	0
		E	0	0	0	0	0	0	0	0	0	0	0	0	0	0	0	0	0	0	0	0	0	0	0	0
	Minor	N	0	0	0	0	0	0	0	0	0	0	0	0	0	0	0	0	0	0	0	0	0	0	0	0
		S	0	0	0	0	0	0	0	0	0	0	0	0	0	0	0	0	0	0	0	0	0	0	0	0
1300	Major	E	0	0	0	0	0	0	0	0	0	0	0	0	0	0	0	0	0	0	0	0	0	0	0	0
		W	0	0	0	0	0	0	0	0	0	0	0	0	0	0	0	0	0	0	0	0	0	0	0	0
	Minor	S	0	0	0	0	0	0	0	0	0	0	0	0	0	0	0	0	0	0	0	0	0	0	0	0
		N	0	0	0	0	0	0	0	0	0	0	0	0	0	0	0	0	0	0	0	0	0	0	0	0
1315	Major	E	0	0	0	0	0	0	0	0	0	0	0	0	0	0	0	0	0	0	0	0	0	0	0	0
		W	0	0	0	0	0	0	0	0	0	0	0	0	0	0	0	0	0	0	0	0	0	0	0	0
	Minor	N	0	0	0	0	0	0	0	0	0	0	0	0	0	0	0	0	0	0	0	0	0	0	0	0
1325	Major	E	0	0	0	0	0	0	0	0	0	0	0	0	0	0	0	0	0	0	0	0	0	0	0	0
		W	0	0	0	0	0	0	0	0	0	0	0	0	0	0	0	0	0	0	0	0	0	0	0	0
	Minor	S	0	0	0	0	0	0	0	0	0	0	0	0	0	0	0	0	0	0	0	0	0	0	0	0
		N	0	0	0	0	0	0	0	0	0	0	0	0	0	0	0	0	0	0	0	0	0	0	0	0
1330	Major	E	0	0	0	0	0	0	0	0	0	0	0	0	0	0	0	0	0	0	0	0	0	0	0	0
		W	0	0	0	0	0	0	0	0	0	0	0	0	0	0	0	0	0	0	0	0	0	0	0	0
	Minor	S	0	0	0	0	0	0	0	0	0	0	0	0	0	0	0	0	0	0	0	0	0	0	0	0
		N	0	0	0	0	0	0	0	0	0	0	0	0	0	0	0	0	0	0	0	0	0	0	0	0
1455	Major	W	0	0	0	0	0	0	0	0	0	0	0	0	0	0	0	0	0	0	0	0	0	0	0	0
		E	0	0	0	0	0	0	0	0	0	0	0	0	0	0	0	0	0	0	0	0	0	0	0	0
	Minor	N	0	0	0	0	0	0	0	0	0	0	0	0	0	0	0	0	0	0	0	0	0	0	0	0
		S	0	0	0	0	0	0	0	0	0	0	0	0	0	0	0	0	0	0	0	0	0	0	0	0
1470	Major	E																								
		W																								
	Minor	S																								
		N																								

1490	Major	W	0	0	0	0	0	0	0	0	0	0	0	0	0	0	0	0	0	0	0	0	0	0	0
		E	0	0	0	0	0	0	0	0	0	0	0	0	0	0	0	0	0	0	0	0	0	0	0
	Minor	N	0	0	0	0	0	0	0	0	0	0	0	0	0	0	0	0	0	0	0	0	0	0	0
		S	0	0	0	0	0	0	0	0	0	0	0	0	0	0	0	0	0	0	0	0	0	0	0
1500	Major	W	0	0	0	0	0	0	0	0	0	0	0	0	0	0	0	0	0	0	0	0	0	0	0
		E	0	0	0	0	0	0	0	0	0	0	0	0	0	0	0	0	0	0	0	0	0	0	0
	Minor	N	0	0	0	0	0	0	0	0	0	0	0	1	1	1	0	1	0	1	0	0	0	0	0
		S	0	0	0	0	0	0	0	0	0	0	0	0	0	1	1	1	1	1	0	0	0	0	0
1555	Major	SE	0	0	0	0	0	0	0	0	0	0	0	0	0	0	0	0	0	0	0	0	0	0	0
		NW	0	0	0	0	0	0	0	0	0	0	0	0	0	0	0	0	0	0	0	0	0	0	0
	Minor	SW	0	0	0	0	0	0	0	0	0	0	0	0	0	0	0	0	0	0	0	0	0	0	0
		NE	0	0	0	0	0	0	0	0	0	0	0	0	0	0	0	0	0	0	0	0	0	0	0
1707	Major	W	0	0	0	0	0	0	0	0	0	0	0	0	0	0	0	0	0	0	0	0	0	0	0
		E	0	0	0	0	0	0	0	0	0	0	0	0	0	0	0	0	0	0	0	0	0	0	0
	Minor	N	0	0	0	0	0	0	0	0	0	0	0	0	0	0	0	0	0	0	0	0	0	0	0
		S	0	0	0	0	0	0	0	0	0	0	0	0	0	0	0	0	0	0	0	0	0	0	0
1725	Major	SE																							
		NW																							
	Minor	S																							
		N																							
1790	Major	W																							
		E																							
	Minor	S																							
1795	Major	W																							
		E																							
	Minor	N																							
1960	Major	W	0	0	0	0	0	0	0	0	0	0	0	0	0	0	0	0	0	0	0	0	0	0	0
		E	0	0	0	0	0	0	0	0	0	0	0	0	0	0	0	0	0	0	0	0	0	0	0
	Minor	N	0	0	0	0	0	0	0	0	0	0	0	0	0	0	0	0	0	0	0	0	0	0	0
		S	0	0	0	0	0	0	0	0	0	0	0	0	0	0	0	0	0	0	0	0	0	0	0
2055	Major	W	0	0	0	0	0	0	0	0	0	0	0	0	0	0	0	0	0	0	0	0	0	0	0
		E	0	0	0	0	0	0	0	0	0	0	0	0	0	0	0	0	0	0	0	0	0	0	0
	Minor	N	0	0	0	0	0	0	0	0	0	0	0	0	0	0	0	0	0	0	0	0	0	0	0
		S	0	1	0	0	0	0	0	0	0	0	0	1	0	0	0	0	0	0	0	0	0	0	0
2485	Major	E	0	0	0	0	0	0	0	0	0	0	0	0	0	0	0	0	0	0	0	0	0	0	0

		W	0	0	0	0	0	0	0	0	0	0	0	0	0	0	0	0	0	0	0	0	0	0	0
	Minor	S	0	0	0	0	0	0	0	0	0	0	0	0	0	0	0	0	0	0	0	0	0	0	0
		N	0	0	0	0	0	0	0	0	0	0	0	0	0	0	0	0	0	0	0	0	0	0	0
2665	Major	W	0	0	0	0	0	0	0	0	0	0	0	0	0	0	0	0	0	0	0	0	0	0	0
		E	0	0	0	0	0	0	0	0	0	0	0	0	0	0	0	0	0	0	0	0	0	0	0
	Minor	N	0	0	0	0	0	0	0	0	0	0	0	0	0	0	0	0	0	0	0	0	0	0	0
		S	0	0	0	0	0	0	0	0	0	0	0	0	0	0	0	0	0	0	0	0	0	0	0

Table A-8. Summary of No Right Turn On Red (k = 0.025)

Signal ID	Approach Type	Approach Direction	Hour of Day (Local Time)																							
			0	1	2	3	4	5	6	7	8	9	10	11	12	13	14	15	16	17	18	19	20	21	22	23
1285	Major	E	0	0	0	0	0	0	0	0	0	0	0	0	0	0	0	0	0	0	0	0	0	0	0	0
		W	0	0	0	0	0	0	0	0	0	0	0	0	0	0	0	0	0	0	0	0	0	0	0	0
	Minor	S	0	0	0	0	0	0	0	0	0	0	0	0	0	0	0	0	0	1	0	0	0	0	0	0
		N	0	0	0	0	0	0	0	0	0	0	0	0	0	0	0	0	0	0	0	0	0	0	0	0
1290	Major	W	0	0	0	0	0	0	0	0	0	0	0	0	0	0	0	0	0	0	0	0	0	0	0	0
		E	0	0	0	0	0	0	0	0	0	0	0	0	0	0	0	0	0	0	0	0	0	0	0	0
	Minor	N	0	0	0	0	0	0	0	0	0	0	0	0	0	0	0	0	0	0	0	0	0	0	0	0
		S	0	0	0	0	0	0	0	0	0	0	0	0	0	0	0	0	0	0	0	0	0	0	0	0
1300	Major	E	0	0	0	0	0	0	0	0	0	0	0	0	0	0	0	0	0	0	0	0	0	0	0	0
		W	0	0	0	0	0	0	0	0	0	0	0	0	0	0	0	0	0	0	0	0	0	0	0	0
	Minor	S	0	0	0	0	0	0	0	0	0	0	0	0	0	0	0	0	0	0	0	0	0	0	0	0
		N	0	0	0	0	0	0	0	0	0	0	0	0	0	0	0	0	0	0	0	0	0	0	0	0
1315	Major	E	0	0	0	0	0	0	0	0	0	0	0	0	0	0	0	0	0	0	0	0	0	0	0	0
		W	0	0	0	0	0	0	0	0	0	0	0	0	0	0	0	0	0	0	0	0	0	0	0	0
	Minor	N	0	0	0	0	0	0	0	0	0	0	0	0	0	0	0	0	0	0	0	0	0	0	0	0
1325	Major	E	0	0	0	0	0	0	0	0	0	0	0	0	0	0	0	0	0	0	0	0	0	0	0	0
		W	0	0	0	0	0	0	0	0	0	0	0	0	0	0	0	0	0	0	0	0	0	0	0	0
	Minor	S	0	0	0	0	0	0	0	0	0	0	0	0	0	0	0	0	0	0	0	0	0	0	0	0
		N	0	0	0	0	0	0	0	0	0	0	0	0	0	0	0	0	0	0	0	0	0	0	0	0
1330	Major	E	0	0	0	0	0	0	0	0	0	0	0	0	0	0	0	0	0	0	0	0	0	0	0	0
		W	0	0	0	0	0	0	0	0	0	0	0	0	0	0	0	0	0	0	0	0	0	0	0	0
	Minor	S	0	0	0	0	0	0	0	0	0	0	0	0	0	0	0	0	0	0	0	0	0	0	0	0
		N	0	0	0	0	0	0	0	0	0	0	0	0	0	0	0	0	0	0	0	0	0	0	0	0
1455	Major	W	0	0	0	0	0	0	0	0	0	0	0	0	0	0	0	0	0	0	0	0	0	0	0	0
		E	0	0	0	0	0	0	0	0	0	0	0	0	0	0	0	0	0	0	0	0	0	0	0	0
	Minor	N	0	0	0	0	0	0	0	0	0	0	0	0	0	0	0	0	0	0	0	0	0	0	0	0
		S	0	0	0	0	0	0	0	0	0	0	0	0	0	0	0	0	0	0	0	0	0	0	0	0
1470	Major	E																								

		W																								
	Minor	S																								
		N																								
1490	Major	W	0	0	0	0	0	0	0	0	0	0	0	0	0	0	0	0	0	0	0	0	0	0	0	0
		E	0	0	0	0	0	0	0	0	0	0	0	0	0	0	0	0	0	0	0	0	0	0	0	0
	Minor	N	0	0	0	0	0	0	0	0	0	0	0	0	0	0	0	0	0	0	0	0	0	0	0	0
		S	0	0	0	0	0	0	0	0	0	0	0	0	0	0	0	0	0	0	0	0	0	0	0	0
1500	Major	W	0	0	0	0	0	0	0	0	0	0	0	0	0	0	0	0	0	0	0	0	0	0	0	0
		E	0	0	0	0	0	0	0	0	0	0	0	0	0	0	0	0	0	0	0	0	0	0	0	0
	Minor	N	0	0	0	0	0	0	0	0	0	0	0	1	1	1	0	1	0	1	0	0	0	0	0	0
		S	0	0	0	0	0	0	0	0	0	0	0	0	0	1	1	1	1	1	0	0	0	0	0	0
1555	Major	SE	0	0	0	0	0	0	0	0	0	0	0	0	0	0	0	0	0	0	0	0	0	0	0	0
		NW	0	0	0	0	0	0	0	0	0	0	0	0	0	0	0	0	0	0	0	0	0	0	0	0
	Minor	SW	0	0	0	0	0	0	0	0	0	0	0	0	0	0	0	0	0	0	0	0	0	0	0	0
		NE	0	0	0	0	0	0	0	0	0	0	0	0	0	0	0	0	0	0	0	0	0	0	0	0
1707	Major	W	0	0	0	0	0	0	0	0	0	0	0	0	0	0	0	0	0	0	0	0	0	0	0	0
		E	0	0	0	0	0	0	0	0	0	0	0	0	0	0	0	0	0	0	0	0	0	0	0	0
	Minor	N	0	0	0	0	0	0	0	0	0	0	0	0	0	0	0	0	0	0	0	0	0	0	0	0
		S	0	0	0	0	0	0	0	0	0	0	0	0	0	0	0	0	0	0	0	0	0	0	0	0
1725	Major	SE																								
		NW																								
	Minor	S																								
		N																								
1790	Major	W																								
		E																								
	Minor	S																								
1795	Major	W																								
		E																								
	Minor	N																								
1960	Major	W	0	0	0	0	0	0	0	0	0	0	0	0	0	0	0	0	0	0	0	0	0	0	0	0
		E	0	0	0	0	0	0	0	0	0	0	0	0	0	0	0	0	0	0	0	0	0	0	0	0
	Minor	N	0	0	0	0	0	0	0	0	0	0	0	0	0	0	0	0	0	0	0	0	0	0	0	0
		S	0	0	0	0	0	0	0	0	0	0	0	0	0	0	0	0	0	0	0	0	0	0	0	0
2055	Major	W	0	0	0	0	0	0	0	0	0	0	0	0	0	0	0	0	0	0	0	0	0	0	0	0

		E	0	0	0	0	0	0	0	0	0	0	0	0	0	0	0	0	0	0	0	0	0	0	0	0
	Minor	N	0	0	0	0	0	0	0	0	0	0	0	0	0	0	0	0	0	0	0	0	0	0	0	0
		S	0	1	0	0	0	0	0	0	0	0	0	1	0	0	0	0	0	0	0	0	0	0	0	0
2485	Major	E	0	0	0	0	0	0	0	0	0	0	0	0	0	0	0	0	0	0	0	0	0	0	0	0
		W	0	0	0	0	0	0	0	0	0	0	0	0	0	0	0	0	0	0	0	0	0	0	0	0
	Minor	S	0	0	0	0	0	0	0	0	0	0	0	0	0	0	0	0	0	0	0	0	0	0	0	0
		N	0	0	0	0	0	0	0	0	0	0	0	0	0	0	0	0	0	0	0	0	0	0	0	0
2665	Major	W	0	0	0	0	0	0	0	0	0	0	0	0	0	0	0	0	0	0	0	0	0	0	0	0
		E	0	0	0	0	0	0	0	0	0	0	0	0	0	0	0	0	0	0	0	0	0	0	0	0
	Minor	N	0	0	0	0	0	0	0	0	0	0	0	0	0	0	0	0	0	0	0	0	0	0	0	0
		S	0	0	0	0	0	0	0	0	0	0	0	0	0	0	0	0	0	0	0	0	0	0	0	0